

Studies in Low and Flood Flow Estimation for Irish River Catchments

Uzzal Krishna Mandal

Ph.D.



**Engineering Hydrology
College of Engineering & Informatics
National University of Ireland, Galway**

September 2011

Studies in Low and Flood Flow Estimation for Irish River Catchments

By

Uzzal Krishna Mandal

B.Sc. Eng. (Civil), MSc.(Hydrology), CEng MIEI

Thesis submitted to the National University of Ireland, Galway in
fulfilment of the requirements for the Degree of Doctor of Philosophy

Supervisor: Professor C. Cunnane
Professor and Head of the Discipline



Engineering Hydrology
College of Engineering & Informatics
National University of Ireland, Galway

September 2011

Studies in Low and Flood Flow Estimation for Irish River Catchments

**Part-A: Low-Flow Estimation for Ungauged
Catchments**

and

**Part-B: Non-Stationarity in Flood Flows and Its
Effect on Flood Frequency Growth Curves
for Irish River Catchments**



**Engineering Hydrology
College of Engineering & Informatics
National University of Ireland, Galway**

September 2011

Acknowledgements

The author would like to express his appreciation and gratitude to Professor C. Cunnane, Head of Engineering Hydrology, National University of Ireland for his excellent guidance, financial support and immense patience through the study period. The author feels privileged of having an opportunity to work with such an eminent hydrologist.

The author also extends his sincere thanks to Professor. Kieran M. O'Connor for his useful advice and encouragement during the study period.

The financial support provided by the Discipline of Engineering Hydrology, National University of Ireland through the Irish Office of Public Works Flood Studies Update Programme is gratefully acknowledged. Sincere thanks to Professor C. Cunnane for organising this financial support.

His sincere thanks to all staff of the Department of Engineering Hydrology, especially to Mr. Dermot McDermott, Mr. Edward Kilcullen and Ms. Carmel King for their sincere co-operation.

Sincere thanks are due to all the author's colleagues, especially Mr. Gerry Carty, Mr. P.J. Griffin and Mr. Christy O'Sullivan for their constant support and encouragement throughout the course of the study.

The author wishes to convey his sincere gratitude to his mother, late father who has a very strong influence on the author's life, his sisters and his brothers, especially his younger brother Utpal for their affection, inspiration and encouragement throughout the study period. Special thanks to the author's father-in-law for his constant affection and encouragement during the entire course of the study.

Last but not least, the author extends his heartfelt thanks to his wife Moushumi and daughters Sushmita and Nandita for their support and encouragement during the course of the study. The patience, support and encouragement provided by Moushumi throughout this hard journey deserves special mention without which the author would not have been able to reach his goal.

Abstract

This study focused on the estimation of low flows for Irish River catchments, particularly for ungauged catchments and on the estimation of flood flows in the context of changing climatic conditions, which is believed may be causing non-stationarity in the streamflow time series. The main objectives of the study were to develop a methodology to estimate low-flows for ungauged river catchments in Ireland, to investigate any evidence of the presence of trends in the Annual Maximum Flood (AMF) records and to investigate the effects of trends / non-stationarity on the design floods (on both growth curve and at-site quantiles) estimated from the conventional statistical frequency analysis techniques applied on a regional scale level. The study was carried out in two parts: (i) Part A deals with low-flows estimates, while (ii) Part B deals with the flood flow estimates in the presence of trends.

In the low-flow studies for Ireland, it was found that a regression-based 1-parameter logarithmic type model provides a good approximation to the lower three-quarter part of the Period-of-Record (POR) daily Flow Duration Curves (FDC) at most of the 125 gauging sites in Ireland. Given the complex shape of the observed FDCs and the higher variability in the high-flow sections of the FDCs, this study focused on modelling of only the lower three-quarter section of FDC (25%ile to 99.99%ile). The parameter of the proposed model has been estimated from the easily measurable/obtainable catchment physiographic and climatological characteristics, such as catchment areas (AREA), mean annual rainfall (SAAR) and mean annual potential evapotranspiration (PE). A sensitivity analysis on the mean daily flow records for 10 Irish River catchments showed that at least 15 to 20 years of observed streamflow records are required to obtain a reliable long-term POR equivalent estimate of the FDCs and associated low-flow indices. The study also showed that the Q_{95} flow estimate from 10 years of records at a site in the study region could deviate (under- or over-estimation) by approximately 20% from the equivalent long-term estimate.

In the search for any evidence of the presence of non-stationarity in Irish AMF records, a number of parametric and non-parametric tests were employed. The results showed that the Irish AMF series are in general dominated by positive serial

correlations. Non-randomness properties were identified at 5% significance level in 17% of the sites, while 30% of sites showed step change in mean (mostly increase) during the post 1976 period. The trend test results identified considerably more trends in Irish AMF records than that would be expected to occur by chance. Significant trends were found at 30% of sites at 5% significance level, with increasing trends at 23% of sites. Some temporal variations in the trend test results are also apparent in the Irish AMF records. The Annual Maximum Rainfall (AMR) records of Ireland (1955-2008) also showed significant increasing trends, with longer rainfall durations showing greater tendency of trends. Some evidence of spatial patterns in trends in AMF and AMR series was detected by a mapping exercise which might indicate that the climate change may be responsible for AMF trends.

The findings of the simulation experiments carried out to identify the power of different trend identification tests (Mann-Kendall, Spearman's Rho and Standardised Linear Regression tests) showed that, in general, the power of a trend test is an increasing function of the trend slope and sample size, i.e. power increases with the increase in trend slope and sample size. This is true in all three tests. The simulation results also showed that the sample variance plays a very important role in detecting whether trend exists or not in the records.

The effects of trends on the regional growth curves and at-site quantiles were investigated through Monte Carlo Simulation techniques and in accordance with the Hosking and Wallis (1997) proposed L-moment algorithm procedures. Two different forms of trends were applied, one additive and the other hybrid, referred to as TF-1 and TF-2 respectively, in three different spatial patterns in the region / pooling group. The simulation results show that any trend causes changes in the population parameters, depending on the form and magnitude of trend and type of population distribution. TF-1 generally causes a flattening of growth curves, while TF-2 has the opposite effect. These changes can be as large as 16% at $T=100$ and trend slope of 1%. Trend effect on quantiles is generally positive, largely caused by an increase in the index flood, with increases up to 17% at $T=100$ and 1% trend slope. Some unrealistic results emerged in the GEV-GEV simulation case where large return period floods showed a decrease caused by the estimated GEV k value being (unexpectedly) positive when estimated from the data containing trends.

CONTENTS

LIST OF FIGURES	ix
LIST OF TABLES	xv
LIST OF SYMBOLS AND ABBREVIATIONS	xviii
1 INTRODUCTION	1
1.1 GENERAL BACKGROUND AND OBJECTIVE OF THE STUDY	1
1.2 SCOPE OF THE STUDY	4
1.3 OUTLINE OF THE THESIS	4
2 LITERATURE REVIEW	6
2.1 INTRODUCTION	6
2.2 PART A - LOW-FLOW ESTIMATION FOR UNGAUGED CATCHMENT	6
2.2.1 Statistical Approaches	9
2.2.2 Parametric Approaches	12
2.2.3 Graphical (Non-parametric) Approaches	13
2.2.4 Estimation of Low-Flows from Short Records Lengths	15
2.3 PART B – NON-STATIONARITY IN FLOOD FLOWS	17
2.3.1 Detection of Trend in Flood Series	17
2.3.2 Power of Trend Tests	22
2.3.3 Effect of Trends on Regional Growth Curves and At-site Quantile Estimates	24
3 LOW-FLOWS - PHYSICAL PROCESSES AND ESTIMATION METHODS	26
3.1 INTRODUCTION	26
3.2 LOW-FLOW HYDROLOGY – CATCHMENT PHYSICAL PROCESSES	26
3.3 LOW-FLOW MEASURES AND INDICES	34
3.4 FLOW-DURATION CURVE (FDC).....	35
3.4.1 Construction and Interpretation	35
3.4.2 Applications	37
3.5 LOW-FLOW ESTIMATION AND PREDICTIONS	38

4	LOW-FLOW PREDICTION FOR UNGAUGED RIVER CATCHMENTS IN IRELAND	40
4.1	INTRODUCTION	40
4.2	LOW-FLOWS IN IRELAND	40
4.2.1	Low-flow Characteristics and Drought History	40
4.2.2	Low-flow Measures Currently in Use in Ireland	41
4.2.3	History of Low-Flow Studies	42
4.3	A FLOW-DURATION CURVE BASED LOW-FLOW ESTIMATION METHOD FOR UNGAUGED RIVER CATCHMENTS IN IRELAND	45
4.3.1	Methodology	45
4.3.2	Data	46
4.3.3	Proposed FDC Model	48
4.3.4	Model Parameter Estimation	50
4.3.5	Model Performance	55
4.3.6	Model Validation	58
4.4	RESULTS SUMMAY AND DISCUSSIONS	60
5	LIMITATIONS OF PERIOD-OF-RECORD FLOW-DURATION CURVE (FDC) AND ITS SENSITIVITY TO RECORD LENGTHS	62
5.1	PERIOD-OF-RECORD FDC AND ITS LIMITATIONS	62
5.2	COMPARISON OF PERIOD OF RECORD AND ANNUAL FLOW DURATION CURVES FOR THE IRISH RIVER CATCHMENT	63
5.3	SENSITIVITY OF LOW-FLOW INDICES TO SAMPLE LENGTHS FOR IRISH RIVER CATCHMENTS	70
5.3.1	Introduction	70
5.3.2	Methodology	70
5.3.3	Data	72
5.3.4	Results	73
5.4	ESTIMATION OF LOW-FLOWs FROM SHORT RECORD LENGTHS	81
6	NON-STATIONARITY IN FLOOD SERIES, ITS CAUSES AND DETECTION METHODS	83
6.1	INTRODUCTION	83
6.2	FLOOD FREQUENCY ANALYSIS AND ITS ASSUMPTIONS	83
6.3	CAUSES OF NON-STATIONANIRITY IN FLOOD MAGNITUDES	84
6.4	IMPACTS OF NON-STATIONARITY IN FLOOD FREQUENCY ANALYSIS	86
6.5	METHODS OF TESTING NON-STATIONARITY IN FLOOD SERIES	87
6.5.1	Test Procedures	87
6.5.2	Parametric and Non-parametric Tests	97
6.5.3	Details of some commonly used tests for Non-stationarity	98

7	DETECTION OF TRENDS IN IRISH ANNUAL MAXIMUM FLOOD (AMF) SERIES.	106
7.1	INTRODUCTION	106
7.2	DATA	106
	7.2.1 Exploratory Data Analysis (EDA).....	108
7.3	METHODOLOGY	116
	7.3.1 General	116
7.4	RESULTS AND DISCUSSIONS	121
	7.4.1 Test for Independence.....	121
	7.4.2 Test for Stationarity.....	127
	7.4.3 Trend Test Results	132
7.5	INVESTIGATION OF THE CAUSES OF TRENDS IN THE ANNUAL MAXIMUM FLOOD SERIES IN IRELAND	143
7.6	RESULTS SUMMARY – NON STATIONARITY IN IRISH AMF SERIES	152
8	POWER OF TREND TESTS	156
8.1	INTRODUCTION	156
8.2	METHODOLOGY	156
8.3	RESULTS & DISCUSSION	161
8.4	RESULT SUMMARY AND DISCUSSIONS	169
9	EFFECT OF TRENDS ON REGIONAL GROWTH CURVES AND AT-SITE QUANTILE ESTIMATES	172
9.1	INTRODUCTION AND OBJECTIVE	172
9.2	SCOPE OF THE STUDY	172
9.3	METHODOLOGY	173
	9.3.1 General.....	173
	9.3.2 Selection of Stationary Region and Random Sample Generation.....	174
	9.3.3 Application of Trends.....	175
	9.3.4 Trend Scenarios.....	177
	9.3.5 Growth Curve and Quantile Estimation Methods.....	178
	9.3.6 Trend Effect Assessments.....	187
9.4	RESULTS	192
	9.4.1 Introduction	192
	9.4.2 Population Properties	193
	9.4.3 Changes in Distribution Parameters.....	203
	9.4.4 Changes in Growth Curves	212
	9.4.5 Changes in At-site Quantiles	219
	9.4.6 Suitability of various Distributions in Trend Impact Study	228
	9.4.7 Result Summary and Discussions.....	237

10	CONCLUSIONS AND RECOMMENDATIONS.....	243
10.1	CONCLUSIONS.....	243
10.2	RECOMMENDATIONS.....	245
	REFERENCES:.....	247
	Appendix A: Data and Catchment Characteristics.....	265
	Appendix B: Critical Values for the Standardised Linear Regression based Test Statistic.....	275
	Appendix C: Heterogeneity Test Measures.....	279

LIST OF FIGURES:

Figure 3.1: Hydrological processes and catchment storages.....	29
Figure 3.2: Shape of FDC represents catchment response behaviour	36
Figure 4.1 Modelled FDC section	45
Figure 4.2: Spatial distribution of the gauging sites.....	48
Figure 4.3: Fitted Log-model to an empirical FDC.....	49
Figure 4.4: Correlation between parameters 'a' & 'b'	50
Figure 4.5: Regression of parameter 'a' on AREA & SAAR	52
Figure 4.6: Regression of Parameter 'a' on MF.....	53
Figure 4.7: Indicative Potential Evapotranspiration Map (PE-Map) for Ireland	54
Figure 4.8: Relationship between the predicted and observed Mean Flows.....	54
Figure 4.9: Scatter Plots – AREA-SAAR Model	57
Figure 4.10: Scatter Plots Mean Flow Model.....	58
Figure 4.11: Observed and predicted FDCs.....	59
Figure 5.1: Plots of mean daily flows and comparison of POR and Annual 95%ile flows for River Suir at Clonmel (Hydrometric station No. 16011)	64
Figure 5.2: Plots of mean daily flows and comparison of POR and Annual 95%ile flows for River Suir at Clonmel (Hydrometric station No. 16011) for the period of 1975 to 1976	64
Figure 5.3: Interannual variation of 95%ile flows with respect to POR value for River Suir at Clonmel (Hydrometric station No. 16011)	65
Figure 5.4: Comparison of FDCs for various record lengths for River Barrow at Portarlinton ..	66
Figure 5.5: Probability Plots and fitted EV1 distribution for the annual time series of low-flow indices of Q_{25} , Q_{50} , Q_{75} and Q_{95}	68
Figure 5.6: Plots of Period of Record FDC and the 2 and 50 year return periods AFDCs.....	69
Figure 5.7: Comparison of period-of record and resampled estimates of Q_{95}	75

Figure 5.8: Comparison of period-of record and resampled estimates of Q_{75}	76
Figure 5.9: Comparison of period-of record and resampled estimates of Q_{50}	77
Figure 5.10: Comparison of period-of record and resampled estimates of Q_{25}	78
Figure 5.11: Temporal variation of AFDC- Q_{95} estimates for the river gauging sites- 27002 and 14005.	79
Figure 5.12: Variation of regional average mean relative errors for various sample lengths.....	80
Figure 5.13: Variation of regional average absolute relative errors for various sample lengths .80	
Figure 5.14: Variation of regional average standard deviation of relative errors for various sample lengths.....	81
Figure 6.1: Hypothesis tests	94
Figure 6.2: Type I error in a hypothetical test (two sided test)	95
Figure 6.3: Type II error and the power of a hypothesis test.....	95
Figure 7.1: Spatial distribution of the gauging sites	107
Figure 7.2: Plots of Annual Maximum Flows against time (EDA analysis).....	109
Figure 7.3: Plots of Annual Maximum Flows against time for the catchments where drainage improvement works were carried out (continued).....	110
Figure 7.4: Percentage of sites with positive and negative Lag-1 serial correlation in AMF series along with respective significant percentage for the selected five timeframes (Original time series, significance level of 5%).....	122
Figure 7.5: Percentage of sites with positive and negative lag-1 serial correlation in AMF series along with respective significant percentage for the selected five timeframes (TF series, significance level of 5%)	123
Figure 7.6: Autocorrelation structure of AMF Series at various lags for the sites with significant Lag-1 autocorrelation at 5% significance level.	125
Figure 7.7: Number of sites with significant non-randomness at 5% significance level	126
Figure 7.8: Plots of average specific annual maximum flows against time (average of 33 sites) for the period of 1955 – 2007.....	127
Figure 7.9: Plots of average annual maximum rainfall records of various durations (1-day, 2-day, 3-day, 4-day, 8-day, 10-day, 16-day, 20-day and 25-day) against time for the period of 1955–2004 (average of 144 sites).....	128

Figure 7.10: Percentage of sites with increase and decrease in mean/median between time periods of 1955-1975 and 1976-2008 in AMF series along with respective significant percentage for the three timeframes (Panel a. T-test and Panel b. MW-U test) 129

Figure 7.11: Plots of the two sub-periods of AMF Series partitioned at 1976 (1955-1975 and 1976-2008) for each sites showing significant non-stationarity i.e. changes in location parameters (contd.) 131

Figure 7.12: Percentage of sites with positive and negative trends indentified by the MK, SPR and SLR tests (panels a-c) in AMF series along with respective significant percentage for the five timeframes (the trend tests were applied to the Original data without removing any effect of autocorrelation) 134

Figure 7.13: Comparison of trend test results for the MK, SPR and SLR tests showing the percentage of sites with significant trends at 5% significance level, in the AMF Series for all timeframes (the trend tests were applied to the Original data without removing any effect of autocorrelation) 134

Figure 7.14: Percentage of sites with positive and negative significant (at 5% significance level) trends obtained with the MK, SPR and SLR trend identification tests when applied to the Original, PW and TFPW form of the AMF data series..... 136

Figure 7.15: Comparison of trend test results showing the percentage of sites with significant trends at 5% significance level) for the Original, PW and TFPW series as identified by the MK, SPR and SLR tests (panel a: MK-test, panel b: SPR test and panel c: SLR-test) 137

Figure 7.16: Spatial distribution of trend test results – POR – Original data series 140

Figure 7.17: Spatial distribution of trend test results – 1965-2008 – Original data series 141

Figure 7.18: Spatial distribution of trend test results – 1975-2008 – Original data series 142

Figure 7.19: Number of stations with significant trends in AMR records for different durations (5% significance level – total stations examined are 144)..... 146

Figure 7.20: Spatial distribution of trend test results for AMR series of 8-day duration 147

Figure 7.21: Spatial distribution of trend test results for AMR series of 16-day duration 148

Figure 7.22: Spatial distribution of trend test results for AMR series of 25-day duration 149

Figure 7.23: Illustration of effect of trends in Annual Maximum Flows (POR Series) and AMR records (25-day duration) 151

Figure 8.1: Changes in the population mean with the increase in trend slopes in both cases of trend forms (a) CV=0.30 (b) CV=0.50 162

Figure 8.2: Changes in the variance with the increase in trend slopes in both cases of trend forms 163

Figure 8.3: Variations of the power of trend identification tests with the increase in trend slopes in the Trend Forms of 1 & 2 (panel a: MK-test, panel b: SPR-test and panel c: SLR-test)..... 164

Figure 8.4: Comparison of the power of the trend identification tests MK, SPR and SLR tests under two trend forms (panel a: for TF-1 and panel b: for TF-2)..... 165

Figure 8.5: Variations of the power of trend identification tests with the increase in trend sample sizes in the Trend Forms of 1 & 2 (panel a: MK-test, panel b: SPR-test and panel c: SLR-test). 166

Figure 8.6: Comparison of the sensitivity of the power of the trend identification tests (MK, SPR and SLR tests) with the increase in sample size under two trend forms (panel a: for TF-1 and panel b: for TF-2). 167

Figure 8.7: Variations of the power of trend identification tests with the increase in sample variance in the trend forms of 1 & 2 for trend slope of 1% (panel a: MK-test, panel b: SPR-test and panel c: SLR-test). 168

Figure 8.8: Comparison of the sensitivity of the power of the trend identification tests (MK, SPR and SLR tests) with the increase in sample variance under two trend forms for trend slope of 1% (panel a: for TF-1 and panel b: for TF-2). 169

Figure 9.1: Graphical presentation of two different trend forms (1% upward trend slope). The no-trend sample was drawn from GEV distribution with location, scale and shape parameters of 0.773, 0.318 and -0.121 respectively (mean =1.0, L-CV=0.25 & L-Skewness=0.25) 177

Figure 9.2: Changes in regional average mean with increase in upward trend slopes for all trend forms and true distribution types (left graphs are for TF-1 & right graphs are for TF-2). Samples were generated from GEV (upper graphs) and EV1 (lower graphs) distributions with sample properties presented in Tables 9.2 and 9.3 respectively 194

Figure 9.3: Changes in L-CV (regional average value) for various trend forms and types (left hand graphs – TF-1 & right hand graphs for TF-2). Samples were generated from GEV (upper graphs) and EV1 (lower graphs) distributions with population sample properties presented in Table 9.2 and 9.3 respectively 195

Figure 9.4: L-moment ratios for all sites in the region for different trend scenarios and forms (left hand graphs are for TF-1 and right hand graphs are for TF-2); Samples were generated from GEV distribution with population sample properties presented in Table 9.2. 197

Figure 9.5: L-moment ratios for all sites in the region for different trend scenarios and forms (left graphs are for trend form-1 and right graphs are for TF-2); Samples were generated from EV1 distribution with population sample properties presented in Table 9.3..... 198

Figure 9.6: Changes in L-Skewness (regional average value) for various trend forms and types (left graphs are for TF-1 & right graphs are for TF-2). Samples were generated from GEV (upper graphs) and EV1 (lower graphs) distributions with population sample properties presented in Table 9.2 and 9.3 respectively 199

Figure 9.7: Comparison of the regional average mean, L-CV & L-Skewness for SUT scenario for various trend slopes; Samples were generated from GEV (left hand graphs) and EV1 (right

hand graphs) distributions with population sample properties presented in Table 9.2 and 9.3 respectively.....203

Figure 9.8: Changes in the GEV location parameter for various trend scenarios and forms (left hand graph is for TF-1 & right hand graph is for TF-2). Samples were generated from GEV distribution with population sample properties presented in Table 9.2.....204

Figure 9.9: Changes in the GEV scale parameter (regional average value) for various trend scenarios and forms (left hand graph is for trend scheme 1 & right hand graph corresponds to trend scheme 2). Samples were generated from GEV distribution with population sample properties presented in Table 9.2.....205

Figure 9.10: Changes in the GEV shape parameter (regional average value) for various trend scenarios and forms (left graph is for TF-1 & right graph corresponds to TF-2). Random samples were generated from GEV distribution with population sample properties presented in Table 9.2.....205

Figure 9.11: Relationship between L-Skewness & GEV shape parameter206

Figure 9.12: Changes in the EV1 location parameter (regional average value) for various trend scenarios and forms (the left graph is for TF-1 & the right graph correspond to TF-2). Samples were generated from EV1 distribution with population sample properties presented in Table 9.3.207

Figure 9.13: Changes in the EV1 scale parameter (regional average value) for various trend scenarios and forms (the left hand graph is for TF-1 & the right hand graph correspond to TF-2).Samples were generated from EV1 distribution with population sample properties presented in Table 9.3.208

Figure 9.14: Comparison of GEV distribution parameters (regional average values- location, scale and shape parameters) for uniform trend scenario; Samples were generated from GEV distribution with population sample properties presented in Table 2.....209

Figure 9.15: Changes in the shape of GEV pdf with the increase in uniform trend slope.....210

Figure 9.16: Comparison of EV1 distribution parameters (regional average values- location and scale parameters) for SUT scenario; Samples were generated from EV1 distribution with population sample properties presented in Table 9.3.....211

Figure 9.17: Comparison of growth curves for SUT scenario and for different combinations of true and fitted distributions (for example GEV-EV1 mean true distribution GEV and fitted distribution EV1).....213

Figure 9.18: Comparison of relative differences in growth curves for different combinations of true and fitted distributions (left graphs correspond to TF-1 & right graphs are for TF-2).....217

Figure 9.19: Comparison of Site 1 quantiles for different combinations of trend forms and true and fitted distributions (left graphs are for TF-1 & the right graphs correspond to TF-2).221

Figure 9.20: Comparison of Site 8 quantiles for different combinations of trend forms and true and fitted distributions (left graphs are for TF-1 & the right graphs correspond to TF-2).222

Figure 9.21: Comparison of Site 15 quantiles for different combinations of trend forms and true and fitted distributions (left graphs are for TF-1 & the right graphs correspond to TF-2).223

Figure 9.22: At-site quantiles for Site 1 (GEV-GEV) for TF-1.....224

Figure 9.23: Comparison of relative differences in quantile estimates for different combinations of true and fitted distributions (left graphs correspond to TF-1 & right graphs are for TF-2).....226

Figure 9.24: Unrealistic quantile estimates in the case of GEV-GEV distribution combination under TF-1 scenario (SUT).....233

Figure 9.25: Changes in quantile functions for Site 1 estimated by GEV-GEV for different larger at-site record lengths (from top to bottom, 100, 200 and 300 years respectively)236

LIST OF TABLES:

Table 4.1: Data Summary	48
Table 4.2: Summary of Results (one-parameter model)	56
Table 4.3: Summary of Results (two-parameter FDC model)	56
Table 4.4: Catchment characteristics for the selected Validation Sites.....	59
Table 5.1: Comparison between POR and Annual FDCs for River Suir at Clonmel.....	63
Table 5.2: Sensitivity of record lengths to FDC for River Barrow at Portarlinton	65
Table 5.3: Catchment characteristics for hydrometric stations 06013 and 14005	67
Table 5.4: Catchment characteristics for hydrometric stations 06013 and 14005	69
Table 5.5: List of streamgauges and their associated catchment characteristics	72
Table 5.6: Comparison of POR and equivalent short sample length estimates of Q_{95} and Q_{25} for all sites	74
Table 5.7: Estimated regional average relative errors (mean, absolute mean and standard deviation) of short resampled estimates of low-flows with respect to the POR estimates for all sample lengths.....	79
Table 6.1: Possible results of a hypothesis test	96
Table 7.1: Stations with significant trends	108
Table 7.2: River catchments with drainage improvement works	110
Table 7.3: Physical and statistical characteristics of the selected river catchments	113
Table 7.4: Study timeframes (AMF Series)	115
Table 7.5: Number of sites showed significant dependency / non-randomness at 5% significance level.....	123
Table 7.6: Sites showed significant lag-1 autocorrelation (at 5% significance level)	124
Table 7.7: The number of sites with significant non-stationarity (at 5% significance level) identified by the T-test and the Mann-Whitney U-test (change point 1976).....	129

Table 7.8: Sites showing significant non-stationarity at 5% significance level (MW-U test) (Data period: 1955-2008, partitioned at 1976 i.e. 1955-1975 and 1976-2008).....	130
Table 7.9: Sites with significant trends (at 5% significance level) when trend identification tests (MK, SPR and SLR) were applied to the Original AMF Series.....	133
Table 7.10: Sites with significant trends (at 5% significance level) when trend identification tests (MK, SPR and SLR) were applied to the PW AMF Series.	135
Table 7.11: Sites with significant trends (at 5% significance level) when trend identification tests (MK, SPR and SLR) were applied to the TFPW AMF Series.....	136
Table 7.12: Comparison of trend test results (percentage of sites with significant trends at 5% significance level) for the Original, PW and TFPW series as identified by the MK, SPR and SLR tests.	137
Table 7.13: Statistical properties of AMR time series of different durations.....	144
Table 7.14: Number of sites with significant trend (at 5% significance level) in AMR records detected by MK-test.....	145
Table 8.1: Variations in the population mean with trend slopes.....	162
Table 8.2: Variations in the variance with the increase in trend slopes.....	163
Table 8.3: Variations in the power of the trend identification test with the trend slopes.....	164
Table 8.4: Variations in the power of the trend identification test with the trend slopes.....	166
Table 8.5: Variations in the power of the trend identification test with the sample variance (trend slope 1%).....	168
Table 9.1: Selected trend scenarios	178
Table 9.2: True at-site properties, distribution parameters and at-site quantile values for GEV distribution (reproduced from Hosking and Wallis, 1993; the mean of all populations is 1.0)...	193
Table 9.3: True at-site properties, distribution parameters and at-site quantile values for EV1 distribution (Note: L-Skewness plays no role in determining the parameters and quantiles. The mean of all populations is 1.0).....	193
Table 9.4: Comparison of the regional average mean, L-CV & L-Skewness for SUT trend scenario for both GEV and EV1 distributions for various trend slopes; (Samples were generated from GEV and EV1 distributions with population sample properties presented in Tables 9.2 and 9.3 respectively. The mean of all populations is 1.0).....	202
Table 9.5: Comparison of GEV distribution parameters (regional average values- location, scale and shape parameters) for uniform trend scenario; Samples were generated from GEV distribution with population sample properties presented in Table 9.2.....	209

Table 9.6: Comparison of EV1 distribution parameters (regional average values- location and scale parameters) for uniform trend scenario; Samples were generated from EV1 distribution with population sample properties presented in Table 9.3.211

Table 9.7: Relative differences in growth factors for various combinations for true and fitted distributions under TF-1 scenario.215

Table 9.8: Relative differences in growth factors for various combinations for true and fitted distributions under TF-2 scenario.216

Table 9.9: Relative differences in regional average at-site quantile estimates for various combinations for true and fitted distributions under trend form TF-1.....224

Table 9.10: Relative differences in regional average at-site quantile estimates for various combinations for true and fitted distributions under trend form TF-2.....225

Table 9.11: Regional Average Relative bias, Abs. bias, RMSE and Standard Error of growth curves and quantiles for various trend slopes estimated from various combinations of trend forms and true and fitted distributions.231

Table 9.12: Relative differences in 1000 year return period growth factor for various record lengths in the case GEV-GEV distribution and TF-1.235

Table 9.13: Relative differences in 1000 year return period quantile for various record lengths in the case GEV-GEV distribution and TF-1.....235

LIST OF SYMBOLS AND ABBREVIATIONS:

LIST OF SYMBOLS:

Q_P :	Daily discharge corresponding to ' p ' percentile
$Q(D)$:	Daily discharge corresponding to ' d ' duration
q_{50} :	50 year return period annual minimum discharge
Q_{obs} :	Observed flow
Q_{est} :	Estimated flow
L :	Record length
ℓ :	Sample length:
$Q_{i,l}^j(d)$:	' d ' duration flow for the j^{th} sample of record length ' l ' for site i
$Q_{i,POR}(d)$:	' d ' duration flow for the Period-Of-Record flow-duration curve for site i
$\varepsilon_{i,l}^j(d)$:	Relative error for site i , sample length l and duration ' d '
$\bar{\varepsilon}_{i,l}(d)$:	Mean relative error for site i , sample length l and duration ' d '
$\sigma_{\varepsilon,i,l}(d)$:	Standard deviation of relative error for site i , sample length l and duration ' d '
$\varepsilon_{R,l}(d)$:	Regional average relative error for sample length and l duration ' d '
$\sigma_{\varepsilon,R,l}(d)$:	Regional average standard deviation of relative error for sample length l and duration ' d '
r_k :	Lag k autocorrelation
H_0 :	Null hypothesis
H_1 :	Alternative hypothesis
α :	Significance level
S :	Test statistics
Z :	Standardised 'z' statistic
$Q_{NS}(T)$:	Non-stationary time series
$Q_S(T)$:	Stationary Time Series

$Q(F)$:	Flood frequency curve in terms of 'F' (Non-exceedance probability)
$Q(T)$	Flood frequency curve in terms of 'T' (Return period)
μ :	Index flood
$q(F)$:	Dimensionless growth curve
γ :	Euler's constant
b_r :	Probability weighted moment
l_r :	Sample L-moments
t_r :	Sample L-moment ratios
λ_r :	L-moment ratios
t_r^R :	Regional average L-moment ratio (r=2,3,4..)
$R_i(F)$:	Relative root mean square error for site i
$B_i(F)$:	Relative bias for site i
$B^R(F)$:	Regional average relative bias
$A^R(F)$:	Regional average absolute relative bias
$SE_i(F)$:	Standard error of at-site quantile for site i
$SE^R(R)$:	Regional average standard error

LIST OF ABBREVIATIONS:

ACF:	Autocorrelation Function
AE:	Actual Evapotranspiration
AF:	Annual Flow
AFDC:	Annual Flow – Duration Curve
AMF:	Annual Maximum Flood
AMR:	Annual Maximum Rainfall
AR(1):	Lag-1 Autoregressive Process
AREA:	Catchment Area
BIAS:	Bias
BFI:	Base Flow Index
BS:	Bootstrap

CV:	Coefficient of Variation
cdf;	Cumulative distribution function
DRAIN D:	Drainage Density
DWF:	Dry Weather Flow
EDA:	Exploratory Data Analysis
ENSO:	EL-Nino Southern Oscillation
EPA:	Environmental Protection Agency
ESB:	Electricity Supply Board
EV1:	Extreme Value Type 1 Distribution
EV2:	Extreme Value Type 2 Distribution
FDC:	Flow – Duration Curve
FEH:	Flood Estimation Handbook
FSU:	Flood Studies Update
GEV:	General Extreme Value Distribution
GIS:	Geographical Information System
HOST:	Hydrology of Soil Types
IID:	Independent and Identically Distributed
IPCC:	International Panel on Climate Change
LAKE:	Lake Index
LFSR:	Low Flow Studies Report
LN2:	Two-parameter Lognormal Distribution
LN3:	Three-parameter Lognormal Distribution
LR:	Linear Regression
MAVF:	Moving Average Flow
MDF:	Mean Daily Flow
MF:	Mean Flow
MK:	Mann-Kendall
MS:	MicroSoft
MSE:	Mean Square Error
MW-U:	Mann Whitney U test

NAO:	North Atlantic Oscillation
NAR:	Net Annual Rainfall
NERC:	Natural Environmet Research Council
OPW:	Office of Public Works
pdf:	Probability Density Function
PDO:	Pacific Decadal Oscillation
PE:	Potential Evapotranspiration
POR:	Period-of-Record
POT:	Peaks – Over -Threshold
PW:	Pre-Whitening
RBD:	River Basin District
RD:	Rank Difference
RMSE:	Root Mean Square Error
ROI:	Region of Influence
RT:	Random Trend
SAAR:	Standard Period Average Annual Rainfall
SLF:	Sustained Low Flows
SLR:	Standardised Linear Regression
SMD:	Soil Moisture Deficit
SPR:	Spearman’s Rho
STRMFRQ:	Stream Frequency
SUT:	Spatially Uniform Trend
SVT:	Spatially Varying Trend
TF:	Trend Free
TFPW:	Trend Free Pre-Whitening
TP:	Turning Points
WFD:	Water Framework Directive
WMO:	World Meteorological Organisation
WRD:	Water Resources Department

1 INTRODUCTION

1.1 GENERAL BACKGROUND AND OBJECTIVE OF THE STUDY

This thesis focuses on the estimation of low and high flows for Irish River catchments, particularly for the ungauged catchments and in the context of changing climatic condition, which is believed may be causing non-stationarity in the stream flow time series.

Reliable estimation of low-flows for any river catchment is vital for proper planning and design of water related projects, so as to assess the waste-load assimilative capacity, to estimate water availability for water supply, power generation, irrigation and for recreation and wildlife conservation purposes. Due to the lack of adequate resources, all streams in the country cannot be gauged. Furthermore, estimation of design low-flows from short periods of records is challenging. It is therefore, essential to estimate low-flows for ungauged stream catchments. The present study focuses on these areas of low-flow estimations for the Irish River catchments.

In statistical flood frequency analysis, the key assumptions are that all observations in a data series are independent and identically distributed (stationary). If the assumption of stationarity is not met, then the current procedures for the estimation of a design flood based on statistical theory would not be applicable anymore. The application of the existing statistical procedure on such non-stationary data would result in under- and/or over-estimation of a design flood quantile. The violations to these assumptions could occur due to changes in stream flows caused either directly by human activities such as urbanisation, reservoir construction, drainage systems, water abstraction and land-use changes (agricultural practices, afforestation / deforestation) or by natural catchment changes (e.g. natural changes in channel morphology, volcanic eruption), long-term climate change and climate variability caused by the atmospheric circulations (ENSO, PDO and NAO phenomena) and also from problems linked to data such as instrumental error, change in measurement techniques, etc. Changes in a stream flow time series can occur in two main ways: e.g. gradually (a trend) or abruptly (a step change). It may affect the mean, median, variance, autocorrelation or other aspects of the data.

Climate change scenarios have shown that the hydro-meteorological regimes will likely be modified significantly over the next 50–100 years (Intergovernmental Panel on Climate Change (IPCC), 2001, 2007). As a result, the frequency of occurrence and magnitude of extreme values may be impacted. Thus, the conventional extreme value analysis, as presented in “Theory of extreme values”, needs to be modified to accommodate these phenomena. This could be accomplished by incorporating the changes that had occurred during the past observation period directly into the frequency analysis techniques in order to extrapolate them into the future. It is possible that the changes that had occurred in the past may not be statistically significant but the time-trends of these changes may be required to formulate future climate change scenarios. In the presence of significant time trends, the assumption of ‘independence’ of extremes may still be valid, but the assumption of ‘identical distribution’ may not be. It is also possible that the statistical characteristics of extreme values change in relation to well established low frequency climate modes (ENSO, PDO and NAO phenomena).

Estimation of design flood flow under the non-stationary hypothesis is very complex. Frequency analysis of a non-stationary time series requires a different approach than the conventional stationary one because the distribution parameters and the distribution itself change in time and so do the estimates of exceedance probability and associated uncertainty of a design value of interest. Thus, any evidence of departure from basic assumptions of independence and stationarity of observations could significantly affect the validity of frequency analysis results (see, for example, Porporato and Riodolfi, 1998; Cox et al., 2002; Cunderlik and Burn, 2003). Therefore, alternate approaches that incorporate the effects of non-independence and non-stationarity should be used and further developed and the assumption of ‘independent and identically distributed (iid)’ data values should be considered only as a first approximation.

Non-stationary frequency analysis is a relatively new modelling approach and the number of published studies is rather small but is continuously increasing (Strupczewski et al., 2001; Strupczewski and Kaczmarek, 2001; Cunderlik and Burn, 2003; Khaliq et al., 2006). A number of approaches were proposed for frequency analysis of dependent observations (Strupczewski et al., 2001; Strupczewski and

Kaczmarek, 2001; Adlouni et al., 2007). However, most of these approaches were based on site-specific limited length records.

Further, the information extracted from limited length records of a small number of sites may not be representative of the regional behaviour and could lead to misdiagnosis (Jain and Lall, 2000; IPCC, 2001). Therefore, it is important to establish the significance of non-stationarity in the regional context, preferably using long observational records where available, using a suitable regional approach (e.g., see Burn and Hag Elnur, 2002 for such an approach). Satisfactory detection of consistent regional changes (increases/decreases) in the statistics of extremes, as compared to just site-specific ones, could be more interesting and useful for decision-making to revise design methodology or to plan adaptability to climate change.

Until now no such acceptable and/or reliable procedure has been developed and/or adopted to deal with these non-stationary properties of data series. Furthermore, only a small numbers of studies so far have explored the effects of non-stationarity in the data series on the design flow estimates using the conventional flood frequency analysis techniques (Cox et al., 2002; Cunderlik and Burn, 2003, Khaliq et al., 2006). The present study therefore focused on determining the effects of non-stationarity/trend on quantile estimates, particularly on the regional growth curves, at various degrees of trend conditions. It is considered that the non-stationarity in the Annual Maximum Flood (AMF) series would have resulted mainly from climate change impact on a regional basis. This trend effect assessment has therefore been focused on a regional scale basis rather than on a single site basis. The findings of this study will help hydrologists to make an allowance in the estimated design flood based on the current statistical procedure.

The main objectives of the study were (i) to develop a methodology to estimate low-flows for ungauged river catchments in Ireland, (ii) to investigate any evidence of the presence of trends in the AMF flows and (iii) to investigate the effect of trends on the design flood estimates obtained from the conventional statistical frequency techniques on a regional scale.

1.2 SCOPE OF THE STUDY

The scope of this thesis includes:

- An extensive literature review on the selected research topics,
- Low-flow estimation for ungauged catchments including:
 - Development of a Flow-Duration Curve (FDC) based low-flow estimation method for the prediction of low-flows for ungauged Irish River Catchments,
 - Examination of the limitations of the period-of-record FDC based low-flow estimations , and
 - Investigation of the sensitivity of the record lengths on the low-flow estimates.
- Study on non-stationarity in flood flows and its effect on flood frequency growth curves including:
 - Detection of non-stationarity / trends in the Irish Annual Maximum Flood Series by using various trend detection methods (parametric and non-parametric tests),
 - Investigation of the power of various trend detection tests, and
 - Investigation of the effect of non-stationarity in the Annual Maximum Flood Series on the regional growth curves and at-site quantile estimates.

1.3 OUTLINE OF THE THESIS

This thesis contains 10 chapters including the present chapter.

Based on the two different stream flow regimes – low and high flows, the thesis has been divided into two parts: Part A and Part B. Part A includes all research carried out on low-flow estimations, while Part B covers all research carried out on the high flow estimations.

Part-A: Low-Flow Estimation for Ungauged Catchments, and

Part B: Non-Stationarity in Flood Flows and Its Effect on Flood Frequency Growth Curves for Irish River Catchments

Chapter 2 reviews the current literature and research on each of the chosen study areas as mentioned in Section 1.2.

The core studies carried out under Part A are presented in Chapters 3, 4 and 5. Chapter 3 describes the catchment physical processes for generating low-flows, a brief review of various low-flow indices and low-estimation methods currently in practice for the ungauged catchments. Chapter 4 presents a Flow Duration Curve (FDC) based methodology for estimating low-flow estimation and prediction for the ungauged River catchments in Ireland. Chapter 5 identifies limitations of the low-flow estimates from the long-term observed mean daily flows, carries out an analysis to investigate the sensitivity of the record lengths on the low-flow estimates and recommends a procedure for estimating long-term equivalent low-flow estimates from a short period of records for Irish River catchments.

The details of the studies carried out on high-flows and the associated findings are presented in Chapters 6, 7, 8 and 9. Chapter 6 explores various methods available for detecting non-stationarity in flood flow time series. Chapter 7 investigates the presence, if any, of non-stationarity / trends in the Irish Annual Maximum Flood Series. Chapter 8 examines the power of a number of selected trend test methods. Chapter 9 investigates the effects of non-stationarity / trends in annual maximum flood series on the estimation of regional growth curves and at-site quantiles.

Chapter 10 outlines the conclusions from the overall study and makes recommendations for further research.

2 LITERATURE REVIEW

2.1 INTRODUCTION

This Chapter explores the existing published literature on the chosen topics of the present study. The previous research in the areas of low-flow estimations for ungauged catchments, trend detection in the flood flow records and the effect of trend on the design flood flow estimates are discussed in the following sections.

2.2 PART A - LOW-FLOW ESTIMATION FOR UNGAUGED CATCHMENT

The scarcity of streamflow data is a common problem in many countries in the world. This condition, along with the worldwide pursuit of the optimal estimation and management of water resources, led to the formulation and proposal of numerous procedures for estimation of low-flows at ungauged river basins or at streamgauges with limited flow records.

The development of regionalized hydrological models for estimating low-flow characteristics for the ungauged catchments has been the subject of international research since the 1970s. Historically these models have been based on multivariate statistical models that relate flow statistics to the physical and climatic characteristics of a catchment.

Smakhtin (2001) provides an extensive review of low-flow hydrology, including the estimation of low-flows at ungauged sites. According to Smakhtin (2001), possible approaches for low estimation in ungauged catchments may be arbitrarily categorised as (i) those which aim at the prediction of either specific low-flow indices (e.g. Q_{95}) or composite low-flow measure (e.g. FDC) using techniques of hydrological regionalisation and (ii) those which allow any low-flow characteristics to be estimated from synthetic flow time series. The latter case implies the application of simulation methods which aim at the generation of a continuous flow time series (at an ungauged site or multiple sites in a river catchment), which may subsequently become subject to low-flow analyses. The regional regression approach is perhaps the most widely used technique in low-flow estimation at ungauged sites. It normally includes several successive steps such as (i) selection of low-flow characteristics for a regression model, (ii) delineation of hydrologically homogeneous regions, and (iii) construction of the regression model. Technically, the regression model is

constructed by means of multiple regression analysis. The 'best' regression model is commonly estimated using a stepwise regression approach where the model is developed one step–one independent variable – at a time. The procedure is described in many textbooks (e.g. Yevjevich, 1972; Haan, 1977; Walpole and Myers, 1978; Holden, 1985; Gordon et al., 1992).

Castellarin et al. (2004) classified all approaches to regionalisation of FDCs into three broad categories: statistical, parametric and graphical (non-parametric) approaches. The procedures belonging to the first category view the FDC as the complement of a cumulative frequency distribution and use stochastic models to present FDCs. The procedures include: (i) selection of a suitable frequency distribution as the parent distribution for the study region, (ii) estimation of distribution parameters on a local basis for the gauged river basins located in the study region using the streamflow observations; (iii) development of regional regression models for predicting the distribution parameters at ungauged basins on the basis of the geo-morphological and climatic characteristics of the basins. Examples of application of such approaches can be found in Fennessey and Vogel (1990), LeBoutillier and Waylen (1993), Singh et al. (2001). The second category (parametric) includes all procedures whose basic idea is the representation of the FDCs by analytical relationships. The parameters of the relationships for ungauged river basins are then estimated through regional models, similarly to the parameters of the parent distribution for the statistical approaches. Examples of application of such approaches can be found in Quimpo et al., (1983), Mimikou and Kaemaki (1985), Franchini and Suppo (1996), and Yu et al. (2002). The third category (graphical) comprises regional procedures that use standardised graphical representations of FDCs with a regional validity instead of analytical relationships. As opposed to the estimation of a single low-flow characteristic for which a regression model has been constructed, the regional prediction curve approach allows the range of low-flow indices of a similar type to be estimated. The graphical approach requires the following major steps: (i) standardise the FDCs for all gauged river basins by dividing the empirical FDCs by an index streamflow (e.g. long-term mean daily flow), (ii) a graphical regional dimensionless FDC is obtained by averaging the standardised empirical FDCs of all gauged river basins in the study region. The FDC for any ungauged river basin located within the study area can then be estimated as the product of the dimensionless regional FDC and an

estimate of the index streamflow. An example of application of such an approach can be found in Smakhtin et al. (1997).

The regionalisation of streamflow characteristics in general is based on the premise that catchments with similar climate, geology, topography, vegetation and soils would normally have similar streamflow responses. A number of studies investigated the relationships between the catchment geology and recession characteristics and/or baseflow index (BFI). BFI is a non-dimensional ratio which is defined as the volume of baseflow divided by the volume of total streamflow. Browne (1981) attempted to represent catchment storage by means of recession characteristics. In the UK Low-Flow Studies Report (Institute of Hydrology, 1980), BFI was found to be a key variable in the estimation procedures. Tjomsland et al. (1978), Pereira and Keller (1982) and Demuth (1989) illustrated relationships of baseflow and recession constants with catchment morphology and climatic characteristics. Bingham (1986) illustrated the significance of geology and drainage area in estimating low-flow recession rate. Ando et al. (1986) derived regional values of recession constants in Japan. Zecharias and Brutsaert (1988) examined regional distribution of recession parameters. The use of baseflow index in regional studies has been illustrated by: Hutchinson (1993) in New Zealand; Pilon and Condie (1986) in Canada; Green (1986) in Fiji; Meigh (1987) in Zimbabwe; and Lacey and Grayson (1998) in Australia. The delineation of regions may be accomplished using convenient boundaries based on geographic, administrative or physiographic considerations. An extensive review on selection of regions is given in Gustard et al. (1992), Robson and Wood (1999), Smakhtin (2001), Gustard et al. (2009) and Vogel et al. (1991).

A large number of regional models for low-flow estimation at ungauged sites have been developed in different parts of the world in the last several decades and the list of such studies will hardly ever be complete. The examples which concentrate predominantly on regression models for low-flows of different frequency of occurrence include: Balco (1976, 1977) in Slovakia; Leith (1978) , Pol (1985), Hamilton (1985) , Pelletier et al. (1986) and Cumming Cockburn Ltd (1990) in Canada; Chang and Boyer (1997), Downer (1981), Armentrout and Wilson (1987), Barnes (1986), Tasker (1989), Risle (1984), Ries (1994), Ludwig and Tasker (1993), Cervione et al. (1993), Hayes (1992) and Dingman and Lawlor (1995) in USA; Mimikou (1984) in Greece; Lundquist and Krokli (1985) in Norway; Institute of Hydrology (1987) in Scotland; Prit and Simpson (1983) and Gustard et al. (1992) in

UK; Demuth (1994) in Germany; FRENDA (1994) in Western Europe; Kobold and Brilly (1994) and Brilly et al., (1997) in Slovenia; Castellarin et al. (2004) in Italy; and Laaha and Blöschl (2004b) in Austria. Gustard et al., (1997) reported the results of European study of Q_{90} . Regional FDCs have been constructed in several states in USA (Singh, 1971; Dingman, (1978), Quimpo et al. (1983) in Philippines, Mimikou and Kaemaki (1985) in Greece, Wilcock and Hanna (1987) in Northern Ireland.

Regional studies of spell characteristics, often referred to as annual or seasonal droughts, have been carried out by Kachroo (1992), Clausen and Pearson (1995), Tallaksen and Hisdal (1997), Tallaksen et al. (1997) and Stahl and Demuth (1999). Midgley et al. (1994) constructed regional deficient flow-duration frequency curves and storage-yield curves for about 80 hydrologically homogeneous zones in South Africa.

The examples of regional statistical FDC models include: Beard (1943), Fennessey and Vogel (1990), LeBoutillier and Waylen (1993), Claps and Fiorentino (1997), Singh et al. (2001), Croker et al. (2003), and Castellarin et al. (2004).

The examples of regional averaged non-parametric FDC models include: FRENDA (1989), Furness (1959); Gustard et al. (1992), Smakhtin et al. (1997), Studley (2001), Holmes et al.(2002) and Ganora et al. (2009).

A brief description of some of the models under the each of the above mentioned categories (statistical, parametric and non-parametric) are presented below:

2.2.1 Statistical Approaches

Fennessey and Vogel (1990) proposed a regional hydrological model for estimating FDCs of daily streamflows at ungauged river basins in Massachusetts in the USA. They approximated the lower half of the daily FDCs using a two-parameter lognormal probability density function. Using the hydrometric and geomorphoclimatic information available for the 23 gauged river basins, the authors identified through multivariate regression analyses, two regional models to estimate the distribution parameters μ and σ at ungauged basins of the study region.

LeBoutillier and Waylen (1993) proposed a stochastic approach for regionalisation of the mean Annual Flow–duration Curve (AFDC) of daily streamflows for the entire Province of British Columbia, Canada. The authors employed the five-parameter mixed lognormal distribution as the parent distribution and utilised cluster analysis to identify groupings of basins having similar streamflow regimes.

Claps and Fiorentino (1997) presented a statistical approach to the regionalisation of AFDCs. The authors considered 14 river basins located in southern Italy and, for each basin, fitted a two parameter lognormal distribution to each empirical annual FDC. The authors developed catchment characteristics based regional models to estimate the parameters of the normal distributions for ungauged sites.

Singh et al. (2001) presented a statistical regional model for the estimation of FDCs for ungauged river basins in the Himalayan region. The authors adopted the normal frequency distribution to represent the standardised and normalised 10-day streamflow series observed in the study region. The standardisation of each series was performed by dividing the observations by the mean annual flow of the corresponding streamgauge, while the normalisation was obtained through a power transformation of the data (Box and Cox, 1964). The estimation of the mean annual flow was performed for ungauged sites through a regional model as a function of the basin area.

Discontinuities in the flow regime of ephemeral rivers make the modeling of FDCs challenging (Croker et al., 2003). An approach based on the theory of total probability was proposed by Croker et al. (2003) to derive daily FDCs for both perennial and ephemeral rivers in Portugal. This approach included a model to predict the percentage of time the river is dry and a model to predict a FDC for the nonzero flow period, with flows normalized by the mean daily flow of nonzero flows. The regional FDC approach presented by Croker et al. (2003) has three components. First, determination of the probability of zero flows occurring (p_{dry}) and derivation of threshold exceedance probability ($1 - p_{dry}$) above which flows are nonzero (p_{nz}). The second component involved a procedure to estimate a FDC for nonzero flows (FDC_{nz}). As p_{dry} and FDC_{nz} were each scaled from zero to one in the

first two steps, finally it was required to combine and rescale the derived distributions over a common probability interval [0,1]. The authors applied the theory of total probability so that:

$$p(i)_t = p(i)p_{nz} \quad (2.1)$$

where $p(i)_t$ is the transformed exceedance probability over the interval [0,1] and $p(i)_{nz}$ is the exceedance probability of a specific nonzero flow (i). The authors developed a regional regression model to estimate p_{dry} in ungauged watersheds from mean annual rainfall.

Castellarin et al. (2004) proposed a stochastic index flow model of flow duration curves. It is a stochastic model of daily streamflow that features the unique characteristic of analytically relating AFDC to Period-of-record (POR) FDC. The fundamental assumption of the index-flow model is that the daily streamflow X is the product of two random variables, an index-flow equal to the annual flow, AF , and a dimensionless daily streamflow X' ,

$$X=AF \cdot X'. \quad (2.2)$$

The random variable AF models the alternation of dry and wet years and it is mainly controlled by annual precipitation. The hydrologic behaviour of the river basin was summarised by the pdf of the standardised daily streamflow X' , $f_{X'}$, which is mainly controlled by climate, size and permeability of the basin. The implementation of the model showed that the four-parameter kappa distribution can be effectively adopted for representing the frequency regime of daily streamflows in 18 unregulated river basins in Italy. The distribution's parameters were estimated from geo-morphological and climatic indexes of the catchment by using multiregression relationship, which were identified through stepwise regression analysis. The results of the study indicate that the regional index-flow model is as reliable as, or more reliable than, the traditional regional models for estimating long-term flow-duration curves.

2.2.2 Parametric Approaches

Quimpo et al. (1983) proposed a regional parametric approach for estimating FDCs at ungauged potential small hydropower sites in the Philippines. The authors suggested the following two-parameter exponential equation to represent FDCs of daily streamflows:

$$Q(d) = Q_A \exp(-cD) \quad (2.3)$$

where $Q(d)$ indicates the daily streamflow associated with duration d , and Q_A and c are the parameters of the equation. In order to evaluate FDCs at ungauged sites, the authors identified a regional model that estimates Q_A as a function of the drainage area and provided a contour map representation of c for the whole archipelago of the Philippines.

Mimikou and Kaemaki (1985) performed a study analogous to the study by Quimpo et al. (1983). The authors considered several analytical equations to represent the monthly FDCs observed in north-western Greece, and suggested to use a third order polynomial equation to estimate $Q(d)$ as

$$Q(d) = a - bd + cd^2 - d'd^3 \quad (2.4)$$

where the parameters a , b , c and d' have to be non-negative. In order to estimate the FDCs at ungauged locations the authors proposed four regional regression models expressing the equation parameters as functions of the mean annual precipitation, the drainage area, the hypsometric fall and the length of the main river course.

Franchini and Suppo (1996) proposed a different parametric approach for estimating daily FDCs in a wide region of southern-central Italy. The authors described the lower portion of the FDC's of daily streamflows (i.e. $d \geq 0.3$) by adopting the following three-parameter analytical equation:

$$Q(d) = c + a(1.0 - d)^b \quad (2.5)$$

where the parameters a , b and c are all greater than zero. Parameter b is associated with physical characteristics of the basin (e.g., imperviousness, size, etc.) and controls the concavity of the FDC (i.e., downward concavity for when $b \in [0,1]$, upward concavity if $b \in [1,+\infty]$). The estimation of the equation parameters was performed by forcing the above equation to honour three points identified by three different durations and the corresponding values of daily streamflow, $[d_i, Q(d_i)]$, with $i \in [1,2,3]$. The authors presented three regional regression models to estimate the values of $Q(d)$, with $i \in [1,2,3]$, as functions of relevant geomorphoclimatic characteristics.

Yu et al. (2002) analysed 15 river basins in Taiwan and identified regional models to estimate the daily discharge Q_p , corresponding to the percentiles $p=10,20,\dots, 90\%$, as functions of several geomorphoclimatic indexes. The regional models of Q_p 's were then used to construct the FDCs at ungauged sites. The authors assessed the reliability of the proposed approach at all 15 sites and determined the confidence intervals for estimated FDCs by using a bootstrap cross-validation.

Wilcock and Hanna (1987) applied the method of synthesizing FDCs outlined in the UK Institute of Hydrology's 1980 Low Flow Studies Report (LFSR) for derivation of FDCs in Northern Ireland. Using the BFI derived from flow records at fourteen gauging stations, the method works well, and there is no systematic tendency to over- or underestimate Q_{95} . High flows, however, do tend to be underestimated. In the absence of BFI maps, an alternative method of synthesizing FDCs from catchment characteristics was considered. The two methods of FDC synthesis were tested on independent data, the LFSR method performed slightly better than the catchment equations at Q_{95} flows, but less well at flows above Q_{90} .

2.2.3 Graphical (Non-parametric) Approaches

Smakhtin et al. (1997) proposed a regional average FDC model for estimating FDC for an ungauged catchment in South Africa. The ordinates of all individual curves constructed on the basis of gauged data in a hydrologically homogeneous region were normalized by the mean daily flow and an average regional non-dimensional FDC was calculated. The actual FDC at an ungauged site may be calculated by

multiplying the nondimensional ordinates of a corresponding regional FDC by the estimate of the mean flow. Regional FDCs may be established for the year, season or for each calendar month.

Holmes et al. (2002) proposed a region of influence (ROI) approach (Burn, 1990a,b, Robson and Reed, 1999) to estimate FDCs at ungauged sites in UK. In this approach, a region of hydrogeologically similar catchments was developed using soils data as a surrogate for hydrogeological data. A catchment was assessed by calculating a weighted Euclidean distance in the Hydrology of Soil Types (HOST) space, between the target catchment and every other catchment within a large data pool of natural gauged catchments. A 'region' is formed around a target catchment by ranking all of the catchments in the data pool by their weighted Euclidean distance in the Hydrology of Soil Types (HOST) space and selecting a set of catchments from the pool that are 'closest' to that target catchment. An estimate of Q_{95} (95%ile flow) for the target catchment was calculated from a weighted average of the observed Q_{95} values for the selected catchments in the region, where the weight is based on the reciprocal of the Euclidean distance measure. When tested over a large set of UK catchments, the performance of the new ROI model was superior to that of the Report 108 model (Gustard et al.1992) as implemented operationally within the Micro LOW FLOWS software package (Young et al. 2000) or applied manually using maps.

Ganora et al. (2009) proposed a new distance-based non-parametric regionalization model for the estimation of dimensionless FDCs (normalised by an index flow – mean annual runoff) in sites with no or limited available data in Italy. The regional approach considers the (dis)similarity between all possible pairs of curves and uses distance measures that can be related to basin descriptors and climatic parameters. The (dis)similarity between curves was computed using a predefined metric based distance matrix. This matrix was then related, by means of linear regression models, to analogous matrices composed of the difference between all possible values of each descriptor within the set of basins. After identification of significant descriptors, a cluster analysis was applied so that the basins can be grouped together. The curves of all basins belonging to the selected cluster were used to build the regional curve. This latter curve was simply estimated point by point as the average of the values of 'q (standardised flow)' relative to each duration for the curves belonging to the selected region. Each region was characterized by a single dimensionless flow

duration curve. The procedure was applied to 95 basins located in north-western Italy and Switzerland. In most of the cases, the distance-based model produces better estimated of the flow duration curves using only a few catchment descriptors.

2.2.4 Estimation of Low-Flows from Short Records Lengths

If the river-flow records within a catchment of interest are short or incomplete, it is always strongly recommend that these should be used to improve the estimates generated using a regional regression model. The primary limitation of short-record data is that the data are unlikely to capture the long-term natural variability of the catchment under investigation. In other words, due to climatic variability and other sources of variability that occur over short time scales, low-flow characteristics estimated from a few years of stream flow data deviate from the long-term average. Because of this, it is usually recommended to use stream flow records of 20 years or more for low-flow estimation (Tallaksen and Van Lanen, 2004). However, in many countries, for a significant part of the gauged catchments, the records are shorter than this recommended period.

A number of methods exist for inferring the long-term low flow characteristics from short records. These methods all adjust low-flow characteristics to longer-term climatic conditions, in some way, and are therefore referred to as climate adjustment methods (Laaha and Blöschl, 2005). They are used to estimate the low-flow characteristics for the site of interest (subject sites) where a short stream flow record is available, based on stream flow data from other catchments (donor sites) where long records are available. The climate adjustment is usually limited to random effects (e.g. random climate variability and measurement errors) and cyclic effects (e.g. climatic variation), while systematic effects such as trends caused by climatic change or changes of catchment response characteristics as a result of human activities are often treated in an explicit way rather than by climate adjustment procedures (e.g. Kundzewicz and Robson, 2000).

Laaha and Blöschl (2005) provided an extensive review of various methods/procedures available for estimating low-flows from short records. According to them the climate adjustment methods consists of three main steps: (a)

selecting donors, (b) calculating adjusted low-flow characteristics at the subject site for each donor by record augmentation techniques, and (c) combining the adjusted values associated with each donor to obtain an estimate of the long-term low flow characteristics at the subject site.

Laaha and Blöschl (2005) examined the relative performance of different climate adjustment techniques for estimating low-flow characteristics (e.g. Q_{95}) from short stream flow records. They examined three donor selection techniques such as (i) using the nearest gauge at the same stream as the subject site, (ii) similarity of physiographic catchment characteristics, and (iii) the Robson and Wood (1999) proposed correlation based procedure. Two record augmentation methods were used: (i) adjusting the low-flow characteristic at the subject site by scaling it by the ratio of Q_{95} calculated from the entire observations period and Q_{95} calculated from the overlap period (e.g. Kroiß et al., 1996) and (ii) the second method uses the same principle, but includes a weighting coefficient to account for the strength of correlation between subject site and donors. The authors suggested that, on average over the study region, 1-year of continuous stream flow data clearly outperforms the more sophisticated regionalisation method. The downstream donor selection method performs best on all scores. The relative performance of the record augmentation methods depends on the donor selection method but, overall, the choice of record augmentation method is less important than the choice of the donor site. The value of the climate adjustment methods is very significant for record lengths shorter than 5 years.

An alternative approach to developing relationships between short- and long-record time series of flows was developed by Hughes and Smakhtin (1996) and is called “spatial interpolation using FDCs”. This approach is used for “patching” or extending the time series of daily flow data using FDCs, which can also be used for generating time series of flow data at ungauged sites if combined with a regional statistical model for estimating the FDC. The approach is based on the assumption that hydrographs from rivers in a broadly climatically homogeneous region will have similar patterns of rises and falls.

Castellarin et al. (2004) carried out a study to identify the minimum record length for which empirical FDCs reproduce long-term (i.e. period-of record) FDCs more

accurately than the best performing regional models. In doing this, they carried out a series of resampling experiments to assess the sensitivity of empirical FDC's to sample lengths. The analysis considered 14 river basins of eastern-central Italy with at least 25 years of daily streamflows. The analysis showed that five years of observed streamflows are sufficient to obtain rather consistent estimates of the long-term FDC, and these estimates are generally more reliable than the estimates produced by the regional models.

2.3 PART B – NON-STATIONARITY IN FLOOD FLOWS

2.3.1 Detection of Trend in Flood Series

As a result of increase in global average surface temperature (IPCC, 1996, 2001 and 2007) changes in climate parameters such as precipitation and evapotranspiration could have occurred and which in turn could have impacted streamflows. These potential impacts of climate change and variability have received a great deal of attention from researchers in a variety of fields. A comprehensive review of the potential impacts of climate change is provided in IPCC (1996, 2007). A range of potential impacts on the hydrologic regime for various geographic areas has been hypothesized in the report. The report indicates that climate change is likely to increase runoff in higher latitude regions because of increased precipitation. Changes in flood frequencies are expected in some locations, particularly in northern latitudes and in catchments experiencing snowmelt-flooding events. The frequency and severity of drought could increase as a result of changes in both precipitation and evapotranspiration. Changes in the hydrologic regime that do occur are not expected to be equally distributed throughout the year. For example, increased temperatures in the winter are expected to lead to earlier snowmelt events and a shift in runoff from the spring to late winter with a corresponding decrease in runoff in the summer period.

Numerous studies have been undertaken in different regions of the world to investigate if changes in the form of trends exist in the time series of hydrological variables. Examples of such country, regional and worldwide scale studies are: Chew and McMahon (1993) in Australia; Lettenmaier et al. (1994), Lins and Slack (1999), Douglas et al. (2000) in USA; Burn (1994a), Westmacott and Burn (1997), Yulianti and Burn (1997), Whitefield and Cannon (2000), Mortsch et al. (2000),

Zhang et al. (2001), Ouarda et al. (1999), Cunderlik and Burn (2002) in Canada; Robson and Reed (1999), Hannaford and Marsh (2006) and Dixon et al. (2006) in the UK; Petrow and Merz (2009), Bronstert (2003), Caspary (2000) and Mudelsee et al. (2003) in Germany; Nobilis and Lorenz (1997) in Austria, Lindstrom and Bergstrom (2004) in Sweden; Xiong and Shenglian (2004) and Yang et al. (2005) in China; Xu et al. (2003) in Japan; Kiely (1999) and Kiely et al. (1998) in Ireland; Rood et al. (2005) in North America, Kundzewicz et al. (2005), Svensson et al. (2005) in Europe and Kundzewicz et al. (2004) and Milly et al. (2002) on a worldwide scale.

In the above studies, both parametric and non-parametric techniques were used. Interestingly, the nonparametric methods have been the favoured choice of most of the studies. The parametric methods involve distributional assumptions about the data being analysed and the form of the trend component as compared to the nonparametric methods (e.g. the Mann-Kendal trend test; Mann, 1945 and Kendall, 1975). For the application of nonparametric methods, no assumptions on parent distribution are necessary for the underlying hydrological regime and that may be the reason behind their popularity. The main reason for using non-parametric statistical tests is that they are thought to be more suitable for non-normally distributed data and for censored data, which are frequently encountered in hydro-meteorological time series.

Kundzewicz and Robson (2004) provide general guidance of the methodology of change detection in time series of hydrological records, giving an overview of preparation of a suitable data set, exploratory analysis, and application of adequate statistical tests and interpretation of results. Yue and Pilon (2004) offer guidance as to the selection of a test (from slope-based, rank-based, parametric, non-parametric and bootstrap-based approaches) for non-normally distributed data – by comparison of test power. Sensitivity of the power tests to the shape of the trend (linear vs nonlinear) has also been examined. A critical review of the parametric approaches can be found in Khaliq et al. (2006). Yue et al. (2002) and Khaliq et al. (2009) provide reviews of various non-parametric approaches.

The most commonly used rank-based non-parametric tests for detecting monotonic trends are the Mann-Kendall (Mann, 1945; Kendall, 1975), the Spearman rank correlation (Lehmann, 1975; Sneyers, 1990) tests and the Normal scores linear

regression (Robson and Reed, 1996), while the most commonly used parametric test for detecting monotonic trend is the least squares linear regression test (Haan, 1977). The other commonly used nonparametric tests for detecting step change in hydrological time series are Mann – Whitney test (Siegel and Castellan, 1988; Helsel and Hirsch, 1992), Distribution-free CUSUM test (Chew and McMahon, 1993; McGilchrist and Woodyer, 1975), the Kruskal – Wallis test (Sneyers, 1975), while the relevant parametric test is the Student t-test. Furthermore, tests are available to test the independence (randomness) in time series such as Kendall’s turning point test (Kendall and Stuart, 1976; Srikanthan and McMahon, 1983), Rank Difference test (Meacham test) (Srikanthan and McMahon, 1983) and Autocorrelation tests (Jenkins and Watts, 1968).

From the non-parametric methods, the rank-based non-parametric Mann-Kendall test (MK test) is widely used as compared to the Spearman rank correlation test (SPR test), though the power of these two tests to identify trends is comparable (e.g. Yue et al., 2002a). Previous reviews and guidelines on the use of non-parametric tests and their bootstrap counterparts may be seen in the work of Kundzewicz and Robson (2000, 2004).

The majority of the studies regarding trend analysis have assumed that recorded streamflow series are serially independent, even though annual mean and annual minimum streamflow may frequently display statistically significant serial correlation. Von Storch (1995) demonstrated that the existence of positive serial correlation within a time series increases the possibility that the MK test detects the significance of a trend. This may lead to rejection of the null hypothesis of no trend, while the null hypothesis is actually true.

In order to eliminate the influence of serial correlation on the MK test, Kulkarni and Von Storch (1995) and Von Storch (1995) proposed to ‘pre-whiten’ a series prior to applying the MK test. That is, the serial correlation component, such as a lag-one autoregressive process (AR(1)) is removed from a time series and the significance of a trend is then evaluated by using the MK test to the pre-whitened series. This method has been used in many trend detection studies (e.g. Douglas et al., 2000; Zhang et al., 2001; Burn and Hag Elnur, 2002). In the case that no trend exists within a time series, von Storch (1995) demonstrated that pre-whitening can

effectively eliminate the effect of serial correlation on the MK test. Douglas et al. (2000) demonstrated that pre-whitening can reduce the detection rate of the significant trend by the MK test. Yue et al. (2002b) investigated this issue by simulation experiments where both a trend and a lag-one autoregressive process (AR(1)) existed in a time series. Their study indicates that pre-whitening a positive AR(1) process will remove a portion of the trend, leading to an acceptance of the null hypothesis of no trend, while the null hypothesis might be false. They also showed that, when trend does exist in a time series, pre-whitening is not suitable for eliminating the influence of serial correlation on the MK test. Based on these, in order to more effectively reduce the effect of serial correlation on the MK test, a modified pre-whitening procedure, termed 'trend-free pre-whitening' (TFPW), was proposed by Yue et al. (2002b). In this method, the time series is detrended before the lag-1 autocorrelation is removed from the time series, and the trend is added to the serial correlation free time series before a trend test is applied. The detail of this procedure is given in Yue and Pilon (2003) and is described later in Section 7.3.1.4. Petrow and Merz (2009) applied this TFPW method for detecting trends in flood magnitudes in German Rivers.

Similar to the existence of serial correlation in a time series, the presence of positive cross-correlation in a network will inflate the rate of rejecting the null hypothesis of no field significance of trends while it is true (Douglas et al., 2000) where field significance is the collective significance of a group of hypothesis tests (Vogel and Kroll, 1989). Douglas et al. (2000) developed a bootstrapping approach preserving the cross-correlation among sites in a network to eliminate the effect of cross-correlation on the assessment results. In their method, an empirical cumulative distribution of the regional average of the MK statistics (S) is obtained by bootstrapping sample data. Yue and Pilon (2003) found that if both upward and downward trends exist within a network, they will cancel each other in the calculation of the regional average MK Statistics S . Thus, the approach proposed by Douglas et al. (2000) might be suitable only for the case where the majority of trends within a network show uniform behaviour, i.e. either upward or downward. In the case that both upward and downward trends exist, it is desirable to assess the field significance of upward and downward trends over the network separately. Yue and Pilon (2003) proposed such an additional bootstrap test, which is similar in spirit to

the method of Douglas et al. (2000), to assess the field significance of upward and downward trends separately.

To incorporate the effect of serial correlation, Kundzewicz and Robson (2000) suggested a block re-sampling approach. In this approach, the original data is re-sampled in predetermined blocks for a large number of times to estimate the significance of the observed test statistic, i.e. the MK or SPR test statistics. The block size depends upon the number of contiguous significant serial correlations.

Kahliq et al. (2009) provide an extensive review of the methods in relation to identification of hydrological trends in the presence of serial and cross correlations and applied these methods to annual flood flow series of Canadian Rivers.

It is important to consider carefully the form and frequency of the data that should be analysed. This usually depends on the focus of the study (Kundzewicz and Robson, 2004). For floods, the biggest flow is often of interest; for droughts, it may be the duration of low flows. Flood trend studies tend to focus on trends in the annual maximum flood series, which means that in years with many high flows still only one flood event per year will be selected, and in years with no large flows at all, a relatively low flow will be extracted. A more representative way of describing the occurrence of floods is to use peaks-over threshold (POT) approach (Fiering, 1949; NERC, 1975; Svensson et al., 2006).

Hydrologic variables are important indicators of climatic change. These variables tend to reflect climatic change and can help in understanding the relationships between hydrology and climate. Numerous studies have suggested different variables for detecting climatic change. Pilon et al. (1991) suggested streamflow variables, while Anderson et al. (1992) considered mean, low and high flow regimes for climate change investigation. Burn and Soulis (1992) suggested studying a large number of hydrologic variables since climatic change is expected to affect various variables in different ways. Burn and Hag (2002) advocated streamflow variables because of the spatially integrated hydrologic response that they provide.

Petrow and Marz (2009) considered eight flood indicators in a study to detect trends in flood magnitude, frequency and seasonality in 145 River catchments in Germany.

They comprise annual maximum streamflow series as well as peaks- over-threshold series (POT).

Robson and Reed (1999) investigated British river flows in the annual maximum series as well as trends in POT magnitude and frequency series, selecting on average 1 and 3 POTs per year. They used four different methods of estimating trends such as Linear Regression, 'Normal scores linear regression, Spearman's rank correlation and Linear Regression using permutation methods. In addition, they used four different distribution-free tests for detecting step change in the flood time series such as – Distribution-free CUSUM test (Statistical Sciences, 1995; Kim and Jennrich, 1973; McGilchrist and Woodyer, 1975). Buishand's Q test for normal scores (Buishand, 1982), Buishand's Q using permutation and Median change-point test using permutation (Siegel and Castellan, 1988; Pettit, 1979).

2.3.2 Power of Trend Tests

When one wants to perform trend detection, it is natural to ask which of the available tests should be applied to detect a trend in a time series. In other words, which test has the highest power to detect a certain amount of trend? Lettenmaier (1976) compared the power of the t test and the Spearman's rho (SPR) test for detecting linear trend in normally distributed series and indicated that the t-test has slightly higher power than the SPR test. Hipel & Mcleod (1994) investigated the powers of the MK test and the lag-one serial correlation test for detecting trends in normally-distributed data, and demonstrated that the MK test is more powerful than a lag-one serial correlation test for identifying deterministic trends.

Yue et al. (2002) reported that MK and SPR tests have the same power and that their power is sensitive to the probability distribution type as well as the statistical properties of sample data. They investigated the power of these tests by Monte Carlo simulation. Simulation results indicate that their power depends on the pre-assigned significance level, magnitude of trend, sample size, and the amount of variation within a time series. That is, the bigger the absolute magnitude of trend, the more powerful are the tests; as the sample size increases, the tests become more powerful; and as the amount of variation increases within a time series, the

power of the tests decrease. When a trend is present, the power is also dependent on the distribution type and skewness of the time series.

Hipel and McLeod (2005) provide discussions on various models for generating data containing trends. Simulation experiments demonstrate that the autocorrelation function (ACF) at lag one is more powerful than Kendall's tau for discovering purely stochastic trends. On the other hand, Kendall's tau is more powerful when deterministic trends are present. The results of these experiments were originally presented by Hipel et al. (1986).

Yue and Pilon (2004) investigated the power of the parametric t-test (refer to Section 6.5.3.1 for the details of this test), non-parametric MK, bootstrap-based slope (BS-slope) and bootstrap-based MK (BS-MK) tests to detect monotonic (linear and non-linear) trends in both normal and non-normal time series. A Monte Carlo simulation technique was used in their study. The simulation results indicated that: (a) the t-test and the BS-slope test, which are both slope based tests, have the same power; (b) the MK and BS-based MK tests, which are rank-based tests, have the same power; (c) for normally-distributed data, the power of the slope based tests is higher than that of the rank-based tests, but the difference is not great; and (d) for non-normally distributed series, such as time series with Pearson type 3 (P3), Gumbel, EV2 and Weibull distributions, the power of the rank-based tests is much higher than that of the slope-based tests. The power of the tests is slightly sensitive to the shape of trend, with upward convex shape having the highest power and upward concave shape having the lowest power except for Weibull distributed data. However, in comparison to the impact of the distribution type on the power of the tests, the influence of the shape of trend on the power of the tests is marginal. This study provides an initial basis for practitioners to select a suitable statistical test based on the sample statistical properties of time series. For approximately normally-distributed series, the slope-based tests should be used to assess the significance of trends, but rank-based tests can also be applied as the power difference between these two kinds of tests is not large. For non-normal series, the rank-based tests should be employed for trend detection due to their increased ability to detect trends in comparison to the slope-based tests.

2.3.3 Effect of Trends on Regional Growth Curves and At-site Quantile Estimates

Frequency analysis is a technique of fitting a probability distribution to a series of observations for defining the probabilities of future occurrences of some events of interest, e.g., an estimate of a flood magnitude corresponding to a chosen risk of failure. The use of this technique has played an important role in engineering practice. The assumptions of independence and stationarity are necessary conditions to proceed with such analyses. However, in the context of climate change, it is possible that these assumptions might no longer hold. The parameters describing the location, scale and shape properties of hydrological time series might have changed over time. Under these circumstances, currently used statistical methods for modelling hydrologic time series and for estimating their extreme values for a given recurrence period cannot be reliably applied. An alternative framework for risk modelling should therefore be developed and disseminated among practitioners.

A time series whose distribution parameters change over time is called non-stationary. It is often characterized by the presence of a trend component (i.e., either linear or non-linear) and/or a sudden jump in the statistical characteristics of data. The source of non-stationary in hydrologic records can be a natural catastrophe or periodicity (forest fires, El Nino, solar activities), anthropogenic activity (land use change due to deforestation, urbanisation) or in changing climate (natural or anthropogenic).

The presence of a trend has a considerable effect on the interpretation of results when fitting a probability distribution to a sample of non-stationary observations. In engineering hydrology over-estimating the design values as a result of ignoring significant decreasing trends in the series may lead to over designed projects and unnecessary expenses. The more serious cases arise from ignoring increasing trends in maximum floods, which may lead to under designed projects and significant losses when more severe floods occur than are expected. Cox et al. (2002) explored the effects of trend (linearly varying deterministic trend) in mean and dispersion on the distribution of extremes using a simple theoretical model (Gumbel distribution). The results showed that if a trend in location and/or scale parameter is likely, prediction of maxima on this basis of the projected parameter

values at the midpoint of the planning horizon is slightly over-optimistic. Based on a non-stationary pooled flood frequency approach, Cunderlik and Burn (2003) showed that ignoring even a weakly significant non-stationarity in the data series (significant at 10% significance level) may seriously bias the quantile estimation for horizons as near as 0-20 years in the future (e.g. the 100-year flood flow can be overestimated by 13% in the future time horizon of 20 years). The results also showed that the 50-year long samples generated from different trend-scenarios assuming GEV distribution yielded relative bias (BIAS) of the estimated slopes in the location (scale) parameter within the range of $\pm 7\%$ ($\pm 15\%$) and to the average relative root mean square error (RMSE) of 60 % (80%).

In the context of classical frequency analysis, there is a wealth of the literature on modelling extreme values. For example, see Cunnane (1989) for a survey of distributions commonly used in flood frequency analysis across different regions of the world and GREHYS (1996), Madsen et al. (1997a,b), Ouarda et al. (1999), Lang et al. (1999) and Smakhtin (2001) for previous reviews and comparisons of frequency analysis techniques and Katz et al. (2002) for a recent review on this subject.

On the other hand, non-stationary frequency analysis is a relatively new modelling approach and the number of studies is rather small but is continuously increasing (Khaliq et al. (2006). North (1980) developed a time-dependent flood frequency model in which both the time of occurrence and the flood magnitude were time-dependent variables. Duckstein et al. (1987) outlined the Bayesian approach to the estimation of the posterior flood distribution. Strupczewski et al. (2001) and Strupczewski and Kaczmarek (2001) developed a non-stationary flood frequency procedure comprising 56 models of flood distribution and trend function. Cunderlik and Burn (2003) proposed a second order, non-stationary approach to pooled flood frequency analysis by assuming at-site non-stationarity in the first two moments (i.e., mean and variance of the time series). Khaliq et al. (2006) provided an extensive review of the various existing approaches of non-stationary frequency analysis. Leclerc and Ouarda (2007) proposed a method for non-stationary flood frequency at ungauged sites. Adlouni et al. (2007) proposed a generalised maximum likelihood parameter estimation based General Extreme Value (GEV) model for estimating quantile in the presence of non-stationarity.

Part-A: Low-Flow Estimation for Ungauged Catchments

3 LOW-FLOWS - PHYSICAL PROCESSES AND ESTIMATION METHODS

3.1 INTRODUCTION

This chapter presents an overview of catchment hydrological process responsible for generating low-flows in a catchment and also identifies various factors that influence the spatial and temporal distributions of low-flows. An understanding of these processes is a key component in developing and understanding the results of hydrological models and in interpreting how changing climate or land use will have an impact on the duration, frequency and magnitude of low-flows

3.2 LOW-FLOW HYDROLOGY – CATCHMENT PHYSICAL PROCESSES

The international glossary of hydrology (WMO, 1974) defines low-flow as ‘flow of water in a stream during prolonged dry weather’. Low-flows are seasonal phenomena and an integral component of a flow regime of any river. Low-flows are normally derived from groundwater discharge or surface discharge from lakes, marshes, or melting glaciers. Lowest annual flow usually occurs in the same season each year. The arbitrary ‘upper bound’ to low-flow hydrology may be given by the *long-term average mean daily flows* or *long-term mean annual flow*. The lowest recorded daily discharge may be referred to as *Absolute Minimum Flow*. Intermittent and ephemeral streams are characterised by natural extended periods of zero flow, which may generally be perceived as the ‘lower bound’ of low-flow.

Smakhtin (2001) provides an extensive review of low-flow hydrology along with a detailed discussion on low-flow generating mechanisms operating in natural conditions and various anthropogenic factors which directly or indirectly affect low-flows. Gustard et al. (2009) also provide a detailed discussion on physical processes for generating low-flows in a catchment. The relationship between hydrological process and low flows and the impact of human influences on droughts are reviewed by Tallaksen and Van Lanen (2004). Dingman (2002) also provides a comprehensive description of catchment processes for low-flows.

Factors controlling the spatial and temporal distribution / variation of low flows:

Low-flows usually occur during a long spell of warm dry weather, typically associated with high pressure systems and subsiding air. High temperatures, high radiation input, low humidity and wind increase evaporation and transpiration rates. Snowfall and snow storage result from temperatures continuously below freezing which are often associated with cold, polar air masses and/or decreasing temperatures at higher altitudes. In the absence of snowmelt, precipitation will accumulate and this will lead to a reduction in low-flow in snowmelt dependent rivers.

In mid- and high-latitude climates, low-flows are often described by the season of occurrence, namely “summer low-flow” and “winter low-flow”. In low latitude climates, there may be one or more dry seasons and, consequently, one or more distinct low-flow periods. As a result of constantly high evaporation rates, the climatic water deficit from the dry season may persist into the wet season. In arid and semi-arid climates, the combination of low precipitation and high evaporation results in minimal river networks and ephemeral rivers. These typically have prolonged periods of zero flow over several months or years and episodic high flows often in the form of flash floods.

Climate determines the magnitude and variation of temperature, precipitation and potential evaporation over the year. However, climate varies spatially, particularly in mountain regions where there are strong altitude-dependent temperature and precipitation gradients. High precipitation (as rain or snow) in mountainous areas is often critical for providing the source of downstream low-flows in arid or semi-arid areas. Climate also varies temporally at inter-annual and decadal timescales. Long-term trends and changes in the climate system will result in changes to the low-flow regime.

Catchment physical processes:

While climate controls may lead to a climatic water surplus in one season and a deficit in another, catchment processes determine how these surpluses and deficits propagate through the vegetation, soil and groundwater system to streamflow. An understanding of these processes is a key component in developing and understanding the results of hydrological models.

A flow in a river is the result of the complex natural processes, which operate on a catchment scale. Conceptually, a river catchment can be perceived as a series of interlinked reservoirs, each of which has components of recharge, storage and discharge. Recharge to the whole system is largely dependent on precipitation, whereas storage and discharge are complex functions of catchment physiographic characteristics. **Figure 3.1** shows a model of a catchment that receives precipitation, which then recharges different catchment storages, that is, soil water, groundwater, snow, glaciers, wetlands and lakes. The outflow from each of these storages contributes to river flow.

Precipitation input may be stored in micro-depressions; once these have been filled, water may flow to the stream as overland flow. This process tends to occur on impermeable urban surfaces and non-vegetated, sloping land with compacted topsoil or exposed rock. Overland flow rates depend on rainfall intensities and whether they exceed infiltration rates to the soil, which are lower on a clay soil than on a sandy soil. During freezing periods, precipitation is stored as snow and ice. When temperatures rise above freezing, liquid water from the snow cover melts and either infiltrates into the soil or flows over frozen ground to the stream as overland flow.

As soil moisture is replenished, soil moisture content increases and water may flow vertically downward to an aquifer to recharge groundwater storage, or move laterally as throughflow towards the stream along a permeable soil layer. The available soil moisture capacity (amount of water that can be stored in the soil) may vary between a few tens to over several hundred millimetres water depth.

Water can also recharge aquifers or flow laterally to the stream without fully replenishing soil moisture. This usually occurs via preferential flow paths such as cracks, macropores and pipes in the soil. In semi-arid and arid climates, a major part of aquifer recharge occurs through the river beds of ephemeral rivers. This indirect recharge often originates from high precipitation in mountainous regions upstream.

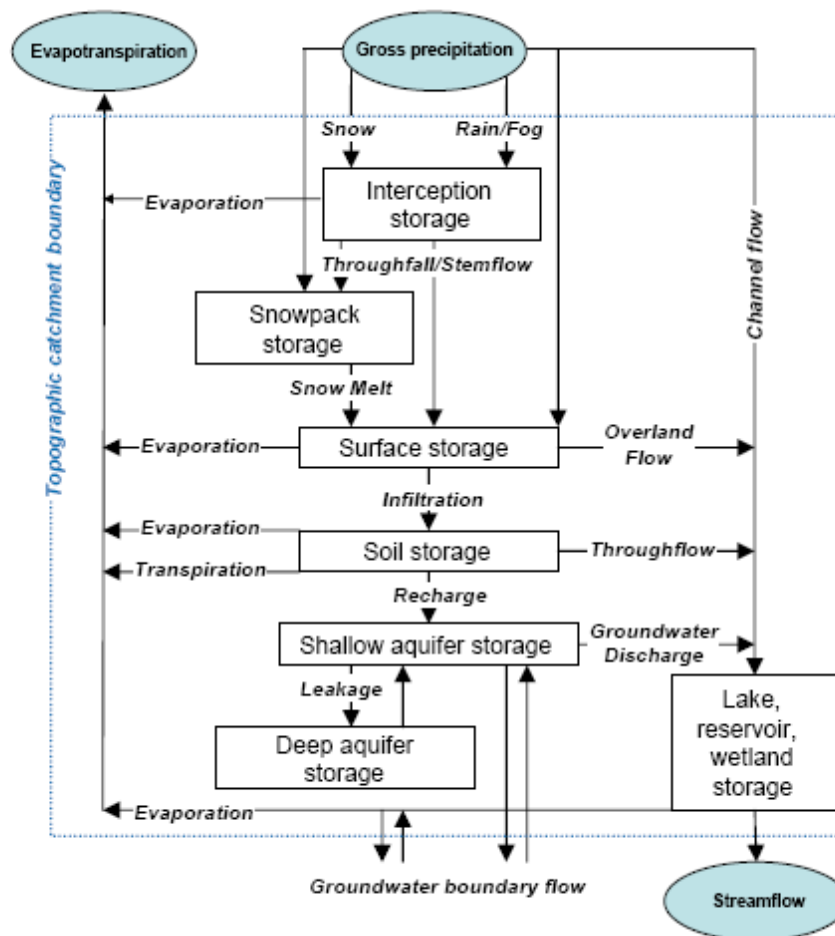


Figure 3.1: Hydrological processes and catchment storages

(courtesy, Gustard et al., 2009, World Meteorological Organisation, Operational Hydrology Report No. 50 and Tallaksen and van Lanen, 2004)

In response to recharge, aquifer storage increases as groundwater levels rise. The groundwater gradient and the transmissivity of the aquifer units (saturated thickness multiplied by hydraulic conductivity) govern the groundwater discharge to the stream. When there is no recharge, groundwater discharge will continue owing to the depletion of storage. In hilly or mountainous regions, discharge from shallow aquifers of weathered hard rock often provides an important source of low-flow during dry periods. In lowland areas or large valleys, aquifers act as large storage systems and are able to feed rivers during prolonged dry conditions.

A river receives water from one or more of three different flow paths: overland flow, through flow and groundwater discharge. Overland flow and through flow respond quickly to rainfall or melting snow, whereas groundwater discharge responds slowly with a time lag of several days, months or years. If groundwater discharge comes

from shallow saturated subsurface flow, then it responds quickly (hours or days) to rainfall or melting snow. Catchments dominated by overland flow, throughflow and/or shallow saturated subsurface flow are therefore classified as quickly responding, 'quick response' or "flashy" catchments. Catchments fed primarily by groundwater discharge are classified as slowly responding catchments with a high base flow. The delayed flow component, commonly referred to as the base flow, represents the proportion of flow that originates from stored sources. A high base-flow proportion would imply that the catchment is able to sustain river flow during dry periods. Base-flow indices are generally highly correlated to the hydrological properties of soils and geology and the presence or absence of lakes in a catchment.

A catchment with a fast/slow response to rainfall usually has fast/slow recession behaviour. Low-flows in the quickly responding catchments are lower than in the slowly responding ones. Low-flows in the slowly responding catchments are more persistent (multi-year effects) than in the quickly responding catchments. These differences are a clear illustration of the influence of hydrological processes and storages on low-flows.

It is clear from the above discussions that the natural factors which influence the various aspects of the low-flow regime of the river include the distribution and infiltration characteristics of soils, the hydraulic characteristics and extent of the aquifers, the rate, frequency and amount of recharge, the evapotranspiration rates from the basin, distribution of vegetation types, topography and climate. These factors and processes may be grouped into those affecting gains and losses to streamflow during the dry season of the year.

Gains in streamflows during dry season:

A number of authors have reported direct relationships between the geologic rock categories and discharge rate during low-flow periods (e.g. Armbruster, 1976; Smith, 1981; Musiaka et al., 1984). Streams flowing through different types of unconsolidated sedimentary rocks normally show low yields during the low-flow period. On the contrary, streams flowing through metamorphosed sedimentary and igneous rock show high flow values relative to their basin size. White (1977) showed that karst, limestone and dolomite rocks have a decreasing effect on low-flows.

Lakes and reservoirs usually have a large impact on low-flows in downstream rivers, with which rivers have direct hydraulic connection. Lakes in a moist and cool climate provide additional catchment storage to maintain low-flows during dry periods. In a semi-arid climate, however, downstream low flows may be smaller than those upstream of a lake due to high lake evaporation losses outweighing any increase in low-flows caused by the regulatory impact. The importance of lakes for low-flows in some regions may be derived from the inclusion of lake related parameters in prediction models for low-flows (FRIEND, 1989; Sakovich, 1990). The effect of reservoirs on low-flows is mainly determined by their operation (outflow control) and normally results in a reduction in discharge downstream of the reservoir. The adequate water level in a lake should be maintained during the dry season to allow lateral outflow into a stream.

In highly seasonal climates, low-flows in different dry seasons (e.g. summer and winter) may be generated by different physical processes. In cold or mountainous regions, in addition to the usual catchment parameters, low-flows are subject to the special influences of ice and snow melting (Bowles and Riley, 1976; Hopkinson and Young, 1998). The release of water from glacier storage may greatly affect the local hydrological cycle by contributing to streamflow in low-flow periods. The principal influence of glaciers in the context of low-flows is similar to that of lakes and includes a decrease in runoff variation and, consequently, more sustained low-flows.

Losses in streamflows during dry season:

In many respects the processes involved in causing streamflow losses are the reverse of those causing gains. Losses to streamflow during dry weather periods may be caused by: (i) direct evaporation from standing or flowing water in a channel, other open water bodies and wetlands; (ii) evaporation and transpiration losses from seepage areas, where groundwater or channel bank soil water drains into the channel; (iii) groundwater recharge from streamflow where the phreatic surface lies below the channel (river channels often follow lines of structural weakness and surface fracturing, offering an ideal opportunity for infiltration into the channel bed), and (iv) bed losses, where unconsolidated alluvial material underlies the river channel (these losses can be substantial not only during low-flows but also during the early stages of flood events); and (v) losses to relatively dry soils forming the

banks of streams (these may be enhanced by the presence of dense riparian vegetation promoting evapotranspiration).

Anthropogenic impacts on low flows:

The natural low-flow generating processes in a river catchment can be affected by various anthropogenic factors. Direct artificial influences on low-flows include the abstraction of water from rivers, lakes and groundwater. Human influences can also indirectly affect low-flows through a change in land use, such as deforestation, afforestation or urbanisation, arterial drainage and the impact of global warming on changing precipitation regimes.

A brief discussion of some of the anthropogenic impacts on low-flow generation processes is given below:

- **Groundwater abstraction within the sub-surface drainage area:** This clearly affects the level of phreatic surfaces and therefore the potential for groundwater re-emergence in stream channels. Localised reductions in the level of the water table may affect either hydraulic gradients or the length of channel that intersects the phreatic surface. The effects of groundwater pumping near the head of a perennial river may result in groundwater table depletion through interception of recharge water and induced recharge of the aquifer from the river itself.
- **Artificial drainage of valley bottom soils for agricultural or building construction purposes:** This can lead to more rapid removal of water from valley bottom storage and a reduction in the sustainability of lateral drainage during dry weather period.
- **Changes to the vegetation regime in valley bottom areas through clearing or planting.** They can modify the levels of evapotranspiration loss from riparian soils, thereby affecting gains or losses to bank or alluvial storage.
- **Afforestation of a whole catchment or parts thereof:** Commercial plantations normally: (i) increase interception loss due to more extensive

canopy cover, leaf area density and increased aerodynamic roughness of the surface; (ii) increase transpiration loss due to increased biomass and total leaf area, deep rooting and evergreen nature of commercial timber tree species; (iii) increase disturbance of the soil structure, infiltration and moisture holding capacity due to site preparation. All these effects modify streamflow and low-flow generating mechanisms.

- **Deforestation** often has a reverse effect on total flow and low flows. It has been demonstrated (e.g. Bosch and Hewlett, 1982), that clearfelling and timber harvesting increase annual water yield, and that in many cases this is due to increase in seasonal low flows. At the same time, decrease in low-flows is also theoretically possible. For example, reduced evapotranspiration, interception and infiltration rates following deforestation may lead to higher soil moisture storage and increased surface runoff, which in their turn lead to reduced recharge and increased gully erosion. Eventually this may result in lowering the groundwater table and reduced low flows, which originate from groundwater storage.
- A wide variety of other effects which may influence the amounts or rates of accumulation of water held in storage during rainfall, and consequently the levels of storage rates of discharge from storage during periods of limited rainfall. A general example is the **modification of land use** over large parts of a catchment which may contribute to changes in the infiltration and/or evaporation characteristics, as well as modifications to the amount of groundwater recharge. One example is catchment urbanisation. In urbanized catchments, low-flows have a tendency to decrease due to the effects of urban impervious surfaces upon direct runoff, infiltration and evapotranspiration (Ferguson and Suckling, 1990).

Apart from the above mentioned indirect anthropogenic impacts on low-flow generating processes, there are human activities, which remove water directly from or add water to the stream.

- **Direct river abstractions for industrial, agricultural or municipal purposes:** These decrease the amount of water flowing downstream and

have a more pronounced effect on streamflow during the dry season. For example, irrigation withdrawals have led to increased frequency of occurrence of low-flow discharges.

- **Direct effluent flows into river channels from industrial or municipal sources:** These can significantly affect the composition of low-flows leading to deterioration of water quality and therefore limiting its availability for downstream users.
- **Irrigation return flows from agricultural fields:** These are widely recognised as contributing to additional sub-surface drainage directly to the river channel or through 'return' canals. Return flows are particularly important if the water for irrigation is imported from outside the catchment.
- **Direct importation of water from outside the catchment** via inter-basin transfer schemes and the use of channels as natural supply conduits
- **Construction of dams and subsequent regulation of a river flow regime:** This regulation can either increase or decrease low-flow discharge levels depending on the operational management of the reservoir.

Owing to the variety of direct impacts, the low-flow regimes of many rivers of the world have been significantly modified and the origin of water in a stream during low-flow conditions has been changed. Many originally perennial streams (particularly in arid regions) have become intermittent (due to various abstractions).

3.3 LOW-FLOW MEASURES AND INDICES

The term '**low-flow measures**' used here, refers to the different methods that have been developed for describing and/or expressing the low-flow regime of a river, often in graphical form, such as Flow-duration Curve (FDC). The term '**low-flow index**' is used predominantly to define particular values obtained from any low-flow measures such as 95%ile flow (Q_{95}).

Some of the commonly used low-flow indices are annual minimum *mean daily flow (MDF)*, *annual minimum m-day sustained low-flow (m-day SLF)*, *annual minimum m-day moving average flow (m-day MAVF)* and *95%ile flow*. The most widely used low-flow indices (particularly in USA) are 7-day 10-year low-flow (7Q-10) and 7-day 2-year low-flow (7Q-2), which are defined as the lowest average flows that occur for a consecutive 7-day period at the recurrence intervals of 10 and 2-years, respectively. The average of the annual series of minimum 7-day average flows known as Dry Weather Flow (DWF) is used in the UK for water abstraction licensing. In Russia and Eastern Europe, the widely used indices are 1-day and 30-day summer and winter low-flows. *Baseflow* (sometimes used as an important low-flow index) is an important genetic component of streamflow, which comes from groundwater storage or other delayed sources (shallow subsurface storage, lakes, melting glaciers, etc.). Another index called, *Baseflow Index (BFI)* is a non-dimensional ratio which is defined as the volume of baseflow divided by the volume of total streamflow. In catchments with high groundwater contribution to streamflow, BFI may be close to 1, but it is equal to zero for ephemeral streams. BFI was found to be a good indicator of the effects of geology on low-flows and for that reason is widely used in many regional low-flow studies (Institute of Hydrology, 1980). Further details of the above mentioned low-flow indices can be found in Smakhtin (2001).

3.4 FLOW-DURATION CURVE (FDC)

3.4.1 Construction and Interpretation

A flow-duration curve (FDC) provides the percentage of time (duration) a daily or monthly (or some other time interval) streamflow is exceeded over a historical period for a particular river basin. It is a relationship between any given discharge value and the percentage of time that this discharge is equalled or exceeded.

An empirical FDC can be easily constructed from streamflow observations using standardised non-parametric procedures, described for example by Vogel and Fennessey (1994). An FDC may be constructed using different time resolutions of streamflow data: annual, monthly or daily. An FDC constructed on the basis of daily flow time series provides the most detailed way of examining the flow-duration characteristics of a river. Curves may also be constructed using some other time intervals, e.g. from m-day or m-month averaged flows calculated from available daily

or monthly data. FDCs may be calculated: (i) on the basis of the entire available record period ('period-of-record FDC, Vogel and Fennessey, 1994), or (ii) on the basis of single year record – Annual FDC (AFDC), or (iii) 'Long-term average annual FDC' (FRIEND, 1989; Smakhtin et al., 1997), which could be obtained from averaging of all available AFDCs.

FDC provides a simple, yet comprehensive, graphical view of the overall historical variability associated with the streamflows in a river basin (Vogel and Fennessey, 1994). An FDC is one of the most informative methods of displaying the complete range of river discharges from low-flows to flood events. Vogel and Fennessey (1990) described FDC as a non-parametric cumulative distribution function (cdf) of daily streamflows at a site.

Vogel and Fennessey (1994) suggested a different interpretation of FDC. They considered FDCs for individual years and treat those annual FDCs (AFDCs) in the way similar to a sequence of annual flow maxima or minima. Such curves represent the exceedance probability of flows in individual years. This approach allows confidence intervals and return periods to be assigned to FDCs.

The shape and general interpretation of any FDC depends on the particular period of record on which it is based (Searcy, 1959; Vogel and Fennessey, 1994)

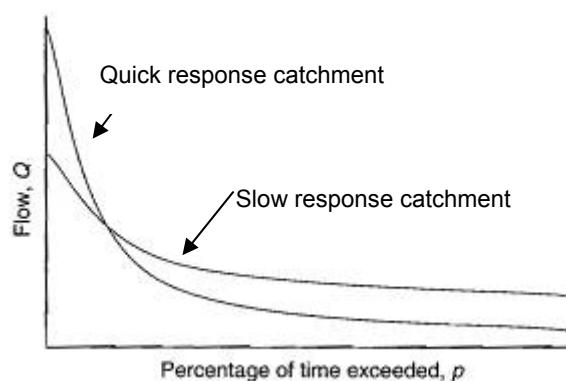


Figure 3.2: Shape of FDC represents catchment response behaviour

The shape of the FDC is an indication of hydrological conditions in the catchment. The entire low-flow section of the curve may be interpreted as an index of groundwater (and/or subsurface flow) contribution to stream flow. If the slope of the

low-flow part of the FDC is small, groundwater/subsurface flow contribution is normally significant and low-flows are sustainable. A steep curve indicates small and/or variable base flow contribution. An FDC is sometimes referred to as the 'signature' of a catchment, as it describes its behaviour and response. A flat FDC indicates little variability in the flow (slow response to rainfall), whereas a steep FDC indicates high variability in the flow magnitude (quick response to rainfall) (**Figure 3.2**).

3.4.2 Applications

FDCs are widely used by hydrologists in water related applications like hydropower generation and planning and design of irrigation systems, management of stream-pollution, river and reservoir sedimentation and fluvial erosion. Vogel and Fennessey (1990) present a comprehensive review of FDC applications in water resources planning and management.

FDCs have been advocated by many researchers and practitioners for use in hydrological studies such as hydropower, water supply, and irrigation planning (Vogel, 1994). Searcy (1959) described additional applications to waste-load allocation and other water quality management problems. FDC can be used to illustrate and evaluate the trade-offs among the variables involved in the selection of a wastewater treatment plant capacity (Male and Ogawa, 1994). The US. Bureau of Reclamation uses FDCs in river basin and reservoir sedimentation studies that examine the frequency of suspended sediment loads and determine the long-term average suspended sediment yield for a given site (Vogel and Fennessey 1994). FDCs can be used for patching and extension of daily observed streamflow time series, for generation of low-flow time series at ungauged sites (Hughes and Smakhtin, 1996). The US Fish and Wildlife Service use FDCs for determining the suitability of habitats in streamflows of different magnitudes and frequencies. Gustard et al. (2009) also provides a comprehensive review of various uses of flow-duration curves.

3.5 LOW-FLOW ESTIMATION AND PREDICTIONS

An extensive review of current literature on low-flow estimation methods both for the gauged and ungauged catchments has been provided in Section 2.2. A general description of various approaches to low-flow estimation is provided below:

For gauged catchments, FDCs are constructed by reassembling the streamflow time series values in decreasing order of magnitude. All ranked flows are plotted against their ranks which are again expressed as a percentage of the total number of time steps. Vogel and Fennessey (1994) suggested a number of non-parametric approaches for constructing empirical flow duration curves.

For ungauged catchments, FDCs can be constructed using various methods, such as:

- (i) **Regional regression approach**, which generally involves developing regional mathematical models by relating low-flow indices or FDCs with catchment physiographic and climatic characteristics,
- (ii) **Regional prediction curve**, where FDCs for a number of gauged catchments of varying size in a homogeneous region can be converted to a similar scale, superimposed and averaged to develop a composite regional curve (e.g. FRENCH, 1989; Beran and Gustard, 1985). To make curves from different catchments comparable, all flows are standardised by catchment area, mean or median flow or other 'index' flow. A curve for an ungauged site may then be constructed by multiplying the ordinates of a regional curve by either catchment area or an estimate of the index low-flow depending on how the flows for the regional curve were standardised. The index flow is estimated either by means of regression equation or from a regional map,
- (iii) **Regional mapping** and other methods of spatial interpolation of low-flow characteristics similar to regression relationships. Flow maps can be constructed on the basis of flow characteristics estimated from the gauged data. For example, a normalised- Q_{95} map was prepared under the Water Framework Directives- River Basin District (WFD-RBD) Projects in Ireland, and

- (iv) **Low-flow estimation from synthetic streamflow time series** - the alternative approach to low-flow estimation at ungauged sites is to utilise a time-series simulation method (stochastic and deterministic) to generate a satisfactorily long length of streamflow data and to calculate a set of low-flow indices and/or FDCs from the simulated series. A detailed description of these methods can be found in Smakhtin (2001).

4 LOW-FLOW PREDICTION FOR UNGAUGED RIVER CATCHMENTS IN IRELAND

4.1 INTRODUCTION

Estimating streamflows for ungauged catchments is always a big challenge. Numerous studies have been carried out worldwide, including Ireland, to-date on high-flows (floods) estimations for ungauged catchments. However, fewer studies have been carried out so far on low-flow estimation of streamflows.

In the above context, this section of the thesis explores the various low-flow measures/indices, their application and estimation techniques currently in use in Ireland. A simple regression based generalised parametric model for the flow-duration curves (FDC) for Irish rivers has been developed which can be used for predicting an FDC for any ungauged catchment from known catchment physiographic and climatological characteristics.

4.2 LOW-FLOWS IN IRELAND

4.2.1 Low-flow Characteristics and Drought History

Low-flows in Ireland generally tend to occur from April to October. In general, a substantial period of insignificant rainfall, ending in September, results in low river flows. In catchments with limited groundwater resources, low river flows occur after a period of insignificant rainfall, irrespective of the time of year at which it occurs.

The pattern of river flow in Ireland reflects the rainfall pattern and, in general, there is a prompt response to rainfall although the rate of response varies from catchment to catchment. Some catchments have a very quick response to rainfall and are regarded as flashy catchments, with little or negligible storage. In other catchments, the rate of increase in runoff resulting from rainfall may not be as severe as water goes into storage and then contributes to river flow from storage. The normal pattern of flow in rivers in Ireland is that the groundwater recession commences in the spring and continues at a steady rate until the autumn. Rainfall in the late Spring/Summer does not alter the trend of the recession once it is established,

although such rainfall may lead to an increase in river flows. Recovery of groundwater flow to normal winter levels depends on the rainfall pattern after the end of the low flow period.

Ireland enjoys a temperate maritime climate, due mainly to its proximity to the Atlantic Ocean and the presence of the Gulf Stream. Due to this, Ireland receives a lot of precipitation, almost all round the year. Drought in Ireland is therefore not a very frequent event. However, a number of noted droughts occurred in Ireland in the past, such as the droughts in 1975, 1976, 1984, 1990, 1991 and 1995. Dooge (1985) provides an account of drought years gleaned from historical sources as far back as the Annals of Clonmacnoise in the 18th century and extending to the 20th century.

MacCarthaigh (1995) produced maps showing “periods of insignificant rainfall” at twelve climate stations in Ireland for the six driest years over the last 30 years, namely 1975, 1976, 1989, 1990, 1991 and 1995. The dry year 1976 produced the lowest flows recorded in Ireland over the past 40 years and most likely the lowest for perhaps the past 60 or 70 years. During this year, all areas except the northwest experienced “insignificant” rainfall for a period of 8 weeks ending around 9th September. The year 1975 had similarly long or slightly longer periods of “insignificant” rainfall between May and July. The minimum flow rates measured in the 1976 drought are the lowest flows on record and are generally used as a benchmark drought against which other droughts can be compared. The extreme low flows measured at the end of the drought in 1995 in many parts of the country were also comparable to the low flows measured at the end of the drought in 1976. The low flows in all of the drought years were independent of the previous year’s low flows and were due to the lack of rainfall in each of the drought years.

4.2.2 Low-flow Measures Currently in Use in Ireland

The most widely used low-flow indices in Ireland are *95%ile flow (Q₉₅)*, *Dry Weather Flow (DWF)* which has been defined by the Environmental Protection Agency (EPA) as the annual minimum daily mean flow rate with a return period of 50 years and *7-day 15-year sustained low-flow*. EPA uses *DWF and 7-day 15-year SLF* for stream water quality management purposes. The Q₉₅ is generally used to assess the stream

waste-load assimilative capacity. Under the Phosphorus Regulations and the Urban Wastewater Treatment Regulations, the 50%ile flow (Q_{50}) is used for phosphorus assimilative capacity assessment.

Systematic flow measurements have been carried out by ESB, OPW and EPA in pursuit of their statutory obligations. Flow measurements have also been carried out by Dublin City Council and its predecessor. In the 1970's the OPW installed Crump weirs at a number of flow gauging stations in order to improve the quality of low flow measurement. The Water Resources Division (WRD) of An Foras Forbartha (later subsumed into EPA) installed a wide network of gauges in order to assist Local Authorities fulfill their role laid down in the Local Government (Water Pollution) Act 1977. The WRD also undertook a very extensive programme of low flow current meter measurements during the dry summers of 1975 and 1976, and its successor, EPA, continues this practice during prolonged dry periods. Recently, EPA has launched a web-based countrywide low-flow database which can be downloaded for use (www.hydronet.epa.ie).

4.2.3 History of Low-Flow Studies

In Ireland much of the assessment of water resources and low-flows has been carried out in the EPA and earlier by An Foras Forbartha, e.g. McCumiskey (1981), Mac Carthaigh (1984, 1987, 1989, 1992, 1996, 1999, and 2002). Martin and Cunnane (1977) examined the frequency distributions of selected Irish low-flow and volumes of deficit series, while Kachroo (1992) generalised the latter. Dooge (1985) provides an account of drought years gleaned from historical sources. Other academic studies include those of Smyth (1984), King (1985), Carty and Cunnane (1990) and Brogan and Cunnane (2005).

A brief description of some of the main studies is given below:

Martin and Cunnane (1977) gave an expression for 50 year return period annual minimum flow, q_{50} (equivalent in meaning to EPA-DWF) as:

$$q_{50} = 14.5 A^{1.6} \times 10^{-6} \text{ m}^3/\text{s} \text{ where } A \text{ is catchment Area in km}^2 \quad (4.1)$$

This study was based on the data of 18 medium to large sized catchments ranging from 194-3401km². It has a very large factorial standard error (FSE) of 2.5, again indicating the imprecision of the relation as an estimating tool.

Smyth (1984), based on examination of probability plots and Chi Square and Kolmogorov goodness of fit tests, concluded that both EV1 and LN2 distributions provided satisfactory description of a little more than half of the 45 series examined in the study, while the LN3 was satisfactory in almost three quarters of cases. Smyth (1984) also gave prediction equations for the location and scale parameters of both EV1 (Extreme value type 1) and LN2 (log-normal 2-parameter) distributions for annual minimum flows. These parameters were related to catchment area and a selection of catchment characteristics of lake-index, mean annual rainfall and 2-day 5-year return period rainfall. When q_{50} was estimated from such an approach, it was shown to have FSE of about 1.5, a considerable improvement on using area alone (Eq. 4.1).

King (1985) examined the characteristic of sustained low flows (SLFs) of several durations ranging from 1 to 30 days for 71 gauging stations in Ireland.

Kachroo (1992) proposed a generalised regression based parametric model for the annual maximum low-flow deficit volume for a number of frequencies of occurrence from using low-flow data for 26 catchments in Ireland. The relationship between the deficit storage and its frequency of occurrence was calculated for various levels of yield on each catchment. A simple model was described in terms of a small number of parameters. For uses on ungauged catchments, those parameters were related to the physical characteristics of the catchments (catchment area, channel slope, stream frequency, catchment soil index, lake index, mean annual rainfall and evaporation) by multiple linear regressions.

MacCarthaigh (2002) presented plots of DWF (EPA) versus catchment area and of Q_{95} versus catchment area for 371 sites where DWF is stated to be the annual minimum daily mean flow of 50 year return period and Q_{95} is the period-of-record 95%ile flow. These plots show considerable scatter about an upward trend. A least

squares line through the origin of each of these plots was described by the equations:

$$\text{EPA-DWF} = 0.0013A \text{ m}^3/\text{s} \quad (4.2)$$

$$\text{and EPA-Q}_{95} = 0.0026 A \text{ m}^3/\text{s} \quad (4.3)$$

where A is catchment area in km²

These equations are largely guided by the values plotted for the larger catchments, that the percentage scatter among values for small catchment is very large and that these equations cannot be used reliably for low flow (Brogan and Cunnane, 2005).

Brogan and Cunnane (2006) examined the suitability of various statistical distributions for the annual minimum mean daily flow series for Irish Rivers (28 stations with record lengths varying from 31 to 47 years). It was found that the EV1 distribution provides a good fit to annual minimum flow data at most stations, while the two-parameter Log-normal distribution (LN2) performs a little less well.

Studies were undertaken for the Water Framework Directive (WFD) where FDCs were required in risk assessments and in preparation of a programme of measures. Initial screening used a national map of 95%ile flow per sq. km. This was subsequently improved on the basis of a 'Region of Influence' approach to non-parametric FDC estimation using meteorological and topographical catchment descriptors, and also a set of soils, subsoils and aquifer descriptors developed by an expert group (Bree et al., 2009). The method has been prepared as a web-based GIS application that allows the user to select a target site of interest and to choose a set of donor gauged catchments, appropriate to the target site of interest, and to transfer flow information from the donor catchments (<http://193.1.208.39/HydroTool>).

4.3 A FLOW-DURATION CURVE BASED LOW-FLOW ESTIMATION METHOD FOR UNGAUGED RIVER CATCHMENTS IN IRELAND

4.3.1 Methodology

Mathematically, an FDC has often been represented by a number of different forms, including power and exponential forms (Quimpo et al. 1983; Mimikou and Kaemaki 1985, Patel, 2007). Beard (1943) suggested constructing an FDC by fitting a 2-parameter lognormal cumulative distribution function (cdf).

FDCs are known to exhibit rather complex shapes, (Searcy 1959, Dingman 1978); three or more parameters are probably necessary to describe the location, shape, and scale of the probability density function. Vogel and Fennessey (1990) pointed out that a complex trade-off exists between the number of parameters required to describe the FDC and our ability to obtain regional regression models that relate those parameters to drainage basin characteristics.

In a study carried on 23 river basins in Massachusetts in USA, Vogel and Fennessey (1990) approximated the lower half of the daily FDCs using a two-parameter lognormal probability density function.

Given the complex shape of the observed FDC and the higher variability in the high-flow sections of the FDCs, the present study focuses on modelling of only the lower three-quarter section of FDC (25%ile to 99.99%ile). Furthermore, for the planning and design of water related schemes, knowledge of the FDC between the limits of 50 & 99.99%ile flows are adequate. Based on this, the objective of this thesis work is to develop a regional regression model for the lower three-quarter portion of FDC (**Figure 4.1**). This approach will also allow the model to be based on a reduced number of parameters.

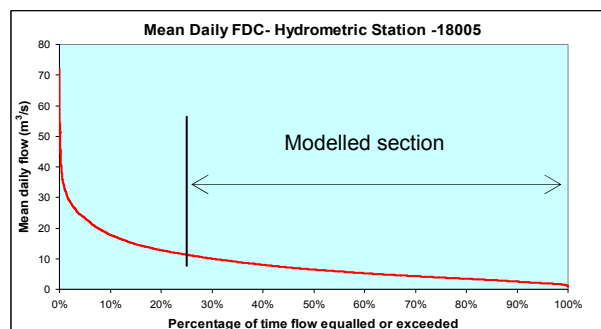


Figure 4.1 Modelled FDC section

4.3.2 Data

Mean daily flow data for 125 gauging sites were obtained from EPA (<http://hydronet.epa.ie/conditions.htm>) and Office of Public Works (OPW) (www.opw.ie/hydro/index.asp) hydrometric databases. FDCs for these gauging stations have also been obtained from EPA. Stations with the following attributes were selected:

1. Good rating curve
2. Rivers are perennial and all streamflows are greater than zero
3. No significant withdrawals, diversions, or artificial recharge areas are involved in the basins

The location of each station is illustrated in **Figure 4.2**. **Table 4.1** provides a summary of the data used in this study. A wide range of catchments have been included, representing catchments with a high variability in annual rainfalls and catchments that differ significantly in terms of their hydrogeology. The record lengths vary from a minimum of 5 years to a maximum of 57 years with a mean value of 25 years. Several other catchment physiographic and climatic characteristics were also obtained from the EPA, OPW and Met Eireann. Climatic characteristics include long-term mean annual rainfall (SAAR) and mean annual potential evapotranspiration (PE). Physiographic characteristics used include catchment area (AREA), drainage density (DRAIND), stream frequency (STRMFRQ), Lake Index (LAKE) and geology as expressed by baseflow index (BFI).

Catchment Area (AREA):

The catchment area (expressed in km²) of each river gauge is directly obtained from the OPW physical catchment descriptor (PCD) database.

Drainage Density (DRAIND):

It is a simple index that relates the length of the upstream hydrological network (km) and the area of the gauge catchment (km²) and is obtained by dividing the upstream stream lengths by the catchment area. These DRAIND values were obtained from the OPW.

Stream Frequency (STRMFRQ):

It records the number of discrete channel elements in the hydrological network above the gauge and is expressed as the number of stream junctions per square kilometre. These were obtained from the OPW.

Standard Period Average Annual Rainfall (SAAR):

The SAAR descriptor, expressed in mm, is derived from a dataset provided by Met Éireann of the long term average annual rainfall for the standard period of 1961-1990. These were obtained from the OPW.

Baseflow Index (BFI):

It is considered as the key variable to index the effect of soils and geology on low flows. It is a dimensionless ratio of the volume of baseflow divided by the volume of total streamflow. These BFI values were obtained from the OPW.

Lake Index (LAKE):

This index measures the proportion of catchment area which drains through a lake or reservoir. These were also obtained from the OPW.

Potential Evapotranspiration (PE):

It is the water flux under non-limiting soil water conditions and is expressed in mm. Met Éireann (Irish Meteorological Department) uses the Penman-Monteith formula to calculate the daily Potential Evapotranspiration, using meteorological data recorded at various locations in Ireland.

Actual Evapotranspiration (AE):

It is the water flux which actually occurs (expressed in mm). This is limited by the amount of moisture available in the soil. Estimates of Actual Evapotranspiration are derived from calculated values of Potential Evapotranspiration and current Soil moisture deficit (SMD) by Met Éireann.

Table 4.1: Data Summary

Data Name	Notation	Median	Mean	Maximum	Minimum	Standard deviation
Catchment area	AREA	122	261	2450	3	409
Mean annual rainfall	SAAR	1157	1226	2585	725	374
Mean Annual Flow	MF	2.87	5.72	39.90	0.09	7.43
Record Length (year)	L	26	25	57	5	12
50%ile Flow (m ³ /s)	Q ₅₀	1.77	3.75	27.80	0.05	5.12
95%ile Flow (m ³ /s)	Q ₉₅	0.29	0.65	5.90	0.01	0.94

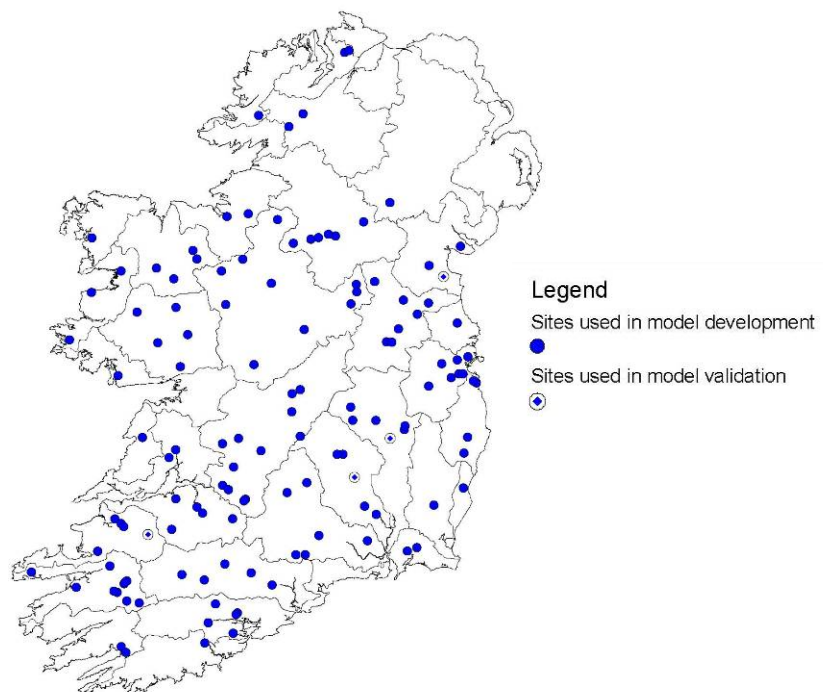


Figure 4.2: Spatial distribution of the gauging sites

4.3.3 Proposed FDC Model

An empirical period-of-record FDC was developed for each gauging site. A best fit curve was fitted to the lower three-quarter section of each of the FDCs using MS Excel's data analysis tool. It was found that a 2-parameter logarithmic type model provides a good approximation to lower three-quarter part of the daily FDCs for almost all of the sites used in this study. The structure of such a model is:

$$Q_p = b - a \ln p \quad (4.4)$$

where Q_p represents the p %ile flow, ' a ' and ' b ' are two model parameters; p is the exceedance percentile for which flow is equalled or exceeded ($25\% \leq p \leq 99.99\%$).

Figure 4.3 shows a plot of the empirical FDC and the fitted logarithmic curve for a site at Killyon on the River Deel. The R^2 - value (coefficient of determination) of 0.9961 suggests a high precision regression model. In most cases R^2 values were greater than 0.98, with a minimum value of 0.92.

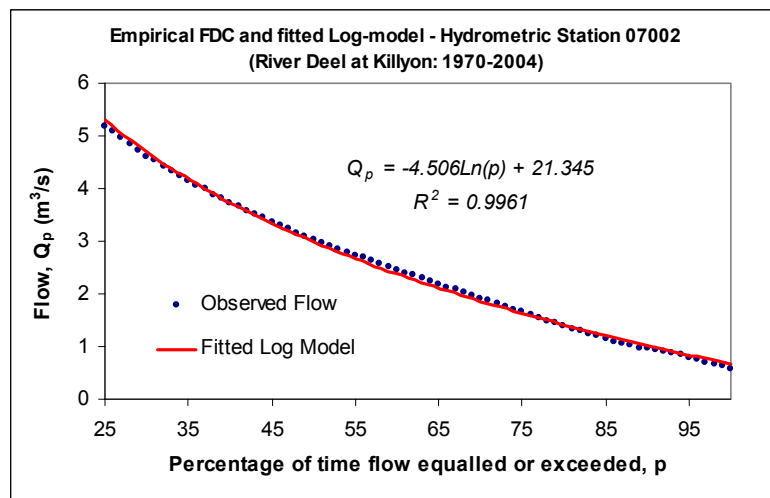


Figure 4.3: Fitted Log-model to an empirical FDC

It was found that the derived model parameters obtained for the 125 study catchments are highly correlated and that the parameter ' b ' is approximately 4.6558 times the parameter ' a ' (i.e. $b=4.6558a$). **Figure 4.4** shows a plot of the parameter ' a ' against parameter ' b '.

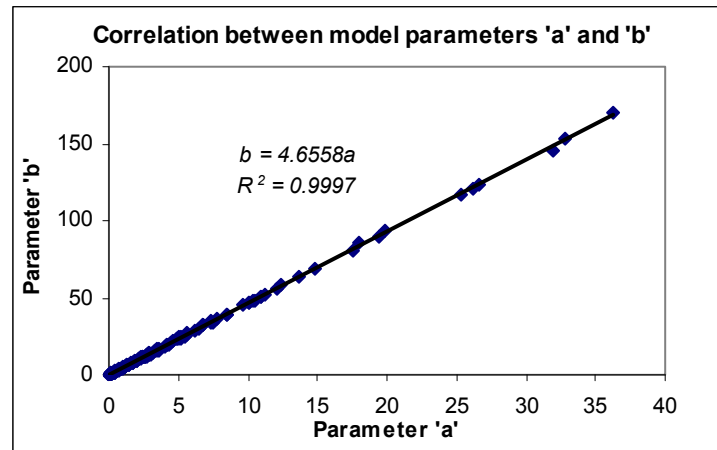


Figure 4.4: Correlation between parameters 'a' & 'b'

Thus the analytical FDC model can be approximated by a single parameter of 'a' as follows:

$$Q_p = a(4.6558 - \ln p) \quad (4.5)$$

It should be mentioned here that this approximation of the parameter 'b' is more reliable than an estimate of 'b' obtained from a regression relationship between 'b' and catchment physiographic and climatic characteristics. Evidence of this is given in Section 4.3.5.

4.3.4 Model Parameter Estimation

The analytical FDC model represented by Eq.4.5 is extended for use at an ungauged site by developing a generalised regression equation for parameter 'a'.

The shape of the FDC has been shown to have a strong dependence on catchment characteristics, particularly hydrogeology (Institute of Hydrology 1980, Gustard et al. 1992a; Vogel and Fennessey 1990). The UK low-flow studies Report (IH, 1980) has highlighted the need to index the hydrogeology of a catchment in order to predict low flows at ungauged locations. The Low-Flow Studies Report recommended the use of BFI. Previous studies in the United States and elsewhere have developed multiple linear equations for estimating low-flow statistics and/or model parameters, by relating with the catchment physiographic, geologic, climatic and/or geomorphic parameters that are easily measured at ungauged sites (Male and Ogawa 1982;

Tasker 1989; Vogel and Kroll 1990). The model derived by Vogel and Fennessey (1990) contains the independent basin parameters of catchment area, average basin slope and the basin relief.

In the present study the attempts have been made to describe the model parameter 'a' using the catchment physiographic parameters: catchment area (AREA), catchment drainage density (DRAIND), stream frequency (STRMFRQ), Baseflow Index (BFI) and the climatic parameters of long-term average annual rainfall (SAAR) and Potential Evapotranspiration (PE). Multivariate regression procedures were employed to test a variety of combinations of model form and independent variables and it was found that catchment area is the most significant, and the fit is improved when this is combined with just one climatological descriptor. Two alternative models were proposed for the model parameter 'a', the details of which are discussed below.

AREA – SAAR Model:

It was found that the parameter 'a' has a good correlation with the catchment area (AREA) and the long-term average annual rainfall (SAAR). The resulting regional regression for the parameter 'a' is:

$$a = k_1 e^{k_2 (\ln AREA)(\ln SAAR)} \quad (4.6)$$

where AREA is in km² and SAAR is in mm; k₁ and k₂ are two regression coefficients, the optimised values of these coefficients are 0.0229 & 0.1393 respectively.

The large R²- value (coefficient of determination) of 0.9428 in the above equation suggests a high precision regression model. In other words, the catchment area and the long-term mean annual rainfall in the form of the above equation (Eq. 4.6 - exponential type) are good predictors of parameter 'a'. Using 'a' in Eq.4.5 one may obtain a regression estimate of Q_p at an ungauged site.

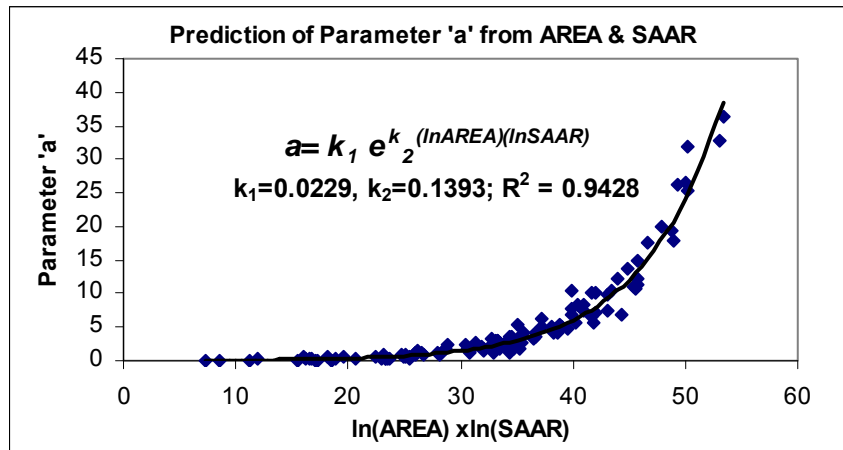


Figure 4.5: Regression of parameter 'a' on AREA & SAAR

Mean Flow Model (MF-Model):

An alternative attempt was made to have a generalised estimate for parameter 'a' from the observed long-term mean annual flow (MF) and mean annual potential evapotranspiration (PE) data for each of the catchments. A regression on the MF with parameter 'a' showed that MF is a good predictor of parameter 'a' and the resulting regression is:

$$a = k(MF) \quad (4.7)$$

where MF is in m^3/s , k is the regression coefficient, the optimised value of which is 0.9301

Conceptually MF could be linked with the catchment area (AREA) and the mean net annual rainfall (NAR) in the following way:

$$\text{i.e } MF = \text{AREA} \times \text{NAR}$$

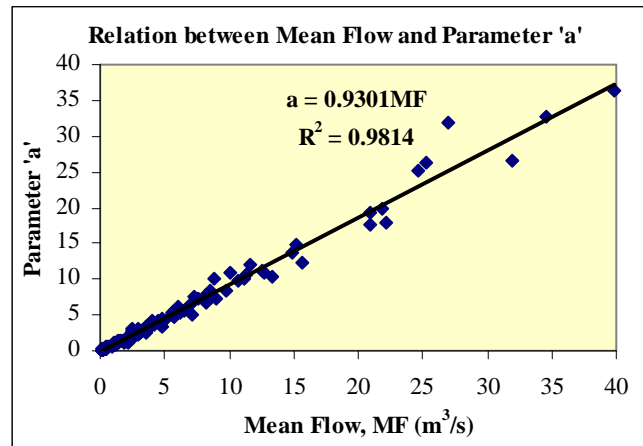


Figure 4.6: Regression of Parameter 'a' on MF

From the known mean annual PE, the NAR at each of the sites was estimated by subtracting it from the observed long-term mean annual rainfall. Mean annual PE for a total of 14 synoptic stations in Ireland were obtained from Met Eireann. Using the MapInfo GIS technique PE values on a 20km x 20km spatial grid resolution have been calculated by linear interpolation and an indicative colour coded map was prepared as shown on **Figure 4.7** (PE-Map). For the sites located outside the limits of the data range/PE-map, the nearest known PE-value was used. By knowing PE and long-term mean annual rainfall, MF at any ungauged site can be calculated as follows:

$$MF = AREA(SAAR - PE) \times 10^3 / (365 * 24 * 60 * 60) \text{ m}^3/\text{s} \quad (4.8)$$

where AREA is in km^2 and PE is in mm

A scatter plot of the observed and estimated MFs shown in **Figure 4.8** indicates a reasonably good performance of the above estimate of MF for an ungauged site. Using Eq. 4.8 'MF' and inserting this in Eq. 4.7 gives an estimate of parameter 'a', which can then be used in Eq. 4.5 to provide an estimate of Q_p for an ungauged site.

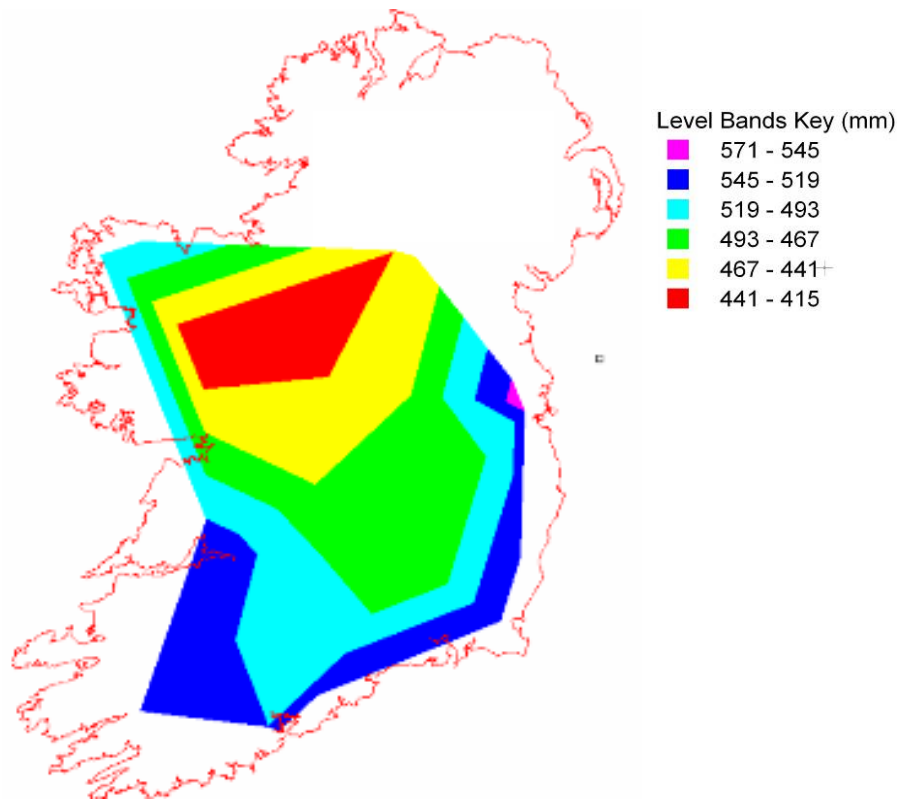


Figure 4.7: Indicative Potential Evapotranspiration Map (PE-Map) for Ireland

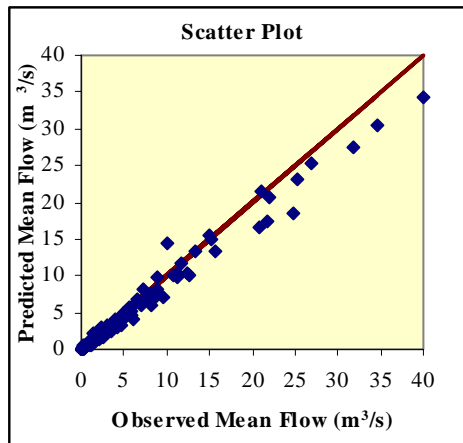


Figure 4.8: Relationship between the predicted and observed Mean Flows

4.3.5 Model Performance

Performance of the generalised FDC model was assessed through both graphical and analytical approaches. Scatter plotting techniques for a number of low-flow indices of Q_{25} , Q_{50} , Q_{75} & Q_{95} were used under the graphical approach where the predicted versus observed flows were plotted. **Figures 4.9** and **4.10** show scatter plots for the above low-flow indices estimated from AREA-SAAR and MF parameter estimation models respectively. In general, these plots show good agreement between the observed and predicted values. A slightly better correlation was observed for the Q_{25} , Q_{50} and Q_{75} flows than for the 95%ile flow in both parameter estimation models. A considerable spread of data is observed around the 45° line for the Q_{95} flow, particularly for higher flow values.

In the analytical approach, two performance indicator statistics, the average bias (BIAS) and root mean sum of squares error (RMSE), as defined below, were used:

$$BIAS = \frac{1}{N} \sum_i^N \left(\frac{Q_{est}^i - Q_{Obs}^i}{Q_{Obs}^i} \right) \times 100\% \quad (4.9)$$

$$RMSE = \sqrt{\frac{1}{N} \sum_{i=1}^N \left(\frac{Q_{est}^i - Q_{Obs}^i}{Q_{Obs}^i} \right)^2} \times 100\% \quad (4.10)$$

where Q_{Obs} = Observed flow
 Q_{est} = Estimated flow
 N = No. of sites

Table 4.2 presents the estimated BIAS and RMSE statistics for the proposed FDC models and the parameter estimation methods. In general, the agreement between the observed and predicted FDCs is reasonably good. The AREA-SAAR Model under-estimates Q_{95} flows by 7.60% while the MF-Model under-estimates Q_{95} by 12.12%.

Table 4.2: Summary of Results (one-parameter model)

Model	BIAS*				RMSE			
	Q ₂₅	Q ₅₀	Q ₇₅	Q ₉₅	Q ₂₅	Q ₅₀	Q ₇₅	Q ₉₅
AREA-SAAR	+1.20%	+7.50%	+10.10%	-7.60%	34.0%	31.0%	35.0%	43%
MF-Model	-9.8%	-1.6%	+2.6%	-12.12%	24.0%	27.0%	38.0%	48.0%

*Note: -ve BIAS: under-estimation, +ve BIAS: over-estimation

As mentioned earlier in Section 4.3.3, the approximation of the parameter ‘*b*’ in the two-parameter FDC model (equation 4.6) by $b=4.6558a$, is more reliable than estimating it from a regression model based on the catchment physiographic and climatic characteristics. Evidence of this can be seen from the results presented in **Table 4.3**, where the bias and RMSE of the FDC model obtained from the regional estimate of both parameters are presented. Since both parameters are highly linearly correlated, the parameter ‘*b*’ also has a similar type of relationship with AREA and SAAR as it has with MF (equations 4.6 and 4.7). It should be mentioned here that these regression models (AREA-SAAR and MF models) give better results for parameter ‘*b*’ than results from any other combinations of independent variables. The estimated bias and RMSE of the Q₉₅ flow estimated from the two-parameter FDC model (equation 4.6) with the AREA–SAAR parameter estimation method are -6.9% and 45% respectively, suggesting that the overall performance of the one-parameter FDC model with $b=4.6558a$ approximation is slightly better than the two-parameter model.

Table 4.3: Summary of Results (two-parameter FDC model)

Model	BIAS*				RMSE			
	Q ₂₅	Q ₅₀	Q ₇₅	Q ₉₅	Q ₂₅	Q ₅₀	Q ₇₅	Q ₉₅
AREA-SAAR	-1.35	+7.90	+10.80%	-6.90%	34.0%	32.0%	36.0%	45%
MF-Model	-10.27%	-2.7%	+0.20%	-18.87%	24.0%	27.0%	37.0%	46.0%

*Note: -ve BIAS: under-estimation, +ve BIAS: over-estimation

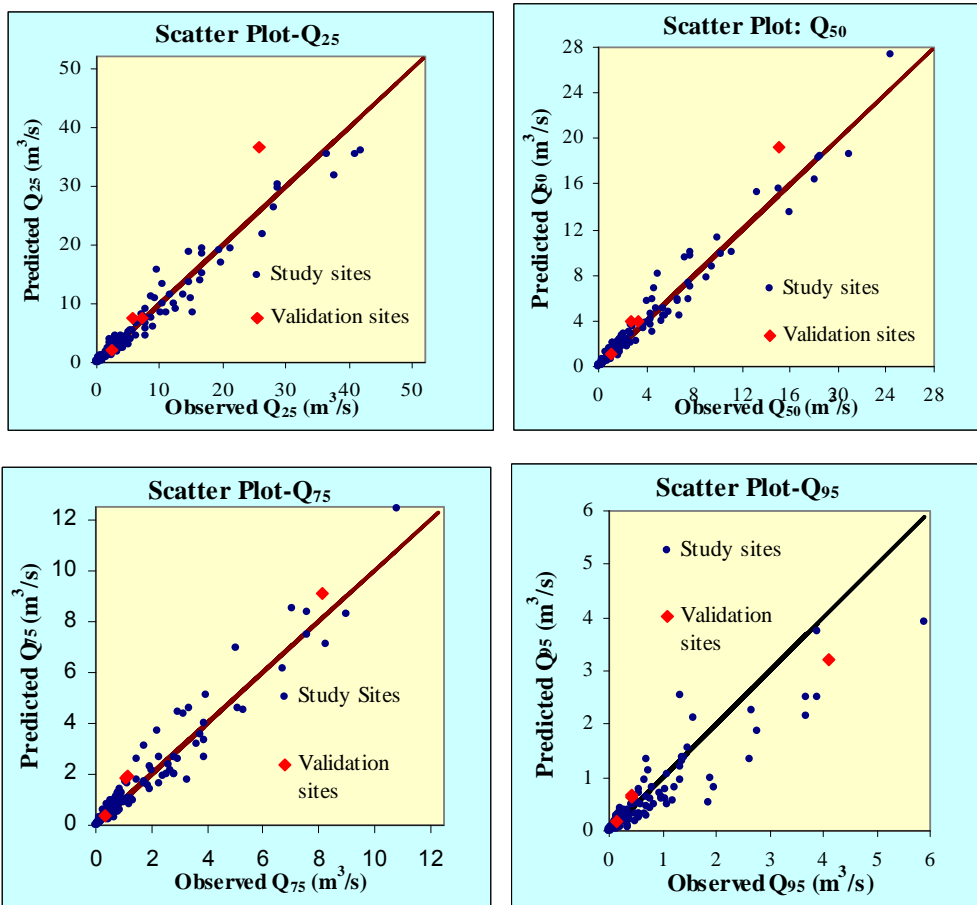


Figure 4.9: Scatter Plots – AREA-SAAR Model

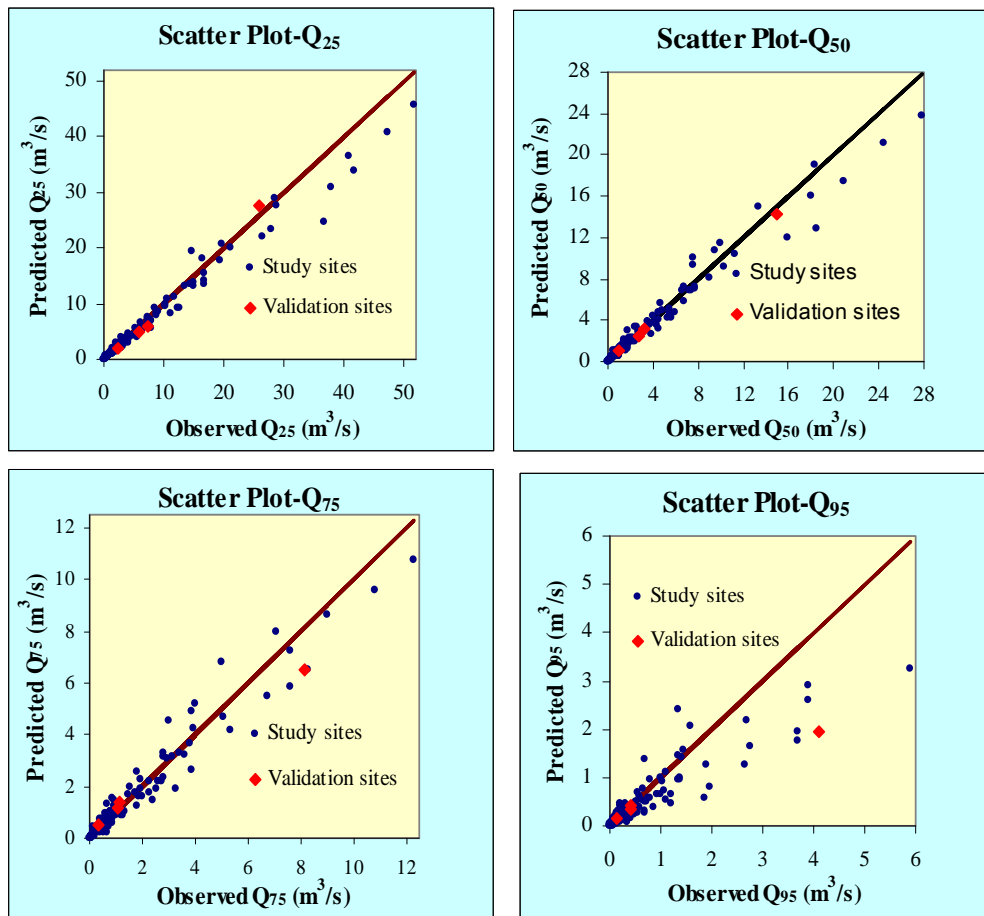


Figure 4.10: Scatter Plots Mean Flow Model

4.3.6 Model Validation

Model validation was carried out on four independent river catchments which were not used in the calibration of the above models. Record lengths, other associated physiographic and climatic characteristics for these stations are summarised in **Table 4.4**. These validation sites are located in different river basins; hence they cover a wide geographic region. **Figure 4.11** depicts the agreement between the observed and the predicted/estimated FDCs. The MF-Model performs better than the AREA-SAAR Model. Overall, the agreement between the observed and the estimated FDCs for the MF model was very good in all four cases. At three sites Q_p estimates with AREA-SAAR model are consistently greater than Q_p observed, particularly at the high-flow end of the FDCs. However, both models predict a slightly better estimate at the low-flow end of the curves.

The regional regression estimator Q_p , based on equations (4.4), (4.5) and (4.6) contains substantial variability due to the inevitable errors associated with the regression models; the sampling errors that arise from fitting the models to short, cross-correlated (in space) and uncorrelated (in time) streamflow sequences; and finally, to the unavoidable errors associated with all streamflow measurements.

Table 4.4: Catchment characteristics for the selected Validation Sites

Data Name	Notation	Hyd. Stn. 14019	Hyd. Stn. 23005	Hyd. Stn. 06013	Hyd. Stn. 15003
Catchment area (km ²)	AREA	1669	62	308	298
Mean annual rainfall (mm)	SAAR	862	1253	873	933
Mean Annual Flow (m ³ /s)	MF	20.20	1.93	4.25	6.16
Record Length (year)	L	26	24	29	33
50%ile Flow (m ³ /s)	Q ₅₀	15	0.998	2.73	3.27
95%ile Flow (m ³ /s)	Q ₉₅	4.12	0.135	0.43	0.43

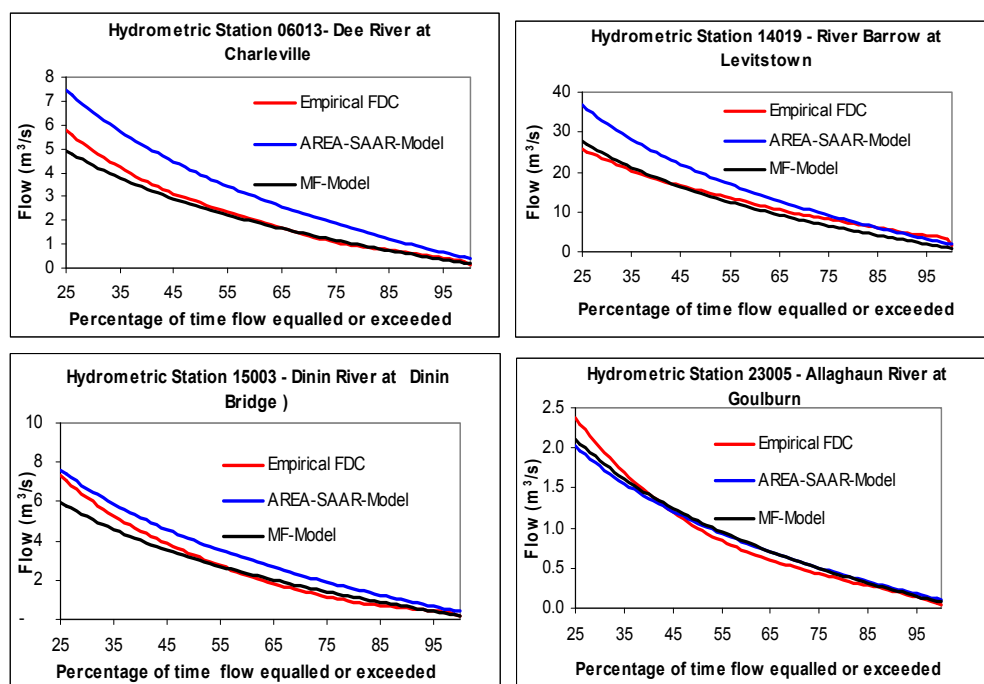


Figure 4.11: Observed and predicted FDCs

4.4 RESULTS SUMMARY AND DISCUSSIONS

The following conclusions can be drawn from the above study:

- (i) Given the complex shape of the observed FDC and the higher variability in the high-flow sections of the FDCs, this study focused on modelling of only the lower three-quarter section of FDC (25%ile to 99.99%ile). It was found that a 2-parameter logarithmic type model provides a good approximation to the lower three-quarter part of the daily FDCs for almost all of the sites used in this study. The model parameters are found to be strongly correlated (the parameter '*b*' is approximately 4.6558 times of the parameter '*a*'). Based on this, the two-parameter FDC model has been approximated by a single parameter model. This approximation of parameter '*b*' was found to be more reliable than estimating it from a catchment physiographic and climatic characteristics based regression procedure.
- (ii) The parameter of the proposed model has been estimated from the easily measurable/obtainable catchment physiographic and climatic characteristics, such as catchment areas (AREA), mean annual rainfall (SAAR) and mean annual potential evapotranspiration. Two alternative regression based models were proposed for estimating the parameter '*a*' namely (i) AREA-SAAR Model and (ii) MF-Model.
- (iii) The AREA-SAAR Model under-estimates the Q_{95} flows by 7.6% while the MF-Model under-estimates Q_{95} by 12.12%. They both perform reasonably well for 25%, 50% and 75%ile flow estimations, but less well for the 95%ile flow estimation.
- (iv) The proposed model provides a reasonably satisfactory basis for the estimation of low-flows for unguaged catchments in Ireland. However, care should be taken when applying the developed models outside the range of catchment descriptors used in the study and in special situations such as karst.

- (v) Further improvement of the model performance can be obtained by incorporating more gauging sites and additional catchment characteristics in estimating model parameter. It is recommended that 2km x 2km grid based maps of 'Potential Evapotraspiration (PE)' and Net Annual Rainfall (NAR) be prepared for Ireland to assist in estimating the model parameter.

5 LIMITATIONS OF PERIOD-OF-RECORD FLOW-DURATION CURVE (FDC) AND ITS SENSITIVITY TO RECORD LENGTHS

5.1 PERIOD-OF-RECORD FDC AND ITS LIMITATIONS

Although FDCs have a long and rich history in hydrology, they are sometimes criticized because, traditionally, their interpretation depends on the particular period of records on which they are based on (Searcy, 1959; Vogel and Fennessey, 1994; Hughes and Smakhtin, 1996; and Smakhtin et al., 1997). A period-of-record (POR) FDC represents the exceedance probability of streamflow over a long period of time. This interpretation can be quite useful, as long as the period of record used to construct the FDC is long enough to provide the 'limiting' distribution of streamflow, or if the period of record corresponds to a particular planning period or design life. However, in many countries, for a significant part of the gauged catchments, the records are shorter than this recommended period. Vogel and Fennessey (1994) explained that the lower tails of such FDCs are highly sensitive to the particular period of record used. Brogan and Cunnane (2006) showed that the POR Q_{95} flow is not necessarily a reliable guide for dry year conditions as flow could be less than full record Q_{95} for up to 70 days during a very dry year (in the context of Irish catchments). This condition may not be ideal to maintain the required aquatic ecological environment for some species to survive.

Because of the above limitations, engineers are always reluctant to use the POR FDC. In order to overcome this, Vogel and Fennessey (1994) suggested a different interpretation of FDC. They considered FDCs for individual years and treated those annual FDCs in the way similar to a sequence of annual flow maxima or minima. Each annual flow-duration curve (AFDC) represents the exceedance probability of the 365 observed values of daily streamflow. From AFDCs, one can easily infer the median AFDC from a group of empirical FDCs. The median AFDC is a hypothetical AFDC that provides a measure of central tendency, describing the annual streamflow regime for a typical hydrological year.

Engineers often wish to estimate quantiles of daily streamflows for use in hydrologic design and planning. The annual-based interpretation of FDCs allows confidence

intervals and return periods to be assigned to FDCs. FDCs can be constructed so as to provide a generalized description of hydrologic frequency analysis using average recurrence intervals (e.g. T-year FDC; Vogel and Fennessey, 1994). Such FDCs provide a description of the frequency and magnitude of the entire continuum of daily streamflows ranging from the T-year annual maximum flood flow to the T-year annual minimum low flow.

5.2 COMPARISON OF PERIOD OF RECORD AND ANNUAL FLOW DURATION CURVES FOR THE IRISH RIVER CATCHMENT

In order to examine the year to year hydrologic variability on low-flows in the Irish context, an examination of the POR FDC for a river gauging station located on the River Suir at Clonmel was carried out. The mean daily flow records for this station were available for a period from 1953 to 2001 and were obtained from the OPW hydrodata website. The river has an upstream catchment area of 2,144km² at Clonmel, a long-term average annual rainfall of 1,125 mm and a mean daily flow of 49.31m³/s. The estimated POR Q₉₅ flow for this station is 11.66m³/s (specific 95%ile flow, (q₉₅) of 0.23m³/s/km²). The annual 95%ile flows from all available year's records have also been estimated. **Table 5.1** presents a summary of these estimates for the River Suir at Clonmel.

Table 5.1: Comparison between POR and Annual FDCs for River Suir at Clonmel

Record length	Long-term average Mean daily flow (MDF) (m ³ /s)	POR Q ₉₅ (m ³ /s)	1975 - AFDC		1976 - AFDC	
			AFDC Q ₉₅ (m ³ /s)	Duration for which mdf was below POR Q ₉₅	AFDC Q ₉₅ (m ³ /s)	Duration for which mdf was below POR Q ₉₅
1953 – 2001 (49 years)	49.31	11.66	8.14	30/7/1975 - 16/9/1975 (49 days)	6.53	23/7/1976 24/9/1976 (64 days)

Figure 5.1 presents the observed mean daily flows for the period of records along with the POR FDC. The estimated POR and annual 95%ile flows are also included in this figure. It can be seen from this figure that the annual Q₉₅ flows were lower than the POR estimate for at least 15 years in the 49 years of observed flow records. This can be expected due to the year-to-year hydrologic variability. The POR Q₉₅ flow was not significantly exceeded for periods of 49 and 64 days during the driest years of 1975 and 1976 respectively (**Figure 5.2**). The estimated annual Q₉₅ flows for these years are 8.14 and 6.53m³/s respectively. These are

approximately 30.19% and 43.90% lower than the POR-Q₉₅ flow respectively. This suggests that if a wastewater treatment plant is designed for the POR-Q₉₅ flow, the receiving water's assimilative capacity would be overestimated and the receiving water's ecological status might not be protected from the worst case scenario, particularly during the long dry periods of 1975 and 1976. **Figure 5.3** illustrates the annual variability of the AFDC- Q₉₅ flows with respect to the POR-Q₉₅ flow.

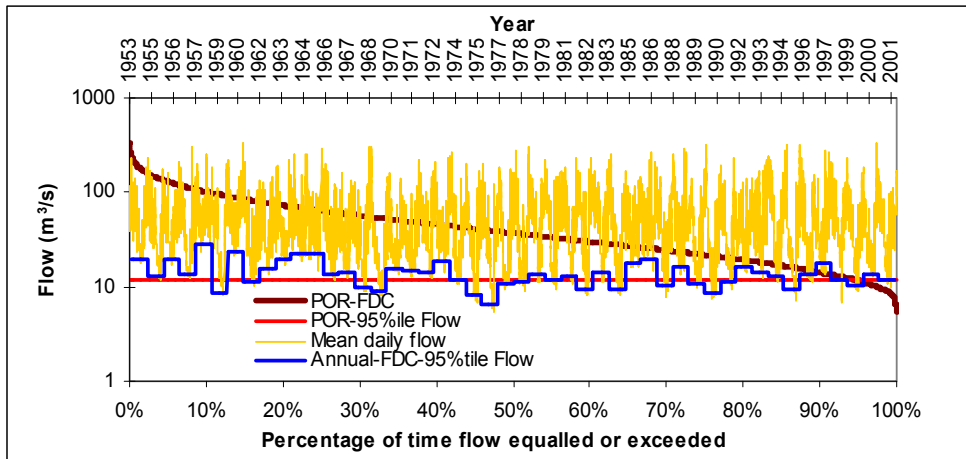


Figure 5.1: Plots of mean daily flows and comparison of POR and Annual 95%ile flows for River Suir at Clonmel (Hydrometric station No. 16011)

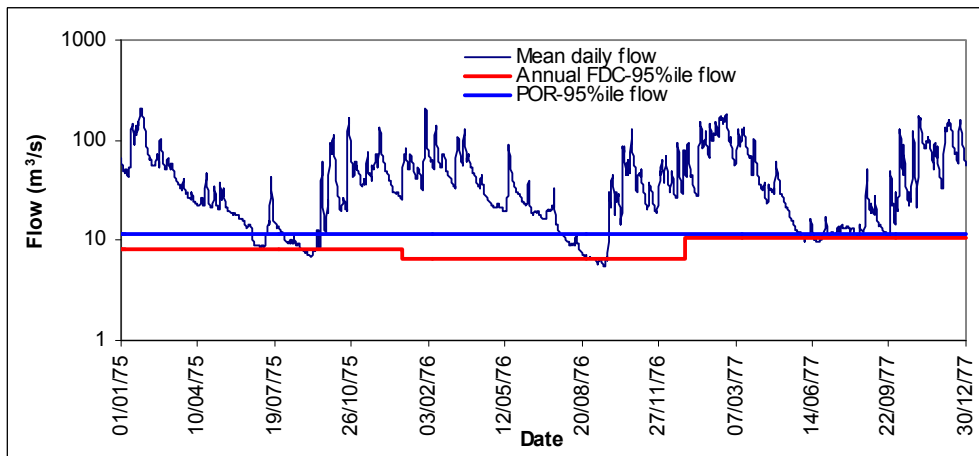


Figure 5.2: Plots of mean daily flows and comparison of POR and Annual 95%ile flows for River Suir at Clonmel (Hydrometric station No. 16011) for the period of 1975 to 1976

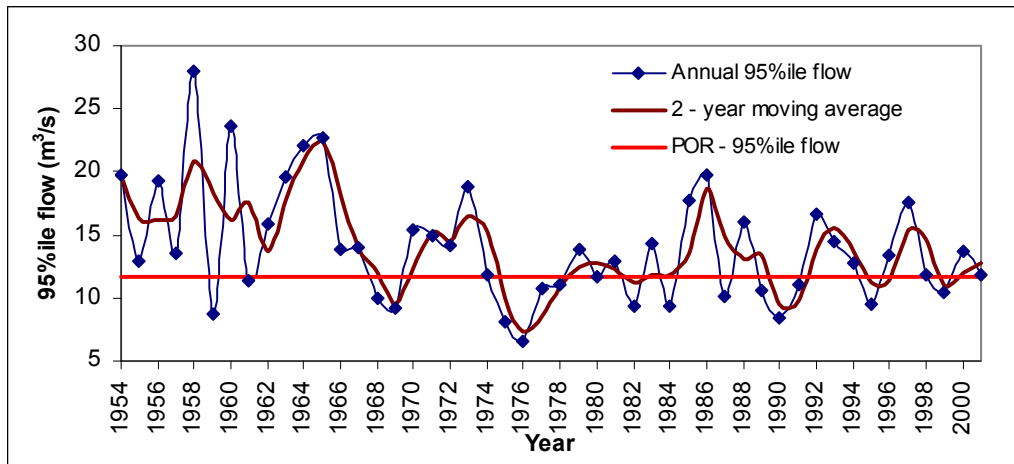


Figure 5.3: Interannual variation of 95%ile flows with respect to POR value for River Suir at Clonmel (Hydrometric station No. 16011)

Furthermore, an examination of the sensitivity of the shape of the FDC to record lengths, particularly at the lower tail of the curve, has been carried out by comparing the POR FDC with the FDCs constructed for two sub-periods of the POR for the hydrometric station located at Portarlinton on the River Barrow. At this location, the River Barrow has an upstream catchment area of 405 km². Mean daily flow records for this station were available from OPW for a period of 45 years (1956-2000). **Figure 5.4** compares the POR- FDC at this site with the FDCs for two sub-periods of 1956 –1978 (23 years) and 1979-2000 (22 years). **Figure 5.4** illustrates how sensitive the lower tail of an FDC can be to the chosen period of record. The period of record 1956-1978 contains the 1975 and 1976's droughts that were more severe than any drought experienced over the 1979-2000 period, hence the FDC for these two periods are quite different. The AFDC for the driest year of 1976 falls below the POR and other two sub-period FDCs for the entire percentile durations. **Table 5.2** presents the estimated Q₉₅ for various periods of record lengths for the River Barrow at Portarlinton.

Table 5.2: Sensitivity of record lengths to FDC for River Barrow at Portarlinton

Record length	Long term average mean daily flow (MDF) (m ³ /s)	POR Q ₉₅ (m ³ /s)	Sub-period 1 1956 -1978	Sub-period 2 1979 -2000	AFDC - 1976
			Q ₉₅ (m ³ /s)	Q ₉₅ (m ³ /s)	Q ₉₅ (m ³ /s)
1956 – 2000 (45 years)	6.45	0.53	0.428	0.648	0.155

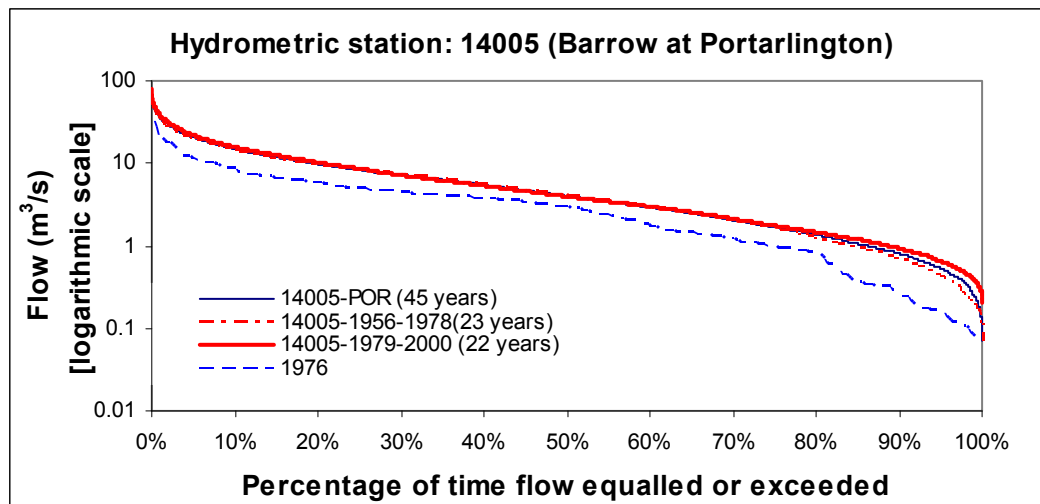


Figure 5.4: Comparison of FDCs for various record lengths for River Barrow at Portarlington

The above findings make it obvious why hydrologists are often reluctant to use the period-of-record FDCs, as their interpretation depends so heavily upon the selected period-of-record. Vogel and Fennessey (1994) argued that the Annual FDCs provide a solution to this dilemma. The authors found that the median annual FDC represents the distribution of daily streamflow in a ‘typical’ or median hypothetical year, and its interpretation is not affected by the observation of abnormally wet or dry periods during the period of record. As discussed above, the annual-based interpretation of FDCs allows confidence intervals and return periods to be assigned to FDCs. Since the POR FDCs often fail to provide protection for the worst case scenario, a design FDC or a low-flow index for a particular recurrence interval (e.g. 50 year return period Q_{95}) can be adopted rather than using the long-term FDC for designing a water related scheme or for maintaining stream or lake water quality.

Based on the above, frequency analysis of the AFDCs for two Irish river basins were carried out and the AFDCs for a number of recurrence intervals were developed in the present study. The procedures included: (i) development of empirical AFDCs for all available record years, (ii) extracting annual series of low-flow indices from the AFDCs for a number of selected exceedance percentages (16 No.) i.e. 0.25, 0.35, 0.45, 0.99, (iii) fitting the annual low-flow time series to a suitable statistical distribution, (iv) estimation of associated low-flow quantile for a number of selected return periods (T), and (v) finally construction of T-year AFDC.

Table 5.3 gives some physical and climatological characteristics of two selected river basins (i) River Dee at Charleville and (ii) River Barrow at Portarlinton. Mean daily flows (MDF) for these hydrometric stations were collected from Office of Public Works (OPW) hydrodata website. MDF records for the River Deel were available for a period of 27 years (1975 – 2002), while for the River Barrow, 46 years (1955 – 2001) of records were available. All records include the driest year of 1976.

Table 5.3: Catchment characteristics for hydrometric stations 06013 and 14005

Station No.	River and location	Data Period	No. of Years	Area (km ²)	BFI	SAAR (mm)	Mean Ann. Flow (m ³ /s)	POR – Q ₉₅ (m ³ /s)	q _{min-50} year *
06013	River Dee at Charleville	1975-2002	27	307	0.617	873	4.31	0.413	0.136
14005	Barrow at Portarlinton	1955-2001	46	398	0.500	981	6.48	0.533	0.114

*Source: Brogan and Cunnane, 2005.

The annual low-flow time series for the selected durations for each station were estimated from the observed MDF records. Frequency analysis of these low-flow time series were conducted by fitting the data to EV1 (Gumbel) statistical distribution. The choice of the EV1 distribution was based on the earlier studies carried out on the annual minimum low-flow time series for Irish Rivers. A number of previous studies showed that the EV1 distribution provides a good fit to annual minimum flow data at most stations in Ireland (King 1985; Brogan and Cunnane 2006). Since the EV1 distribution is an unbounded distribution, its applicability in the low-flow frequency analysis is theoretically not justified because low-flow has a lower limit of zero flow. However, the Irish Low-flow series has skewness similar to EV1 distribution and the lack of lower bound in the low-flow time series would not have such serious effect in its frequency analysis.

In this study the EV1 distribution was also found to be a good descriptor of all the selected low-flow indices considered. **Figure 5.5** shows the probability plots and the fitted EV1 distribution to the annual time series of the low-flow indices of Q₂₅, Q₅₀, Q₇₅ and Q₉₅.

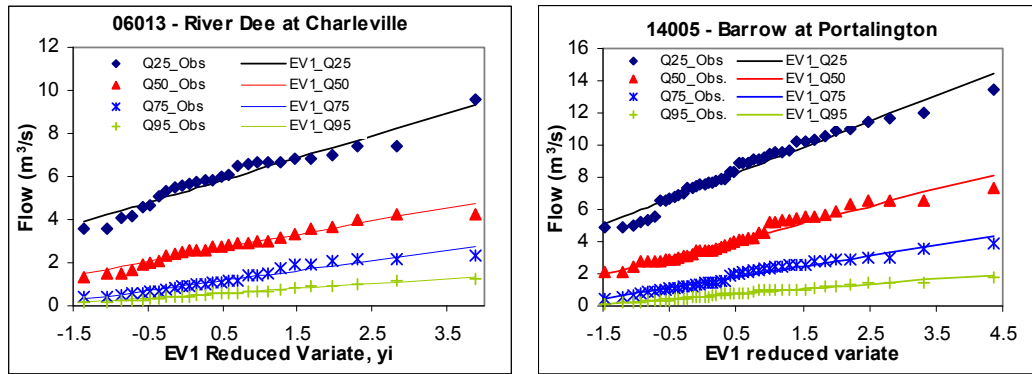


Figure 5.5: Probability Plots and fitted EV1 distribution for the annual time series of low-flow indices of Q_{25} , Q_{50} , Q_{75} and Q_{95}

Table 5.4 presents the estimated low-flow indices for the return periods of 2 and 50 years for the two river basins along with their corresponding POR estimates. These estimates are plotted in **Figure 5.6**. It can be seen from this figure that the POR-FDC has an approximate return period of 2 year which is a median year FDC. The fitting of the POR-FDC with the 2-year return period AFDC is slightly better for the larger flows than the Q_{95} flows. In both cases, the 50-year return period AFDCs fall below the POR FDCs. The estimated 50-year return period annual Q_{95} flows are 0.156 and 0.174 m^3/s for the River Dee and Barrow respectively, while the POR Q_{95} flow for these stations are 0.413 and 0.533 m^3/s . This suggests that the POR Q_{95} flow is on average 2.86 times higher than the 50 year return period annual Q_{95} flow. The estimated 50-year return period annual minimum flows for these stations are 0.136 and 0.144 m^3/s , suggesting that they are on average 1.18 times lower than the 50-year return period annual Q_{95} flow. The observed 1976 AFDC- Q_{95} flow for the River Dee and Barrow are 0.184 and 154 m^3/s respectively. This shows that the 1976 AFDC- Q_{95} has an approximate return period of 50 years at both sites.

Table 5.4: Catchment characteristics for hydrometric stations 06013 and 14005

Percentage of Time flow exceeded	Hydrometric station - 06013			Hydrometric Station - 14005		
	POR_FDC	T-year FDC		POR_FDC	T-year FDC	
		2-year	50-year		2-year	50-year
25%	5.888	5.688	3.893	8.409	8.042	5.271
30%	5.007	4.939	3.328	7.227	6.911	4.415
35%	4.283	4.291	2.952	6.294	5.996	3.694
40%	3.690	3.638	2.527	5.426	5.207	3.095
45%	3.174	3.028	1.931	4.645	4.524	2.499
50%	2.781	2.591	1.510	4.006	3.936	2.109
55%	2.393	2.152	1.082	3.431	3.397	1.657
60%	2.029	1.789	0.775	2.950	2.854	1.229
65%	1.692	1.530	0.574	2.510	2.425	0.951
70%	1.352	1.307	0.441	2.063	2.063	0.750
75%	1.081	1.109	0.306	1.698	1.706	0.570
80%	0.888	0.952	0.241	1.367	1.369	0.364
85%	0.730	0.803	0.183	1.061	1.115	0.275
90%	0.582	0.674	0.171	0.806	0.913	0.226
95%	0.413	0.545	0.156	0.533	0.707	0.174
100%	0.156	0.440	0.106	0.071	0.485	0.069

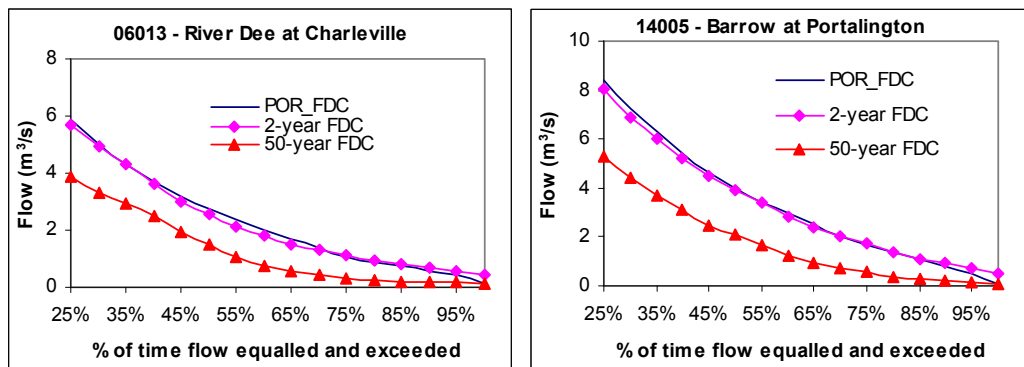


Figure 5.6: Plots of Period of Record FDC and the 2 and 50 year return periods AFDCs

The above findings suggest that, designing a water resource scheme for the POR record low-flow indices will provide protection only for the low-flow frequency of 2 years. It is, therefore, important to review the traditional approach of designing of many water resources schemes based on the POR low-flow estimates. The estimates of AFDC based low-flow indices with an appropriate frequency should be used/adopted rather than the POR based estimates in designing the water resources scheme. It should be mentioned here that Irish Office of Public Works recognised this as early as the 1970's and they provided tables of AFDC values and also plots of these (Cunnane and Martin, 1977).

5.3 SENSITIVITY OF LOW-FLOW INDICES TO SAMPLE LENGTHS FOR IRISH RIVER CATCHMENTS

5.3.1 Introduction

The primary limitation of short-record data is that the data are unlikely to capture the long-term natural variability of the catchment under investigation. In other words, due to climatic variability and other sources of variability that occur over short time scales, low-flow characteristics estimated from a few years of stream flow records deviate from the long-term average. However, in many countries, for a significant part of the gauged catchments, the records are shorter than this recommended period.

This section examines the effect of climate variability in low-flows in Ireland and determines the minimum length of records that are to be required to obtain a period-of-record equivalent low-flow estimate.

5.3.2 Methodology

A series of resampling experiments has been performed to assess the sensitivity of empirical FDCs to sample length. The analysis consisted of the following steps:

- (a) From the L years of mean daily flows of the historical sample, $m = L - l + 1$ consecutive overlapping sub-samples with length equal to l years were extracted,
- (b) Empirical FDCs of each sub-sample were constructed and compared with the empirical POR-FDC.

The comparison of step (b) was performed for 4 arbitrarily selected flow-durations (d) of 25, 50, 75 and 95 percentiles. Twenty five sub sample lengths ranging from 1 to 25 years were considered. This was based on the available flow records for ten river basins selected for this experiment.

The comparison between the POR and resampled FDCs is performed by means of several statistical indices as discussed below:

- (i) Relative Error (with respect to POR) for site i , sample length l and duration 'd'

$$: \quad \varepsilon_{i,l}^j(d) = \left(\frac{Q_{i,l}^j(d) - Q_{i,POR}(d)}{Q_{i,POR}(d)} \right) , \quad (5.1)$$

- (ii) Mean Relative Error for site i , sample length l and duration 'd' :

$$\bar{\varepsilon}_{i,l}(d) = \frac{1}{m} \sum_{j=1}^m \varepsilon_{i,l}^j(d) , \quad (5.2)$$

- (iii) Standard deviation of relative error for site i , sample length l and duration 'd':

$$\sigma_{\varepsilon,i,l}(d) = \sqrt{\frac{1}{m-1} \sum_{j=1}^m \left(\varepsilon_{i,l}^j - \bar{\varepsilon}_{i,l}(d) \right)^2} , \quad (5.3)$$

- (iv) Regional average relative error for sample length l and duration 'd':

$$\varepsilon_{R,l}(d) = \frac{1}{N} \sum_{i=1}^N \bar{\varepsilon}_{i,l}(d) , \text{ and} \quad (5.4)$$

- (v) Regional average standard deviation of relative error for sample length l and duration 'd':

$$\sigma_{\varepsilon,R,l}(d) = \frac{1}{N} \sum_{i=1}^N \sigma_{\varepsilon,i,l}(d) \quad (5.5)$$

where,

$j= 1$ to m ($m=$ no. samples with length l drawn from the period of records)

$Q_{i,l}^j(d) =$ 'd'-percentile flow for the j^{th} sample of record length ' l ' for site i

$Q_{i,POR}(d) =$ 'd'-percentile flow for the period of record for site i

$N=$ no. of sites in the region (or No. of sites considered in the experiment).

The mean relative error ($\bar{\varepsilon}_{i,l}(d)$) and the standard deviation of relative error ($\sigma_{\varepsilon,i,l}(d)$) computed as shown in equations (5.2) and (5.3) represents the errors (between the period-of-record and short sample FDCs) associated with site i and sample length l , and the average of the N values of $\bar{\varepsilon}_{i,l}(d)$ and $\sigma_{\varepsilon,i,l}(d)$ represent corresponding regional average errors.

In addition to the regional average mean relative error, another index, such as, regional average absolute relative error was also used. The regional average relative error measures the tendency of FDC estimates from short samples to be uniformly too high or too low across the whole region, while the regional average absolute relative error measures the tendency of FDC estimates from the short sample to be consistently high at some sites and low at others with respect to POR estimates. This occurs in a heterogeneous region, in such cases the absolute mean relative error indicates the magnitude of the relative error at a typical site and is more useful than the mean relative error, in which the contributions of negative and positive errors may cancel out to give a misleading small value of error. In a homogeneous region, however, the error could be expected to be the same at each site, and therefore both measures should be equal.

5.3.3 Data

Mean daily flow (MDF) records for 10 Irish streamgauges were used in this sensitivity analysis. The location details of these gauging sites, record lengths and some catchment characteristics are given in **Table 5.5**. All stations have at least 25 years of records (ranging from 25 to 48 years) with an average record length of 35 years. The catchment areas range from 309 to 2,144 km² with a mean size of 784 km². The selected river catchments are spatially well scattered across Ireland and have different climatic and geomorphological characteristics.

Table 5.5: List of streamgauges and their associated catchment characteristics

Hydro. Station	Rivers and locations	Catchment area (km ²)	Rainfall SAAR (mm)	Record lengths [range(years)]	Mean annual flow (m ³ /s)	95%ile flow (m ³ /s)	50%ile flow (m ³ /s)
06013	Dee at Charleville	309	873	1976-2002(27)	4.25	0.413	2.781
07003	Blackwater at Castlerickard	182	809	1976-2001(26)	2.39	0.398	1.660
14005	Barrow at Portalington	405	1015	1956-1999(44)	6.41	0.533	4.006
14019	Barrow at Levistown	1697	861	1972-2001(30)	20.20	1.394	10.752
15001	Kings at Annamult	444	935	1972-2004(33)	7.02	0.568	4.088
16011	Suir at Clonmel	2144	1125	1954-2001(48)	45.28	11.649	36.867
18005	Funshion at Downing	378	1190	1972-2007(36)	8.96	2.014	6.442

Hydro. Station	Rivers and locations	Catchment area (km ²)	Rainfall SAAR (mm)	Record lengths [range(years)]	Mean annual flow (m ³ /s)	95%ile flow (m ³ /s)	50%ile flow (m ³ /s)
	Bridge						
25002	Newport at Barrington's Bridge	222	1300	1972-1996(25)	5.65	0.660	3.896
27002	Fergus at Ballycorey	564	1336	1957-2000(44)	10.00	0.689	7.776
36019	Erne at Belturbet	1492	971	1958-1997(40)	26.90	1.309	20.554

5.3.4 Results

Figures 5.7 - 5.10 illustrate the variation of low-flow estimates (Q_{95} , Q_{75} , Q_{50} and Q_{25} respectively) with various sample lengths and compare these estimates with the period of record estimates for all sites studied. The rightmost point in each graph is the period-of record estimate. A generalised over- and under-estimation of the selected low flow indices can be seen for the shorter durations and the flow estimates converge toward the period of record estimates as the record lengths increases. This was expected, as short-term FDCs are affected significantly by the observation of abnormally wet and dry periods during these periods, while the longer durations FDCs are constructed from the combined streamflow records (both dry and wet years), thus consequently reduce the sensitivity of the very wet and dry period records to any associated long-term low flow indices. It can be seen from the above mentioned figures that at least 15 to 20 years of observed streamflows are required to obtain a reliable estimate of the POR FDCs and associated low flow indices. **Table 5.6** presents the period-of-record and equivalent short sample estimates of the Q_{95} and Q_{50} flows for all stations. The requirement of this longer record length in the Irish context can be attributed to the significant irregular pattern in decadal climate variability and its impacts on streamflows in contrast to the usual interannual and seasonal variability. **Figure 5.11** illustrates the temporal variation of AFDC- Q_{95} estimates for two river gauging sites of 27002 (River Fergus at Ballycorey) and 14005 (River Barrow at Portarlinton).

Table 5.6: Comparison of POR and equivalent short sample length estimates of Q_{95} and Q_{25} for all sites

Hydro. Station	Record lengths (years)	POR estimates		Equivalent short sample estimates			
		95%ile flow (m^3/s)	50%ile flow (m^3/s)	95%ile flow		50%ile flow	
				Flow (m^3/s)	Sample length (years)	Flow (m^3/s)	Sample length (years)
06013	27	0.413	2.781	0.378	15	2.707	15
07003	26	0.398	1.660	0.376	15	1.542	15
14005	44	0.533	4.006	0.486	24	3.936	20
14019	30	1.394	10.752	1.254	15	11.308	24
15001	33	0.568	4.088	0.568	15	4.17	20
16011	48	11.649	36.867	11.70	20	35.82	20
18005	36	2.014	6.442	1.967	15	6.633	15
25002	25	0.660	3.896	0.777	15	4.074	15
27002	44	0.689	7.776	0.582	20	7.704	20
36019	40	1.309	20.554	1.125	20	19.918	20

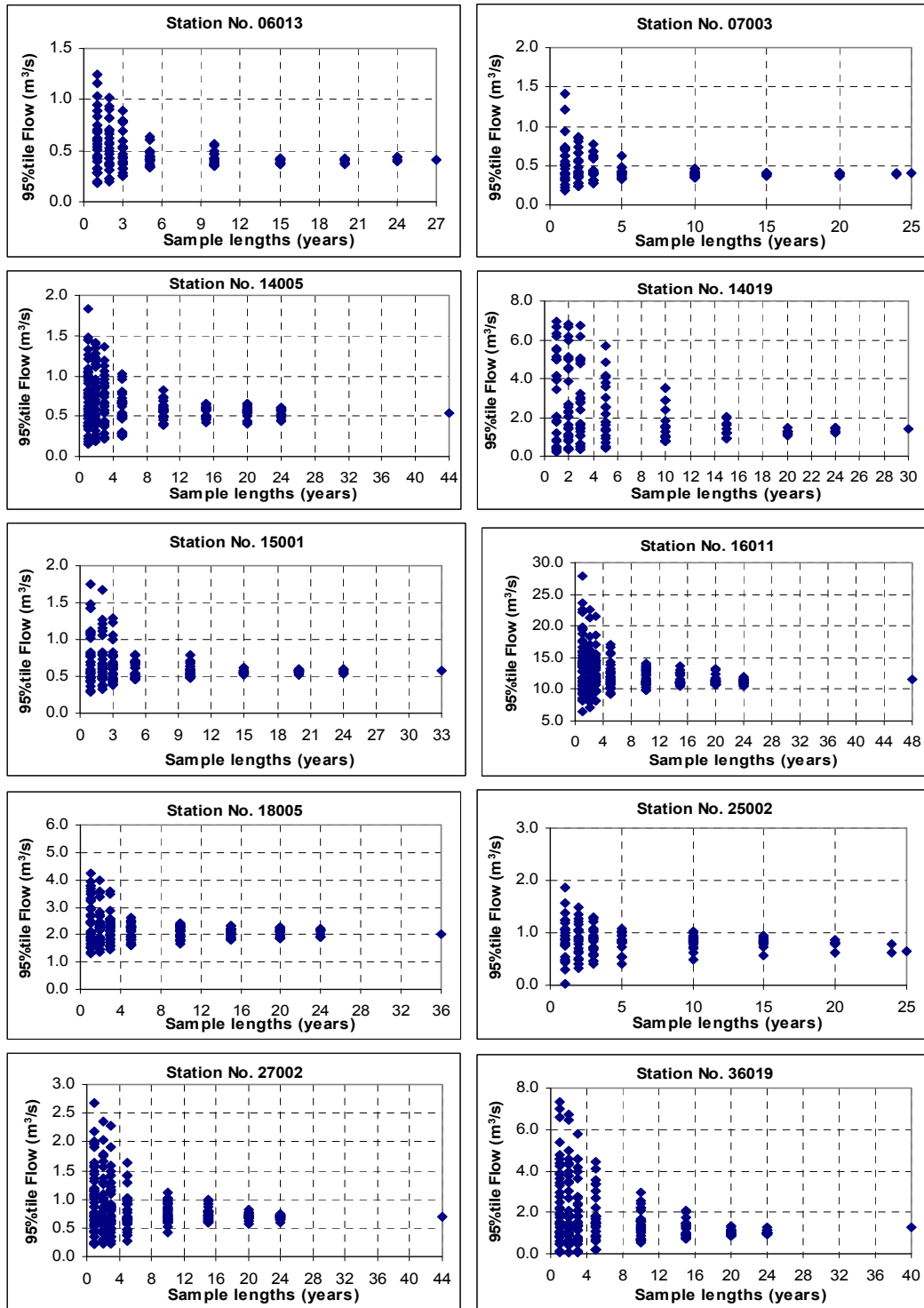


Figure 5.7: Comparison of period-of-record and resampled estimates of Q_{95}

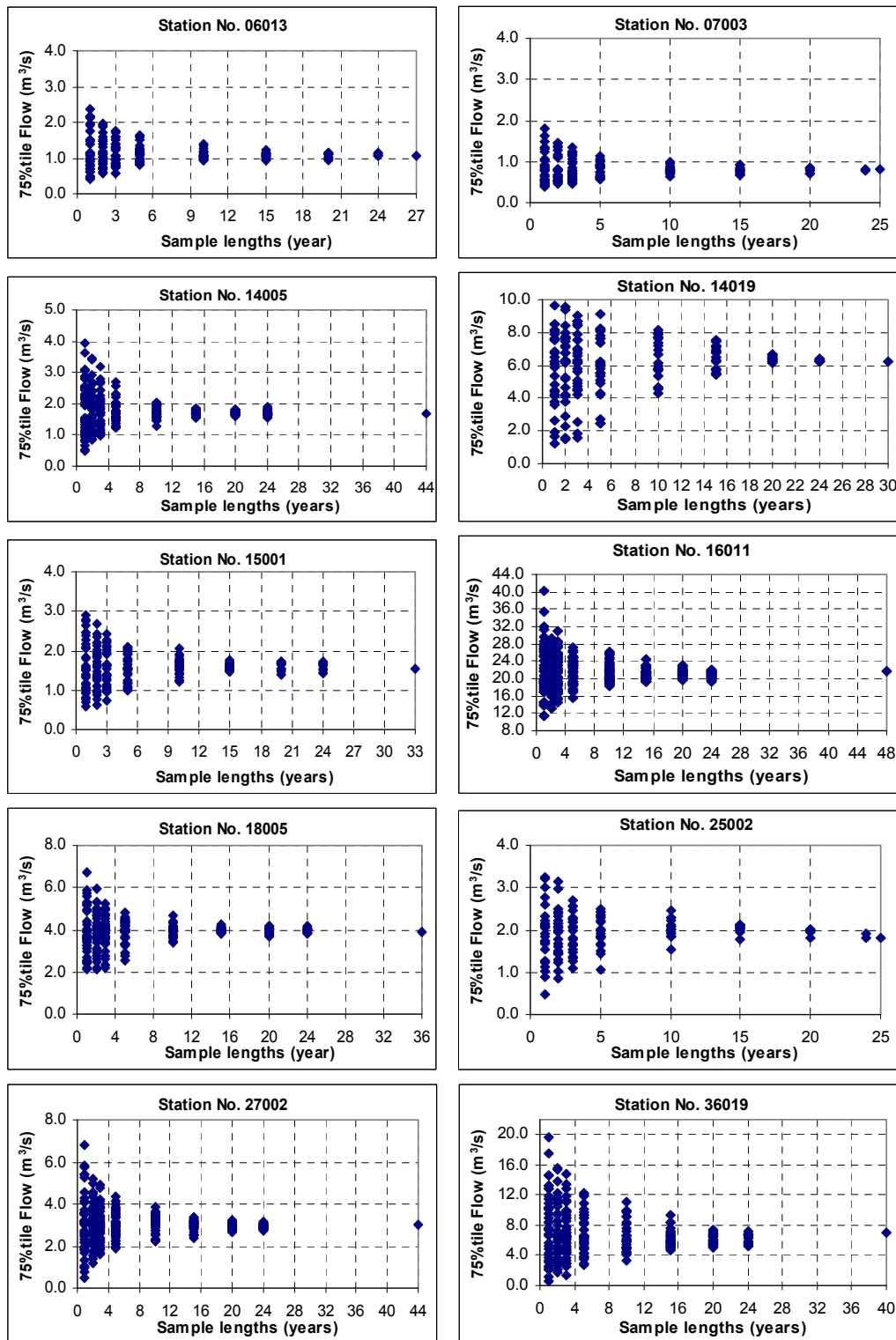


Figure 5.8: Comparison of period-of-record and resampled estimates of Q_{75}

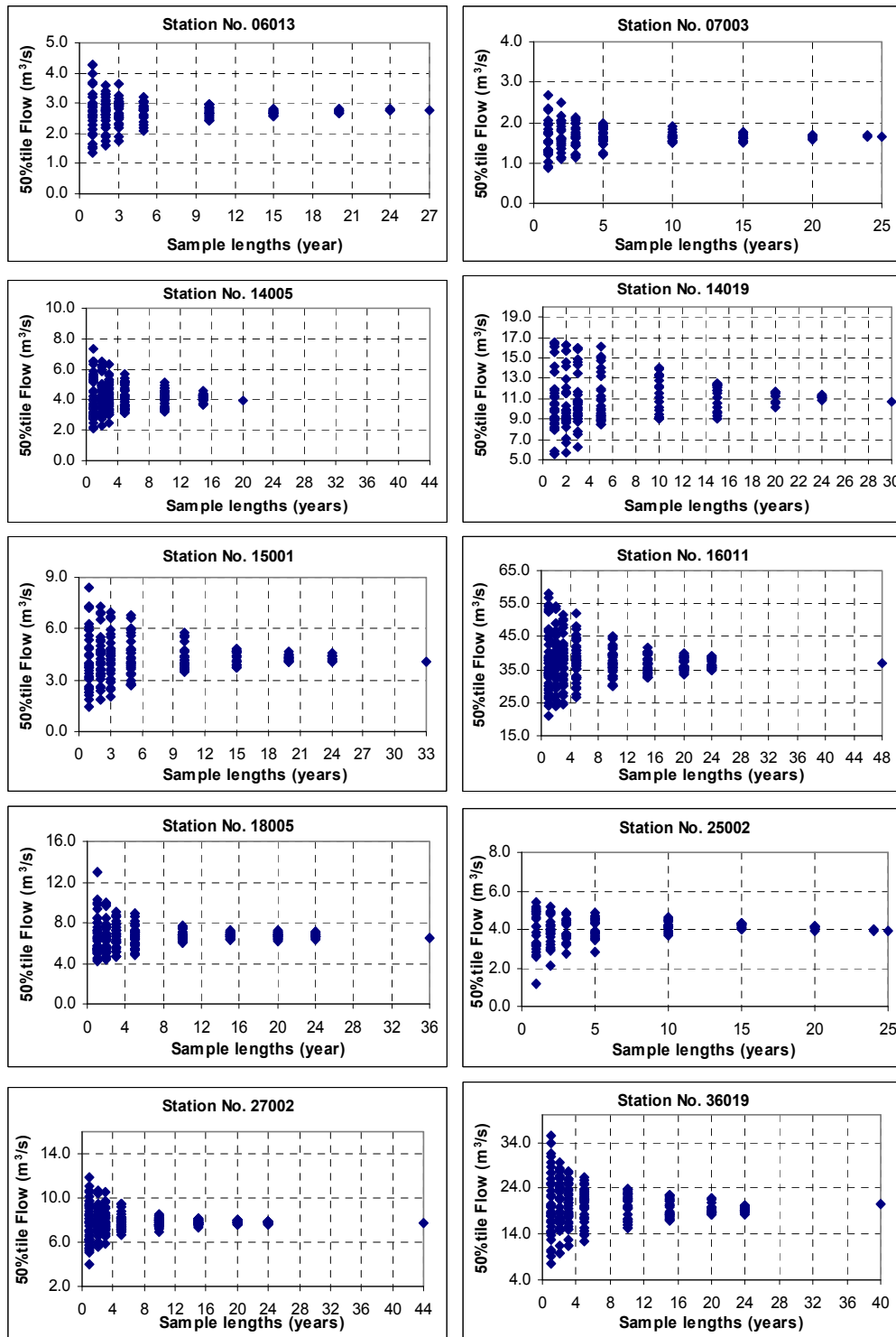


Figure 5.9: Comparison of period-of record and resampled estimates of Q_{50}

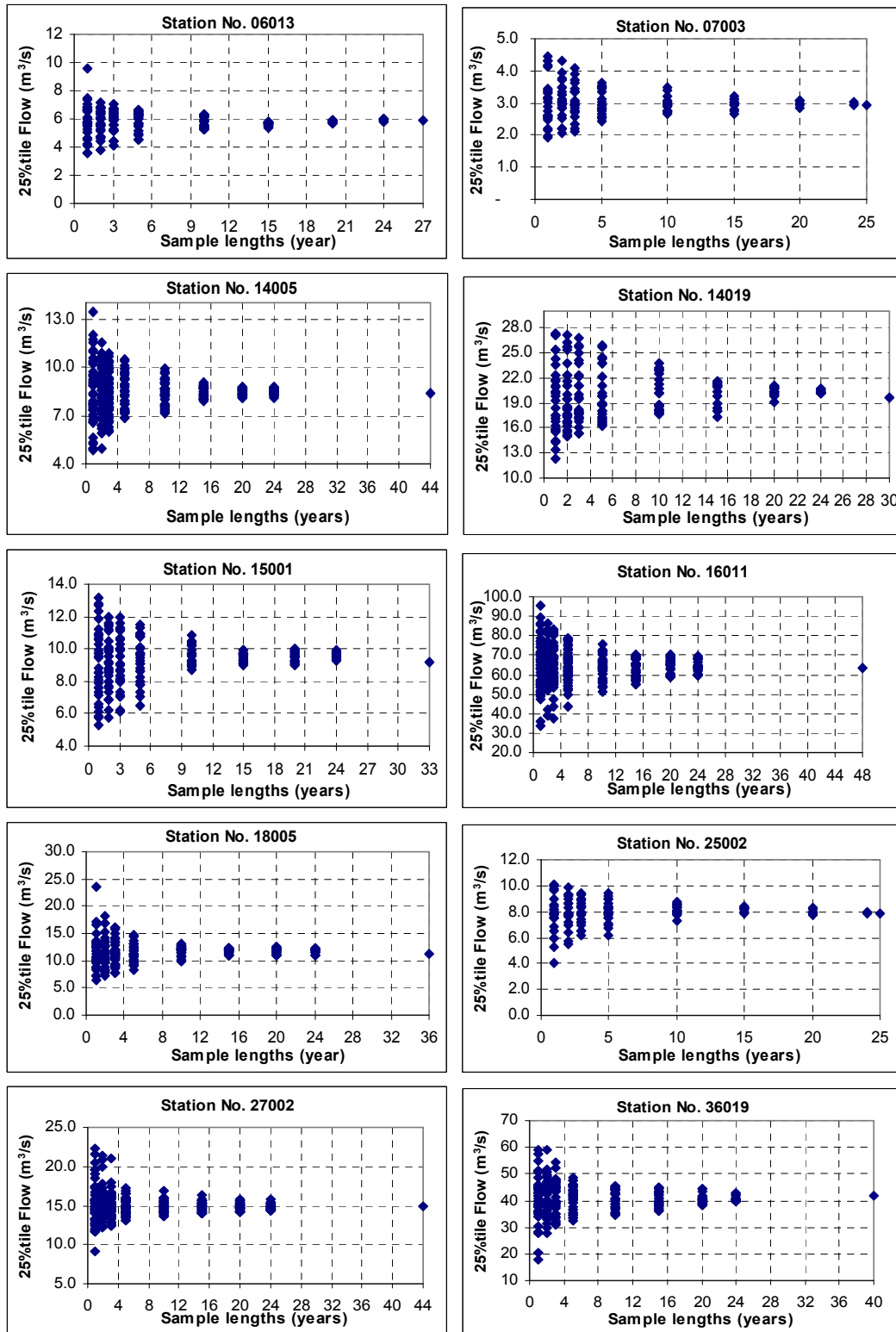


Figure 5.10: Comparison of period-of record and resampled estimates of Q_{25}

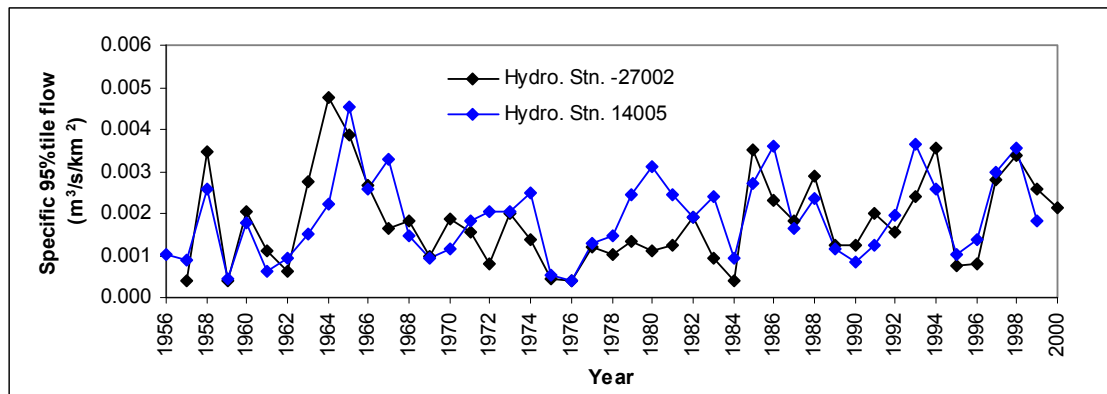


Figure 5.11: Temporal variation of AFDC- Q95 estimates for the river gauging sites- 27002 and 14005.

The regional average relative deviations/errors of FDC estimates (for 25, 50, 75 and 95 percentiles) from various shortened samples with respect to the period-of-record estimates are presented in **Table 5.7**. These results are graphically illustrated in **Figures 5.12 – 5.14**. The results show a general decrease in relative errors with the increase in sample lengths. They also show that the errors are smaller for the low-duration flows (i.e. high flows). For example, the regional average mean relative errors for the Q_{25} and Q_{95} flow estimates from 15 years records, with respect to 35 years of period-of-record estimates are 0.6% and 0.9% respectively.

Table 5.7: Estimated regional average relative errors (mean, absolute mean and standard deviation) of short resampled estimates of low-flows with respect to the POR estimates for all sample lengths.

Sample length (years)	Mean relative errors over the POR estimates (%)				Absolute mean relative errors over the POR estimates (%)				Standard dev. of relative error (%)			
	Q_{25}	Q_{50}	Q_{75}	Q_{95}	Q_{25}	Q_{50}	Q_{75}	Q_{95}	Q_{25}	Q_{50}	Q_{75}	Q_{95}
1	0.3%	0.5%	5.4%	53.3%	17.8%	24.2%	36.9%	74.2%	22.7%	30.2%	45.7%	84.4%
2	0.5%	0.8%	3.2%	34.2%	13.8%	18.2%	28.1%	55.6%	17.5%	22.9%	34.9%	69.0%
3	0.6%	1.2%	2.6%	23.1%	12.5%	16.1%	24.3%	43.8%	15.5%	20.1%	29.8%	56.7%
4	0.7%	1.6%	1.9%	17.4%	11.2%	14.2%	20.7%	36.3%	13.7%	18.0%	25.7%	47.4%
5	0.6%	1.8%	1.5%	14.6%	10.2%	12.9%	18.4%	31.6%	12.5%	16.1%	22.6%	38.7%
6	0.9%	2.0%	1.2%	12.3%	9.2%	11.6%	16.5%	28.6%	11.3%	14.5%	20.1%	34.4%
7	1.1%	2.1%	1.3%	10.7%	8.5%	10.9%	15.3%	26.4%	10.5%	13.4%	18.6%	31.5%
8	1.6%	2.7%	3.8%	9.1%	7.0%	9.1%	12.2%	19.1%	8.3%	10.8%	14.1%	21.8%
9	1.1%	2.2%	1.7%	7.9%	7.3%	9.7%	13.5%	22.3%	8.5%	11.3%	15.8%	27.0%
10	1.0%	2.2%	1.7%	6.1%	6.8%	9.1%	12.4%	20.6%	7.8%	10.5%	14.4%	24.1%
11	0.9%	2.0%	1.6%	4.1%	6.2%	8.3%	10.8%	18.4%	6.8%	9.3%	12.5%	21.0%
12	0.8%	1.8%	1.3%	2.6%	5.7%	7.7%	10.0%	16.5%	6.1%	8.3%	10.9%	18.3%
13	0.6%	1.6%	1.1%	1.7%	5.4%	7.2%	9.4%	15.0%	5.5%	7.5%	9.8%	15.9%
14	0.7%	1.5%	1.1%	-0.2%	4.8%	6.4%	8.1%	11.9%	4.6%	6.3%	7.9%	11.7%

Sample length (years)	Mean relative errors over the POR estimates (%)				Absolute mean relative errors over the POR estimates (%)				Standard dev. of relative error (%)			
	Q ₂₅	Q ₅₀	Q ₇₅	Q ₉₅	Q ₂₅	Q ₅₀	Q ₇₅	Q ₉₅	Q ₂₅	Q ₅₀	Q ₇₅	Q ₉₅
15	0.6%	1.4%	0.8%	0.9%	4.8%	6.2%	8.1%	12.7%	4.7%	5.9%	8.1%	12.7%
16	0.6%	1.4%	0.6%	0.3%	4.5%	5.8%	7.6%	11.9%	4.5%	5.4%	7.5%	11.6%
17	0.7%	1.4%	0.5%	-0.3%	4.2%	5.3%	7.0%	10.9%	4.3%	4.7%	6.7%	10.2%
18	0.8%	1.4%	0.3%	-0.9%	3.9%	4.8%	6.5%	10.0%	4.0%	4.3%	6.2%	8.8%
19	0.9%	1.4%	0.0%	-1.3%	3.6%	4.4%	6.2%	9.6%	3.7%	3.8%	5.8%	7.9%
20	1.0%	1.4%	-0.2%	-1.7%	3.4%	4.2%	6.0%	9.4%	3.4%	3.6%	5.6%	7.6%
21	1.1%	1.4%	-0.2%	-1.8%	3.3%	4.0%	5.6%	8.7%	3.2%	3.3%	5.3%	6.8%
22	1.2%	1.4%	-0.1%	-1.5%	3.2%	3.7%	5.4%	8.0%	2.9%	3.0%	5.0%	6.5%
23	1.3%	1.4%	-0.2%	-1.3%	2.9%	3.5%	4.8%	7.8%	2.5%	2.6%	4.3%	6.2%
24	1.1%	1.2%	-0.5%	-1.6%	2.7%	3.2%	4.2%	7.5%	2.3%	2.5%	4.2%	6.7%
25	1.0%	0.9%	-1.0%	-2.1%	2.3%	2.8%	3.5%	5.9%	1.8%	2.0%	3.4%	4.7%

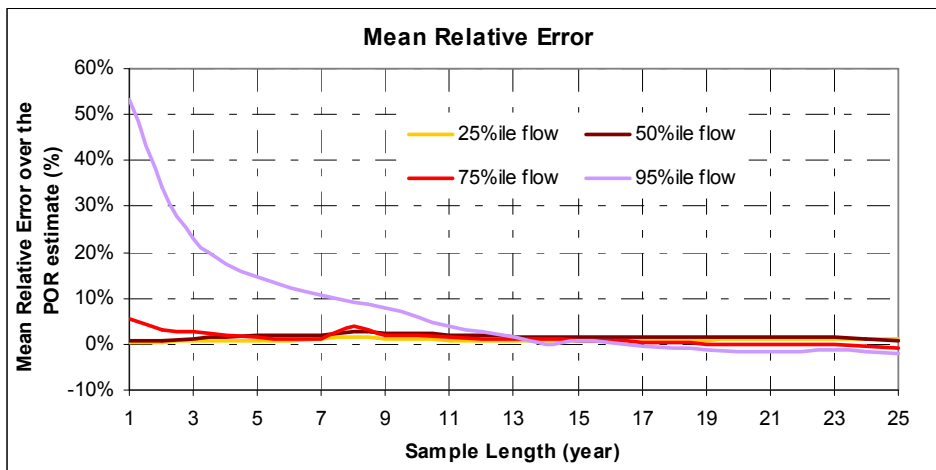


Figure 5.12: Variation of regional average mean relative errors for various sample lengths

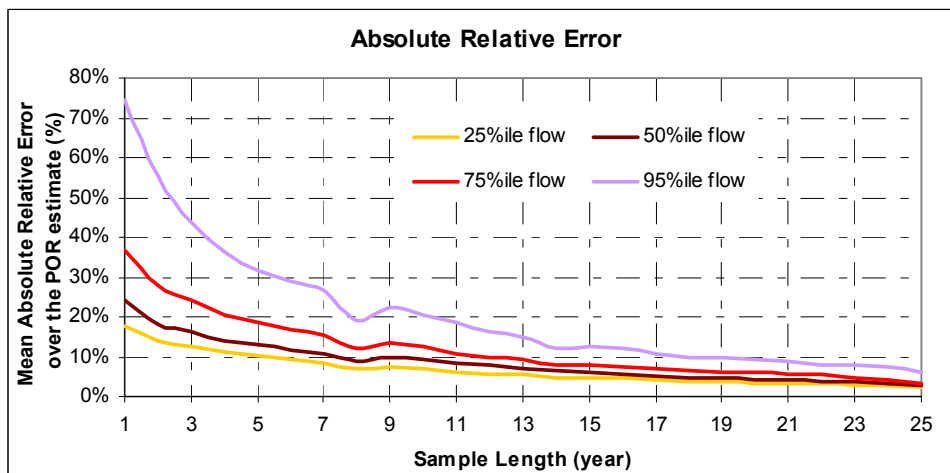


Figure 5.13: Variation of regional average absolute relative errors for various sample lengths

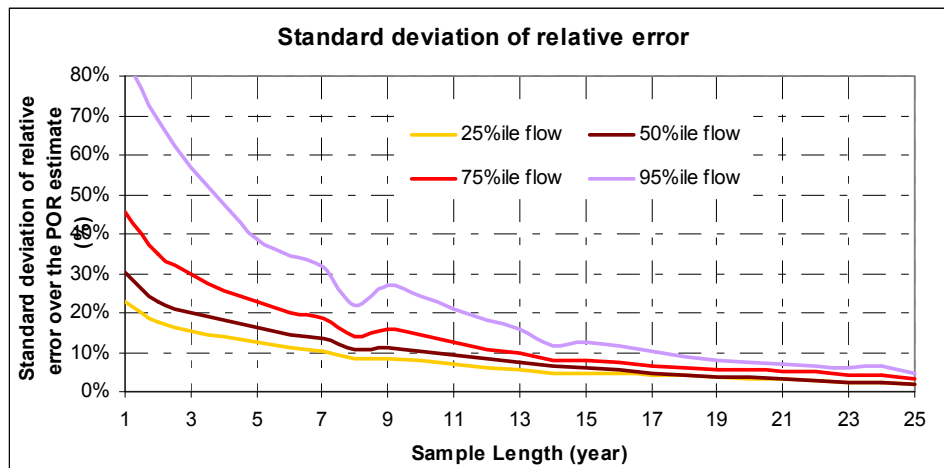


Figure 5.14: Variation of regional average standard deviation of relative errors for various sample lengths

Figure 5.12 illustrates the variation in regional average mean errors for various sample lengths. It can be seen from this graph that at least 13-15 years of records are required to have long-term equivalent low-flow estimates. However, it should be mentioned here that due to the regional heterogeneity and the interannual variability in streamflow records at a site, a frequent under-and over – estimations of POR FDCs can occur as can be seen in **Figures 5.7 – 5.10**. These positive and negative variations in flow estimates cancel out each other and give a very low regional average mean relative error. **Figure 5.13** thus illustrates the more realistic picture of relative variation at a typical site in terms of absolute relative mean error as discussed in Section 5.3.2. For example, the Q_{95} flow estimate from 10 years of records at a site in the study region could deviate (under- or over-estimation) by 20.6% from the long-term equivalent estimate (see **Table 5.7**).

5.4 ESTIMATION OF LOW-FLOWS FROM SHORT RECORD LENGTHS

As shown above estimation of low-flows from short records is not reliable and in the Irish context at least 15 to 20 years of records are required to have a long-term equivalent estimate. This is due to the fact that the short-record data are unlikely to capture the long-term natural variability of the catchments. However, in many countries, for a significant part of the gauged catchments the records are shorter than the recommended period. While these short records are unlikely to provide the full information of long records, they do provide some information which may be

used in estimating the long-term low flow characteristics for these stream gauge locations (Laaha and Bloschl, 2005).

A number of methods exist for inferring the long-term low-flow characteristics from short records. These methods all adjust low flow characteristics to longer-term climatic conditions, in some way, and are therefore referred to as climatic adjustment methods (Laaha and Bloschl, 2005). They could be used to estimate the low-flow characteristics for a site of interest. The climate adjustment methods consist of two steps: donor site selection and record augmentation. An extensive discussion on various procedures/methods for donor site selection and record augmentation methods are given in the literature review chapter (Chapter 2, Section 2.2).

It is recommended that an appropriate procedure for estimating low-flows from short records should be developed for Ireland. However, the above estimated absolute error factor, such as 20% adjustment factor, can be applied for estimating long-term equivalent Q_{95} flow from a 10 years of short records. In the case of low-flow estimates, it is generally advisable to reduce the short-sample estimate by this factor, to avoid any risk of uncertainty in design failure (such as water supply scheme or water quality management measures). A more reliable regional adjustment factor can be obtained through the above mentioned resampling experiments and by forming a larger homogeneous region.

**Part-B: Non-Stationarity in Flood Flows
and Its Effect on Flood
Frequency Growth Curves for
Irish River Catchments**

6 NON-STATIONARITY IN FLOOD SERIES, ITS CAUSES AND DETECTION METHODS

6.1 INTRODUCTION

Frequency analysis is a technique of fitting a probability distribution to a series of observations for defining the probabilities of occurrences of some events of interest, e.g., an estimate of a flood magnitude corresponding to a chosen risk of failure. The use of this technique has played an important role in engineering practice. The assumptions of independence and stationarity of variables are necessary classical conditions to proceed with such analyses. However, in the context of climate change, it is possible that these assumptions might no longer hold and the results of conventional frequency analysis would become less reliable. It is therefore essential to examine the validity of these assumptions before applying the classical frequency analysis technique to hydrological variables. If violation of these assumptions occurs in the data series, new approaches are required which will incorporate the non-independence and non-stationarity of hydrometeorological extremes or at the very least the sensitivity of results to these violations needs to be investigated.

The chapter describes various potential causes of non-stationarity in hydrological variables, its identification techniques and its impact on classical frequency analysis.

6.2 FLOOD FREQUENCY ANALYSIS AND ITS ASSUMPTIONS

In flood frequency analysis a major assumption is that all observations in a data set are independent and identically distributed (IID). If the observation of a variable X , at time t depends (linearly) on the observation at time $t-k$, for $k=1,2,\dots$, then the time series is called serially correlated, or correlated in time. Otherwise, it is uncorrelated. An uncorrelated time series is generally called an independent series. However, some other complex non-linear dependency might exist between the observations, due to which the independent assumption of a data set may not be valid. A hydrologic time series is stationary if it is free of trends, shifts, or periodicity (cyclicality). This implies that the statistical parameters of the series, such as the mean and variance, remain constant through time. Otherwise the time series is non-stationary.

6.3 CAUSES OF NON-STATIONARITY IN FLOOD MAGNITUDES

The source of non-stationarity in hydrologic records can be a natural catastrophe or periodicity (forest fires, El Nino, solar activities), anthropogenic activity (land use change due to deforestation, urbanisation) or changing climate (natural or anthropogenic). Generally, hydrologic time series defined on an annual time scale are stationary, although this assumption may be incorrect as a result of large-scale climate variability, natural disruptions like a volcanic eruption, and human-induced changes such as the effect of reservoir construction on downstream flow. Hydrologic time series defined at time scales smaller than a year, such as monthly series, are typically nonstationary, mainly because of the annual cycle.

The changes in river flow can be caused directly by human activities such as urbanization, reservoirs, drainage systems, water abstraction, landuse changes or by natural catchment changes (e.g. natural changes in channel morphology), climate variability and problems linked to data such as instrumental error, change in measurement techniques, etc. However, climate is the most important driver of the hydrological cycle. Since the climate system and water cycle are intimately linked, any change in one of the systems induces a change in another. Change in a data series can occur either gradually (a trend) or abruptly (a step-change). It may affect the mean, median, variance, autocorrelation, or almost any other aspect of data.

In general, natural and human-induced factors may produce gradual and instantaneous trends and shifts (jumps) in hydrologic series. For example, a large forest fire in a river basin can immediately affect the runoff, producing a shift in the runoff series, whereas a gradual killing of a forest (for instance by an insect infestation that takes years for its population to build up) can result in gradual changes or trends in the runoff series. An important source of trends and shifts in stream-flow series arises from changes in land use and the development of reservoirs and diversion structures.

The current concern about global warming and climatic changes is making hydrologists more aware of the occurrence of trends and shifts in hydrologic time series. Hydrologic time series defined at time intervals smaller than a year (such as monthly series) generally exhibit distinct seasonal (or periodic) patterns. These

result from the annual revolution of the earth around the sun and the angle of tilt of earth's axis which produce the annual cycle in most hydrologic processes. It is very important to understand the difference between climate variability and climate change, where the former is the natural variation in the climate from one period to the next, while the latter refers to a long-term alteration in the climate. Climate variability appears to have a very marked effect on many hydrological series. This has two important consequences: (i) Climate variability can easily give rise to apparent trend when records are short – these are trends that would be expected to disappear once more data had been collected, and (ii) Climate variability obscures other changes, because climate variability is typically large, it can effectively obscure any underlying changes due either to climate change or to urbanisation (Kundzewicz and Robson, 2004).

Autocorrelation or dependence in some hydrologic time series such as streamflow usually arises from the effect of storage, such as surface, soil, and groundwater storages which causes the water to remain in the system through subsequent time periods. For instance, basins with significant surface storage in the form of lakes, swamps, or glaciers produce annual streamflow series showing significant autocorrelation. Likewise, subsurface storage, especially groundwater storage, also produces significant autocorrelation in the streamflow series which are derived mainly from groundwater outflow. The time series of annual precipitation and annual maximum flows (peak flows) are usually not serially correlated. Conversely the time series of mean daily flows are highly correlated.

If x and y are flow time series of two neighbouring rivers/gauging sites, then if y_t at time t depends (linearly) on x_{t-k} , for $k=1, \dots$, then the two time series are cross correlated. For instance, it is possible that both series x_t and y_t are uncorrelated serially in time, yet are cross-correlated with one another. Likewise, it is possible that each series can be autocorrelated, yet there is no cross-correlation between them. Just as there are physical reasons why some hydrologic time series are autocorrelated, there are physical reasons why two or more series are cross-correlated. Examples are precipitation series at two nearby sites and streamflow at two nearby gauging stations. In both cases, one would expect that the time series will be cross-correlated because the sites are relatively close to each other and therefore subject to similar climatic and hydrologic events. As the sites considered

become further apart, their cross-correlations decrease. Likewise, one would expect a significant cross-correlation between stream-flow time series and the corresponding areal average precipitation time series over the same basin, because they are related by cause and effect.

6.4 IMPACTS OF NON-STATIONARITY IN FLOOD FREQUENCY ANALYSIS

Traditionally, design rules are based on the assumption of stationary hydrology, resulting in the principle that the past is the key to the future. If the stationarity assumption is not correct i.e. if the parameters describing the location, scale and shape properties of hydrological time series change over time then the existing procedures for designing water-related structures: dams, dikes, etc. will have to be revised. Otherwise, systems would be over- or under-designed, and might not serve their purpose adequately, or be over costly. In engineering hydrology, overestimating the design values as a result of ignoring significant decreasing trends in the series may lead to over-designed objects and unnecessary expenditure. The more serious cases arise from ignoring increasing trends in maximum floods, which may lead to under designed projects and significant losses when more severe floods occur than are expected.

Research carried out at the country, regional and global levels have shown some evidence of non-stationarity in the hydrological variables (Cunderlik and Burn, 2002; Milly et al., 2002 Kundzewicz et al., 2004; Svensson et al., 2004; Kundzewicz et al., 2004a; Petrow and Merz, 2009). In these circumstances, the classical notions of 'probability of exceedance' and 'return period' are no longer valid or have to be re-interpreted and therefore currently used statistical methods for modelling hydrologic time series and for estimating their extreme values for a given recurrence period have to be reconsidered. Under such circumstances, new approaches for hydrological frequency analysis are required which will incorporate the non-independence and non-stationarity of hydrometeorological extremes.

6.5 METHODS OF TESTING NON-STATIONARITY IN FLOOD SERIES

6.5.1 Test Procedures

Detection of abrupt or gradual changes in hydrological records, and river discharge in particular, is of considerable scientific and practical importance, being fundamental for planning of future water resources and flood protection. Statisticians have developed many test procedures for detecting changes (non-stationarity) in time series which may also be applied to hydrological time series.

The main stages of a statistical analysis of change in hydrological data include (Kundzewicz, 2004):

- Decide what type of series/variable to test depending on the issue of interest (e.g. monthly averages, annual maxima, Peaks-Over-Threshold (POT) series, etc.).
- Decide what type of change is of interest (gradual or step change).
- Check out data assumptions (e.g. use exploratory data analysis, or a formal test).
- Select a statistical test. This means selecting a test statistic and selecting a method for evaluating significance levels.
- Evaluate significance levels.
- Investigate and interpret results

Data selection:

The selection of the form of data depends on the objective of the study, i.e. if the long-term trend in the hydrological behavior is to be investigated, the relevant time series is to be selected. If the trend in the frequency of the flood magnitude is to be investigated, then POT data will provide more information. For flood seasonality analysis, monthly seasonal data is important. Robson and Reed (1999) investigated British river flow trends in the annual maximum series as well as trends in POT magnitude and frequency series, selecting on average 1 and 3 POTs per year.

Petrow and Merz (2009) investigated trends in eight flood indicators for 145 discharge gauges in Germany, which were extracted from annual maximum and

peaks over threshold series and included: the annual maximum daily mean streamflow, annual winter and summer maximum daily mean streamflows, peaks over threshold flood magnitude, annual peaks over threshold frequency (on average three events per year), and seasonal (summer and winter) peak over threshold frequency.

Burn and Hag (2002) investigated trends on 18 hydrologic variables for 225 hydrometric stations in Canada. These variables include the annual mean flow, annual maximum daily flow, and the monthly mean flow for each month. Variables related to the timing of hydrological events that were investigated included the date of occurrence of the annual maximum daily flow, the date when ice conditions start, the date when ice conditions end, and a variable reflecting the duration of hydrologic events including the number of days with ice conditions. This collection of variables was analysed in order to gain a broad understanding of the hydrologic response to climate change.

Data are the backbone of any attempt to detect trend or other change in hydrological data (Kundzewicz and Robson, 2004). Data should be quality-controlled before commencing an analysis of change. Examples of problems linked to the data that can cause apparent change in a data series are:

- Typographical errors,
- Instruments malfunctioning,
- Change in measurement techniques, instrumentation, or instrument location,
- Change in accuracy of data, or change of data units, and
- Changes in data conversions (e.g. altered rating equations).

Selection of which stations to use in a study is also important (Kundzewicz and Robson, 2004). For example, to study climate change signature in river flow records, data should ideally be taken from pristine/baseline rivers and should be of high quality and extend over a long period. Where pristine sites are not available, it may be possible to eliminate other influences or reconstruct natural flows, or using conceptual flow naturalization. Hence, catchments featuring strong changes in land-use and land-cover change (e.g. deforestation, urbanization), river regulation (e.g. dikes or dams) are not appropriate. Detailed suggestions as to how to select a

network of stations for climate change are given in Pilon (2000) and Harvey et al. (1999).

The choice of stations should be made based on the following criteria (Harvey et al., 1999; Pilon, 2000; Kundzewicz and Robson, 2004):

- Data accuracy: Data accuracy should be assessed qualitatively by local experts based on knowledge of the hydraulic condition of the stations to ensure that only stations with good quality data are included in the network,
- Availability of long series (the longer the better); at least 40 years of data would be required.
- Absence of significant regulations or diversions: Priority should be given to smaller catchments without strong anthropogenic influence.
- No such missing records or gaps which could contaminate the series of annual maxima should be admitted in the records,. Problems arise if data gaps result from destruction of a gauge. The consequence of such a gap is that high flows are may be missed.
- Geographical distribution: Avoid many neighbouring stations. The data set should be selected in such a way that it represents large-scale variations in the time series over a country.

It would be ideal if the datasets are available in common time intervals. Selecting a common period of record facilitates investigation of variable climatic conditions during the (common) prescribed period. The investigation of all available data through the 'All Records' study period (all of the available records at each station) allows for an optimal spatial coverage, although the periods of record reflected at each station will potentially differ, making interpretation of the results more difficult. The partitioning of the study period into a number of fixed period timeframes can be useful for temporal evolution of data series (i.e. to address the uncertainty associated with the temporal change signal to the length of historical record). Burn and Hag (2002) performed trend detection procedures on five study periods for the Canadian river network. These periods started in 1940, 1950, 1960 and 1970 and ended in 1997. Khaliq et al. (2009) investigated temporal evolution of annual mean

daily flow series for four time frames: (1) 1974-2003 (30 years), (2) 1964-2003 (40 years), (3) 1954-2003 (50 years) and (4) 1944-2003 (60 years).

Data assumption:

In carrying out a statistical test it is always necessary to consider whether the following assumptions are valid:

- (i) Independence: This assumption is violated if there is autocorrelation or, in the case of a multi-site study, spatial correlation (correlation between sites).
- (ii) A specified form of distribution: (e.g. assuming that the data are normally distributed). This assumption is violated if the data do not follow the specified distribution.
- (iii) Constancy of distribution: (i.e. all data points have an identical distribution). This assumption is violated if there are seasonal variations or any other cycles in the data, or if there is an alteration over time in the variance or any other feature of the data that is not allowed for in the test.

If the assumptions made in a statistical test are not fulfilled by the data, then test results can be meaningless, in the sense that the estimates of significance level would be incorrect. Hydrological data are often strongly non-normal and this means that tests which assume an underlying normal distribution are less appropriate or inadequate. Hydrological data may also show either autocorrelation, or spatial correlation and therefore data values may not be independent. They may also display seasonality, which violates assumptions of constancy of distribution.

Examination of data assumption:

Exploratory data analysis (EDA) is a visual examination of the data and forms an integral part of any study of change (Tukey, 1977). It involves using graphs to explore, understand and present data, and is an essential component of any statistical analysis. The first use of EDA is usually to examine the raw data in order to identify such features as data problems (outliers, gaps in the record, etc.); temporal patterns (e.g. trend or step-change, seasonality); and regional and spatial patterns. Exploratory data analysis also plays an important role in checking out test assumptions such as independence, or statistical distribution of data values.

Common types of graph that can be useful for hydrological data series include histograms and normal probability plots, autocorrelation plots, scatter plots and smoothing curves. A well-conducted EDA is such a powerful tool that it can sometimes eliminate the need for a formal statistical analysis (Kundzewicz, 2004). A good EDA involves plotting, studying and refining graphs so as to highlight important features of the data and thus identify further graphs that are needed. Excellent presentations of general principles of EDA can also be found in Tufte (1983), Cleveland (1984) and Grubb & Robson (2000).

Some of the most commonly used EDA tools are discussed briefly below :

One of the simplest and more useful exploratory graphical tools is to ***plot the data against time***. Characteristics of the data which may be easily discovered from a perusal of a graph include the detection of extreme values, trends, known and unknown interventions, dependencies among observations, seasonality, need for a data transformation, non-stationarity, and long term cycles.

Histograms are plots of bars whose height is the number n_i , or fraction n_i/n of data falling into one of several intervals of equal width. It provides information about the distribution of the data.

Quantile Plots or cumulative distribution functions (cdfs) portray the quantiles of the distribution of sample data. They are also called empirical distribution functions (edfs). Quantiles of importance such as the median are easily discerned from the plot. The spread and skewness of the data, as well as any bimodal character it possesses, can also be examined. A specified form of the quantile plot is the probability plot using specially designed graph paper such that a given theoretical probability distribution function would plot as a straight line. An example is the normal probability plot. The sample data plotting close to straight line in this plot is an indication that these data are approximately normal.

A box plot is a concise graphical display for summarizing the distribution of a data set. Box plots provide visual summaries that provide at a glance an idea of the central tendency of the data, the variability, the symmetry, and the presence of outliers. Box plots are useful for examining the characteristics of a single data set,

and, when plotted side by side on the same scale, they are particularly useful for comparing several related data sets. A box plot-and-whisker graph is based upon what is called a 5-number summary (Tukey, 1977). For a given data set, the 5-number summary consists of the smallest and largest values, the median, and the 0.25 and 0.75 quantiles which are called hinges. When the data are ranked from the smallest to largest value, the first data point is the smallest value while the last entry is the largest value. This distance between the first and third quartile is called the interquartile range. This distance, which can be used to judge the spread of the data, is referred to by Tukey (1997) as the H spread. Box plots provide a ready visual check on the symmetry of a data set.

The autocorrelation function (ACF) at lag k , r_k , for a given time series reflects the linear dependence between values which are separated by k time lag. The estimate for the ACF at lag k , r_k , for an evenly spaced series x_t , of length n can be calculated using

$$r_k = \frac{\sum_{t=1}^{n-k} (x_t - \bar{x})(x_{t+k} - \bar{x})}{\sum_{t=1}^n (x_t - \bar{x})^2}, \quad k > 0 \quad (6.1)$$

as in Jenkins and Watts (1968).

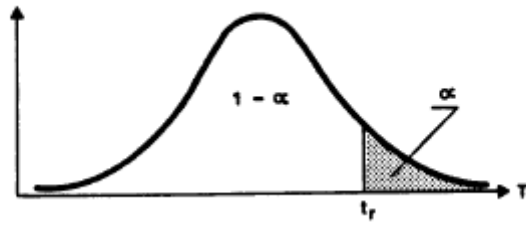
where \bar{x} is the mean of the x_t series. The value of r_k can range from -1 to +1 where r_0 has value of unity. When the theoretical ACF is zero and, therefore, the series is white noise, r_k is asymptotically normally distributed with mean of zero and variance of $1/n$. If the ACF function with lag 1 is found to be significant at a given significance level, the time series is serially correlated and are not independent. The ACF furnishes a method for interpreting data independence. If, for example, there is a large positive correlation at lag one, this means that data are autocorrelated and they are not independent.

Statistical test procedures:

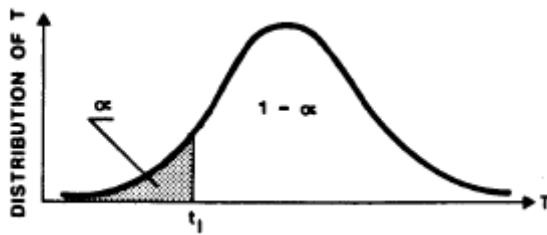
The steps in any statistical test includes (i) naming a null hypothesis, (ii) naming a test statistic and its distribution under the null hypothesis, (iii) naming a critical region for the test statistic in which, under the null hypothesis, the value of the test statistic falls with probability α , (iv) computing the test statistic from a sample, and

(v) rejecting the null hypothesis or not according to whether the observed test statistic value falls in the critical region.

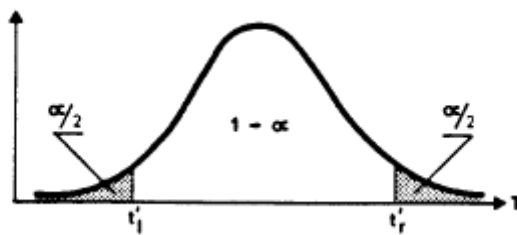
Suppose one would like to determine whether or not a data set possesses a certain property. For example, one may wish to ascertain the existence or nonexistence of a certain kind of trend in a hydrological time series. Typically, the null hypothesis, H_0 , which is sometimes called the hypothesis under test, is that the population, from which the sample data set is drawn, does not possess a property like trend. The alternative hypothesis, H_1 , which specifies a direction of departure from H_0 , is that the data set does exhibit the property. In order to choose between H_0 and H_1 , a test statistic, T , which is a function of the data set $X=(x_1, x_2, \dots, x_n)$, is defined. When the hypothesis H_0 is true, the distribution of T must be known, at least approximately, so that the hypothesis test can be executed. By knowing the probability distribution of T , the probability of the sample statistic falling within or outside a given interval can be determined. As shown in **Figure 6.1** for one sided and two sided tests, let t_r and t_l stand for the right and left values of T , respectively, for the two possible one sided tests, and let t'_r and t'_l define the right and left ends, respectively of an interval in two sided test. A chosen significance level, α , is the probability that the sample test statistic value falls outside a specified range of values, given that H_0 is true. For the one tailed or one sided tests, α represents the area in one of the tails of the distribution. In **Figure 6.1(a)**, $\Pr(t >= t_r) = \alpha$, and consequently, if one were checking for the absence of an increasing trend, the hypothesis H_0 would be rejected if $t_x >= t_r$ and hence H_1 would be accepted, where t_x is the sample or estimated value of T calculated using the sample X . Alternatively, H_0 would be accepted if $t_x < t_r$. The one tailed test in **Figure 6.1(b)** works in a similar manner. Suppose that H_0 indicates the absence of a decreasing trend. If $t_x <= t_l$, then H_0 would be rejected and H_1 thereby accepted, whereas when $t_x > t_l$, H_0 would be considered to be correct. A two sided test would be used in trend detection when one wishes to test for the presence of a trend which could be increasing or decreasing. For the case of the two sided test in **Figure 6.1(c)**, H_0 is accepted when $t'_l < t_x < t'_r$, and is rejected when $t_x >= t'_r$ or $t_x <= t'_l$.



(a) One sided hypothesis test on the right



(b) One sided hypothesis test on the left



(c) Two sided hypothesis test

Figure 6.1: Hypothesis tests

Notice from the above figures, that the probability of selecting H_0 when H_0 is true is, $1 - \alpha$ which is referred to as the confidence level.

When executing a hypothesis test, two types of errors can arise. These are illustrated in **Figures 6.2** and **6.3**. The act rejecting H_0 when H_0 is true is called a *type 1 error* or error of the first kind. The probability of committing a type 1 error is α for both one and two sided tests. If the hypothesis H_0 is accepted when it should be rejected, this is called *type 2 error*, or *error of the second kind*. Letting β present the probability of committing a type 2 error, the probability of not making a type 2 error, is $1 - \beta$. The probability of rejecting H_0 when H_1 is true, or equivalently, the probability of not making a type 2 error, is called the power of the hypothesis test. If,

for example, one were testing for the presence of a trend, the power, given by $1 - \beta$, can be interpreted as the probability of detecting a trend when a trend is actually present in the data.

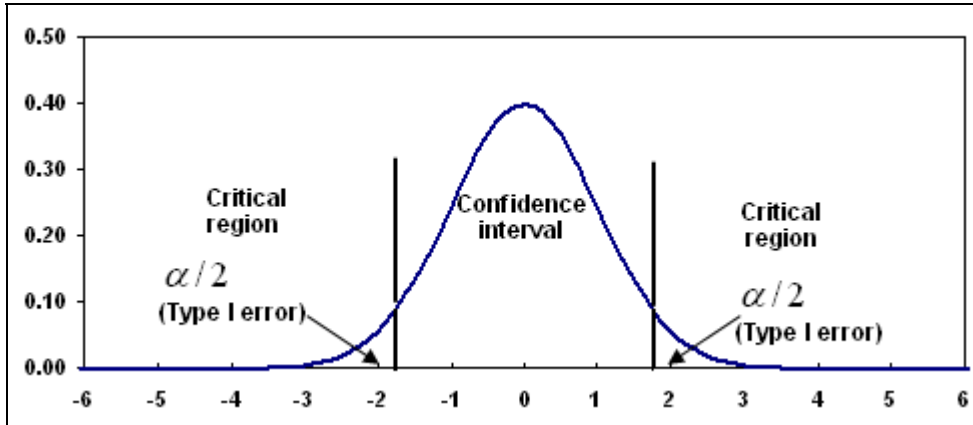


Figure 6.2: Type I error in a hypothetical test (two sided test)

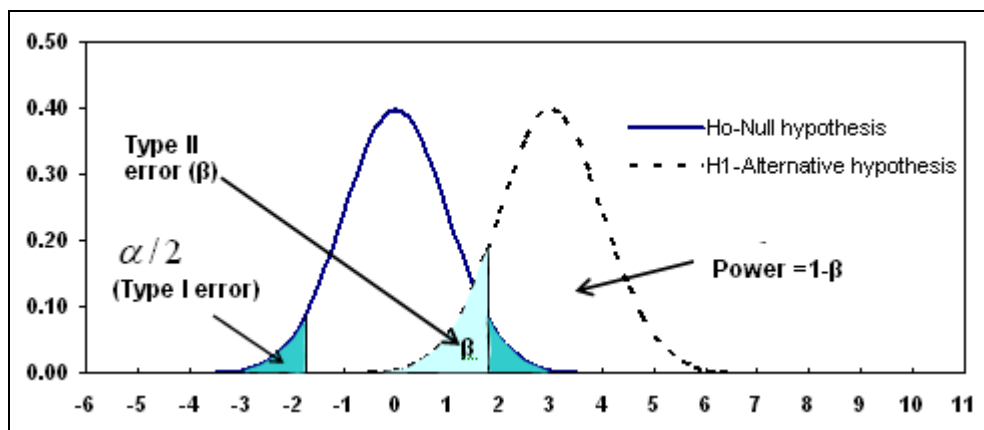


Figure 6.3: Type II error and the power of a hypothesis test

Again, when performing a hypothesis test, one of the four situations given in **Table 6.1** can arise. Notice that two of the four outcomes to a hypothesis test result in either a type 1 or type 2 error. In general, the power, $1 - \beta$ (**Figure 6.3**), and the confidence level, $1 - \alpha$, are inversely related. Consequently, increasing the confidence level decreases the power and vice versa. For a specified significance level, α , the power of a test may be made greater by increasing the sample size.

Table 6.1: Possible results of a hypothesis test

True situation	Action	
	Accept H_0	Reject H_0
H_0 is true	No error (Pr= $1-\alpha$) Confidence level	Type 1 error (Pr= α)
H_1 is true	Type 2 error (Pr= β)	No error (Pr= $1-\beta$) Power

The choice of a significance level (α) is completely arbitrary (Fisher, 1958), but the values $\alpha = 0.05$ and $\alpha = 0.01$ are the most frequently used. A possible interpretation of the significance level might be (Chiew and Lionel, 2005):

- $\alpha > 0.1$ - little evidence against H_0
- $0.05 < \alpha < 0.1$ - possible evidence against H_0
- $0.01 < \alpha < 0.05$ - strong evidence against H_0
- $< \alpha < 0.01$ - very strong evidence against H_0 .

An alternative way to conclude a test of hypotheses is to compare the p-value of the sample test statistic with significance level (α). The p-value of the sample test statistic is the smallest level of significance for which we can reject H_0 . In other words, the p-value of a statistical hypothesis test is the probability of getting a value of the test statistic, by chance alone, as extreme as, or more extreme than that observed, if the null hypothesis, H_0 , is true. The p-value is compared with the actual significance level of the test and, if it is smaller, the result is significant. That is, if the null hypothesis were to be rejected at the 5% significance level, this would be reported as “ $p < 0.05$ ”. The smaller it is, the more convincing is the rejection of the null hypothesis. It indicates the strength of evidence for rejecting the null hypothesis H_0 , rather than simply concluding “Reject H_0 ” or “Do not reject H_0 ”. The p-value serves a valuable purpose in the evaluation and interpretation of research findings. It enables the researchers to set their own level of significance and to reject or accept the null hypothesis in accordance with their own criterion rather than that of fixed level of significance.

For most traditional statistical methods, critical test statistic values for various significance levels can be looked up in statistical tables or calculated from simple formulae, provided that the test assumptions are satisfied or by simulation methods

if algebraic solution is not possible. Where test assumptions are violated, resampling methods can be used to estimate the significance level of a test statistic.

For detecting trend/change of any direction, the critical test statistic value at $\alpha/2$ is used (two-sided tail). For detecting trend/change in a pre-specified direction (e.g., an increasing trend), the critical test statistic value at α is used (one-sided tail).

6.5.2 Parametric and Non-parametric Tests

Test procedures for detecting any trend in hydrological time series. They are mainly classified as parametric and non-parametric. If any test does not depend on the form of parent distribution from which the sample is drawn, then the test is distribution free or non-parametric, otherwise it is a parametric test. Non-parametric tests require few assumptions about the shapes of the underlying population distributions. Parametric tests make use of information consistent with interval scale measurement, whereas non-parametric tests typically make use of ordinal information only. The selection of a test to be used is sometimes difficult.

Non parametric tests are less powerful, because parametric tests use more of the information available in a set of numbers. Therefore, when the assumptions for a parametric test are met, it is preferable to use the parametric test rather than a non-parametric test. If the assumptions made in a statistical test are not fulfilled by the data, then test results can be meaningless, in the sense that the estimates of significance level would be incorrect (Kundzewicz, 2004).

Hydrological data are often strongly non-normal and this means that tests which assume underlying normal distribution are not appropriate. Distribution-free non-parametric methods are recommended because they allow minimal assumptions to be made about the data and are therefore particularly suited to hydrological series, which are often neither normally distributed nor independent (Kundzewicz, 2004).

6.5.3 Details of some commonly used tests for Non-stationarity

6.5.3.1 Test of independence assumption (i.e. testing presence of non-randomness and serial dependency of time series)

The following three tests are commonly used to test non-randomness and/or serial dependency of time series:

- (i) Autocorrelation test – Lag 1 (Parametric test for serial dependency of data)
- (ii) Turning points test (Kendall non-parametric test for randomness)
- iii) Rank Difference (Meachem non-parametric test for randomness)

Autocorrelation test-Lag 1:

The linear dependence (or autocorrelation) in samples of hydro-meteorological variables is usually characterised by the persistence phenomenon. This means that for a sample y_1, y_2, \dots, y_n , the value of y_t at time point t depends on values at earlier neighbouring time points. The strength of dependence among observations is measured by estimating autocorrelation coefficients, r_k , with lags 1, 2, ..., k (Salas et al., 1980). If some autocorrelation coefficients are significant, i.e., they lie outside the chosen confidence interval (e.g., 90%, 95%, 99%, etc.), then most likely the observations in the sample are not independent and consequently the assumption of independence of observations, required for conventional frequency analysis, is not fulfilled. The autocorrelation coefficient at lag one is often referred to as the serial correlation coefficient at lag one or first serial correlation coefficient. If the lag one autocorrelation is found to be significant at a given significance level, the time series are serially correlated and are not independent. In this case, in the plot of a series a sequence of high values will often be grouped together and low values will frequently follow under low values.

The lag-one autocorrelation (r_1) can be obtained by putting $k=1$ in Equation 6.1. If the time series data come from a random process then r_1 is approximately normally distributed and the mean and variance of r_1 are:

$$\text{mean} = -1/n \quad (6.2)$$

$$\text{variance} = (n^3 - 3n^2 + 4) / \{n^2(n^2 - 1)\} \quad (6.3)$$

The test statistic, z is calculated from:

$$z = \frac{|r_1 - \text{mean}|}{\text{variance}^{0.5}} \quad (6.4)$$

The critical test statistic values for various significance levels can be obtained from normal probability tables.

Turning points test (Kendall's test):

This is a non-parametric test and is based on counting "turning points" in the series, i.e. triplets of successive values x_{i-1}, x_i, x_{i+1} such that $x_{i-1} < x_i > x_{i+1}$ or $x_{i-1} > x_i < x_{i+1}$. If N is the number of turning points, then the test statistic is

$$S = \frac{(3N - 2n + 4)\sqrt{10}}{\sqrt{16n - 29}} \quad (6.5)$$

Under the null hypothesis of independent, identically distributed values, this test statistic is normally distributed with mean 0 and variance 1 (Srikanthan and MacMahon, 1983).

Rank difference test (Meacham test):

This is a nonparametric test. It involves computing differences between the ranks of subsequent values in the series. If U denotes the sum of absolute values of such rank differences then the test statistic is

$$S = \frac{(3U - n^2 + 1)\sqrt{10}}{\sqrt{(n-2)(n+1)(4n-7)}} \quad (6.6)$$

Under the null hypothesis of independent, identically distributed values, this statistic is normally distributed with mean 0 and variance 1 (Srikanthan and MacMahon, 1983).

6.5.3.2 Tests for step change (stationarity assumption test)

The following two tests are commonly used to test the step change (shift) in the data series:

- (i) Mann-Whitney U test (non-parametric test for step jump in mean/median)
- (ii) T-test (Parametric test for step jump in mean)

These methods test whether the means/medians in two different periods are different. Both tests assume that the point of change in a data series is known. However, when the point of change is not known, Bayesian analysis can be used to detect the point of change and its amount.

Mann-Whitney U test (Rank-Sum Test):

This is a non-parametric test for testing location difference between two sub-samples. Suppose that $y_t, t=1, \dots, N$ is an annual hydrologic series that can be divided into two subseries y_1, \dots, y_{N_1} and y_{N_1+1}, \dots, y_N of series N_1 and N_2 respectively such that $N_1+N_2=N$. A new series, $z_t, t=1, \dots, N$, is defined by rearranging the original data y_t in increasing order of magnitude. One can test the hypothesis that the mean of the first subseries is equal to the mean of second subseries by using the statistic:

$$U = \frac{\sum_{t=1}^{N_1} R(y_t) - N_1(N_1 + N_2 + 1) / 2}{[N_1 N_2 (N_1 + N_2 + 1) / 12]^{1/2}} \quad (6.7)$$

where $R(y_t)$ is the rank of the observation y_t in ordered series z_t ; when both sub-samples are larger than 20, U is approximately normally distributed with mean $n_1 n_2 / 2$ and standard deviation $[n_1 n_2 (n_1 + n_2 + 1)]^{1/2} / 12$. The hypothesis of equal means of the two subseries is rejected if $|U| > u_{1-\alpha/2}$, where $u_{1-\alpha/2}$ is the $1 - \alpha / 2$ quantile of the standard normal distribution and α is the significance level of the test. The critical values for this test statistic are tabulated by Siegel (1956). The test statistic can be modified for the case of groups of values that are tied.

T-test:

The t-test is the most widely used method for comparing two independent groups of data.

Suppose that $y_t, t=1, \dots, N$ is an annual hydrologic series which is uncorrelated and normally distributed with mean μ and standard deviation σ and N =sample size. The series is divided into two subseries of sizes N_1 and N_2 such that $N_1+N_2=N$. The

first subseries y_t , $t=1,2,\dots,N_1$, has mean μ_1 and standard deviation σ , and the second subseries y_t , $t=N_1+1, N_1+2,\dots,N$, is assumed to have mean μ_2 and standard deviation σ . The simple t-test can be used to test the hypothesis $\mu_1 = \mu_2$ when the two subseries have the same standard deviation σ . Rejection of hypothesis can be considered as a detection of a shift. The test statistic in this case is given by:

$$T_c = \frac{\left| \bar{y}_2 - \bar{y}_1 \right|}{S \sqrt{\frac{1}{N_1} + \frac{1}{N_2}}} \quad (6.8)$$

where S is the sample standard deviation of the entire N_1 and N_2 observations, and can be calculated by:

$$S = \sqrt{\frac{(N_1 - 1)s_1^2 + (N_2 - 1)s_2^2}{N - 2}} \quad (6.9)$$

where \bar{y}_1 and \bar{y}_2 and s_1^2 and s_2^2 are the estimated means and variances of the first and the second subseries respectively. The hypothesis $\mu_1 = \mu_2$ is rejected if $T_c > T_{1-\alpha/2, \nu}$ where $T_{1-\alpha/2, \nu}$ is the $1 - \alpha/2$ quantile of the Student's t distribution with $\nu = N - 2$ degrees of freedom and α is the significance level of the test.

6.5.3.3 Test for monotonic trends

The following three tests are frequently used in trend detection in hydrological variables:

- i) Mann-Kendall test
- ii) Spearman's Rho test
- iii) Linear Regression test

The first two tests are non-parametric tests and the third test is a parametric test. The details of these tests are discussed below:

Mann-Kendall (MK) Test:

This method tests whether there is a trend in the time series data. It is a non-parametric test (Kendall, 1938). The n time series values ($X_1, X_2, X_3, \dots, X_n$) are replaced by their relative ranks ($R_1, R_2, R_3, \dots, R_n$) (starting at 1 for the lowest up to n). The test statistic S (Kendall's sum) is:

$$S = \sum_{i=1}^{n-1} \left[\sum_{j=i+1}^n \text{sgn}(R_i - R_j) \right] \quad (6.10)$$

where $\text{sgn}(x) = 1$ for $x > 0$

$\text{sgn}(x) = 0$ for $x = 0$

$\text{sgn}(x) = -1$ for $x < 0$

Mann (1945) and Kendall (1975) have documented that if the null hypothesis H_0 is true then for $n \geq 8$, the statistic S is approximately normally distributed with the mean and the variance as follows:

$$\text{Mean: } E(S) = 0 \quad (6.11)$$

$$\text{variance: } V(S) = \frac{n(n-1)(2n+5) - \sum_{i=1}^n t_i i(i-1)(2i+5)}{18} \quad (6.12)$$

where t_i is the number of ties of extent i . The standardized test statistic Z is computed by:

$$Z_{MK} = \begin{cases} \frac{S-1}{\sqrt{\text{Var}(S)}} & S > 0 \\ 0 & S = 0 \\ \frac{S+1}{\sqrt{\text{Var}(S)}} & S < 0 \end{cases} \quad (6.13)$$

The standardized MK statistic Z follows the standard normal distribution with mean of zero and variance of one.

The P-value of the MK statistic (S) of sample data can be estimated using the normal cdf,

$$p = 0.5 - \Phi(|Z|) \quad (Z=Z_{MK}) \quad (6.14)$$

$$\left(\Phi(|Z|) = \frac{1}{\sqrt{2\pi}} \int_0^{|Z|} e^{-t^2/2} dt \right) \quad (6.15)$$

If the P-value is small enough, the trend is quite unlikely to be caused by random sampling. At the significance level of 0.05, if $p \leq 0.05$, then the existing trend is considered to be statistically significant.

Critical test statistic values for various significance levels can be obtained from normal probability tables. A positive value of S indicates that there is an increasing trend and vice versa. The MK test searches for a trend in a time series without specifying whether the trend is linear or nonlinear.

Spearman's Rho (SPR) Test:

This is a rank-based test that determines whether the correlation between two variables is significant. In trend analysis, one variable is taken as the time itself (years) and the other as the corresponding time series data. Both variables are replaced by their ranks. If the time series consists of n distinct values, the ranks will be the numbers from 1 to n, with n corresponding to the highest value in the series, n-1 to the second highest, and so on. If there are ties (equal values) in the series, each value in the tie group is assigned the same (mean) rank.

Given a sample data set $\{X_i, i=1,2,\dots,n\}$, the null hypothesis H_0 of the Spearman's Rho test against trend tests is that all the X_i are independent and identically distributed; the alternative hypothesis is that X_i increases or decreases with i , that is, trend exists. The test statistic 'D' is given by (Sneyers, 1990)

$$D = 1 - \frac{6 \sum_{i=1}^n [R(X_i) - i]^2}{n(n^2 - 1)} \quad (6.16)$$

where $R(X_i)$ is the rank of i th observation X_i in the sample of size n.

Under the null hypothesis, the distribution of 'D' is asymptotically normal with the mean and variance as follows (Lehmann, 1975; Sneyers, 1990).

$$E(D) = 0 \quad (6.17)$$

$$V(D) = \frac{1}{n-1} \quad (6.18)$$

The P-value of the D of the observed sample data is estimated using the normal cumulative distribution function (cdf) as its statistics are approximately normally distributed with mean of zero and variance of V(D) for the SPR statistic. Using the following standardization,

$$Z_{SR} = \frac{D}{\sqrt{V(D)}} \quad (6.19)$$

the standardized statistics Z follows the standard normal distribution $Z \sim N(0,1)$.

The P-value of the SPR statistic (D) of sample data can be estimated using the normal cdf,

$$p = 0.5 - \Phi(|Z|) \quad (Z=Z_{SR}) \quad (6.20)$$

$$\left(\Phi(|Z|) = \frac{1}{\sqrt{2\pi}} \int_0^{|Z|} e^{-t^2/2} dt \right) \quad (6.21)$$

If the P-value is small enough, the trend is quite unlikely to be caused by random sampling. At the significance level of 0.05, if $p \leq 0.05$, then the existing trend is considered to be statistically significant.

Linear Regression (LR) Test:

This is a parametric test that assumes that the data are normally distributed. It tests whether there is a linear trend by examining the relationship between time x (with mean \bar{x}) and the variable of interest y (with mean \bar{y}).

The regression gradient is estimated by:

$$b = \frac{\sum_{i=1}^n (x_i - \bar{x})(y_i - \bar{y})}{\sum_{i=1}^n (x_i - \bar{x})^2} \quad (6.22)$$

and the intercept is estimated as:

$$a = \bar{y} - b\bar{x} \quad (6.23)$$

The test statistic S is:

$$S = \frac{b}{\sigma} \quad (6.24)$$

$$\text{where } \sigma = \sqrt{\frac{12 \sum_{i=1}^n (y_i - a - bx_i)^2}{n(n-2)(n^2-1)}} \quad (6.25)$$

The test statistic S follows a Student-t distribution with n-2 degrees of freedom under the null hypothesis (critical test statistics values for various significance levels can be obtained from Student's t statistic tables).

The linear regression test assumes that the data are normally distributed and that the errors (deviation from the trend) are independent and follows the same normal distribution with zero mean. An adaptation of this type of test for non-normal data, is introduced later in Section 7.3.1.3.

7 DETECTION OF TRENDS IN IRISH ANNUAL MAXIMUM FLOOD (AMF) SERIES

7.1 INTRODUCTION

This chapter investigates the presence of non-stationarity in the Irish Annual Maximum Flood (AMF) Series and subsequently examines its causes, including any linkage with climate change. A number of statistical tests have been employed for this purpose, the details of which are discussed in the following sections.

7.2 DATA

In flood frequency analysis, the Annual Maximum flood model is generally used in Ireland. It is therefore decided to investigate possible changes in AMF Series for the Irish River catchments. The AMF records for 117 gauging stations have been obtained from the Office of Public Works hydrometric database (www.opw.ie/hydro/index.aspata.ie). The selection of these stations was based on the following factors:

1. Good rating quality (A1 & A2¹ category stations) - stations that have good stage-discharge ratings for determining high flood flows,
2. Minimum data gaps /missing records,
3. Long record length, and
4. Minimum anthropogenic influence (e.g. no flow regulation, minimum abstraction etc.)

Out of 117 stations, 79 stations have continuous records with the lengths ranging from 17 to 58 years. The remaining 38 stations have intermittent missing records with the successive missing values in the series ranging from 1 to 16. The locations of these 117 stations are illustrated in **Figure 7.1**. Further details of these stations including their associated catchment characteristics are provided in **Appendix A**.

¹A1 sites – confirmed ratings good for flood flows well above Q_{med} with the highest gauged flow greater than $1.3 \times Q_{med}$ and/or with a good confidence of extrapolation up to 2 times Q_{med} , bankfull or, using suitable survey data, including flows across the flood plain. A2 sites – Ratings confirmed to measure Q_{med} and up to around 1.3 times the flow above Q_{med} .

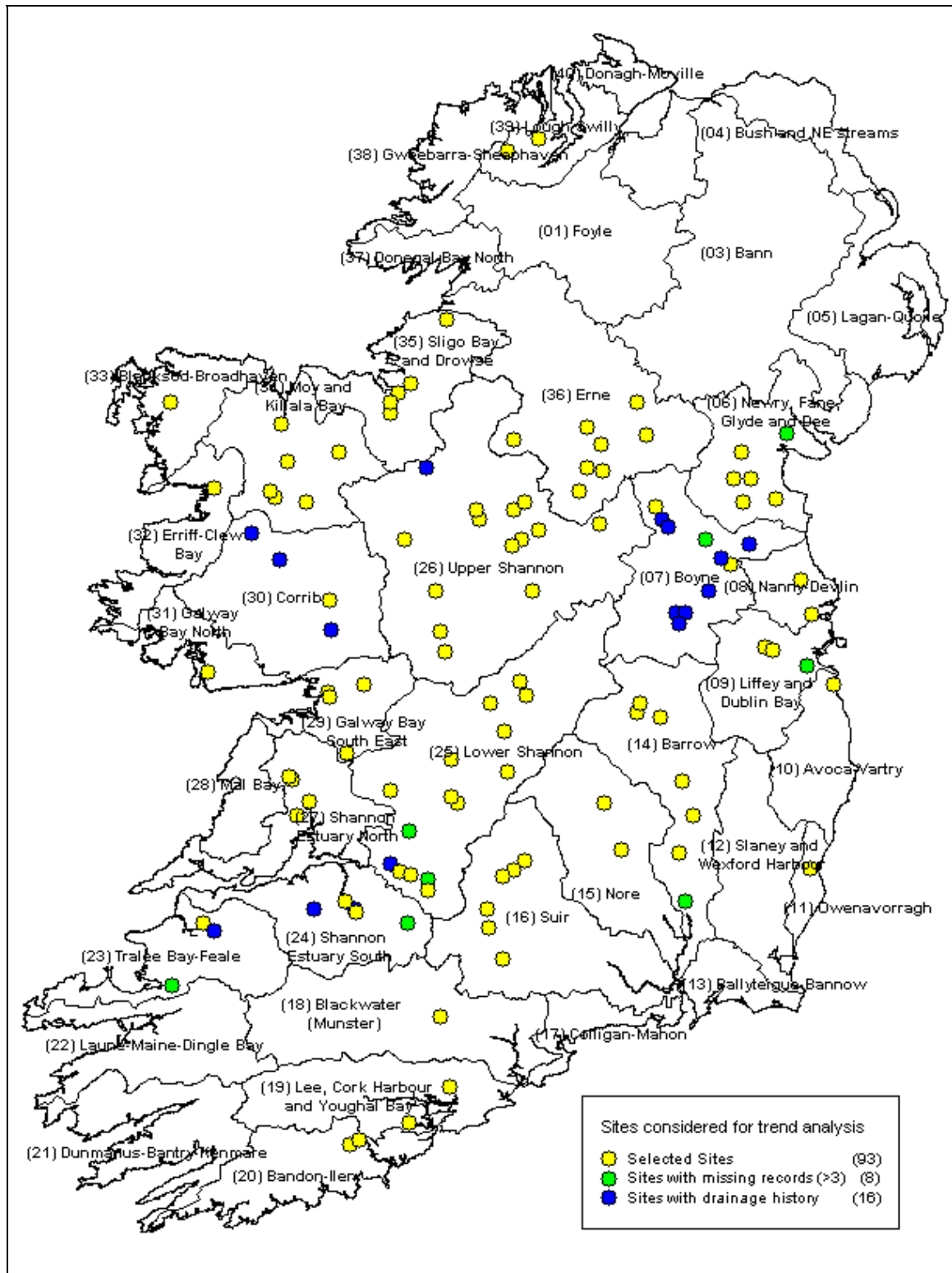


Figure 7.1: Spatial distribution of the gauging sites

7.2.1 Exploratory Data Analysis (EDA)

In order to refine the preliminary selection of the AMF data set for trend analysis and to examine further any evidence of the presence of any undesirable record properties such as outliers, missing records, effect of drainage works, some Exploratory Data Analysis are carried out. Data for each of the selected stations have been plotted in a graph (time series plot technique) and a trend line (linear) is set to each of the AMF series using the Excel data analysis tool. The EDA shows that most of the AM Flood series are well scattered about the mean, while outliers occurred in some of the series. Out of 117 time series, 11 series showed notable upward or downward trends when plotted against time. **Table 7.1** lists these stations and **Figure 7.2** shows the plots of their records against time. The River Nore at MacMahon's Bridge, the Mulkear River at Abington and the Nenagh River at Clarianna showed significant downward trends, while the remainder (8 AMF Series) showed upward trends.

Table 7.1: Stations with significant trends

Station ID.	Waterbody / River Name	Gauge location
15004	Nore	McMahons Br.
16003	Clodiagh	Rathkennan
24001	Maigue	Croom
25002	Newport	Barrington's Br.
25003	Mulkear	Abington
25014	Silver	Millbrook
25023	Little Brosna	Milltown
25029	Nenagh	Clarianna
26005	Suck	Derrycahill
34018	Castlebar	Turlough
36011	Erne	Bellahillan

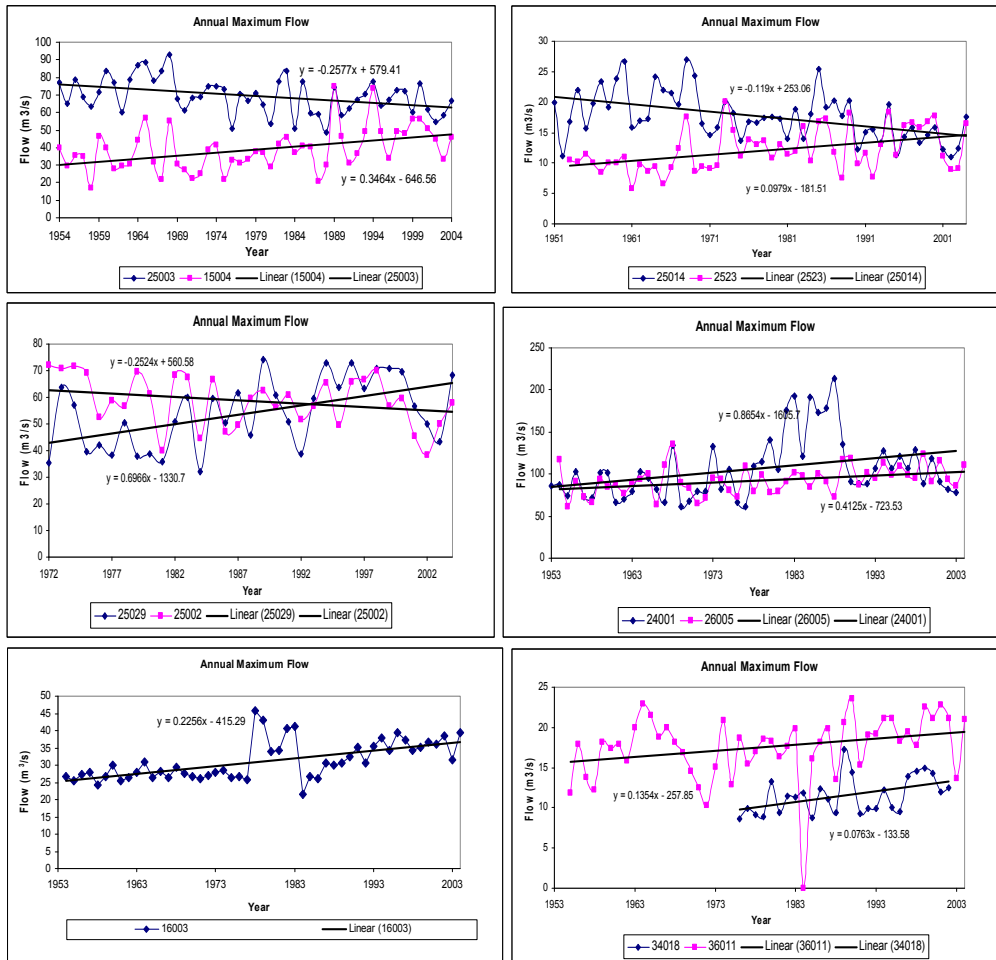


Figure 7.2: Plots of Annual Maximum Flows against time (EDA analysis)

The impact of drainage improvement works on AMF series in some of the catchments (16 sites) is also evident from the graphical plots. These stations have been listed in **Table 7.2** and their records are plotted in **Figure 7.3**. The history of the drainage improvement works in these catchments has been obtained from OPW. In most cases, an upward step change occurred in the AMF series at the beginning of the post-drainage stage as shown in the plots. However, the Mulkear River at Annacotty and the Aille river at Cartronbower each showed a slight downward trend.

Table 7.2: River catchments with drainage improvement works

Station ID.	Waterbody / River Name	Gauge location
7002	Deel	Killyon
7003	Blackwater (Enfield)	Castlerickard
7004	Blackwater (Kells)	Stramatt
7005	Boyne	Trim
7007	Boyne	Boyne Aqueduct
7010	Blackwater (Kells)	Liscartan
7011	Blackwater (Kells)	O'daly's Br.
7012	Boyne	Slane Castle
23002	Feale	Listowel
24001	Maigne	Croom
24013	Deel	Rathkeale
25001	Mulkear	Annacotty
26012	Boyle	Tinacarra
30001	Aille	Cartronbower
30004	Clare	Corrofin
30005	Robe	Foxhill

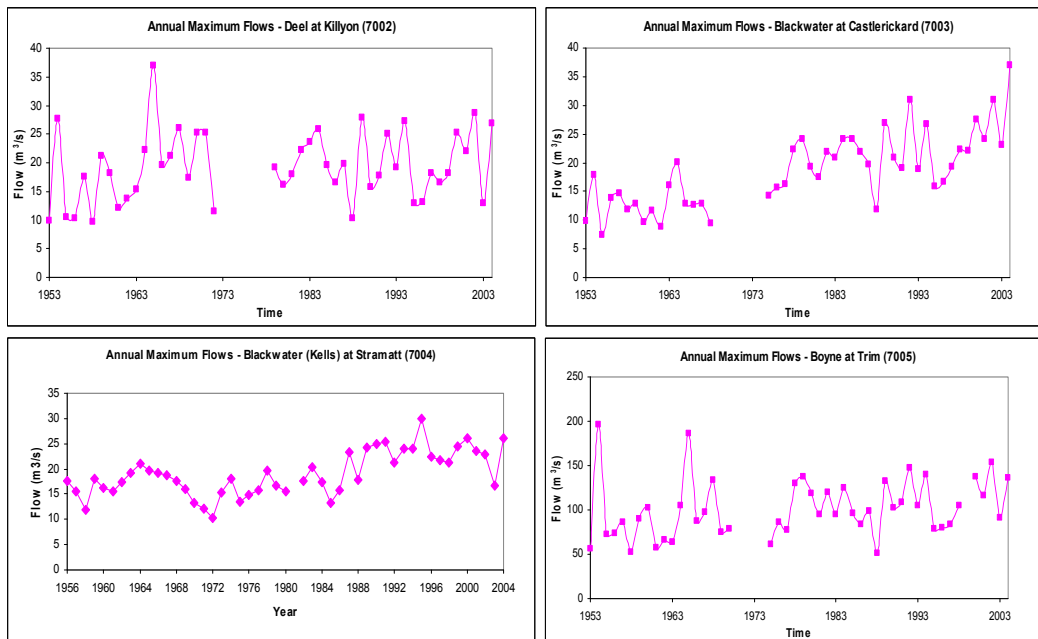


Figure 7.3: Plots of Annual Maximum Flows against time for the catchments where drainage improvement works were carried out (continued)

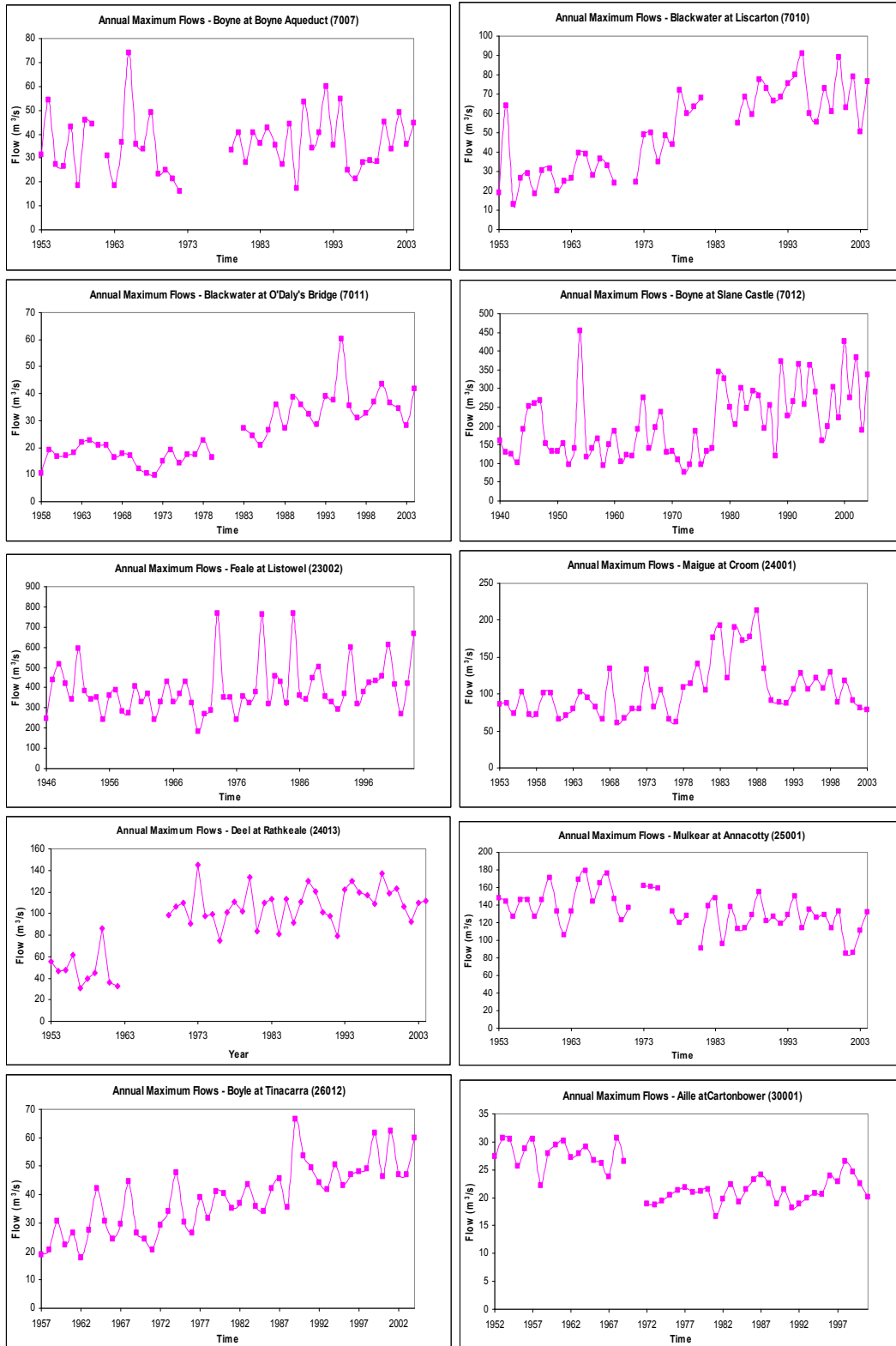


Figure 7.3: Plots of Annual Maximum Flows against time for the catchments where drainage improvement works were carried out (continued)

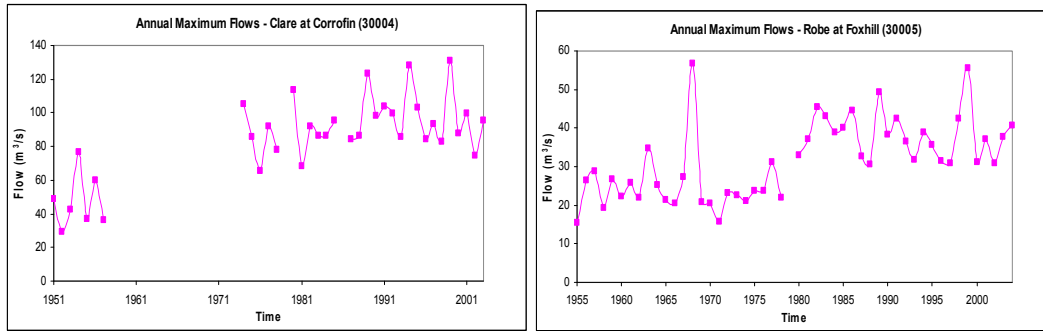


Figure 7.3 Plots of Annual Maximum Flows against time for the catchments where drainage improvement works were carried out.

Further, it was found that 8 AMF Series have more than 3 consecutive years missing records.

Based on the above findings, it was decided to exclude the following stations from trend analysis:

- (i) all river catchments that have undergone arterial drainage works (**16 stations**) and
- (ii) all AMF Series that have more than 3 consecutive years missing records (**8 stations**)

A total of 93 stations / AMF Series have thus been selected out of 117 A1 & A2 category stations for trend analysis. The locations of these stations are illustrated by yellow circles in **Figure 7.1**. The selected stations are relatively homogeneously distributed across Ireland except in the southwest part of the country. Twenty six stations are located in the River Shannon catchment, 8 in the River Erne catchment, the River Suir, Moy and Barrow each have 6 stations and the River Nore catchment has 2 stations.

Table 7.3 presents some physical and statistical characteristics for these stations. The catchment sizes associated with these sites range from 23 km² to 7,980 km² with a median size of 229 km². The record lengths range from 21 years to 61 years, with a median record length of 39 years. All stations have at least 20 years of record, with an average record length of 42 years; 66% of the stations have 30 or more years of record. The specific mean annual maximum flow among the sites range from 0.05 to 1.0 m³/s/km² with a median value of 0.114 m³/s/km². The coefficient of variation (CV) of the AMF series vary from 0.107 to 0.831 with a

median value of 0.227 and the median skewness of 0.60. These values suggest a wide variation in data characteristics.

Irrespective of any significance level, approximately 30% (28 out of 93) sites show downward trends (based on Sen's slope; Sen, 1968), while 70% shows upward trends although not of all of these trends are necessarily significant. The estimated trend slopes in the selected data sets range from 0 to 1.7% with a median value of 0.39% (slope per year). Approximately 65% of sites show positive autocorrelation.

Table 7.3: Physical and statistical characteristics of the selected river catchments

Station		Area (km ²)	Record length (years)	Mean flow (m ³ /s)	Std. deviation	CV	Skewness	Lag 1 Auto. Correlation	Slope (m ³ /s/yr)	Unit slope (per year)
No.	Identifier									
1	06011	229	51	15.906	3.127	0.197	0.647	0.013	0.0403	0.0025
2	06013	309	34	27.049	7.412	0.274	0.241	0.041	-0.1729	-0.0064
3	06014	270	34	22.162	5.827	0.263	1.146	0.101	-0.1440	-0.0065
4	06025	176	34	18.431	2.817	0.153	-0.181	-0.182	0.1050	0.0057
5	06026	148	50	13.620	4.396	0.323	0.935	0.085	-0.0857	-0.0063
6	07009	1658	33	162.079	60.163	0.371	0.712	-0.065	0.4919	0.0030
7	07033	125	25	14.934	3.623	0.243	1.298	0.052	0.1539	0.0103
8	08002	33	21	5.712	1.211	0.212	1.141	-0.142	0.0141	0.0025
9	08008	108	29	43.608	27.450	0.629	1.257	-0.167	-0.4076	-0.0093
10	09001	210	52	38.663	17.075	0.442	0.977	-0.029	-0.0909	-0.0024
11	09002	35	25	7.099	5.896	0.831	1.834	0.058	0.1004	0.0141
12	10021	33	24	7.871	2.931	0.372	0.704	-0.103	0.1028	0.0131
13	11001	155	36	49.919	16.096	0.322	2.414	-0.039	-0.0078	-0.0002
14	14005	405	52	42.140	12.879	0.306	1.577	0.247	-0.1643	-0.0039
15	14006	1064	55	84.392	17.682	0.210	1.121	0.041	-0.2763	-0.0033
16	14009	68	29	6.612	1.717	0.260	0.894	-0.317	-0.0674	-0.0102
17	14013	154	50	16.537	4.343	0.263	0.312	-0.135	-0.0464	-0.0028
18	14018	2419	55	142.391	34.473	0.242	0.180	-0.032	0.5502	0.0039
19	14019	1697	55	103.299	26.285	0.254	0.453	-0.022	-0.0501	-0.0005
20	15003	299	55	142.854	31.173	0.218	-0.825	0.049	0.1520	0.0011
21	15004	491	55	39.511	12.314	0.312	0.704	0.259	0.3533	0.0089
22	16002	486	55	55.236	16.402	0.297	1.384	0.027	-0.1900	-0.0034
23	16003	243	55	31.567	5.581	0.177	0.572	0.559	0.2200	0.0070
24	16004	229	51	22.274	4.231	0.190	0.385	0.058	-0.0218	-0.0010
25	16005	84	34	23.003	4.041	0.176	0.925	0.101	0.0000	0.0000
26	16008	1090	55	91.485	11.924	0.130	-0.191	0.121	0.3274	0.0036
27	16009	1583	56	159.612	26.937	0.169	-0.380	-0.096	0.3855	0.0024
28	18005	378	54	57.006	15.221	0.267	1.287	-0.210	0.1880	0.0033
29	19001	103	52	15.921	2.643	0.166	0.413	0.042	0.0101	0.0006
30	19020	74	28	24.630	8.285	0.336	0.093	0.119	-0.4019	-0.0163
31	20001	406	48	146.494	41.486	0.283	0.428	0.064	1.2209	0.0083
32	20002	424	35	139.657	49.047	0.351	1.799	-0.159	0.0000	0.0000
33	23001	192	46	97.493	31.991	0.328	1.023	-0.036	0.3513	0.0036
34	24008	806	34	118.166	33.606	0.284	-0.111	0.064	0.1771	0.0015
35	24082	763	32	135.505	33.685	0.249	-0.177	0.199	1.1134	0.0082
36	25002	222	55	60.240	10.079	0.167	-0.536	0.301	-0.2932	-0.0049
37	25003	399	55	68.754	10.088	0.147	0.152	0.221	-0.2790	-0.0041
38	25005	193	47	28.661	3.057	0.107	-0.757	0.131	0.0345	0.0012
39	25006	1163	56	86.838	21.068	0.243	0.576	0.166	-0.1172	-0.0013

Station		Area (km ²)	Record length (years)	Mean flow (m ³ /s)	Std. deviation	CV	Skew- ness	Lag 1 Auto. Correlation	Slope (m ³ /s/yr)	Unit slope (per year)
No.	Identifier									
40	25014	164	58	17.595	3.949	0.224	0.511	0.372	-0.1076	-0.0061
41	25017	7980	59	415.097	87.672	0.211	0.114	-0.134	1.2707	0.0031
42	25021	479	48	28.193	3.874	0.137	-0.156	0.146	0.1118	0.0040
43	25023	114	56	12.544	3.774	0.301	0.514	0.318	0.1248	0.0099
44	25025	161	35	10.614	3.448	0.325	0.494	0.185	0.2090	0.0197
45	25027	119	47	23.698	6.593	0.278	0.178	0.026	0.1413	0.0060
46	25029	293	37	54.367	12.540	0.231	-0.110	0.280	0.5417	0.0100
47	25030	280	52	44.078	13.659	0.310	0.811	-0.147	0.2015	0.0046
48	26002	641	57	56.835	12.776	0.225	1.833	-0.086	0.0212	0.0004
49	26005	1085	55	92.465	16.418	0.178	0.156	0.012	0.3497	0.0038
50	26006	185	57	27.414	10.027	0.366	2.790	0.057	0.1105	0.0040
51	26007	1207	57	91.591	18.974	0.207	0.591	-0.267	0.0749	0.0008
52	26008	280	54	23.524	5.090	0.216	0.321	0.122	0.0927	0.0039
53	26009	98	39	13.653	2.111	0.155	0.760	-0.145	-0.0236	-0.0017
54	26017	216	53	11.676	1.645	0.141	0.169	0.148	0.0197	0.0017
55	26018	119	53	9.307	1.856	0.199	0.521	0.289	0.0367	0.0039
56	26019	253	55	22.134	5.509	0.249	1.074	0.012	-0.0906	-0.0041
57	26020	122	33	11.001	2.366	0.215	-0.433	0.048	0.0789	0.0072
58	26021	1099	34	71.293	21.998	0.309	0.393	0.403	0.8365	0.0117
59	26022	62	37	6.475	1.966	0.304	0.485	0.061	-0.0495	-0.0076
60	26059	257	23	12.793	2.351	0.184	-0.079	-0.102	-0.1400	-0.0109
61	27001	47	36	20.807	3.796	0.182	1.101	-0.097	-0.0659	-0.0032
62	27002	564	55	34.867	8.386	0.241	1.071	0.064	0.1100	0.0032
63	27003	166	52	24.335	5.550	0.228	0.453	-0.058	0.0121	0.0005
64	27070	144	29	19.200	5.674	0.296	0.968	0.758	-0.1425	-0.0074
65	29001	115	44	14.477	2.830	0.195	0.254	0.175	0.0873	0.0060
66	29004	121	35	11.356	1.614	0.142	0.668	-0.212	0.0083	0.0007
67	29011	354	26	34.066	10.585	0.311	1.579	0.402	0.5874	0.0172
68	29071	124	29	15.679	3.724	0.237	0.612	-0.059	0.1498	0.0096
69	30007	470	35	61.827	12.644	0.205	0.921	-0.075	-0.1480	-0.0024
70	31002	71	26	12.890	3.138	0.243	1.451	0.310	0.0600	0.0047
71	32012	146	24	30.058	3.745	0.125	-0.091	0.006	0.0431	0.0014
72	33070	88	28	7.897	1.299	0.164	0.914	0.231	0.0095	0.0012
73	34001	1975	39	174.653	34.314	0.196	0.647	0.155	0.9290	0.0053
74	34003	1802	29	180.415	31.397	0.174	0.978	-0.066	0.1995	0.0011
75	34009	117	37	28.083	4.844	0.172	0.390	0.167	-0.0454	-0.0016
76	34011	143	34	18.813	3.123	0.166	0.507	0.144	0.0731	0.0039
77	34018	95	33	11.926	2.773	0.233	0.951	0.237	0.1332	0.0112
78	34024	127	29	20.293	3.209	0.158	-1.620	-0.029	0.0154	0.0008
79	35001	299	35	34.674	11.240	0.324	1.002	0.513	0.3400	0.0098
80	35002	89	34	51.784	8.781	0.170	0.055	0.066	0.1800	0.0035
81	35005	640	61	78.640	19.834	0.252	0.782	0.223	0.4957	0.0063
82	35071	247	31	26.525	5.282	0.199	0.151	0.018	0.0908	0.0034
83	35073	384	30	54.807	11.986	0.219	0.269	-0.182	-0.0667	-0.0012
84	36010	772	54	67.409	15.322	0.227	0.831	0.201	0.2160	0.0032
85	36011	321	53	18.042	3.397	0.188	-0.184	0.154	0.0861	0.0048
86	36012	262	50	14.160	3.176	0.224	0.212	0.310	0.0775	0.0055
87	36015	153	37	24.042	7.849	0.326	1.651	0.012	0.2707	0.0113
88	36018	234	54	15.874	2.995	0.189	0.308	-0.114	0.0580	0.0037
89	36019	1492	51	90.748	17.912	0.197	0.318	0.211	0.5276	0.0058
90	36021	23	31	25.054	5.412	0.216	1.309	-0.102	-0.0150	-0.0006
91	36031	64	30	6.851	1.532	0.224	3.264	0.041	0.0267	0.0039
92	39008	78	37	28.256	7.266	0.257	0.456	-0.277	0.0345	0.0012
93	39009	207	33	45.912	11.754	0.256	0.817	-0.042	0.0556	0.0012

In order to examine the uncertainty associated with the temporal change signal to the length of historical records, partitioning of record lengths of all AMF series into a number of timeframes was considered. Based on the available record lengths, the following five timeframes were selected:

- (1) 1955–2008 (54 years),
- (2) 1965–2008 (44 years),
- (3) 1975–2008 (34 years),
- (4) 1985–2008 (24-years)
- (5) Period-of-Records (POR) (average 42 years)

The number of stations used for each timeframe is different with the maximum of 69 sites for 24 year period, 66 for the 34-year, 42 for the 44-year and 29 for the 54-year timeframes (see **Table 7.4** for details). The Period-of-Record (POR) timeframe comprises of all available records for all 93 sites and has an average record length of 42 years. **Table 7.4** summarises some properties of these timeframes.

In addition to the annual maximum data form, trend analysis was also carried out for a 5-yearly median series of the observed AMF Series. This series was derived from all 117 A1 & A2 gauging sites. The median series are considered in order to compensate for any undesirable data properties such as presence of outliers, high autocorrelations etc.

Table 7.4: Study timeframes (AMF Series)

Study periods	Length of record (years)	No. of Sites	Area [range(mean)] (km ²)
1955-2008	54	29	114 – 7980 (918)
1965 - 2008	44	42	103 – 7980 (731)
1975 - 2008	34	66	47 – 7980 (614)
1985 - 2008	24	69	23 – 7980 (633)
Period of Records	42 (average)	93	23 – 7980 (495)
Median Series	-	117	23 – 7980 (495)

7.3 METHODOLOGY

7.3.1 General

The purpose of trend testing is to determine if the values of a random variable generally increase (or decrease) over some period of time in statistical terms (Helsel and Hirsch, 1992).

Hydrological data are often strongly non-normal and this means that tests which assume an underlying normal distribution are not adequate. In general, parametric tests are more powerful when the variable is normally distributed, but much less powerful when it is not, compared with the non-parametric tests (Hirsch et al., 1991). The non-parametric (often called distribution-free) methods are normally used because they allow minimal assumptions to be made about the data and are therefore particularly suited to hydrological series, which are often neither normally distributed nor independent (Kundzewicz, 2004).

The null hypothesis, H_0 , for the tests for trend test is that there is no trend in the data. The null hypothesis, H_0 , for the tests for changes or difference in means/medians is that there are no changes or difference in the means/medians between two data periods. The null hypothesis H_0 for the tests for randomness (independence) is that the data come from a random process. It is considered that the alternative hypotheses for all tests are non-directional i.e. all tests are two tailed tests. All tests were carried out for a significance level of 5%.

Based on the above and since it was found during the 1975-UK Flood Studies (NERC, 1975) and very recently in the Flood Studies Update Programme (OPW, 2009) that the two-parameter Extreme Value type 1 (Gumbel) distribution can adequately describe the Irish Annual Maximum Flood Series, the use of normality based parametric tests was not considered to be appropriate in this case. Hence non-parametric tests are mainly used. However, in order to compare the power of the tests and to have a reliable result, a number of parametric tests are used.

7.3.1.1 Test of Independence

As indicated earlier in Chapter 6, in most trend tests, it is always necessary to assume that the observations are independent and come from a common distribution (stationarity). If these assumptions are not fulfilled by the data, then the test results can be meaningless, in the sense that the estimates of significance level would be grossly incorrect. For this, it is very important to test the validity of these assumptions. The following three tests have been employed to test the assumption of 'independence' in the Irish AMF Series:

- (i) Autocorrelation test – Lag 1 (parametric test for independence)
- (ii) Turning points (TP) test (Kendall non-parametric test for randomness)
- iii) Rank Difference (RD) test (Meachem non-parametric test for randomness)

The theoretical details of these tests are discussed in the previous chapter (Section 6.5.3.1).

7.3.1.2 Test for step change / stationarity assumption test

The following two tests are used to test the stationarity assumption in the data series:

- (i) Mann-Whitney U (MW-U) test (non-parametric test for step jump in mean/median)
- (ii) T-test (Parametric test for step jump in mean)

These tests examine whether the means/medians in two different sub-periods in a data series are different. The Mann-Whitney U test (MW-U test) is a non-parametric test, whereas the t-test is a parametric test. The theoretical details of these tests are discussed Section 6.5.3.2.

7.3.1.3 Test for monotonic trends

The following three tests were employed to identify any existence of trend in the Irish AMF Series:

- i) Mann-Kendall (MK-test, non-parametric test for trend)
- ii) Spearman's Rho (SPR-test, non-parametric test for trend)
- iii) Standardised Linear Regression test (SLR test, parametric test for trend)

The first two tests are non-parametric tests and the third one is a parametric test. The details of the two non-parametric tests have been discussed in the previous chapter. The SLR test is discussed below:

Standardised Linear Regression Test

This test determines whether there is a linear trend by examining the relationship between time (x) and the variable of interest (y). It is similar to the linear regression test. The test statistic was defined by:

$$b_s = \frac{b}{\bar{y}} \quad (7.1)$$

where, b is the regression gradient and \bar{y} is the mean of the time series, $\bar{y} = \frac{1}{n} \sum_{i=1}^n y_i$. The regression gradient is estimated by:

$$b = \frac{\sum_{i=1}^n (x_i - \bar{x})(y_i - \bar{y})}{\sum_{i=1}^n (x_i - \bar{x})^2} \quad (7.2)$$

The critical values for the test statistic, b_s , for various significance levels were calculated from the sampling distribution, which was obtained by Monte Carlo simulation. Ten thousand time series with sizes ranging from 10 to 50 years were generated from an EV1 distribution with a population mean (μ) and coefficient of variation (CV) of 1.0 and 0.3 (a typical value of CV for the Irish AMF Series) respectively. The selection of EV1 distribution was based on its suitability for the Irish AMF Series as discussed earlier. An examination of the distribution of b_s

showed that, for sample sizes larger than 10, it follows the normal distribution. Refer to **Appendix B** for the estimated critical values for b_s .

7.3.1.4 Approaches for incorporating the effect of serial correlation for estimating trends in hydrological time series

The assumption of independence of observations is inherent in the application of trend identification tests. Therefore, it is important to take into account the effect of serial correlation (autocorrelation) of the hydrological time series for evaluating significance of trends at local scale because failure to do so could result in erroneous conclusions. [Kulkarni and von Storch \(1995\)](#) found that if a time series is positively correlated then the trend identification tests (e.g. the MK test) will suggest a significant trend more often than it will for an independent series.

In order to eliminate the influence of serial correlation, many approaches have been suggested. [Kulkarni and Von Storch \(1995\)](#) and [Von Storch \(1995\)](#) proposed to pre-whiten a series prior to applying the trend test. That is, the serial correlation component if significant, such as a lag-one autoregressive process (AR(1)) is removed from a time series and the significance of a trend is then evaluated by using the MK test on the modified pre-whitened (PW) series. [Douglas et al. \(2000\)](#) demonstrated that pre-whitening can reduce the detection rate of the significant trend by the MK test. [Yue et al. \(2002b\)](#) investigated this issue by simulation experiments where both a trend and a lag-one autoregressive process (AR(1)) existed in a time series. Their study indicated that pre-whitening a positive AR(1) process will remove a portion of the trend, hence leading to an acceptance of the null hypothesis of no trend, while the null hypothesis might be false. They also showed that, when trend does exist in a time series, pre-whitening is not suitable for eliminating the influence of serial correlation of the MK test. In order to more effectively reduce the effect of serial correlation on the MK test, a modified pre-whitening procedure, termed as trend-free pre-whitening (TFPW), was proposed by [Yue et al. \(2002b\)](#). In this method, the time series is detrended before the lag-1 autocorrelation is removed from the time series, and the trend is added to the serial correlation free time series before a trend test is applied. [Kundzewicz and Robson \(2000\)](#) suggested a block resampling approach. In this approach, the original data is resampled in predetermined blocks for a large number of times to estimate the

significance of the observed test statistic, i.e. the MK or SPR test statistics. The block size depends upon the number of contiguous significant serial correlations.

In the current study, both the PW (Kulkarni and Von Storch, 1995; Von Storch, 1995) and TFPW (Yue et al., 2002b, 2003) procedures have been applied to correct the effect of serial correlation in the Irish AMF Series.

The steps involved in implementing the PW approach are summarized below:

- (1) Firstly, compute the lag-1 autocorrelation coefficient, r_1 ,
- (2) if r_1 is found non-significant at the chosen significance level α then the trend identification is applied to the original time series (y_1, y_2, \dots, y_n) and otherwise
- (3) the trend identification test is applied to the pre-whitened time series $(y_2 - r_1 y_1, y_3 - r_1 y_2, \dots, y_n - r_1 y_{n-1})$.

The TFPW approach includes the following steps:

- (1) Firstly estimate the slope of the trend using the non parametric trend slope estimator developed by Sen (1968). This estimation of the trend slope β is more robust than a normal linear regression slope (Yue et al., 2003).

$$\beta = \text{median} \left[\frac{y_i - y_j}{i - j} \right] \text{ for all } j < i \quad (7.3)$$

where y_i and y_j are the data at time points i and j , respectively. If there are N values in the time series then one can get as many as $n = N(N-1)/2$ slope estimates and the Sen's Slope (Sen, 1968) is taken as the median of these n values.

- (2) Secondly, detrend the time series being analysed under the assumption of a linear trend

$$x_t = y_t - \beta.t \quad (7.4)$$

where x_t is the detrended time series and y_t is the original time series.

- (3) Thirdly, estimate the first serial correlation coefficient r_1 (lag-1 autocorrelation) from the detrended series,

- (4) if r_1 is non-significant at a chosen significant level then the trend identification test is applied to the original time series, and otherwise
- (5) the trend identification test is applied to the detrended pre-whitened series as follows:

$$x'_t = x_t - r_1 y_{t-1} \quad (7.5)$$

the x'_t time series should now be free of a trend and serial correlation.

Finally, the initially removed trend is included back into the time series.

$$x''_t = x'_t + \beta.t \quad (7.6)$$

The resulting time series x''_t is a blended time series which includes the original trend but without autocorrelation.

All three trend tests chosen for this study (MK-test, SPR-test and the SLR-test) have been applied to the x''_t series. In addition, the trend tests have also been applied on the original AMF Series. The effects of serial correlation in the AMF Series on trend test results then have been examined by comparing the PW and TFPW results with the original test results. These procedures have been applied in the AMF Series of all study timeframes as outlined in Section 7.2.1.

7.4 RESULTS AND DISCUSSIONS

7.4.1 Test for Independence

The independence assumption of the AMF Series is examined here through three statistical tests: (i) Autocorrelation test – Lag 1 (r_1), (ii) Turning points test (TP-test) and (iii) Rank Difference (RD-test). The serial correlation structure of the data series were investigated using the first test, while the randomness nature of the data series was investigated through the last two tests.

Serial structure of the AMF Series:

The serial structure of the Irish AMF series has been investigated by estimating the Lag-1 autocorrelation for the 'Original' and 'Trend Free (TF)' Series. The TF series

was used to identify the effect of trend on the serial correlation structure of data series. In the TF case, the slope of the trend in the AMF records was estimated using the non-parametric Sen's Slope (Sen, 1968) method and subsequently the AMF series was detrended in accordance with method described in Section 7.3.13 (Yue et al., 2003).

Table 7.5 and **Figure 7.4** present the serial correlation structure of the Original AMF records in terms of Lag-1 autocorrelation. **Figure 7.4** illustrates the percentage of stations/sites with positive and negative Lag-1 autocorrelation (r_1) along with its significant proportions identified in Irish AMF series for all selected timeframes. The results suggest that the Irish AMF series is mainly dominated by positive serial correlations. In the POR data scenario 12 sites (13%) showed significant serial correlations (11 positive and 1 negative). In the timeframes of 24 (1985-2008), 34 (1975-2008), 44 (1965-2008) and 54 (1955-2008) years, the estimated significant r_1 were found in 13%, 11%, 10% and 24% of sites respectively. Over 50% of these in each case are positively serially correlated.

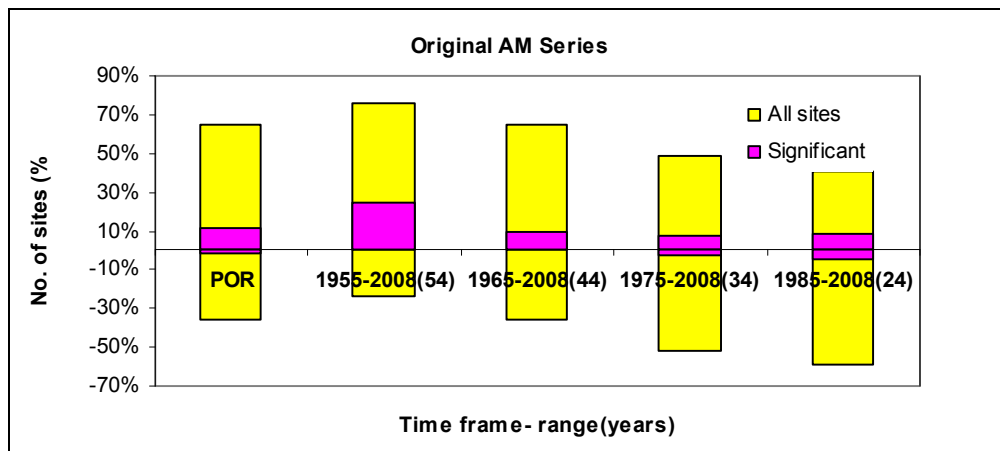


Figure 7.4: Percentage of sites with positive and negative Lag-1 serial correlation in AMF series along with respective significant percentage for the selected five timeframes (Original time series, significance level of 5%)

Table 7.5: Number of sites showed significant dependency / non-randomness at 5% significance level

No.	Study time frames	Length of records (years)	No. of Sites	No. of sites – significant at 5% significance level			
				Lag-1 AutoCor. (Original data)	Lag-1 AutoCor. (Trend-free data)	TP-test	RD-test
1	POR	42	93	12 (13%)	8 (9%)	7 (8%)	16 (17%)
2	1955-2008	54	29	7 (24%)	2 (7%)	3 (10%)	9 (31%)
3	1965 - 2008	44	42	4 (10%)	2 (5%)	3 (7%)	9 (21%)
4	1975 - 2008	34	66	7 (11%)	9 (14%)	4 (6%)	9 (14%)
5	1985 - 2008	24	69	9 (13%)	8 (12%)	4 (6%)	6 (9%)

Figure 7.5 and **Table 7.5** presents the correlation structures of the TF data series. It can be seen that detrending of data series reduces the number of significant serially correlated sites in all cases of timeframes except in the 34 (1975-2008) year timeframe. In the POR case, 9% sites showed significant autocorrelation, which is 4% lower than the original time series case. However, the detrending process slightly increases the number of negatively significant sites.

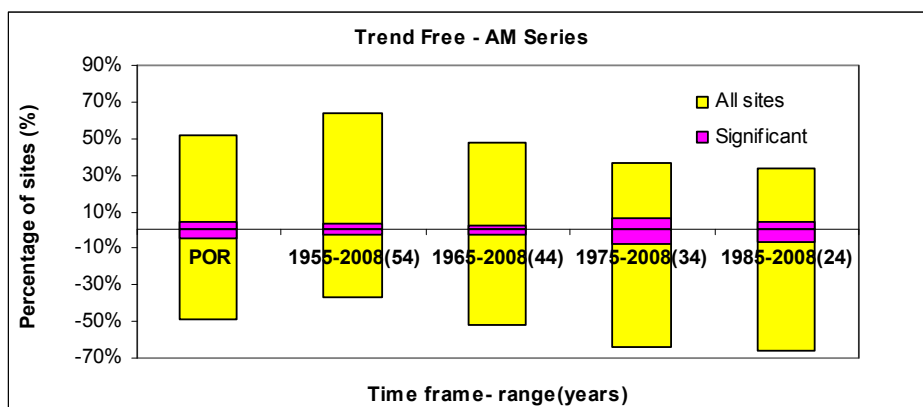


Figure 7.5: Percentage of sites with positive and negative lag-1 serial correlation in AMF series along with respective significant percentage for the selected five timeframes (TF series, significance level of 5%)

The estimated autocorrelations for various lags (1 to 10) for the sites with significant Lag-1 autocorrelations and their 95% confidence intervals ($\pm 2/\sqrt{N}$) in the POR data scenario are plotted in **Figure 7.6**. The location details of these sites are given in **Table 7.6**.

Table 7.6: Sites showed significant lag-1 autocorrelation (at 5% significance level)

Station ID.	River name and site location	Record length (year)	r_1	Direction of lag-1 autocorrelation	95% confidence intervals ($\pm 2/\sqrt{N}$)
15004	River Nore at McMahons Br.	55	0.27	Positive	± 0.27
16003	Clodiagh River at Rathkennan	55	0.56	Positive	± 0.27
25002	Newport River at Barrington's Br.	55	0.30	Positive	± 0.27
25014	Silver River at Millbrook	58	0.37	Positive	± 0.26
25023	Little Brosna River at Milltown	56	0.32	Positive	± 0.27
26007	Suck River at Bellagill	57	-0.27	Negative	± 0.26
26018	Owenure River at Bellavahan	53	0.29	Positive	± 0.27
26021	Inny River at Ballymahon	34	0.40	Positive	± 0.34
27070	Baunkyle River at L. Inchiqui	29	0.76	Positive	± 0.37
29011	Dunkellin River at Kilcolgan	26	0.40	Positive	± 0.39
35001	Owenmore River at Ballynacarrow	35	0.51	Positive	± 0.34
36012	Erne River at Sallaghan	50	0.31	Positive	± 0.26

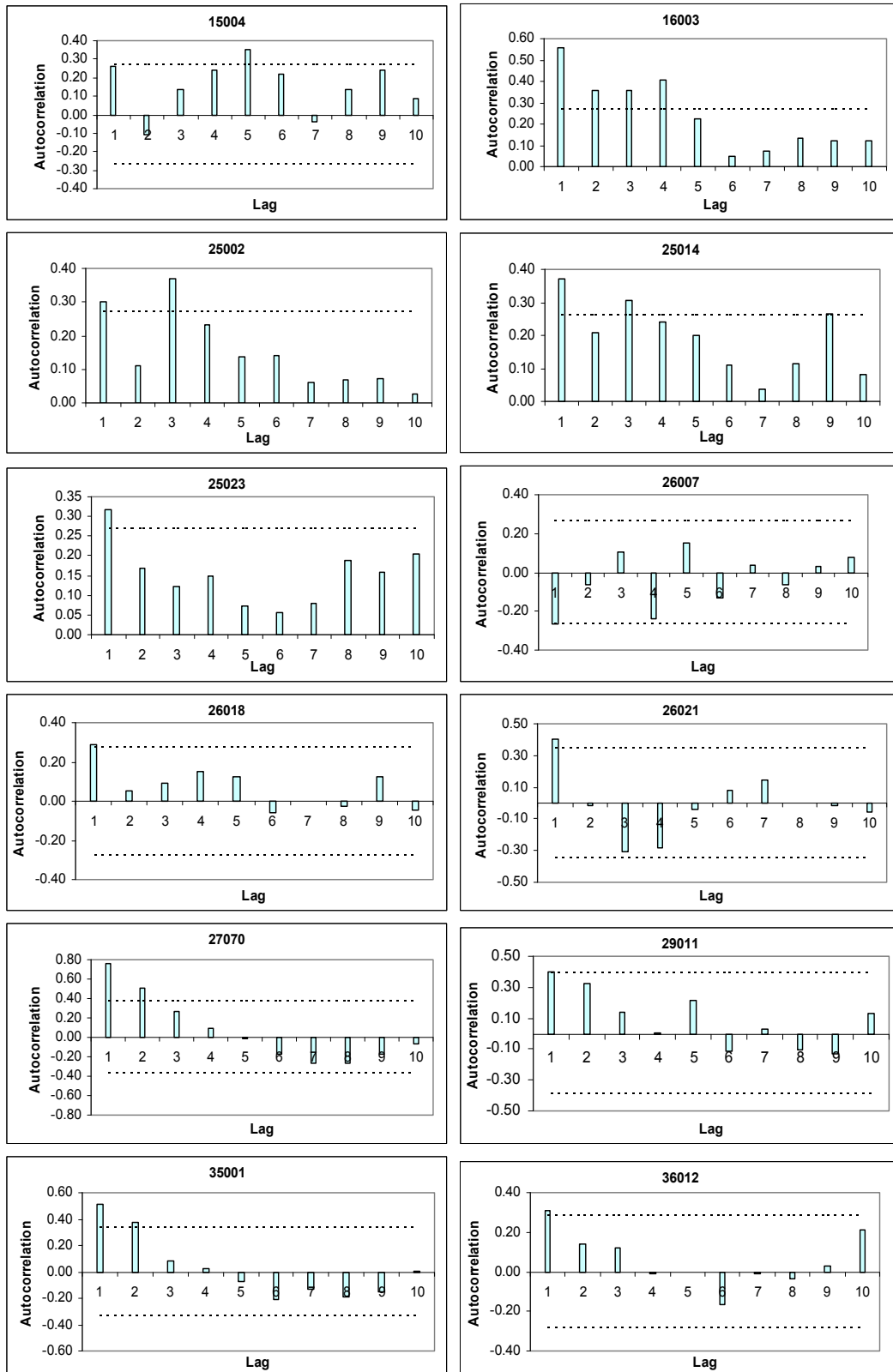


Figure 7.6: Autocorrelation structure of AMF Series at various lags for the sites with significant Lag-1 autocorrelation at 5% significance level.

The above autocorrelation plots show that the majority of AMF records that exhibit significant Lag-1 autocorrelation are not autocorrelated significantly at larger lags. However, 4 out of 12 stations showed significant autocorrelations at larger lags (lag >2 year) [*River Nore at McMahons Bridge (15004)*, *Clodiagh River at Rathkennan (16003)*, *Newport River at Barrington's Bridge (25002)* and *Silver River at Millbrook (25014)*]. The significant low lag autocorrelations (e.g. Lag-1 autocorrelation) are less likely to occur by chance, rather they represent persistence in their associated catchment physical systems (e.g. effect of reservoir storage system on streamflows).

Non-randomness in the AMF Series:

Figure 7.7 and **Table 7.5** shows the percentage of stations/sites with significant non-randomness properties as identified by the TP and RD tests. The number of sites with significant non-randomness properties identified by the RD-test is higher than that by the TP-test, suggesting that the power of the RD-test is higher than the TP-test. In both cases, power of the tests decreases with the decrease in record lengths. In the POR data scenario, 16 sites (17%) showed significant non-randomness by the RD-test, while in the timeframes of 24, 34, 44 and 54 years the estimated significant sites are 9%, 14%, 21% and 31% respectively.

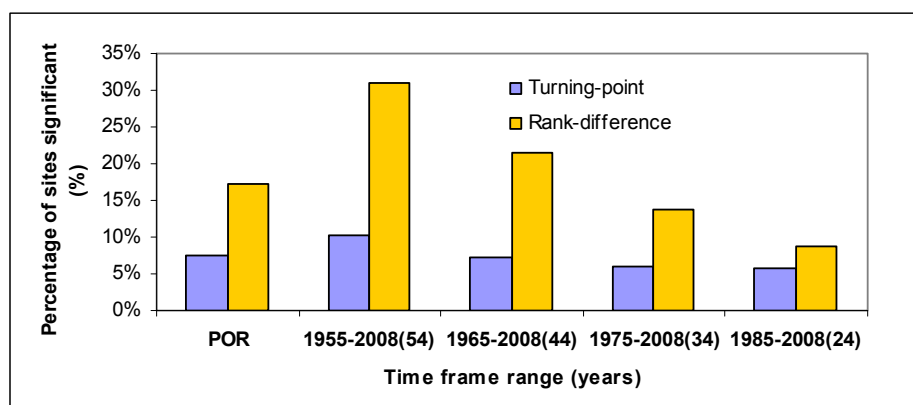


Figure 7.7: Number of sites with significant non-randomness at 5% significance level

7.4.2 Test for Stationarity

Any evidence of non-stationarity or step changes in the AMF Series has been examined using two tests, the parametric t-test and the non-parametric Mann-Whitney U-test (MW-U test). A common point of change for all AMF Series has been identified by plotting the AMF data and the associated rainfall records against time. **Figure 7.8** shows the plots of average specific AMF records (average of 33 sites across Ireland) for the period of 1955-2007 along with a 5-year moving average curve and a linear regression line. An abrupt change in the records during the seventies, particularly during the years of 1974 and 1976 can be noticed in this figure. These changes in the records are also evident in the time series plots of average annual maximum rainfall records (average of 144 sites) for various durations (1-day, 2-day, 3-day, 4-day, 8-day, 10-day, 16-day, 20-day and 25-day) as can be seen in **Figure 7.9**. Kiely (1999) also identified 1975 as a break/turning point in the Irish AMF series.

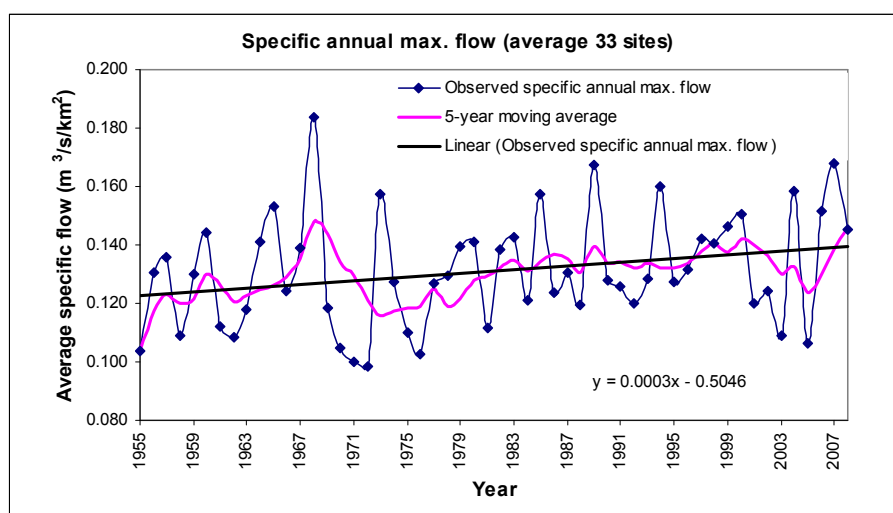


Figure 7.8: Plots of average specific annual maximum flows against time (average of 33 sites) for the period of 1955 – 2007.

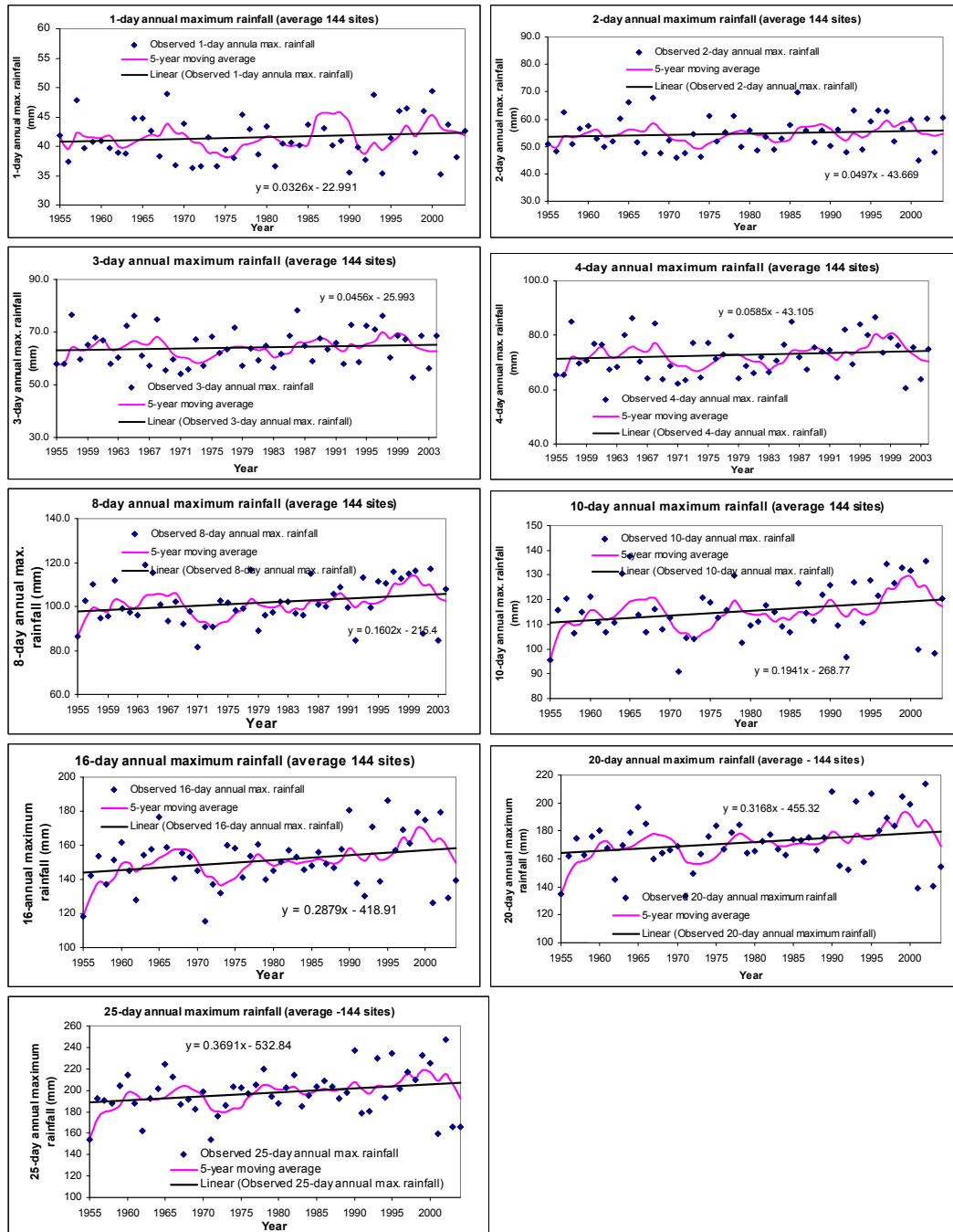


Figure 7.9: Plots of average annual maximum rainfall records of various durations (1-day, 2-day, 3-day, 4-day, 8-day, 10-day, 16-day, 20-day and 25-day) against time for the period of 1955–2004 (average of 144 sites)

Based on the above, the AMF data series have been partitioned at 1976 for the purpose of detecting step change in the data series. Due to the shorter record lengths, the step change tests were applied only on two data timeframes, 1955-2008 and 1965-2008. The tests were also applied on the POR data scenario. In this case, 46 sites with longer record lengths were identified from 93 sites.

Table 7.7 and **Figure 7.10** present the percentage of sites with progressive decreases and increases of mean or median of AMF Series for all selected timeframes for the two sub-periods considered. The proportion of stations with significant step change in mean/median (at 5% significance level) is also shown therein. The results suggest that in the majority of the stations at all timeframes, the mean/median annual maximum flows for the post 1976 period have increased. In the POR data scenario, 14 sites (30%) showed significant step change (9 increases and 5 decreases) by the MW-U test. In the timeframes of 1955-2008 and 1965-2008, significant step changes were identified at 41% and 21% sites by the MW-U test. The parametric t-test also showed almost similar results.

Table 7.7: The number of sites with significant non-stationarity (at 5% significance level) identified by the T-test and the Mann-Whitney U-test (change point 1976)

No.	Study time frames	Record length (years)	No. of Sites	No. of sites – significant at 5% significance level					
				T-test			Mann-Whitney U-test		
				Total	Increas	Decrease	Total	Increase	Decrease
1	POR	42	46	12 (26%)	8 (17%)	4 (9%)	14 (30%)	9 (19%)	5 (11%)
2	1955-2008	54	29	10 (34%)	7 (24%)	3 (10%)	12 (41%)	7 (24%)	5 (17%)
3	1965-2008	44	42	8 (19%)	5 (12%)	3 (7%)	9 (21%)	6 (14%)	3 (7%)

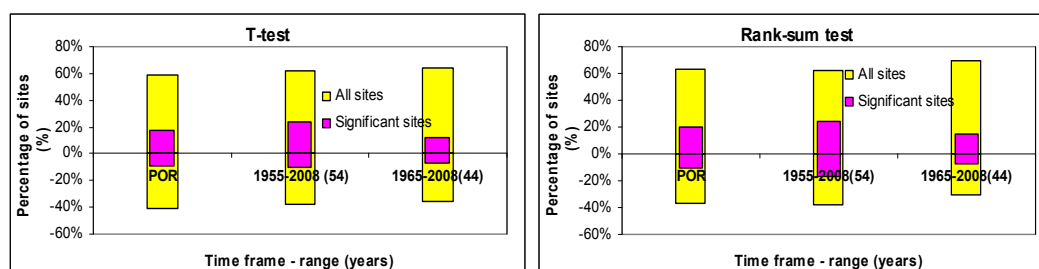


Figure 7.10: Percentage of sites with increase and decrease in mean/median between time periods of 1955-1975 and 1976-2008 in AMF series along with respective significant percentage for the three timeframes (Panel a. T-test and Panel b. MW-U test)

Table 7.8 lists the sites which showed significant non-stationarity as detected by the MW-U test in the longest timeframe of 1955-2008. Out of 29 sites, 12 sites showed significant step change in mean/median at 5% significance level, of which 7 showed upward change and 5 showed downward change. In order to examine the nature of changes in various statistical properties of the 12 sites between the two sub-periods of 1955-1975 and 1976-2008, box plots of the AMF records for these sub-periods

have been prepared as shown in **Figure 7.11**. These plots suggest that, in addition to changes in mean/medians, the variability in the data series has also been changed (increased/decreased).

Table 7.8: Sites showing significant non-stationarity at 5% significance level (MW-U test) (Data period: 1955-2008, partitioned at 1976 i.e. 1955-1975 and 1976-2008)

Station	River and Location	Direction of changes of mean / median	Results (MW-U test statistic)
14005	Barrow at Portalington	Decrease	2.005
15004	Nore at McMahons Br.	Increase	-2.857
16003	Clodiagh at Rathkennan	Increase	-4.631
16008	Suir at Newbridge	Increase	-2.369
25002	Newport at Barrington's Br.	Decrease	3.692
25003	Mulkear at Abington	Decrease	3.451
25014	Silver at Millbrook	Decrease	3.105
25023	Little Brosna at Milltown	Increase	-3.309
26005	Suck at Derrycahill	Increase	-2.564
26019	Camlin at Mullagh	Decrease	2.091
35005	Ballysadare at Ballysadare	Increase	-2.756
36011	Erne at Bellahillan	Increase	-2.255

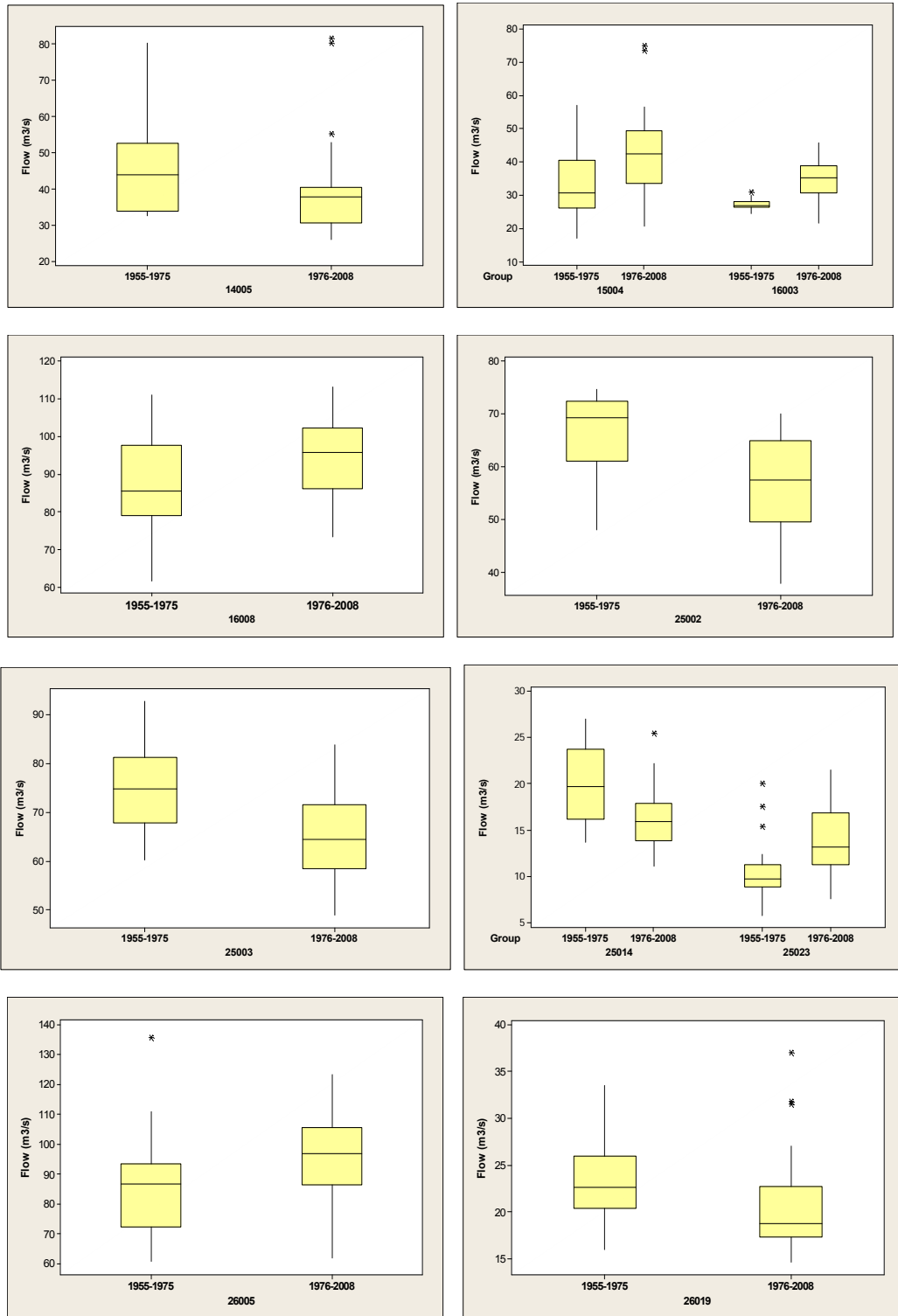


Figure 7.11: Plots of the two sub-periods of AMF Series partitioned at 1976 (1955-1975 and 1976-2008) for each sites showing significant non-stationarity i.e. changes in location parameters (contd.)

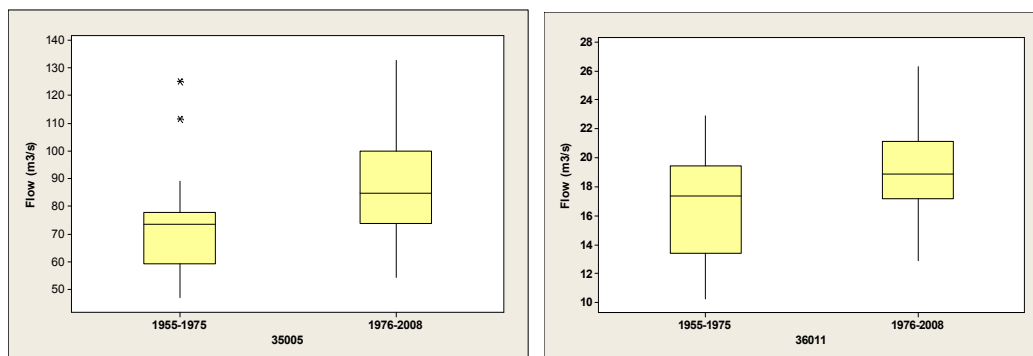


Figure 7.11: Plots of the two sub-periods of AMF Series partitioned at 1976 (1955-1975 and 1976-2008) for each sites showing significant non-stationarity i.e. changes in location parameters.

7.4.3 Trend Test Results

Any evidence of the presence of monotonic trends in the Irish AMF Series has been investigated by using two non-parametric (MK and SPR tests) and one parametric test (SLR test). The results of these tests are presented and discussed in a number of separate sections:

- (i) first, the trends in the Original data series, i.e. without considering the serial correlation structure of the records, were explored,
- (ii) the effect of serial correlation on the significance of identified trends was then examined,
- (iii) a discussion on the overall trend results is presented, and
- (iv) finally, the spatial distribution of the trend test results across Ireland is explored.

(i) Trends in Irish AMF records (Original data series)

The number of sites with positive and negative trends identified by the MK, SPR and SLR tests in Irish AMF series along with the respective significant proportions, for all timeframes are presented in **Table 7.9** and are graphically illustrated in **Figure 7.12**. It should be noted here that these trend tests were applied to the original data series without removing any effect of autocorrelation. In general, it can be seen in **Figure 7.12** that the majority of the selected sites in Ireland show increasing trends in the AMF Series. For example, in the POR data scenario, out of 93 sites, the MK, SPR and SLR tests identified increasing trends in 64 (69%), 64(69%) and 65 (70%) sites, respectively (irrespective of significance level).

However, in terms of significance level, these numbers are smaller. At 5% significance level, the non-parametric MK and SPR tests each identified increasing significant trends at 23 (25%) sites, while the SLR tests detected significant trends at 13 (14%) sites in the POR timeframe. On the other hand, significant decreasing trends were identified at 7% sites by the MK and SPR tests and at 5% sites by the SLR test. Irrespective of the direction of trends, significant trends were identified at 32% sites (30 out of 93) by the MK and SPR tests and at 19% sites by the SLR test.

Table 7.9: Sites with significant trends (at 5% significance level) when trend identification tests (MK, SPR and SLR) were applied to the Original AMF Series.

Time frame	Record length (years)	No. of Sites	No. of sites – significant at 5% significance level								
			Mann-Kendall test			Spearman Rho test			SLR test		
			Total	Up	Down	Total	Up	Down	Total	Up	Down
1955-2008	54	29	14 (48%)	11 (38%)	3 (10%)	14 (48%)	11 (38%)	3 (10%)	6 (21%)	4 (14%)	2 (7%)
1965-2008	44	42	19 (45%)	16 (38%)	3 (7%)	18 (43%)	15 (38%)	3 (7%)	8 (19%)	6 (14%)	2 (5%)
1975-2008	34	66	22 (33%)	21 (32%)	1 (1%)	20 (30%)	19 (29%)	1 (1%)	13 (20%)	13 (20%)	0 (0%)
1985-2008	24	69	10 (15%)	8 (12%)	2 (3%)	11 (16%)	8 (12%)	3 (4%)	8 (12%)	7 (10%)	1 (2%)
POR	42	93	30 (32%)	23 (25%)	7 (7%)	30 (32%)	23 (25%)	7 (7%)	18 (19%)	13 (14%)	5 (5%)
Median Series	-	117	14 (12%)	11 (9%)	3 (3%)	14 (12%)	11 (9%)	3 (3%)	6 (5%)	4 (3%)	2 (2%)

The above results suggest that the performance of the MK and SPR tests are comparable and both have similar power in identifying trends in the AMF series, while the SLR test has less power. Similar patterns can be noticed in other timeframes considered as illustrated in **Figure 7.12**.

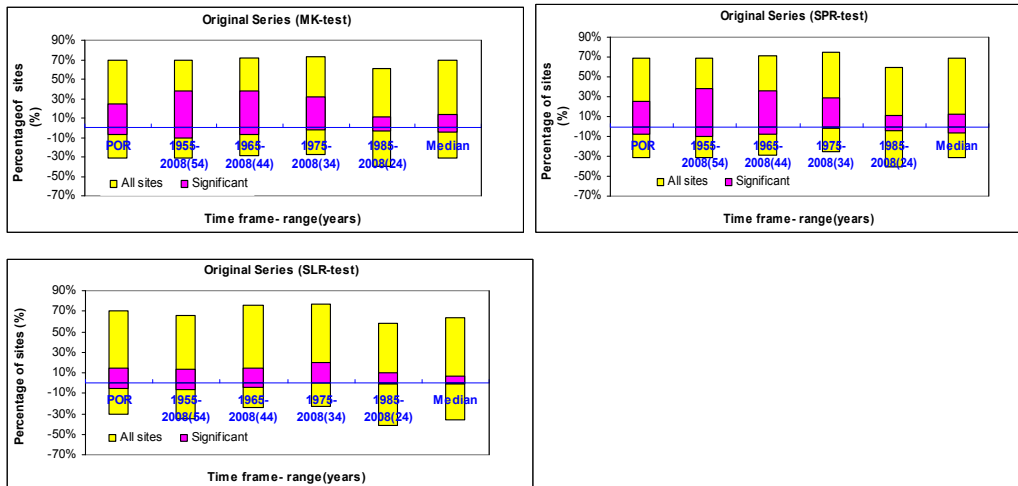


Figure 7.12: Percentage of sites with positive and negative trends identified by the MK, SPR and SLR tests (panels a-c) in AMF series along with respective significant percentage for the five timeframes (the trend tests were applied to the Original data without removing any effect of autocorrelation)

The temporal variations in the trend test results are also apparent from **Figure 7.13**. All three tests identified the highest percentage of sites with significant trends in the longest timeframe of 1955-2008 and the numbers have gradually decreased with the decrease in record lengths (in the 1965-2008, 1975-2008 and 1985-2008 timeframes). This suggests that the power of the tests is a decreasing function of the record lengths, i.e. power decreases with the decrease in record lengths. The rate of decrease is higher and is almost equal for the two non-parametric MK and SPR tests in comparison to the parametric SLR test. This interpretation of the power of trend detection test in the case of POR and median data scenarios is difficult to make, because of the variation in record lengths in the selected data set.

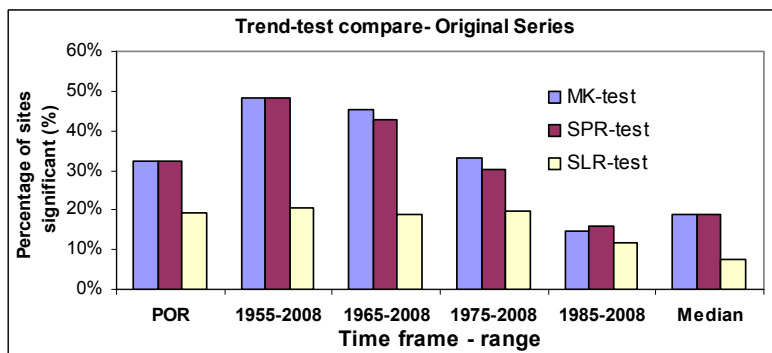


Figure 7.13: Comparison of trend test results for the MK, SPR and SLR tests showing the percentage of sites with significant trends at 5% significance level, in the AMF Series for all timeframes (the trend tests were applied to the Original data without removing any effect of autocorrelation)

(ii) Effect of serial correlation in the AMF records on the significance of identified trends:

The effect of serial correlation on the significance of the observed MK, SPR and SLR tests statistics is investigated by applying these tests to the PW and TFPW data series and comparing them with that of the original time series as discussed in Section 7.3.1.3. The numbers of stations with significant trends identified through the PW and TFPW approaches are presented in **Tables 7.10** and **7.11** respectively. **Figure 7.14** graphically presents these results (along with the results of Original series) showing the percentage of stations with statistically significant positive and negative trends for all timeframes. The results for the Original and PW and TFPW AMF time series are shown in panels a, b and c respectively in this figure. A further comparison of the trend test results associated with these three approaches is presented in **Table 7.12** and is graphically illustrated in **Figure 7.15**.

Table 7.10: Sites with significant trends (at 5% significance level) when trend identification tests (MK, SPR and SLR) were applied to the PW AMF Series.

Time frame	Record length (years)	No. of Sites	No. of sites – significant at 5% significance level								
			Mann-Kendall test			Spearman Rho test			SLR test		
			Total	Up	Down	Total	Up	Down	Total	Up	Down
1955-2008	54	29	14 (48%)	11 (38%)	3 (10%)	14 (48%)	11 (38%)	3 (10%)	6 (21%)	4 (14%)	2 (7%)
1965-2008	44	42	19 (45%)	16 (38%)	3 (7%)	18 (43%)	15 (36%)	3 (7%)	7 (17%)	5 (12%)	2 (5%)
1975-2008	34	66	19 (29%)	18 (27%)	1 (2%)	19 (29%)	18 (27%)	1 (2%)	11 (17%)	11 (17%)	0 (0%)
1985-2008	24	69	7 (10%)	5 (7%)	2 (3%)	8 (11%)	5 (7%)	3 (4%)	7 (10%)	6 (9%)	1 (1%)
POR	42	93	28 (30%)	21 (23%)	7 (7%)	28 (30%)	21 (22%)	7 (8%)	17 (18%)	12 (13%)	5 (5%)
Median Series	-	117	14 (12%)	11 (9%)	3 (3%)	14(12 %)	11 (9%)	3 (3%)	6 (5%)	4 (3%)	2 (2%)

Table 7.11: Sites with significant trends (at 5% significance level) when trend identification tests (MK, SPR and SLR) were applied to the TFPW AMF Series.

Time frame	Record length (years)	No. of Sites	No. of sites – significant at 5% significance level								
			Mann-Kendall test			Spearman Rho test			SLR test		
			Total	Up	Down	Total	Up	Down	Total	Up	Down
1955-2008	54	29	15 (51%)	12 (41%)	3 (10%)	15 (51%)	12 (41%)	3 (10%)	6 (21%)	4 (14%)	2 (7%)
1965-2008	44	42	19 (45%)	16 (38%)	3 (7%)	18 (43%)	15 (36%)	3 (7%)	8 (19%)	6 (14%)	2 (5%)
1975-2008	34	66	23 (35%)	22 (33%)	1 (2%)	22 (33%)	21 (32%)	1 (1%)	12 (18%)	12 (18%)	0 (0%)
1985-2008	24	69	9 (13%)	7 (10%)	2 (3%)	10 (15%)	7 (10%)	3 (5%)	7 (10%)	6 (9%)	1 (1%)
POR	42	93	32 (34%)	25 (27%)	7 (7%)	31 (33%)	26 (28%)	5 (5%)	17 (18%)	13 (14%)	4 (4%)
Median Series	-	117	15 (13%)	12 (10%)	3 (3%)	15 (13%)	12 (10%)	3 (3%)	6 (5%)	4 (3%)	2 (2%)

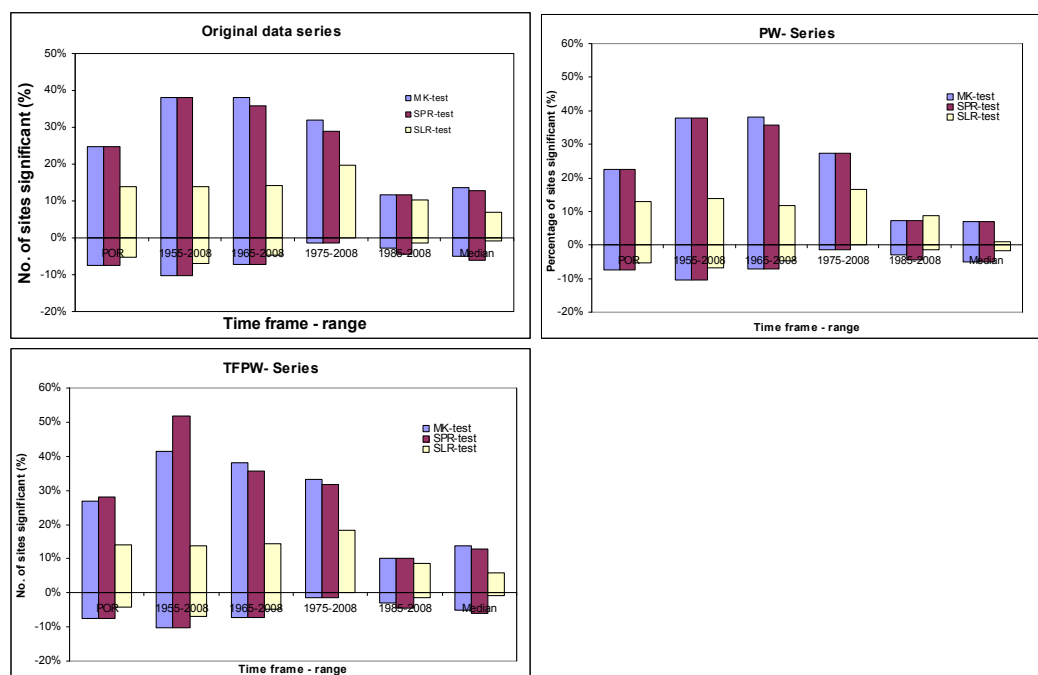


Figure 7.14: Percentage of sites with positive and negative significant (at 5% significance level) trends obtained with the MK, SPR and SLR trend identification tests when applied to the Original, PW and TFPW form of the AMF data series.

Table 7.12: Comparison of trend test results (percentage of sites with significant trends at 5% significance level) for the Original, PW and TFPW series as identified by the MK, SPR and SLR tests.

Time frame	MK-test			SPR-test			SLR-test		
	Original Series	PW Series	TFPW Series	Original Series	PW Series	TFPW Series	Original Series	PW Series	TFPW Series
1955-2008	48%	48%	51%	48%	48%	51%	21%	21%	21%
1965-2008	45%	45%	45%	43%	43%	43%	19%	17%	19%
1975-2008	33%	29%	35%	30%	29%	33%	20%	17%	18%
1985-2008	15%	10%	13%	16%	11%	15%	12%	10%	10%
POR	32%	30%	34%	32%	30%	33%	19%	18%	18%
Median	12%	12%	13%	12%	12%	13%	5%	5%	5%

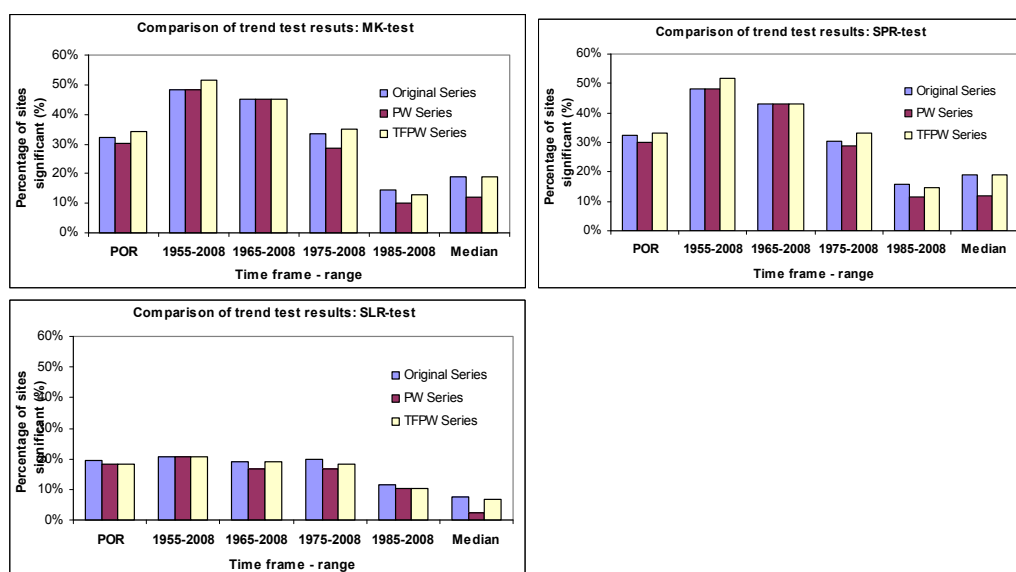


Figure 7.15: Comparison of trend test results showing the percentage of sites with significant trends at 5% significance level) for the Original, PW and TFPW series as identified by the MK, SPR and SLR tests (panel a: MK-test, panel b: SPR test and panel c: SLR-test)

It is obvious from the above that the highest number of stations with significant trends is found when Original data series are employed (i.e. when the effect of serial correlations is not taken into account), with some exceptions for the TFPW approach. For example, the MK-test identified significant trends at 32% sites in the Original POR data scenario, while 30% sites were identified in the PW data scenario. This is not surprising because compared to independent cases, the trend identification tests tend to produce more significant results in the presence of positive serial correlation, which occurs in many of the selected Irish AMF series (**Figure 7.4**). However, the TFPW data series showed slightly higher number of significant sites than the original series. The possible reason for this could be that

serial correlations are estimated from trend-free data for the TFPW approach and that results in a different number of serially correlated time series. This could also be due to a complex trade-off between the autocorrelation and trend and the difficulty in effectively isolating them. Thus, if the serial structure of time series is removed (e.g. using the PW), then the trend identification tests should identify fewer stations with significant trends. However, these numbers are not so striking in the case of Irish AMF series.

(iii) Overall trends in the Irish AMF Series:

Irrespective of the trend identification test, the percentage of stations with significant increasing trends in Irish AMF series (PW case) vary from 7% to 9% for the 24-year timeframe (1985-2008), 17% to 27% for the 34-year timeframe (1975-2008), 12% to 38% for the 44-year timeframe (1965-2008), 14% to 38% for the 54-year timeframe (1955-2008) and 13% to 23% for the POR timeframe (**Table 7.10, Figure 7.14**). Similarly, the percentage of stations with decreasing trends vary from 1% to 4% for the 24-year timeframe (1985-2008), 0% to 2% for the 34-year timeframe (1975-2008), 5% to 7% for the 44-year timeframe (1965-2008), 7% to 10% for the 54 year-timeframe (1955-2008) and 5% to 8% for the POR timeframe. Regardless of the direction of trends, significant trends in Irish AMF series (PW series) vary from 10% to 11% sites for the 1985-2008 timeframe, 17% to 29% for the 1975-2008 timeframe, 17% to 45% for the 1965-2008 timeframe, 21% to 48% for the 1955-2008 timeframe and 18% to 30% for the POR timeframe (**Table 7.12**).

The above results demonstrate that the Irish river catchments are dominated by positive (increasing) trends in AMF time series. Based on the robust MK-test results on the PW - POR AMF series, 30% of sites (28 sites out of 93) showed significant trends at 5% significance level, with increasing trends at 23% of sites. In the case of 1965-2008 timeframe, the MK-test on the PW AMF Series showed significant trends at 45% (19 out of 42) sites with 38% increasing trends. The results in the later case may be more realistic than the POR case, because the POR dataset ignore the effect of sample length on the power of the test. *“Selecting a common period of record facilitates investigation of variable climatic conditions during the (common) prescribed period. Although the POR case provides good spatial coverage, the*

different record lengths at the stations included in the analysis makes it more difficult to interpret the results (Burn and Hag, 2002)".

(iv) Spatial distribution of the trend test results across Ireland:

The results for trend tests include both decreasing and increasing trends. To examine the spatial consistency of the observed trends, maps were created displaying the locations of catchments with decreasing and increasing trends.

Figures 7.16, 7.17 and 7.18 illustrate the spatial distribution of trend test results obtained from MK-test for the data timeframes of POR, 1965-2008 and 1975-2008 respectively. Because of poor spatial coverage the 1955-2008 timeframe was not used. All maps show both the significant and non-significant sites along with their direction of trends (decreasing/increasing). The non-significant sites are shown by the thick smaller arrows and the significant sites are shown by thin long arrows. The decreasing trends are illustrated by downward blue arrow and the upward red arrows represent the increasing trends.

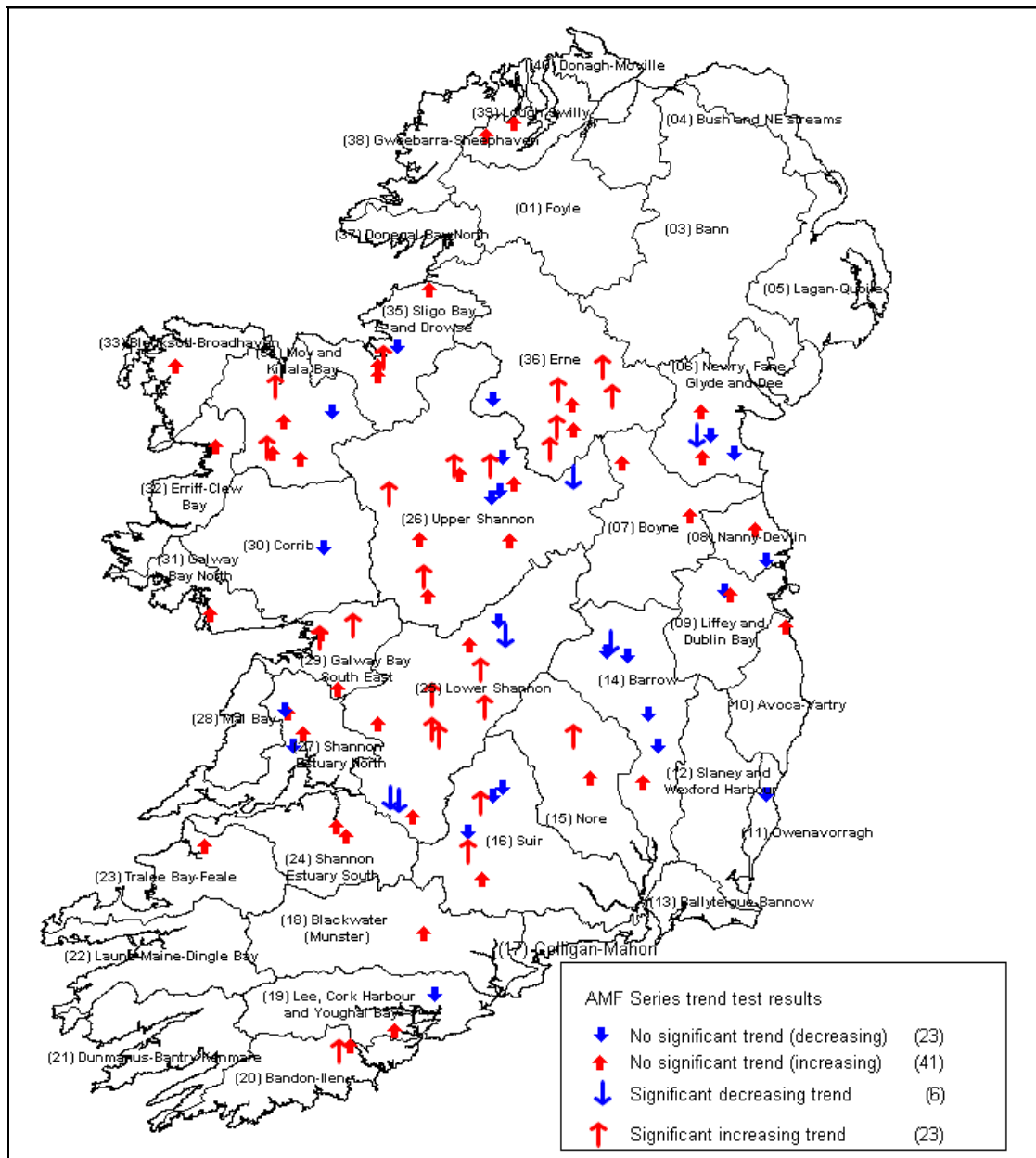


Figure 7.16: Spatial distribution of trend test results – POR – Original data series

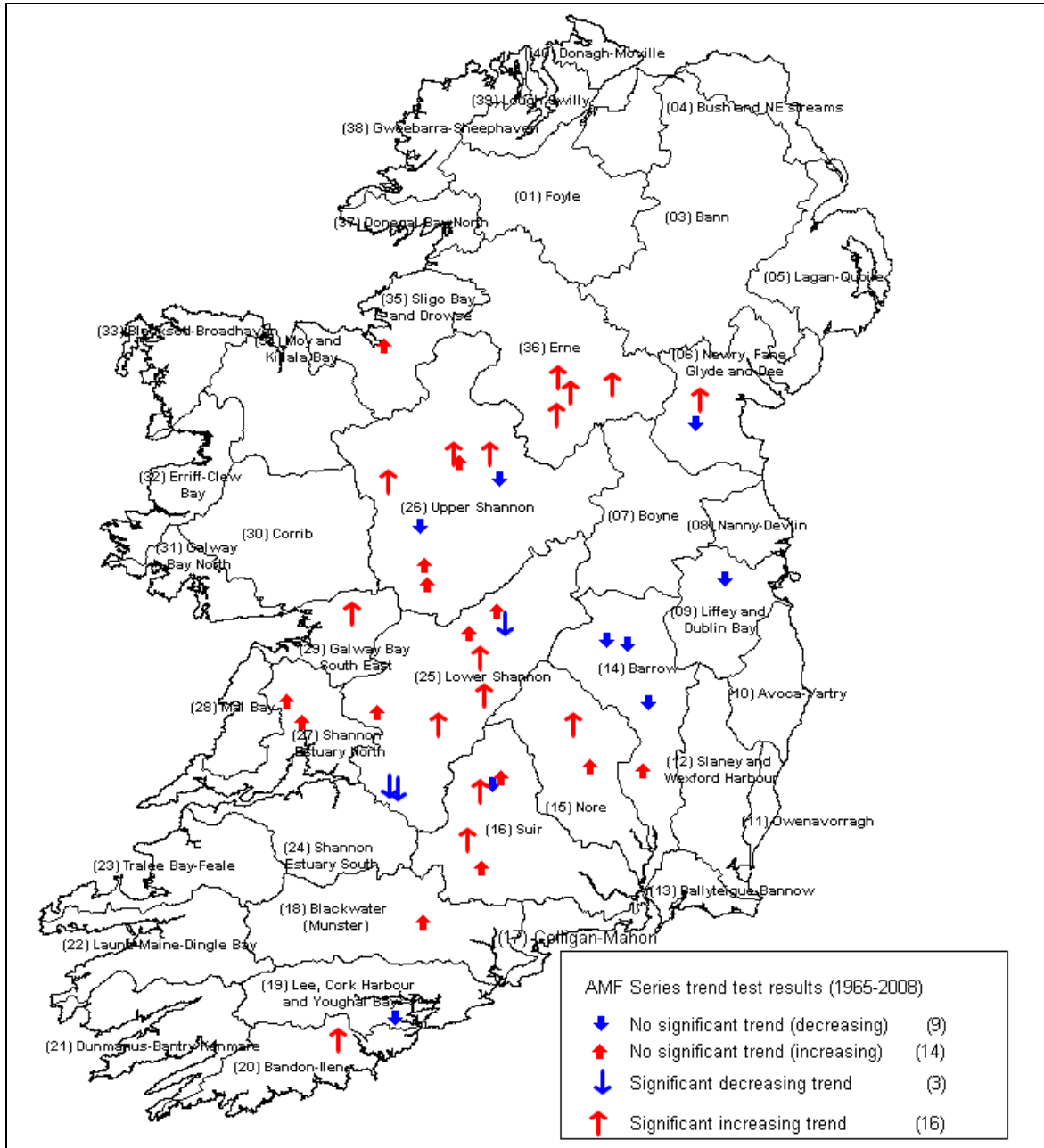


Figure 7.17: Spatial distribution of trend test results – 1965-2008 – Original data series

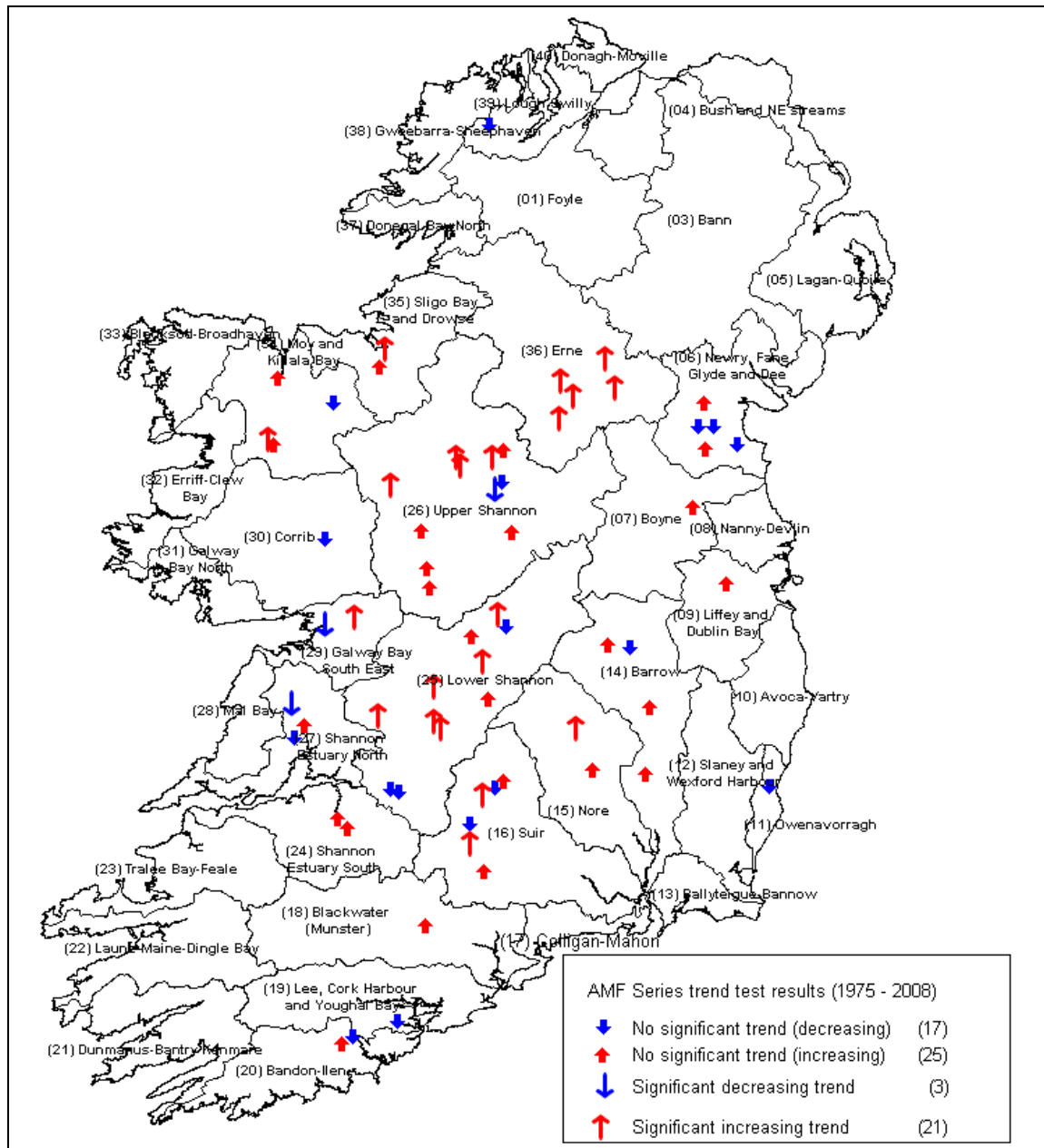


Figure 7.18: Spatial distribution of trend test results – 1975-2008 – Original data series

The above figures show that the Irish AMF data series is dominated by the increasing trend (irrespective of the significance level) and which is generally homogeneously distributed across the country. However, some degree of spatial patterns in the significant sites can be noticed in these figures. In general, significant increased trends occurred in the middle (especially in the River Shannon catchment), north and western parts of the country.

7.5 INVESTIGATION OF THE CAUSES OF TRENDS IN THE ANNUAL MAXIMUM FLOOD SERIES IN IRELAND

The ultimate purpose of a test for trend is to provide information to the engineer in charge of the water resources projects on the current attributes of the streamflow. However, even if the test indicates a significant trend, the engineer is justified in changing his assumption concerning the magnitude of the flow characteristic only if this change is permanent for the life of the project. To ascertain this, it is necessary to complement the detection test with an attribution study, i.e. to determine the nature of the changes in the input variables of the basin system (temperature, precipitation, basin characteristics, etc.) that result in streamflow trends. It is also necessary to establish if the nature of these changes is likely to persist over the design life of the project. Only after the attribution study can the engineer say whether the statistically significant test is also of practical significance.

Common causes of change in streamflows could include:

- Changes directly caused by man (urbanisation, reservoirs, drainage systems, water abstraction, land-use change, river training, river erosion (man made) etc.),
- Natural catchment changes (e.g. natural changes in channel morphology),
- Climate variability,
- Climate change,
- Problems linked to data (measurement errors, instrument malfunctioning etc.)

The best way to improve understanding of changes is to gather as much as information as possible (Kundzewicz, 2004). Examples include:

- Historical information about changes in the catchment, land-use changes etc.
- Historical information about data collection methods etc.,
- Data from nearby sites – if data from other nearby sites show similar patterns then the cause is probably widespread (e.g. linked to climate, or to extensive land-use change)

- Related variables – information on temperature and rainfall can help determine whether changes in flow can be explained by climate factors,
- Record lengths – a primary problem with many hydrological records is that they are too short. If related data can be obtained that extend to a longer period than this may be of assistance.

In the current study, an attempt was made to investigate the effect of climate change on the Irish AMF Series. It is assumed that any trend in the rainfall records would be caused by climate change. Therefore, investigation of trend in the rainfall records would be reasonable in order to investigate the impact of climate change on the flood flows.

Annual Maximum Rainfall (AMR) time series of 9 different durations such as 1-day, 2-day, 3-day, 4-day, 8-day, 10-day, 16-day, 20-day and 25-day for 144 rain gauging stations across Ireland were obtained from Met Eireann. All time series have a common record length of 49 years (1955-2004). The selection of AMR time series durations was based on the different durations of time-of-concentrations for the selected river catchments with different sizes. **Figure 7.20** illustrates the spatial distributions of the selected rain gauging stations across Ireland. They are homogeneously distributed and correspond to the rainfall inputs associated with the selected AMF data set. **Table 7.13** presents some statistical properties of the AMR records.

Table 7.13: Statistical properties of AMR time series of different durations.

No.	Time series (Annual Maximum Series)	Mean Value (mm)	Standard deviation	Coefficient. Variation
1	1-day	41.52	12.28	0.295
2	2-day	54.62	15.26	0.279
3	3-day	64.17	16.48	0.257
4	4-day	72.69	17.67	0.244
5	8-day	101.55	20.92	0.207
6	10-day	115.71	23.03	0.201
7	16-day	151.00	28.69	0.190
8	20-day	171.94	32.07	0.187
9	25-day	197.94	36.57	0.185

The following procedures were applied to examine the effect of climate change on AMF Series in Ireland:

- (i) Firstly, trends in the AMR series were tested using the methodology proposed for the AMF Series using a non-parametric test, such as MK-test.
- (ii) Secondly, the trend test results for both the rainfall and flow records were compared by spatially displaying them in a map.

Table 7.14 presents the trend test results for the rainfall records. In general, the results show an increasing trend in the AMR records of all durations with a large number of sites with significant increasing trends, particularly for the longer duration series. The number of sites with significant increasing trends is an increasing function of rainfall durations, i.e. the significant site numbers increase with the increase in rainfall durations. For the 1-day duration series, only 2% sites showed significant upward trends (3 out of 144 sites), while for the 16-day duration series, 24% sites showed significant upward trends (34 out of 144 sites). The results are graphically illustrated in **Figure 7.19**.

Table 7.14: Number of sites with significant trend (at 5% significance level) in AMR records detected by MK-test.

Durations	All sites			Significant sites (at 5% significance level)		
	Total	Up	Down	Total	Up	Down
1-day	144	78	66	6 (4%)	3 (2%)	3
2-day	144	89	55	7 (5%)	4 (3%)	3
3-day	144	86	58	5 (3%)	5 (3%)	0
4-day	144	93	51	8 (6%)	8 (6%)	0
8-day	144	94	50	26 (18%)	25 (17%)	1
10-day	144	96	48	29 (20%)	28 (19%)	1
16-day	144	108	36	35 (24%)	34 (24%)	1
20-day	144	103	41	33 (23%)	32 (22%)	1
25-day	144	103	41	41(28%)	41 (28%)	0

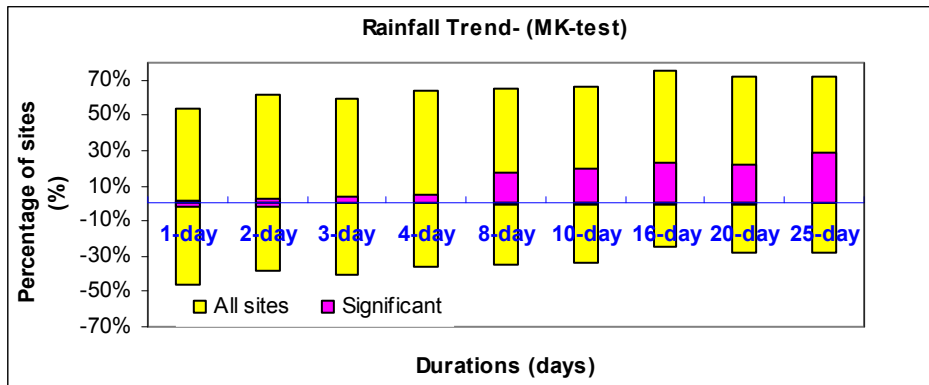


Figure 7.19: Number of stations with significant trends in AMR records for different durations (5% significance level – total stations examined are 144)

To examine the spatial consistency of the observed trends in the AMR records, maps were created displaying the locations of gauging sites with decreasing and increasing trends. **Figures 7.20, 7.21 and 7.22** illustrate the spatial distribution of trend test results obtained from the MK-test for the rainfall durations of 8-day, 16-day and 25-day respectively. All maps show both the significant and non-significant sites along with their direction of trends (decreasing/increasing). The non-significant sites are shown by the thick smaller arrows and the significant sites are shown by thin long arrows. The decreasing trends are shown by downward blue arrow and the upward red arrows represent the increasing trends.

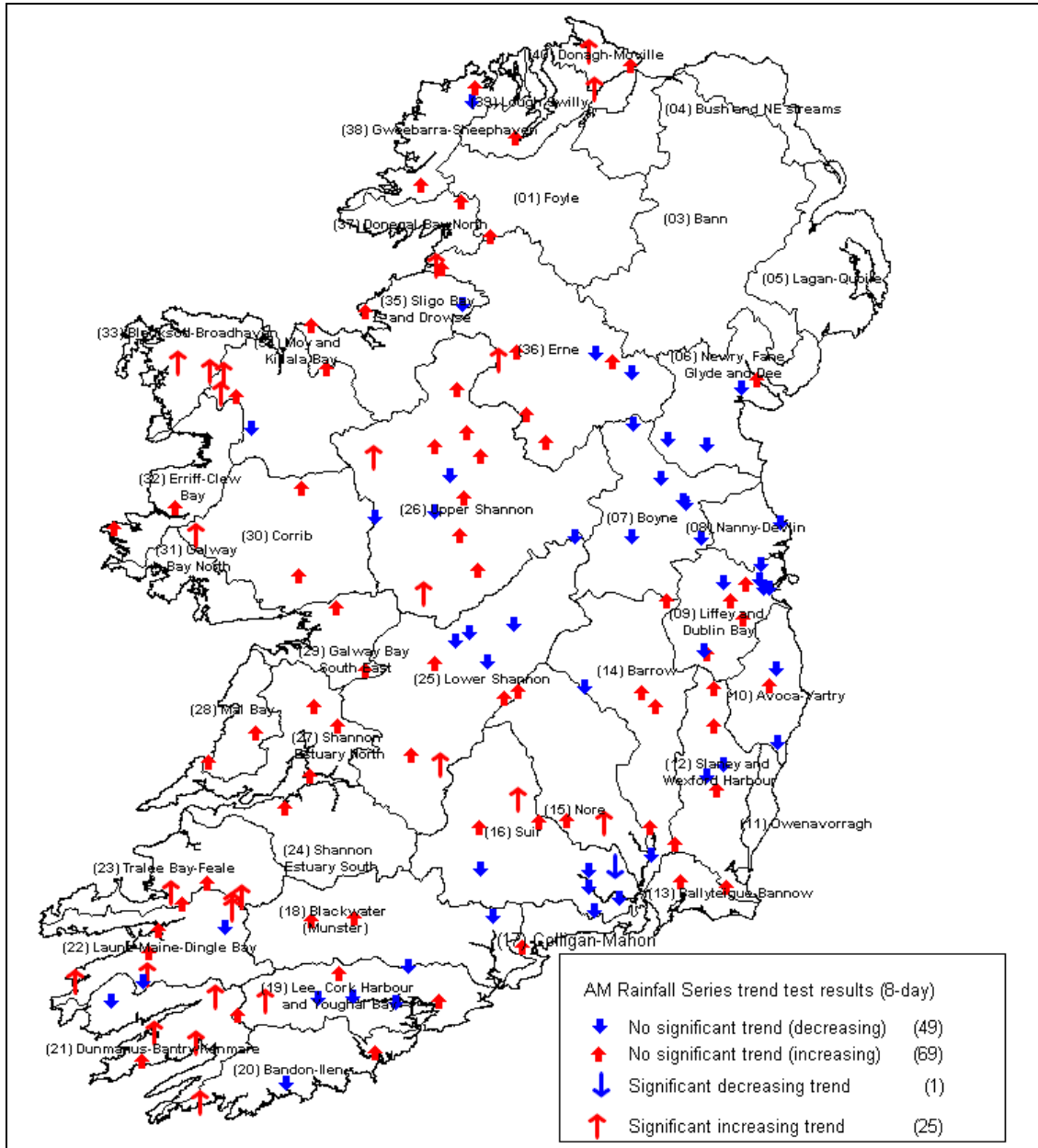


Figure 7.20: Spatial distribution of trend test results for AMR series of 8-day duration

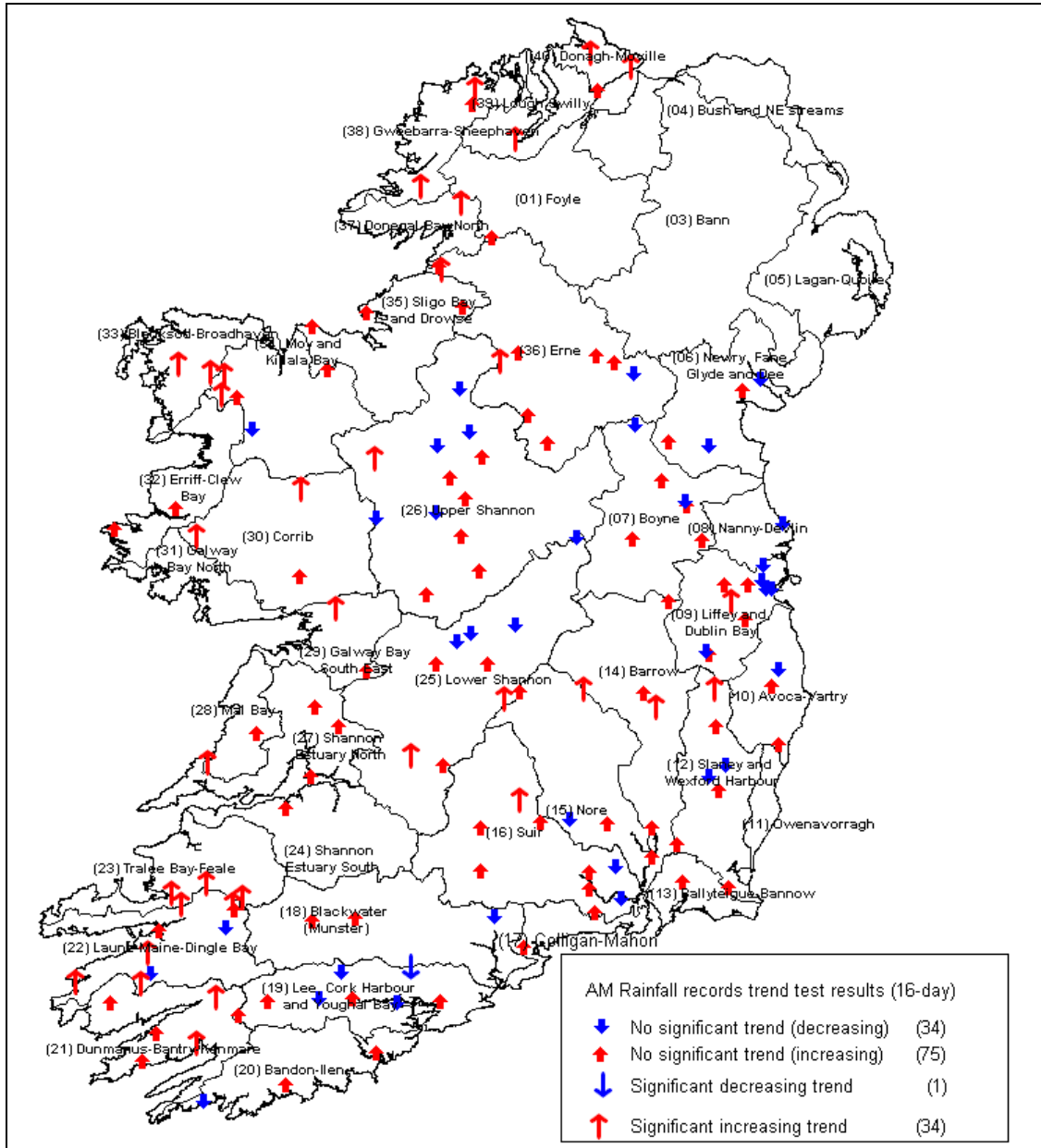


Figure 7.21: Spatial distribution of trend test results for AMR series of 16-day duration

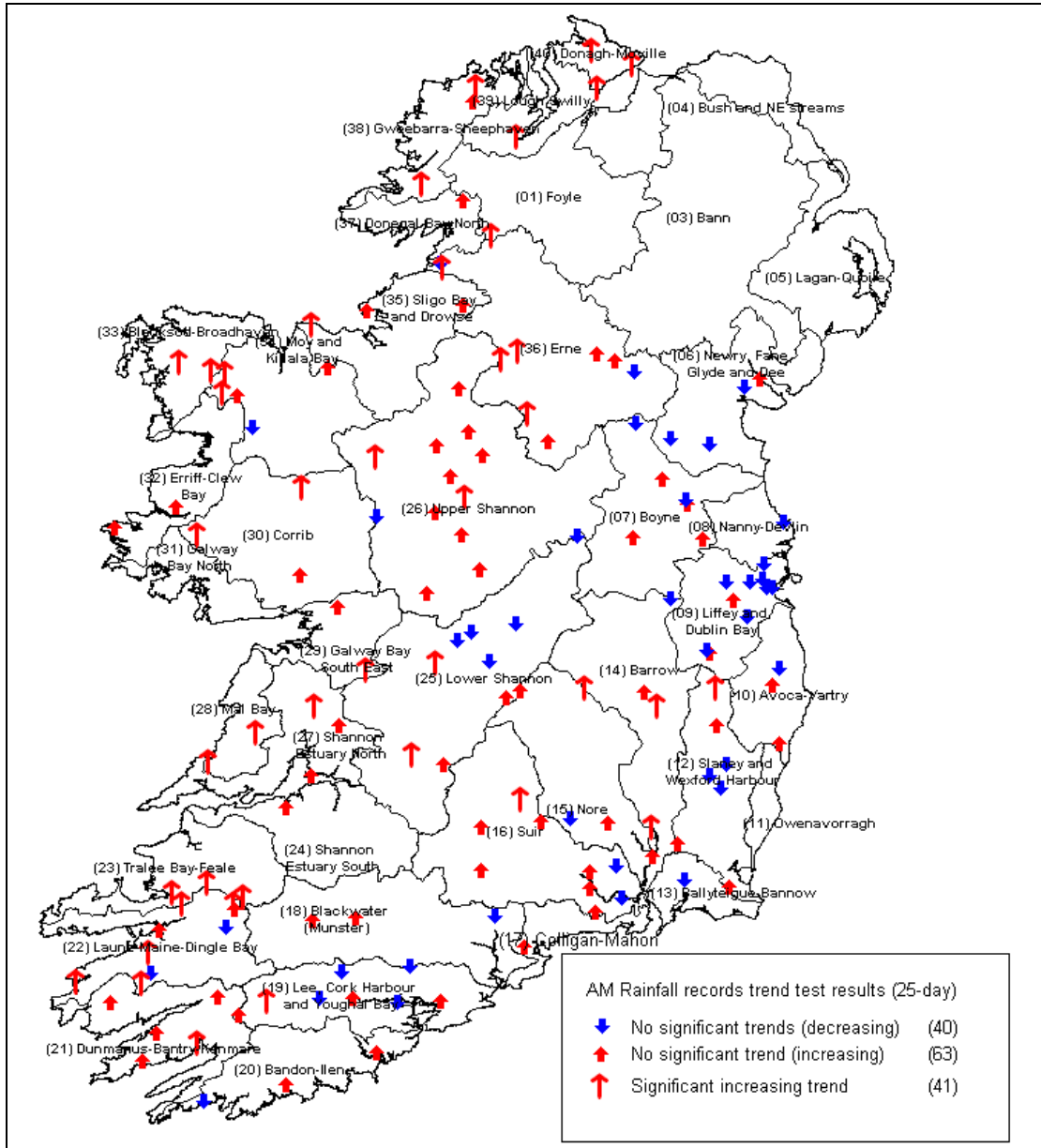


Figure 7.22: Spatial distribution of trend test results for AMR series of 25-day duration

It can be seen from the above figures that, similar to AMF records, AMR records are also dominated by the increasing trends (irrespective of the significance level) and these are generally homogeneously distributed across the country. However, similar to AMF records, some degree of spatial patterns in the significant sites can be noticed in these figures. The significant increasing trends can be noticed along the western and north-western coasts of Ireland in all three AMR series (8-day, 16-day and 25-day durations). A collection of decreasing points can be seen in the River Barrow catchment, located in the eastern part of the country. The 8-day duration

AMR series shows slightly more significant trends in the south-western part of the county compared to the 16- and 25-day durations AMR series (**Figure 7.20**).

Figure 7.23 illustrates the correlation between the significant trends in the AMF records and the corresponding AMR records for Ireland. All sites with significant increasing and decreasing trends as identified by the MK-test both in the POR AMF and the 25-day AMR series are shown in this figure. Some degree of spatial correlation between the significant trends in AMR and AMF records can be noticed all across Ireland with some exceptions in the mid-eastern part. This suggests that the trends in the flow records might be arising from the trends in the associated rainfall records.

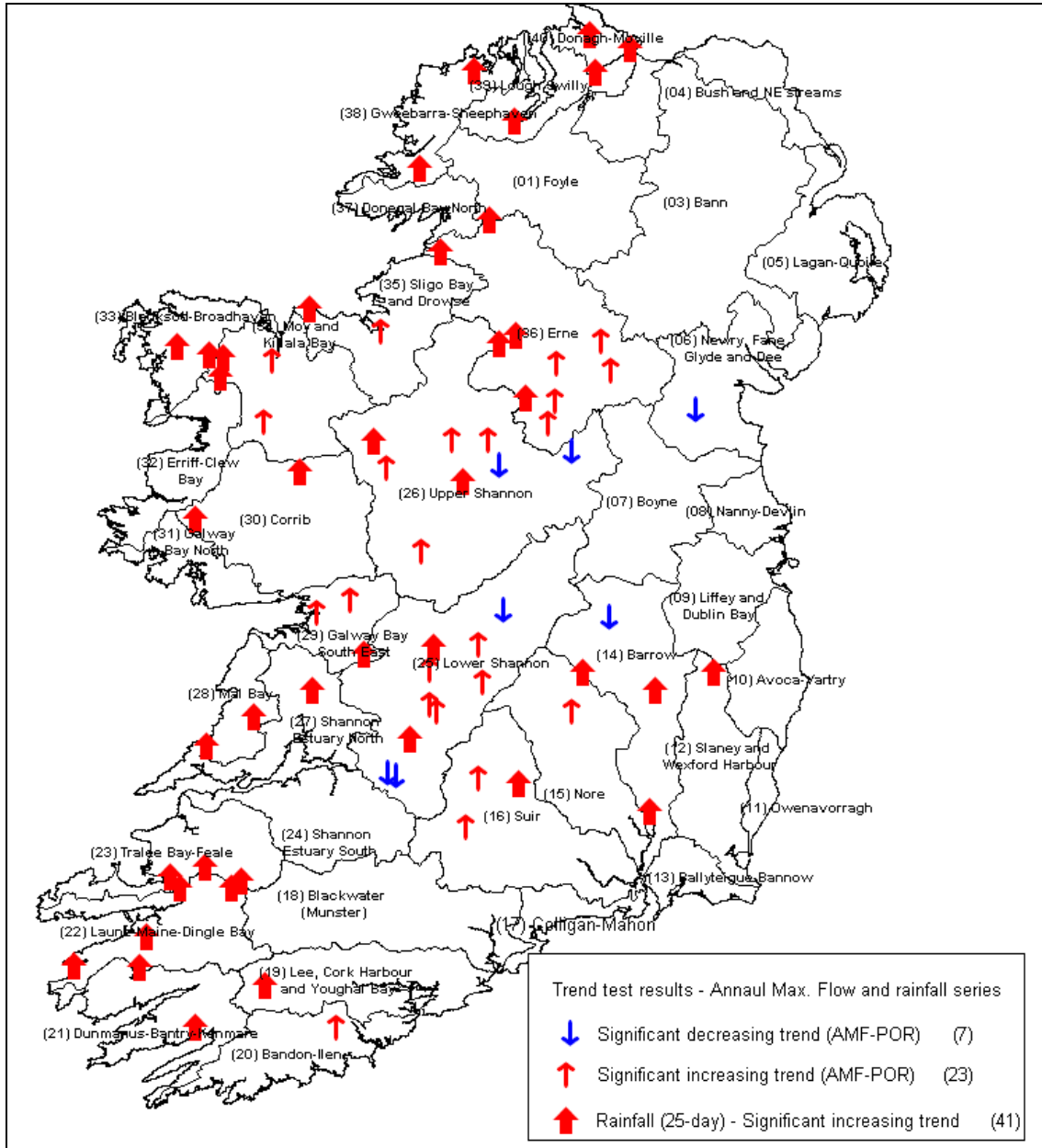


Figure 7.23: Illustration of effect of trends in Annual Maximum Flows (POR Series) and AMR records (25-day duration)

7.6 RESULTS SUMMARY – NON STATIONARITY IN IRISH AMF SERIES

The following conclusions can be drawn from the above study:

- (i) In general, the Irish AMF series are dominated by positive serial correlations. Irrespective of significance level, approximately 65% of sites (60 out of 93) showed positive serial correlations. In terms of significance level these numbers are smaller. In the POR data scenario, 13% of sites (12 out of 93) showed significant Lag-1 autocorrelations at 5% significance level (11 positive and 1 negative). In the timeframes of 1985-2008 (24 years), 1975-2008 (34 years), 1965-2008 (44 years) and 1955-2008 (54 years), significant Lag-1 autocorrelations were found in 13%, 11%, 10% and 24% of sites respectively. Over 50% of these in each case are positively serially correlated.

The Kulkarni and Von Storch (1995) proposed pre-whitened (PW) series, however, showed a slightly smaller number of significant sites. In the POR data scenario, only 9% of sites showed significant Lag-1 autocorrelations, which is 4% less than the Original time series.

An examination of autocorrelation plots for a range of lags (1-10) showed that the majority of AMF records that exhibit significant Lag-1 autocorrelation are not autocorrelated significantly at larger lags. However, 4 out of 12 stations showed significant autocorrelations at larger lags (lag >2 year).

The above results suggest that the autocorrelations, even in the AMF time series, cannot be ignored. The significant low lag autocorrelations (e.g. Lag-1 autocorrelation) are less likely to occur by chance, rather they represent persistence in their associated catchment physical systems. This could be due to the effect of reservoir or groundwater discharge to streamflows, etc.

The TP and RD tests showed some evidence of significant non-randomness properties in Irish AMF series. The RD test identified significant non-randomness at 9%, 14%, 21%, 31% and 17% of sites in the timeframes of 1985-2008, 1975-2008, 1965-2008, 1955-2008 and POR respectively.

- (ii) Any evidence of step changes in the AMF Series i.e. whether the means/medians in two different sub-periods in a data series are different or not was examined using two tests - the parametric T-test and the non-parametric Mann-Whitney U-test (MW-U test). Through graphical explorations of the AMF and associated annual AMR records, a turning point was identified in both series at 1976. The AMF data series were partitioned at 1976 for the purpose of detecting step change in the data series. The test results suggest that, irrespective of any significance level, the mean/median AMF for the post 1976 period have increased in the majority of the stations at all timeframes. In the POR data scenario 30% of sites showed significant step change at 5% significance level (9 increases and 5 decreases) by the MW-U test. In the timeframes of 1955-2008 and 1965-2008, significant step changes were identified at 41% and 21% of sites by the MW-U test. The parametric T-test also showed similar results.

Box plots of the above mentioned significant AMF records for two sub-periods showed that, in addition to changes in mean/medians, variability in the data series has also changed (increased/decreased). Along with the land-use changes, this could also be caused by climate change.

- (iii) The trend test results showed that there are considerably more trends in Irish AMF records than that would be expected to occur by chance.

The robust MK-test identified significant trends at 30% of sites (28 out of 93) at 5% significance level, with increasing trends at 23% of sites (21 out of 93) in the POR AMF Series (PW case). In the timeframes of 1955-2008, 1965-2008, 1975-2008 and 1985-2008, the corresponding detected significant trends proportions are 48% (14 out of 29) 45% (19 out of 42) 29% (19 out of 66) and 10% (7 out of 24) of sites respectively. The majority of these are increasing trends (38%, 38%, 27% and 7% in the 1955-2008, 1965-2008, 1975-2008 and 1985-2008 timeframes respectively).

The above results demonstrate that the Irish river catchments are dominated by positive (increasing) trends in AMF time series. These results are comparable with other studies carried out on European Rivers (Kiely, 1999 in Ireland; Petrow and Merz, 2009 in Germany; Robson and Reed, 1999 in UK;

Lindstróm and Bergstróm, 2004 in Sweden and Nobilis and Lorenz, 1997 in Austria). Petrow and Merz, 2009 found significant increasing trends in the AMF (1951-2002) in Germany at 28% of sites (41 out of 145) at 10% significance level.

The effect of serial correlation in the trend test results showed that, any presence of positive serial correlations in the records would increase the number of sites with significant trends. However, these numbers are not so striking in the case of Irish AMF series. For example, the MK-test identified significant trends at 32% sites in the Original POR data scenario, while 30% sites were indentified in the PW data scenario. The Yue and Pilon (2003) proposed TFPW method identified a slightly larger number of significant sites than the Original series. This finding agrees with the results of (Khaliq et al., 2009). The possible reason for this could be that serial correlations are estimated from trend-free data for the TFPW approach and that results in a different type of serially correlated time series. This could also be due to a complex trade-off between the autocorrelations and trends and the difficulty in effectively isolating them.

- (iv) Some temporal variations in the trend test results are also apparent in Irish AMF records. For example, the robust MK-test identified significant trends at 48%, 45%, 29% and 10% of sites in the timeframes of 1955-2008, 1965-2008, 1975-2008 and 1985-2008 respectively. These results might be suggesting that the trend detection ability of a trend test is a decreasing function of the record lengths, i.e. power decreases with the decrease in record lengths. The rate of decrease is slightly higher and is almost equal for the two non-parametric MK and SPR tests in comparison to the parametric SLR test. This interpretation of the power of a trend test in the case of POR timeframe is difficult to make, because of the variations in record lengths in the selected data set. This temporal variation could be due to the variation of sample size, or could be due to catchment anthropogenic impact or climate change in Ireland.
- (v) The trend test results of AMF Series show some evidence of spatial patterns in the significant sites in Ireland. In general, significant increased trends

occurred in the middle (especially in the River Shannon catchment), north and western parts of the country.

- (vi) The non-parametric tests are found to be more powerful in identifying trends in Irish AMF Series compared to the parametric tests. The power of the MK and SPR tests are equal and comparable. This agrees with the results of Yue and Pilon (2002).
- (vii) The AMR series of Ireland also showed significant increasing trends. The number of significant trends showed an increasing tendency with the rainfall durations, i.e. as the rainfall durations increases, the significant site numbers increase. The 1-day AMR series showed a minimal significant trend (only at 4% of sites), while the 25-day AMR series showed significant trends at 28% sites (41 out of 144).

Similar to AMF records, some degree of spatial patterns in the significant trends in Irish AMR records was also observed. The significant increasing trends are observed along the western and north-western coasts of Ireland in all three AMR series (8-day, 16-day and 25-day durations). A collection of decreasing points can be seen in the River Barrow catchment, located in the eastern part of the country. The 8-day duration AMR series shows slightly more significant trends in the south-western part of the county compared to the 16- and 25-day durations AMR series.

- (viii) The graphical comparison (spatial distribution) of the trend test results for both the AMR and AMF records showed some degree of spatial correlation between the significant increasing trends in the AMR and AMF records all across Ireland. This suggests that the trends in the flow records might be arising from the trends in the associated rainfall records. The evidence of the effect of climate change on the Irish AMF series, therefore, can not be dismissed. A further site specific study along with the examination of other changes in the catchment characteristics (such as urbanization, forestation, drainage network, flow regulation abstractions etc) should be carried out before to coming to a conclusion on the climate change impact on the Irish AMF.

8 POWER OF TREND TESTS

8.1 INTRODUCTION

The power of a statistical hypothesis test measures the test's ability to reject the null hypothesis when it is actually false - that is, to make a correct decision. In detecting trends in a hydrological time series, both parametric and non-parametric tests are used. Parametric tests assume that the test statistic, time series data and the errors (deviations from the trend) follow a particular distribution (usually normal distribution). In contrast, the non-parametric tests are rank-based tests and assumptions on the distribution of data are not required. Since many hydrological data sets are positively skewed, non-parametric tests are recommended for detecting trends in hydrological variables (Yue et al., 2002, Yue and Pilon, 2004).

If the distributional assumptions of the parametric tests are correct, the power (for a given significance level) of the parametric tests are generally higher than the power of the non-parametric alternative. However, if the data distributions depart substantially from the assumed distribution, then the non-parametric tests can be more powerful than the parametric test. In many cases, the differences in power between the parametric and non-parametric tests become smaller as the sample size increases.

The power of the available trend tests has not been well documented in the literature. In this chapter, the power of tests used for identifying trends in Irish AMF Series is investigated by Monte Carlo simulation (Yue et al., 2002; Yue and Pilon, 2004).

8.2 METHDOLOGY

When executing a hypothesis test, two types of errors can arise. A type I error occurs when the null hypothesis (H_0) is rejected when it is in fact true; that is, H_0 is wrongly rejected. The probability of a type I error is the significance level (α) of a hypothesis test. A type II error occurs when the null hypothesis is accepted wrongly when it should be rejected. The power of a statistical hypothesis test measures the test's ability to reject the null hypothesis when it is actually false - that is, to make a correct decision, which is measured as the probability of not committing a type 2

error. Letting β present the probability of committing a type 2 error, the probability of not making a type 2 error, is $1 - \beta$.

$$\text{Power} = 1 - P(\text{type II error}) = (1 - \beta) \quad (8.1)$$

The maximum power a test can have is 1, the minimum is 0. Ideally we want a test to have high power, close to 1. **Figure 6.3** in Section 6.5.1 shows a schematic illustration of the Type I and Type II errors and the power of a hypothesis test.

In a simulation experiment when sampling from a population that represents the case where the null hypothesis is false, the power can be estimated by (Yue et al., 2002; Yue and Pilon, 2004):

$$\text{Power} = \frac{N_{rej}}{N} \quad (8.2)$$

where N is the total number of simulation experiments and N_{rej} is the number of experiments that fall in the critical region.

A type I error is often considered to be more serious, and therefore more important to avoid, than a type II error. The hypothesis test procedure, therefore, should be adjusted so that there is a guaranteed 'low' probability of rejecting the null hypothesis wrongly. For any given set of data, type I and type II errors are inversely related; the smaller the risk of one, the higher the risk of the other.

Power test algorithm:

The study was carried out using a Monte Carlo Simulation technique. The steps of this simulation procedure are as follows:

1. Select a distribution and its parameters (population values) for generating random stationary samples,
2. For each of N repetitions of the simulation procedure, carry out the following steps:
 - (i) Generate a random sample of size n_i (non-trend condition)
 - (ii) Apply trend on the simulated random sample using an appropriate trend model (trend condition)

- (iii) Undertake trend tests using a parametric or non-parametric method as discussed in Chapter 6, Section 6.5.3.3.
3. Count the number of times that the null hypothesis is rejected out of N repetitions (N_{rej}), and
 4. Calculate the power of the test using equation 8.2.

Distribution choice:

The random sample was drawn from EV1 population, since this distribution has been found suitable for the Irish AMF Series (NERC, 1975; OPW,FSU, 2009).

Application of Trend and various Trend Forms considered:

The true form of trend in the historical time series is not known, and it could be either linear or non-linear in nature. Hipel and McLeod (2005) provide a general discussion on various trend application methods/models. These models either could contain deterministic trends or could contain purely stochastic trends.

For the case of a purely deterministic trend component, the time series, x_t , may be written as:

$$x_t = f(t) + a_t \tag{8.3}$$

where $f(t)$ is function of time only and hence is a pure deterministic trend, while a_t is an independent and identically distributed (IID) sequence.

On the other hand, a time series having a purely stochastic trend may be defined as

$$x_t = f(x_{t-1}, x_{t-2}, \dots) + a_t \tag{8.4}$$

where $f(x_{t-1}, x_{t-2}, \dots)$ is a function of the past data and a_t is an innovation series assumed to be IID and with the property of $E[a_t \cdot x_{t-k}] = 0$, $k=1,2,\dots$

Box and Jenkins (1976) suggested that for forecasting purposes it is usually better to use a purely stochastic trend model. However, where the interest is to test any

changes in a time series, a model with a possible deterministic trend component may seem more suitable.

Examples of deterministic models:

- (i) Linear model: the linear regression models are generally used as alternative hypothesis (Lettenmaier, 1976; Hirsch et al., 1982). Assume x_t is given by the linear model which can be written as:

$$x_t = c + bt + a_t, \quad t = 1, 2, \dots, n \quad (8.5)$$

where $a_t = N(0, \sigma_a^2)$, and c and b are constants.

- (ii) Logistic Model - it is possible for a series to change rapidly at the start and then gradually approach a limit, a logistic model constitutes a reasonable choice for an alternative model. This model is defined as (Cleary and Levenbach, 1982):

$$x_t = M / [1 - c \{ \exp(-bt) \}] + a_t, \quad t = 1, 2, \dots, n \quad (8.6)$$

where $N(0,1)$, M is the limit of x_t as t tends to infinity, and b and c are constants.

- (iii) Step Function Model (Hipel and McLeod, 2005): The Step function model is defined as

$$x_t = \begin{cases} a_t & 0 \leq t \leq n/2 \\ c + a_t & n/2 < t \leq n \end{cases} \quad (8.7)$$

where $a_t = N(0, \sigma_a^2)$, and c is the average change in the level of the series after time $t = n/2$.

Examples of a few stochastic models include:

- (i) Barnard's Model (Barnard, 1959):
The Barnard model is defined as (Barnard, 1959)

$$x_t = x_{t-1} + \sum_{i=1}^{n_t} \delta_i + a_t, \quad t = 1, 2, \dots, n \quad (8.8)$$

where n_t follows a Poisson distribution with parameter λ , $\delta_i \approx N(0, \sigma_i^2)$ and $a_t = N(0, 1)$.

(ii) Second order Autoregressive Model (AR(2)) which may be written as:

$$x_t = \phi_1 x_{t-1} + \phi_2 x_{t-2} + a_t, \quad t=1, 2, \dots, n \quad (8.9)$$

where $a_t \approx N(0, \sigma_a^2)$

(iii) Threshold Autoregressive Model:

A particular model proposed by Tong et al. (1985) for modelling and forecasting flows for the Vatnsdalsa River in Iceland is:

$$x_t = \begin{cases} 1.79 + 0.76x_{t-1} - 0.05x_{t-2} + a_t^{(1)} & \text{if } J_t < -1 \\ 0.87 + 1.3x_{t-1} - 0.71x_{t-2} + 0.34x_{t-3} + a_t^{(2)}, & \text{otherwise} \end{cases} \quad (8.10)$$

where x_t is the volume of riverflow in $m^3/s/day$, J_t is the temperature in degrees centigrade, and $a_t^{(1)} = N(0, 0.69)$ and $a_t^{(2)} = N(0, 7.18)$.

Further details of these models can be found in Hipel and McLeod (2005).

Yue and Pilon (2004) used two non-linear trend models with (i) upward convex shape and (ii) upward concave shape to investigate the sensitivity of trend shape on the power of trend identification tests. The changing rate of trend slopes in these trend models increases at the beginning and starts to decrease after a certain turning point. The details of these trend models are given in Yue and Pilon (2004).

In order to simplify our understanding, a linear type trend model is considered in this study. It is again assumed that the first moment of the sample's true distribution will be more sensitive to the long-term climate change effect than the other higher order moments.

The following two deterministic trend forms / models have been employed to introduce trend in the stationary time series:

(i) Trend Form 1 (TF-1) (additive model): $Q_{NS}(t) = Q_S(t) + T_S t$ (8.11)

(ii) Trend Form 2 (TF-2) (hybrid model): $Q_{NS}(t) = Q_S(t)[1 + T_S t]$ (8.12)

where

$Q_{NS}(t)$ = non-stationary time series,

$Q_S(t)$ = population/stationary time series,

T_S = upward trend slope (per unit time step)

t = time step (year), 1 to 50 years

Trend Form 1 is similar to those used by Lettenmaier, 1976 and Yue et al., 2002, while the TF-2 is a hybrid type model proposed in the current study. Some statistical properties of this hybrid type model are discussed in Section 9.3.3.

For detecting trends, three tests have been employed, of which two tests are non-parametric tests (MK and SPR tests) and the third one is a parametric test (SLR-test). The details of these tests are discussed in Chapters 6 (Section 6.5.3.3) and 7 (Section 7.3.1.3).

8.3 RESULTS & DISCUSSION

The results of the power test experiments are discussed in a number of separate sections:

- (i) firstly, the changes in population properties with the increase in trend slopes are investigated,
- (ii) secondly, the sensitivity of the power of trend tests on the magnitude of trend slopes has been investigated and compared for all three tests (MK, SPR and SLR tests),
- (iii) thirdly, the influence of sample sizes on the power of the tests is examined, and
- (iv) finally, the sensitivity of the power of the trend identification tests on sample variance is investigated.

In each of the above cases, 5000 independent samples each with a size of 50, were generated from the EV1 distribution with the population mean (μ) and co-efficient of variation (CV) of 1.0 and 0.30 respectively.

(i) Changes in population properties with the increase in trend slopes:

An examination of the changes in population mean with the increase in trend slopes showed that the population mean increases linearly with trend slopes in both cases of trend forms (**Table 8.1** and **Figure 8.1**). Likewise, the variance is increased. However, the changes in population CV are not easily predictable. These changes are investigated below. Also **Table 8.1** shows the effect of trend on the mean is independent of the original population CV.

Table 8.1: Variations in the population mean with trend slopes

Trend Slope (%)	Change in Mean			
	CV=0.30		CV=0.50	
	TF-1	TF-2	TF-1	TF-2
0.00%	1.000	1.000	1.000	1.000
0.20%	1.052	1.052	1.051	1.051
0.40%	1.101	1.101	1.101	1.101
0.60%	1.152	1.152	1.154	1.154
0.80%	1.204	1.204	1.205	1.205
1.00%	1.254	1.254	1.254	1.254
1.20%	1.305	1.305	1.306	1.306
1.40%	1.356	1.356	1.358	1.358
1.60%	1.408	1.408	1.409	1.409
1.80%	1.459	1.459	1.458	1.458
2.00%	1.508	1.508	1.509	1.509

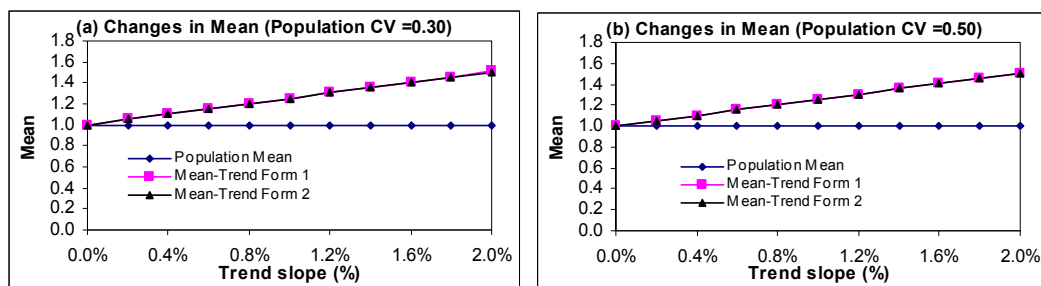


Figure 8.1: Changes in the population mean with the increase in trend slopes in both cases of trend forms (a) CV=0.30 (b) CV=0.50

The simulation results show that variance increases with the increase in trend slopes in different fashions in the two trend forms considered (**Table 8.2** and **Figure 8.2**). In the case of TF-1, population CV decreases with the increase in trend slopes

of up to 1% and increases again for larger trend, while CV increases in the case of TF-2. Again it can be seen that the change rate in CV depends on the magnitude of the population CV. In the case of TF-2, the change rate is slower for the higher population CV value, while in the TF-1 case it is higher for larger population CV. The change pattern in CV, in the TF-1, is slightly non-linear, where in the TF-2 it is almost linear.

Table 8.2: Variations in the variance with the increase in trend slopes

Change in CV				
Trend Slope (%)	Population CV=0.30		Population CV=0.50	
	TF-1	TF-2	TF-1	TF-2
0.00%	0.296	0.296	0.494	0.494
0.20%	0.283	0.298	0.472	0.496
0.40%	0.274	0.301	0.452	0.498
0.60%	0.268	0.306	0.435	0.501
0.80%	0.265	0.312	0.421	0.505
1.00%	0.264	0.320	0.410	0.510
1.20%	0.264	0.328	0.402	0.516
1.40%	0.265	0.334	0.395	0.523
1.60%	0.268	0.342	0.388	0.526
1.80%	0.272	0.351	0.383	0.532
2.00%	0.276	0.357	0.381	0.538

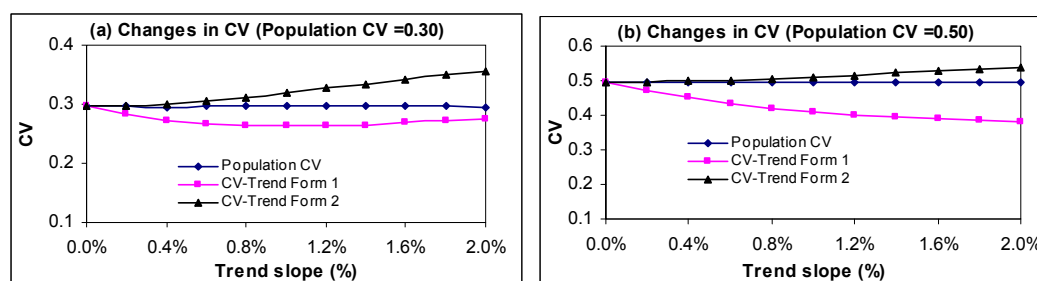


Figure 8.2: Changes in the variance with the increase in trend slopes in both cases of trend forms

(ii) Sensitivity of the power of trend tests to the magnitude of the trend slopes:

Table 8.3 shows the variations of the power of the trend tests (MK, SPR and SLR tests) with the increase in trend slopes under both trend forms considered. The various trend slopes used are ranging from 0% (no-trend condition) to 2%. These are based on the estimated trend slopes in Irish AMF Series as discussed in Section 7.2.1 (**Table 7.3**). **Figure 8.3** illustrates the variation of trend test power with the increase in trend slope. It can be seen that, irrespective of the trend tests and trend

forms, the power of a test is an increasing function of the trend slope, i.e. as the trend slope increases, the power of the test increases leading to an increased ability to discern the existence of trend. Conversely if the trend amount is small, $\leq 0.6\%$ say, the power is so low as to suggest that the test could not detect it effectively.

Table 8.3: Variations in the power of the trend identification test with the trend slopes

Trend slope	Power					
	TF-1			TF-2		
	MK	SPR	SLR	MK	SPR	SLR
0.00%	0.045	0.051	0.064	0.048	0.050	0.061
0.20%	0.112	0.118	0.099	0.095	0.095	0.114
0.40%	0.301	0.316	0.235	0.234	0.245	0.267
0.60%	0.581	0.591	0.458	0.426	0.436	0.452
0.80%	0.834	0.829	0.677	0.622	0.624	0.646
1.00%	0.946	0.943	0.850	0.780	0.773	0.793
1.20%	0.986	0.987	0.944	0.885	0.885	0.899
1.40%	0.998	0.999	0.988	0.944	0.942	0.948
1.60%	1.000	1.000	0.998	0.971	0.977	0.980
1.80%	1.000	1.000	1.000	0.990	0.988	0.991
2.00%	1.000	1.000	1.000	0.994	0.995	0.998

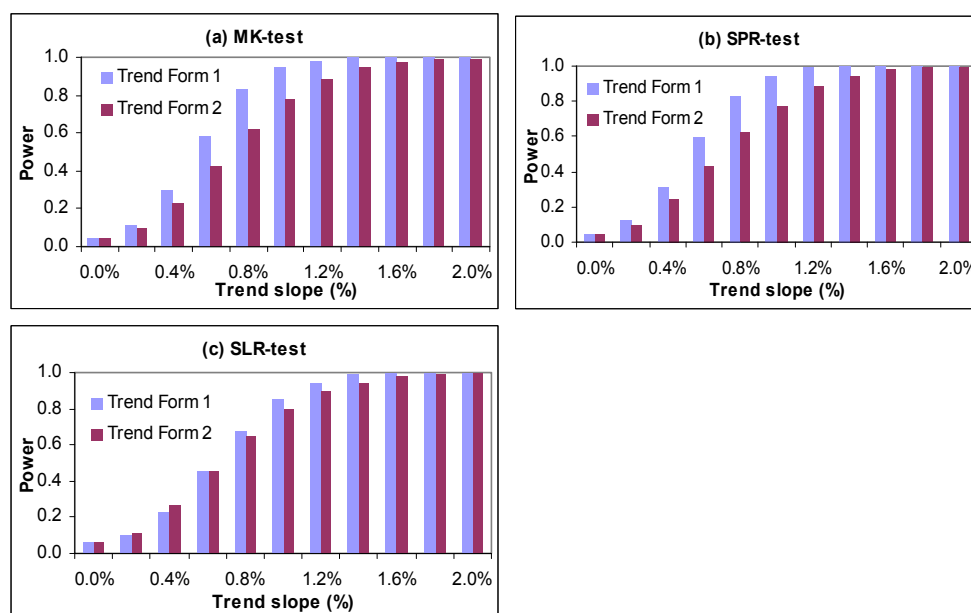


Figure 8.3: Variations of the power of trend identification tests with the increase in trend slopes in the Trend Forms of 1 & 2 (panel a: MK-test, panel b: SPR-test and panel c: SLR-test).

Figure 8.3 also illustrates that the trend detection ability for all three tests is slightly higher, if trends in the records present in the type of TF-1 (equation 8.11), particularly for the trend slope less than 1.6%.

A comparison of the power of the selected three trend tests under both trend forms are illustrated in **Figure 8.4** (panel (a) is for TF-1 and panel b is form TF-2). It can be seen from this figure that the power of all three trend tests are almost equal and 100% for the trend slopes greater than 1.6% in both trend forms. The MK-test and SPR-test have almost similar power in both cases of trend forms. The parametric SLR test shows significantly less power in the TF-1, but slightly higher power for the TF-2 compared to the non-parametric MK and SPR tests. For TF-1, at 1.0% trend slope, the power of the MK, SPR and SLR tests are 94.6%, 94.3% and 85.0% respectively, while in the case of TF-2, these are 78.0%, 77.3% and 79.3% respectively.

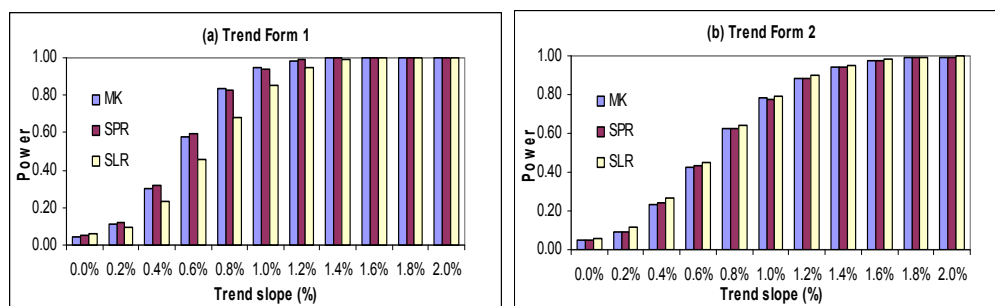


Figure 8.4: Comparison of the power of the trend identification tests MK, SPR and SLR tests under two trend forms (panel a: for TF-1 and panel b: for TF-2).

(iii) Effect of sample sizes on the power of the trend identification tests:

In order to investigate the effect of sample sizes on the power of the trend identification tests, the power test algorithm was applied for sample sizes ranging from 10 to 100 with an increment of 10 (10 sizes). **Table 8.4** presents the variations of the power of the three selected trend identification tests (MK, SPR and SLR tests) with the increase in sample sizes for the trend slope of 1.0% under both Trend Forms 1 and 2. **Figure 8.5** illustrates these variations. It can be seen from this figure that the power of all three tests is an increasing function of sample sizes i.e. the power of the trend tests increases with the increase in sample sizes.

For any sample sizes smaller than 70, the trend detection ability for all three tests is slightly higher, in case of TF-1. For all sample sizes equal to or greater than 70, the power of all three tests is almost 100% in both cases of trend forms.

Table 8.4: Variations in the power of the trend identification test with the trend slopes

Sample length (years)	Power - 1% trend					
	TF-1			TF-2		
	MK	SPR	SLR	MK	SPR	SLR
10	0.061	0.055	0.053	0.060	0.042	0.069
20	0.137	0.135	0.121	0.119	0.119	0.127
30	0.373	0.387	0.298	0.266	0.269	0.300
40	0.720	0.736	0.572	0.531	0.513	0.553
50	0.949	0.943	0.867	0.779	0.780	0.788
60	0.997	0.996	0.978	0.934	0.930	0.933
70	1.000	1.000	0.999	0.988	0.986	0.990
80	1.000	1.000	1.000	0.999	1.000	1.000
90	1.000	1.000	1.000	1.000	1.000	1.000
100	1.000	1.000	1.000	1.000	1.000	1.000

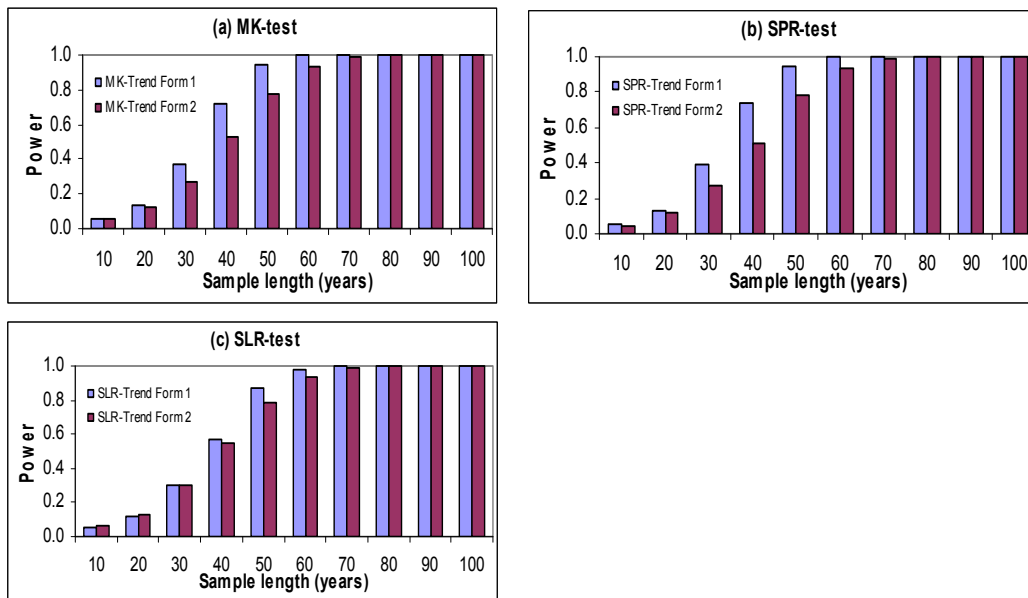


Figure 8.5: Variations of the power of trend identification tests with the increase in trend sample sizes in the Trend Forms of 1 & 2 (panel a: MK-test, panel b: SPR-test and panel c: SLR-test).

Figure 8.6 compares the sensitivity of the power of the three trend identification tests (MK, SPR and SLR tests) to sample sizes under two trend forms for the trend slope of 1.0%. It can be seen from this figure that power of all three trend tests are almost equal and 100% for the any sample sizes equal to 70 and greater. The MK-test and SPR-test have almost similar power in both cases of trend forms. The parametric SLR test shows significantly less power in the TF-1, but slightly higher power in the case of TF-2 compared to the two non-parametric tests (MK and SPR tests). For example, for sample size 40, power of the MK, SPR and SLR tests are 72.0%, 73.6% and 57.2% respectively in the case of TF-1, while these are 53.1%, 51.3% and 55.3% respectively in the case of TF-2.

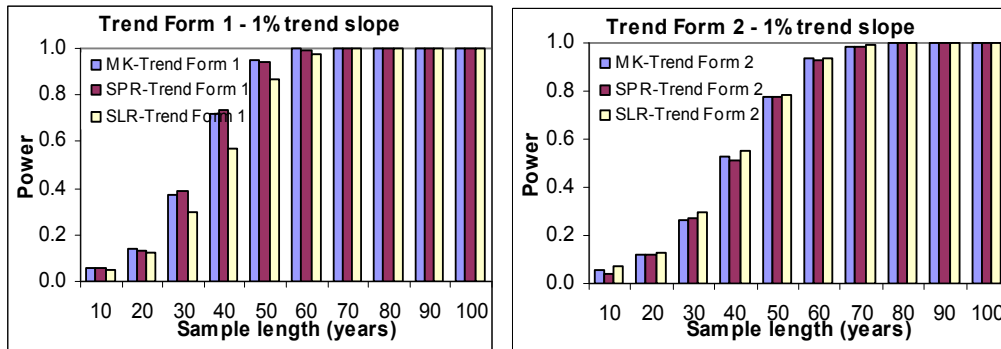


Figure 8.6: Comparison of the sensitivity of the power of the trend identification tests (MK, SPR and SLR tests) with the increase in sample size under two trend forms (panel a: for TF-1 and panel b: for TF-2).

(iv) Sensitivity of the power of trend identification tests on sample variance:

In order to investigate the effect of sample variance on the power of the trend identification tests, power test algorithms were applied for a range of sample coefficients of variations (CV) values of the AMF series ranging from 0.10 to 2.00 with an increment of 0.10. **Table 8.5** presents the variations of the power of the three selected trend identification tests (MK, SPR and SLR tests) with the increase in sample CVs for the trend slope of 1.0% under both trend forms. **Figure 8.7** illustrates these variations. It can be seen from this figure that the power of the two non-parametric tests is a decreasing function of sample variance i.e. the power decreases with the increase in sample variance. However, in the parametric SLR test, power is almost invariant for any increase in CV value greater than 0.50, i.e. the power of the SLR test is a decreasing function of sample variance up to a CV value of 0.50, for any further increase in CV value, power does not decrease further but actually increases. The trend detection ability (power) of the two non-parametric tests is significantly higher in case of TF-1, for any CV value greater than 0.20, than for TF-2. However, in the case of SLR test the power is almost equal for both Trend Forms (**Table 8.5**).

Table 8.5: Variations in the power of the trend identification test with the sample variance (trend slope 1%)

CV	TF-1			TF-2		
	MK	SPR	SLR	MK	SPR	SLR
0.10	1.000	1.000	0.998	1.000	1.000	0.995
0.20	1.000	0.999	0.944	0.984	0.986	0.896
0.30	0.947	0.944	0.853	0.776	0.772	0.787
0.40	0.767	0.767	0.785	0.511	0.516	0.735
0.50	0.581	0.593	0.737	0.334	0.348	0.678
0.60	0.441	0.450	0.707	0.237	0.243	0.666
0.70	0.338	0.341	0.687	0.182	0.189	0.660
0.80	0.275	0.270	0.671	0.145	0.141	0.666
0.90	0.228	0.231	0.669	0.120	0.118	0.663
1.00	0.198	0.202	0.667	0.101	0.096	0.699
1.10	0.169	0.163	0.678	0.088	0.085	0.696
1.20	0.141	0.155	0.677	0.073	0.080	0.718
1.30	0.137	0.134	0.680	0.067	0.076	0.730
1.40	0.120	0.122	0.696	0.070	0.066	0.738
1.50	0.112	0.123	0.716	0.069	0.066	0.759
1.60	0.098	0.106	0.721	0.060	0.062	0.764
1.70	0.099	0.101	0.737	0.060	0.055	0.778
1.80	0.091	0.089	0.730	0.055	0.061	0.776
1.90	0.085	0.084	0.749	0.054	0.060	0.777
2.00	0.086	0.085	0.753	0.057	0.053	0.796

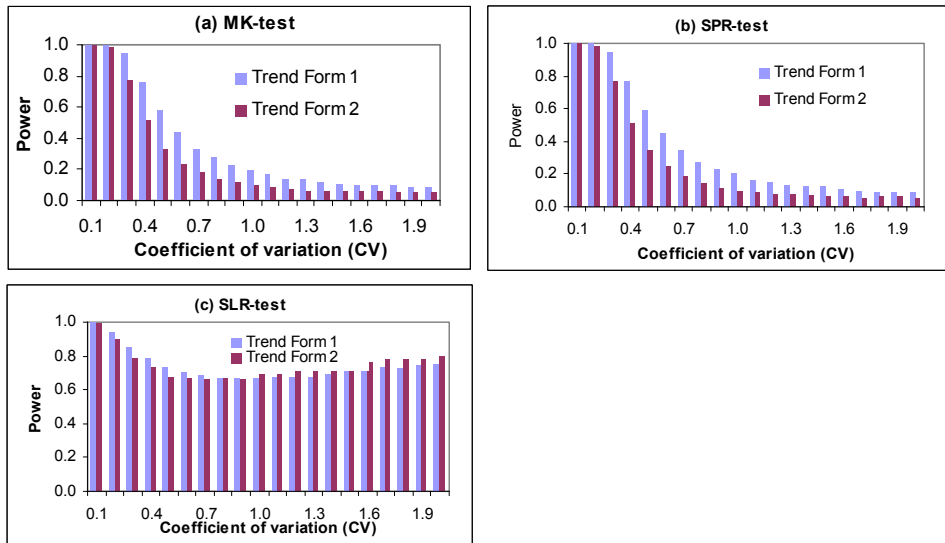


Figure 8.7: Variations of the power of trend identification tests with the increase in sample variance in the trend forms of 1 & 2 for trend slope of 1% (panel a: MK-test, panel b: SPR-test and panel c: SLR-test).

Figure 8.8 compares the sensitivity of the power of the trend identification tests (MK, SPR and SLR tests) with the increase in sample variance under two trend forms for the trend slope of 1.0%. It can be seen from this figure that power of the two non-parametric tests are almost equal in both trend forms. The SLR test has

significantly higher power than the MK and SPR tests in both trend forms for any CV values greater than 0.40. For example, for a sample CV of 0.50, the power of the MK, SPR and SLR tests are 58.1%, 59.3% and 73.7% respectively in the case of TF-1, while in the case of TF-2, these are 33.4%, 34.8% and 67.8% respectively.

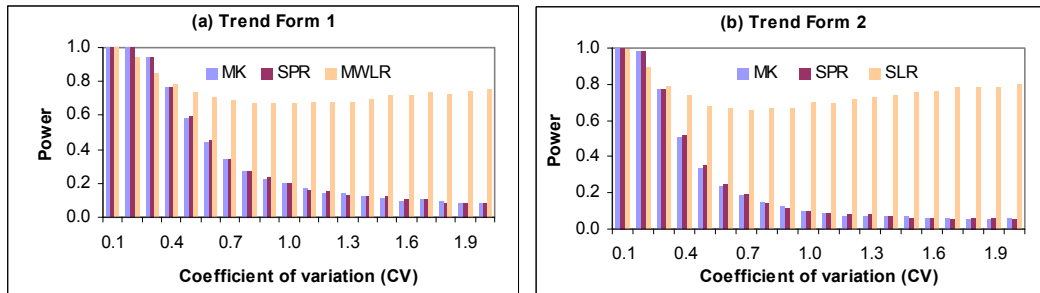


Figure 8.8: Comparison of the sensitivity of the power of the trend identification tests (MK, SPR and SLR tests) with the increase in sample variance under two trend forms for trend slope of 1% (panel a: for TF-1 and panel b: for TF-2).

8.4 RESULT SUMMARY AND DISCUSSIONS

The findings of the simulation experiments carried out to identify the power of various trend identification tests are summarised below:

1. In general, the power of a trend test is an increasing function of the trend slope. This is true for all three trend identification tests considered (MK, SPR and SLR tests) in the experiment. The power of the non-parametric MK and SPR tests changes in a similar fashion (both have almost equal power) with the changes in trend slopes and is significantly influenced by the form of the trends in the records, whilst the influence of trend form on the power of the parametric SLR test is not very noticeable.

The above findings, in the case of MK and SPR tests, agree with the results of Yue et al. (2002), i.e. the power of these two tests increases at a similar rate, both in magnitude and change rate, with the increase in trend slopes. No parametric test was considered by Yue et al. (2002).

2. Irrespective of the type of trend tests, the power of a trend identification test is an increasing function of sample size i.e. power increases with the increase in sample size. The change rate of power, for both non-parametric tests is almost

equal and comparable. Similar to trend slopes, the effect of trend form on power, is slightly more significant in the case of non-parametric test than the parametric test. However, this effect diminishes for any sample size greater than 70, i.e. both the non-parametric and parametric tests show similar power for sample size greater than 70 for both type of trend forms.

3. Regardless of the trend forms, the power of the non-parametric tests (MK and SPR test) is a decreasing function of sample variance. In the case of the parametric SLR test, power is almost invariant for any increase in CV value greater than 0.50 in both trend forms.
4. The sample mean increases linearly and equally with the increase in trend slopes in both cases of trend forms regardless of any variations in the sample variance. In contrast, the sample variance increases with the increase in trend slopes in different fashions in the two trend forms considered. In the case of TF-1, population CV decreases with the increase in trend slopes, while increases in the case of TF-2. Again, it was found that the change rate in sample CV depends on the magnitude of the population CV. In the case of TF-2, the change rate is slower for the higher population CV values, while in the TF-1 case it is faster for larger population CV. The change pattern in the sample CV, in the TF-1, is slightly non-linear, whereas in the TF-2 it is almost linear.

The above suggests that the TF-2 introduces more variation in the records, while the TF-1 reduces it. It is shown earlier that power of a trend test is significantly influenced by the variance of records, i.e. the power decreases with the increase in sample variation, particularly in the non-parametric tests.

It is therefore clear from above that the detection ability of a trend test of a time series with trend in the type of TF-1 would be higher than the TF-2. This effect is very significant in the case of non-parametric tests. In the case of the parametric test, the power is less sensitive to the changes in sample variance. Since in the TF-1, CV value decreases with the increase in trend slopes, the power of the test increases. This decrease rate in CV could be attributed to the faster increase rate in sample mean than in the variations of the data series.

However, in the real world, the sample CV could remain unchanged or could vary slowly with the increase in trend slope. In this case, the suggestion of the power of a trend test is an increasing function of trend slope may not be true. The TF-2 used in this study provides evidence of this.

From the above findings it can be concluded that the sample variance plays a very important role in detecting whether trend exists or not. The parametric tests are more suitable and powerful for testing trend of a time series with high variability. However, in order to get a clear picture for true trend in a data series it is recommended to apply both the non-parametric and parametric tests.

9 EFFECT OF TRENDS ON REGIONAL GROWTH CURVES AND AT-SITE QUANTILE ESTIMATES

9.1 INTRODUCTION AND OBJECTIVE

This chapter investigates the effect of trends in annual maximum flood series on the estimation of regional growth curve and at-site quantiles. It is intuitively felt that quantiles estimated from data series that contain upward trend would be larger than those estimated from trend free data, but judgement about the effect of trend on growth curve quantiles is not so clearcut as the denominator of the quantity plotted in the growth curve is affected by the trend also. As a result, it is intuitively felt that the effect of trend on the growth curve may not be so great as for quantiles. The objective of this chapter is to examine these effects. The study was carried out using Monte Carlo simulation technique. The details of the methodology and the results are discussed in the following sections.

9.2 SCOPE OF THE STUDY

The scope of the study includes:

- Selection of an appropriate trend application method,
- Selection of a region (pooling group) and population distribution (true distribution),
- Investigation of the effect of trend on sample properties and the population distribution parameters,
- Investigation of the effect of trend on regional growth curves and at-site quantile estimates for various combinations of true and fitted distributions,
- Determination of the extent of trend at which the growth curve and at-site quantile estimates significantly deviate from the baseline no-trend condition estimates, and
- Suitability assessments of various combinations of true and fitted distributions at various extents of trend slopes.

9.3 METHODOLOGY

9.3.1 General

The study was carried out using a Monte Carlo Simulation technique. Initially, the effect of trends on sample properties such as the first three sample moments (Mean, L-CV and L-Skewness) were investigated. Subsequently, any effects of trend on the underlying population moments and parameters were examined. Finally, any changes in the estimates of regional growth curves and at-site quantiles (over the stationary condition) were investigated for various trend scenarios.

The steps of this simulation procedure are given as follows:

1. Specify the number of sites, N and for each of the N sites its record length n_i and the L-moments of its frequency distribution.
2. Calculate the parameters of the at-site frequency distribution from their specified L-moment ratios,
3. Calculate the population estimates of the regional growth curve and at-site quantiles (stationary condition)
4. For each of M repetitions of the simulation procedure, carry out the following steps:
 - (i) Generate a random sample of data of size n_i for each site from the frequency distribution (hereafter referred to as the stationary sample)
 - (ii) Apply trend on the simulated random sample for each of the N sites (hereafter referred to as the non-stationary sample)
 - (iii) Apply the regional L-moment algorithm (Hosking and Wallis, 1997) to the non-stationary sample of the regional data. This involves the following steps:
 - (a) Calculate the at-site and regional average L-moment ratios,
 - (b) Fit the chosen distribution from the regional average L-moment ratios,
 - (c) Calculate estimates of the regional growth curves and at-site quantiles,
 - (d) Calculate the relative difference of the estimated non-stationary regional growth curves and at-site quantiles over the stationary condition.

5. Calculate overall regional measures of the relative differences of the estimated quantiles and regional growth curves for various trend scenarios.

9.3.2 Selection of Stationary Region and Random Sample Generation

It is considered that the non-stationarity in the AMF series would result mainly from climate change impact on a regional basis. This trend effect assessment has therefore been focused on a regional scale basis rather than on a single site basis.

The region (pooling group) was specified as follows:

- No. of sites in the region, N : 15,
- Sample size, n_i : 30 years, fixed for each site, a total of 450 station-years,
- Region is moderately heterogeneous (The Hosking-Wallis Heterogeneity measure statistic, $H1$ has a value of 1.74. Refer to **Appendix C** for the details of this measure) with L-CV and L-Skewness both linearly varying from 0.20 at site 1 to 0.30 at site 15 with a range of 0.10. A true distribution mean of 1.0 was used. This linear variation of L-moment ratios is a plausible form of variation for the sites in a region. In practical applications, it will often be the case that sites with high L-CV also tend to have high L-Skewness. For example, Lu and Stedinger (1992b) found this to be the case for annual maximum streamflow data, and
- The flood-like extreme value type distributions (GEV and EV1) were used for random sample generation using the Monte Carlo simulation technique.

The selection of a region with 15 sites and the site record length of 30 were based on the findings of the sensitivity study carried out by Hosking and Wallis (1997). The authors found that “*there is a little to be gained by using regions larger than 20 sites*”, and also showed that “*in heterogeneous regions, the presence of bias does not vanish with the increase in record lengths; when $n > 40$ the at-site estimate is more accurate than regional estimate for the $F=0.9$ quantile*”. The consideration for a moderately heterogeneous region was felt appropriate in the context of real world data. For example, Das and Cunnane (2011) found that the most of the Irish pooling groups of AMF series exhibits a degree of heterogeneity among the group members. Based on the $H2$ heterogeneity measure (Hosking and Wallis, 1997; also refer to **Appendix C** for the details of this measure), 86% (73 out of 85) of the Irish pooling groups showed heterogeneity with $H2$ values less than 4. This result is very

similar to what was found for the UK pooling groups (Flood Estimation Handbook (FEH), 1999, vol.3, p.176). FEH revised the heterogeneity criteria based on the H^2 statistics, suggesting that if $2 < H^2 < 4$, a region could be considered as heterogeneous, whereas if $H^2 > 4$ it could be considered as strongly heterogeneous. The selection of GEV and EV1 distributions was based on the finding of a study carried out under the Irish Flood Studies Update (FSU) Programme, where GEV and EV1 distributions were found suitable for the Irish AMF data (FSU, OPW, 2009).

Four combinations of extreme value type distributions were used for simulating and fitting the data to estimate the regional growth curve and quantiles for various return periods. These include:

- (i) **GEV-GEV**: where both generation and fitting were carried out using the GEV distribution,
- (ii) **GEV-EV1**: where true distribution is GEV and the fitted distribution is EV1,
- (iii) **EV1-EV1**: where both generation and fitting were carried out using the EV1 (Gumbel) distribution, and
- (iv) **EV1-GEV**: where random samples were generated from EV1 distribution and were fitted to GEV distribution.

9.3.3 Application of Trends

The true form of trend in the historical time series is not known, most likely it would be non-linear in nature. However, in order to simplify our understanding, a linear upward type trend model, which is easy to formulate mathematically, was considered in this study. It was assumed that the first moment of the sample's true distribution will be much more sensitive to the long-term climate change effect than the other higher order moments. Therefore, upward linear trend is applied to the population mean.

The following two deterministic trend forms have been employed to introduce trend in the stationary time series:

$$(i) \quad \text{Trend Form 1 (TF-1): } Q_{NS}(t) = Q_S(t) + T_S t \quad (9.1)$$

$$(ii) \quad \text{Trend Form 2 (TF-2): } Q_{NS}(t) = Q_S(t)[1 + T_S t] \quad (9.2)$$

where

$Q_{NS}(t)$ = non-stationary time series,

$Q_S(t)$ = population/stationary time series,

T_S = upward trend slope (per unit time step)

t = time step (year), 1 to 30 years

It can be seen from the above equations that the TF-1 is an additive type trend application scheme, while the TF-2 is a hybrid type. **Figure 9.1** shows a graphical comparison of these two trend forms. The red line represents a sample of a stationary time series with 30 years record length, which has been drawn from GEV distribution with mean, L-CV and L-Skewness of 1.0, 0.25 and 0.25 respectively (corresponding location, scale and shape parameters are 0.773, 0.318 and -0.121 respectively). The blue and pink lines represent the corresponding non-stationary time series where Trend Forms 1 and 2 respectively with an upward trend slope of 1% having been applied. Changes in time series magnitude over the record length are visible in the plots. A linear regression trend line has been estimated for each of the non-stationary samples with different trend forms, the thin dashed line is for TF-1 and the thick solid line is for TF-2. It can be seen from these plots that the estimated slope of the regression line for the TF-1 is slightly greater than that of the TF-2. However, it can be seen that the TF-2 introduces more variability in the time series than the TF-1.

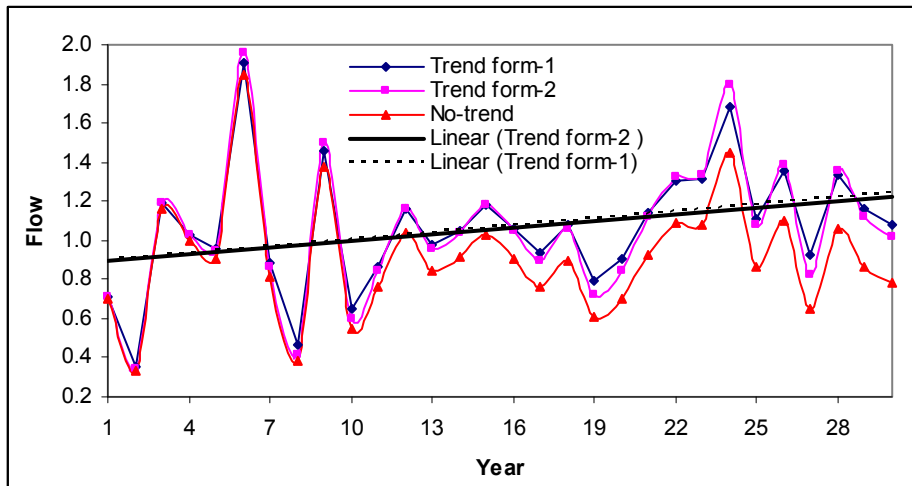


Figure 9.1: Graphical presentation of two different trend forms (1% upward trend slope). The no-trend sample was drawn from GEV distribution with location, scale and shape parameters of 0.773, 0.318 and -0.121 respectively (mean =1.0, L-CV=0.25 & L-Skewness=0.25)

9.3.4 Trend Scenarios

If the cause of trend is mainly believed to be climate change, then it is reasonable to assume uniformity of trend across the region (i.e. a fixed rate trend applies to all sites in the region). However, some degree of variability can be expected among the sites due to the regional variations in climate change and variability in the changes of soil moisture characteristics in their relevant catchments. Based on this, the trend impact assessment was carried out for a number of spatial trend scenarios as discussed below:

- (i) **Spatially Uniform Trend (SUT)** (fixed rate trend across the region): A range of upward trend slopes starting from 0.2% to 4% with an increment of 0.2% was considered. These trend magnitudes were based on the identified upward trend slopes in the Irish AMF series as discussed in Chapter 7 (Section 7.2.1),
- (ii) **Spatially Varying Trend (SVT):** Variable upward trend slopes of 0.2% at site 1 and 2% at site 15 with a range of 1.8% (**Forward SVT**), i.e. a trend slope of 0.2% was applied at site 1 which has true L-CV & L-Skewness of 0.2 each and a trend slope of 2% at site 15 which has true L-CV and L-Skewness of 0.3 each, and

- (iii) **Random Trend (RT):** The effect of trend in a single site in the region on the regional growth curve and at-site quantile estimates was also examined. This type of trend could result from the catchment land use changes and/or from upgrading of catchment drainage systems. In this scenario uniform trend as discussed in (i) has been applied to only one site in the region (Site 8). However, trend could be applied to more than one site on a random basis.

These trend simulation scenarios are summarised in **Table 9.1**.

Table 9.1: Selected trend scenarios

Trend scenarios	Descriptions
SUT	21 trend run-scenarios for 21 upward trend slope magnitudes of - 0% (no-trend condition), 0.2%, 0.4%, 0.6%, 0.8%, 1%, 1.2%, 1.4%, 1.6%, 1.8%, 2%, 2.2%, 2.4%, 2.6%, 2.8%, 3%, 3.2%, 3.4%, 3.6%, 3.8% and 4%
SVT	Variable upward trends across 15 sites in the region with 0.2% at site 1 and 2% at site 15 with a range of 1.8% among sites in the region.
RT	Trends on only site 8 (21 trend slopes)

9.3.5 Growth Curve and Quantile Estimation Methods

The at-site quantiles were estimated using the 'Index-flood and L-moment parameter estimation method' as recommended by Hosking and Wallis (1985a, 1993, 1997). The index-flood used in this study is the at-site sample mean.

As mentioned previously, random samples are generated from the extreme value type distributions as the suitability of these distributions for the Irish AMF series have been identified in a study carried out under the Flood Studies Update (FSU) Programme (Office of Public Works, 2009). Details of the GEV and EV1 distributions, their parameter estimation methods and the growth curves used in this study are provided below:

9.3.5.1 Statistical Distributions

The pdf and cdf of the **GEV distribution** are defined as:

$$\text{GEV pdf: } f(x) = \frac{1}{\alpha} \left[1 - k \left(\frac{x-u}{\alpha} \right) \right]^{\left(\frac{1}{k}\right)-1} \exp \left\{ - \left[1 - k \left(\frac{x-u}{\alpha} \right) \right]^{\frac{1}{k}} \right\} \quad (9.3)$$

$$\text{GEV cdf: } F(x) = \exp \left\{ - \left[1 - k \left(\frac{x-u}{\alpha} \right) \right]^{\frac{1}{k}} \right\} \text{ for } \alpha > 0 \quad (9.4)$$

where u is the location parameter, α the scale parameter and k the shape parameter. The shape parameter k governs the tail behaviour of the distribution. The special case corresponding to $k = 0$ is the Gumbel (GEV type I) distribution. If $k < 0$ the distribution is known as a type II GEV distribution (Fréchet). If $k > 0$, the distribution is known as a type III GEV distribution and is closely related to the Weibull distribution. The range of possible values for the GEV distribution is:

$$-\infty < x \leq u + \frac{\alpha}{k} \quad \text{if } k > 0$$

$$u + \frac{\alpha}{k} \leq x < \infty \quad \text{if } k < 0$$

$$-\infty < x < \infty \quad \text{if } k = 0$$

Thus the GEV distribution is bounded above if $k > 0$ and bounded below for $k < 0$.

The **EV1 distribution** has two parameters (location and scale) and is an unbounded distribution (i.e. $-\infty < x < \infty$). The pdf and cdf of the EV1 distribution are given by:

$$\text{EV1 pdf: } f(x) = \frac{1}{\alpha} \exp \left[- \left(\frac{x-u}{\alpha} \right) - \exp \left\{ - \left(\frac{x-u}{\alpha} \right) \right\} \right] \quad (9.5)$$

$$\text{EV1 cdf: } F(x) = \exp\left\{-\exp\left[-\left(\frac{x-u}{\alpha}\right)\right]\right\} \quad (9.6)$$

Flood frequency curve:

A flood frequency curve relates flood-size to flood-rarity. Flood frequency curve can be expressed in equation form in terms of either the return period T or the non-exceedance probability F and is derived from the cdf of the relevant distribution.

The GEV distribution flood frequency curve is defined by:

$$Q(F) = u + \frac{\alpha}{k} \left\{ 1 - (-\ln F)^k \right\} \quad (9.7)$$

$$Q_T = u + \frac{\alpha}{k} \left\{ 1 - \left(-\ln\left(1 - \frac{1}{T}\right) \right)^k \right\} \quad (9.8)$$

where $Q(F)$ is the flood peak corresponding to non-exceedance probability of F and Q_T is the T-year flood quantile, and where $F=1-1/T$.

In the case of the EV1 distribution, the flood frequency curve takes the form:

$$Q(F) = u + \alpha \left\{ -\ln(-\ln F) \right\} \text{ in terms of F and} \quad (9.9)$$

$$Q_T = u + \alpha \left\{ -\ln\left(-\ln\left(1 - \frac{1}{T}\right)\right) \right\} \text{ in terms of T} \quad (9.10)$$

9.3.5.2 Growth Curve and Index Flood Method

Index flood procedures are a convenient way of pooling summary statistics from different data samples. Suppose that data are available at N sites, with site i having sample size n_i and observed data $Q_{i,j}, j=1, \dots, n_i$. The key assumption of an index-flood procedure is that the sites form a homogeneous region, that is, that the frequency distributions of the N sites are identical apart from a site-specific factor, the index flood. Let $Q_i(F)$, $0 < F < 1$, be the quantile function of the frequency distribution at site i. It can then be written that:

$$Q_i(F) = \mu_i q(F), \quad i=1, \dots, N \quad (9.11)$$

where μ_i is the index flood and $q(F)$ is the dimensionless growth curve ordinate.

μ_i can be thought of as a typical flood for a particular catchment. It tends to increase with catchment size and with average annual rainfall. The index flood is used to link the flood frequency and growth curves. The flood frequency curve is obtained by multiplying the index flood and the growth curve. In the present study, the mean of the at-site frequency distribution was used as the index flood (Q_{mean}). The index flood was naturally estimated by the sample mean of the data at site i ($\hat{\mu}_i$).

The remaining factor $q(F)$ in equation 9.11, is the regional growth curve, a dimensionless quantile function common to every site. It is the quantile function of the regional frequency distribution, the common distribution of all sites in the region. The growth curve can be thought of as a scaled version of the flood frequency curve. It has the same shape parameter as the flood frequency curve, but is scaled to have a value of 1.0 at the frequency or return period of the index flood. Since all growth curves are scaled to have a value of 1.0 at the index flood, the growth curves from different catchments can be easily compared. For pooled analysis, the pooled growth curve represents an average of all the individual growth curves from sites in the pooling-group which are assumed to differ from one another by random amounts only. The growth factor is the value of the growth curve at a particular return period. The T-year growth factor can be defined as, $X_T = Q_T / \mu_i$.

The index-flood procedure makes the following assumptions:

- (i) Observations at any given site are identically distributed,
- (ii) Observations at any given site are serially independent,
- (iii) Observations at different sites are independent – no cross correlation,
- (iv) Frequency distributions at different sites are identical apart from a scale factor, and
- (v) The mathematical form of the regional growth curve is correctly specified.

9.3.5.3 Steps in Flood Frequency Analysis

Flood frequency analysis can be carried out on a single site basis or a pooled sites basis. Single-site analysis is used when there is a reliable and long record at the site of interest and when the target return period T is not too long. Pooled frequency analysis is required unless the flood record is particularly long, i.e. at least as long as the return period of interest. The basic principle of the pooling approach is to combine data from the subject site with flood data from other similar sites. The flood frequency curve is estimated using this more extensive data set.

The main steps in flood frequency analysis in the pooled analysis case are: (i) estimation of the index flood, and (ii) derivation of the growth curve. The index flood is estimated either from the at-site flood data or from the catchment descriptor equations depending on whether the site is gauged or ungauged. Derivation of the growth curve involves selection of the distribution and estimation of the growth curve parameters. The distribution parameters are estimated by pooling information from all sites in the region, in this case by averaging the dimensionless L-Moments t_2 and t_3 . Once the growth curve has been derived, the flood frequency curve is obtained by multiplying the growth curve by at-site index flood (equation 9.11).

9.3.5.4 Derivation of Growth Curve

GEV distribution:

The GEV frequency curve is given by:

$$Q(F) = u + \frac{\alpha}{k} \left\{ 1 - (-\ln F)^k \right\} \quad (9.12)$$

The mean of the GEV distribution is given by:

$$Q_{mean} = u + \frac{\alpha}{k} \left\{ 1 - \Gamma(1+k) \right\} \quad \text{if } k \neq 0, k < 1 \quad (9.13)$$

The growth curve is obtained from the flood frequency curve by substituting in $x(F) = \frac{Q(F)}{Q_{mean}}$ and rearranging to give:

$$x(F) = 1 + \frac{\beta}{k} \left\{ \Gamma(1+k) - (-\ln(F))^k \right\} \quad (9.14)$$

$$\text{where } \beta = \frac{\alpha}{u + \frac{\alpha}{k} \left\{ 1 - \Gamma(1+k) \right\}} \quad (9.15)$$

The GEV growth curve can also be written in terms of the return period T:

$$x_T = 1 + \frac{\beta}{k} \left\{ \Gamma(1+k) - \left(-\ln\left(1 - \frac{1}{T}\right) \right)^k \right\} \quad (9.16)$$

EV1 distribution:

Similarly the EV1 growth curve can be derived as follows:

$$\text{EV1 frequency curve: } Q(F) = u + \alpha \left\{ -\ln(-\ln F) \right\} \quad (9.17)$$

$$\text{EV1 mean: } Q_{mean} = u + \alpha\gamma \quad (9.18)$$

Thus the derived EV1 growth curve:

$$x(F) = 1 + \beta \left\{ -\ln(-\ln F) - \gamma \right\} \quad (9.19)$$

$$\text{where, } \beta = \frac{\alpha}{u + \alpha\gamma} \quad (9.20)$$

In terms of return period the EV1 growth curve is:

$$x_T = 1 + \beta \left\{ -\ln\left(-\ln\left(1 - \frac{1}{T}\right)\right) - \gamma \right\} \quad (9.21)$$

The growth curve has a value of 1.0 at the index flood's return period which means that only two parameters are required to describe the GEV growth curve, whereas three parameters are needed for the GEV flood frequency curve. For the EV1 distribution only one parameter is required to describe its growth curve. In general, a growth curve distribution requires specification of one parameter fewer than the corresponding flood frequency distribution.

9.3.5.5 Growth Curve Parameter Estimation

A simple method of fitting a statistical distribution to the data involves choosing a distribution for which the distribution (or population) mean, variance and skewness match the sample mean, variance and skewness. A distribution is often described in terms of the mean, variance and skewness (and occasionally the kurtosis). The mean locates the 'middle' of the distribution. The variance measures the spread in the distribution. The skewness summarises any asymmetry in the distribution and the kurtosis says whether the distribution is peaky or flat.

Common approaches to distribution fitting include: L-moment approach, conventional moment approach and the maximum likelihood techniques. The L-Moment approach is similar to the method of moments, but is based on L-moments rather than conventional moments. It is a development of probability weighted moments and is computationally convenient.

For pooled analyses, the sample L-moments effectively characterises the shape of a distribution; L-moment ratios of sites in the pooling group are averaged to give pooled L-moment values (Hosking and Wallis, 1993, 1997).

Probability Weighted Moments and L-moments:

From a sample of size n , arranged in ascending order ($X_1 \leq X_2 \leq \dots \leq X_n$), the sample probability weighted moments can be calculated from the following equation (Landwehr et al., 1979a):

$$b_r = n^{-1} \sum_{j=r+1}^n \frac{(j-1)(j-2)\dots(j-r)}{(n-1)(n-2)\dots(n-r)} X_j \quad (9.22)$$

L-moments are an alternative system of describing the shapes of probability distributions. Historically, they arose as modifications of the 'probability weighted moments' of Greenwood et al. (1979). In terms of probability weighted moments, L-moments are given by the following equations (Hosking, Wallis and Wood, 1985b):

$$\left. \begin{aligned} l_1 &= b_0 \\ l_2 &= 2b_1 - b_0 \\ l_3 &= 6b_2 - 6b_1 + b_0 \\ l_4 &= 20b_3 - 30b_2 + 12b_1 - b_0 \end{aligned} \right\} \quad (9.23)$$

where l_1, l_2, l_3 and l_4 are the first four sample L-moments, and b_0, b_1, b_2 and b_3 are the sample probability weighted moments.

The first L -moment is the sample mean, a measure of location. The second L -moment is a measure of the dispersion of the data values about their mean. The L -moment analogue of the coefficient of variation (standard deviation divided by the mean), is the L -CV, defined by, $t_2 = l_2 / l_1$.

By dividing the higher order L-moments by the dispersion measure, l_2 , we can obtain some dimensionless quantities, which are called L-moment ratios. For example, $t_3 = l_3 / l_2$ and $t_4 = l_4 / l_2$, which are the measures of the sample's skewness and kurtosis, and are called L-Skewness and L-kurtosis respectively.

Parameter Estimations by L-moments:

In the method of L-moments, the distribution's parameters are estimated by equating the population L-moments of the distribution to the sample L-moments calculated from the data. Assuming the region to be homogeneous, sample L-moment ratios calculated from the re-scaled data for different sites can be combined to give regional average L-moment ratios. To allow for the greater variability of L-moment ratios in small samples, averages are weighted proportionally to the sites' record lengths.

Suppose that the region has N sites, with Site i having record length n_i , sample mean l_1^i , and sample L-moment ratios $t_2^i, t_3^i, t_4^i, \dots$. Denoting by $t_2^R, t_3^R, t_4^R, \dots$, the regional average L-moment ratios, weighted proportionally to the sites' record length are calculated as:

$$t_2^R = \frac{\sum_{i=1}^N n_i t_2^i}{\sum_{i=1}^N n_i}, t_r^R = \frac{\sum_{i=1}^N n_i t_r^i}{\sum_{i=1}^N n_i}, r=3,4,\dots \quad (9.24)$$

Set the regional average mean to 1 that is $l_1^R = 1$.

Fit the distribution by equating its L-moment ratios $\lambda_1, \tau, \tau_3, \tau_4, \dots$, to the regional average L-moment ratios $l_1^R, t_2^R, t_3^R, t_4^R, \dots$ calculated above.

GEV-distribution – growth curve parameter estimation:

As shown earlier in equation 9.14, the GEV growth curve has two parameters, β and k , where β was expressed, equation 9.15, in terms of the distribution's location and shape parameter as,

$$\beta = \frac{\alpha}{u + \frac{\alpha}{k} \{1 - \Gamma(1+k)\}}.$$

The shape parameter k is estimated from the sample L-Skewness (t_3) via an approximation proposed by Hosking et al, (1985b) as shown below. This has accuracy better than 9×10^{-4} for $-0.5 \leq \tau_3 \leq 0.50$.

$$k \approx 7.8590c + 2.9554c^2 \text{ where } c = \frac{2}{3+t_3} - \frac{\ln 2}{\ln 3} \quad (9.25)$$

In terms of L-moments, the location and scale parameters of the distribution are given by:

$$\alpha = \frac{\lambda_2 k}{(1 - 2^{-k}) \Gamma(1+k)} \quad (9.26)$$

$$u = \lambda_1 - \alpha \{1 - \Gamma(1+k)\} / k \quad (9.27)$$

where λ_1 and λ_2 are the first two L-moments and Γ denotes the gamma function

$$\Gamma(x) = \int_0^{\infty} t^{x-1} e^{-t} dt. \quad (9.28)$$

From the above, the β parameter can be expressed in terms of distribution's shape parameter (k) and L-CV (τ) as follows:

$$\beta = \frac{\tau k}{(1 - 2^{-k})\Gamma(1 + k)} \quad (9.29)$$

where, L-CV, $\tau = \lambda_2 / \lambda_1$; Hence by knowing the sample L-CV, t_2 and the shape parameter, k , the β parameter can be estimated from equation 9.29.

EV1-distribution – growth curve parameter estimation:

The β parameter of the EV1 growth curve (equation 9.20) can be estimated from the sample L-CV using

$$\beta = \frac{t_2}{\ln 2} \quad (9.30)$$

9.3.6 Trend Effect Assessments

The presence of trend in flood records could cause changes (increase or decrease) in various properties such as mean, L-CV and L-Skewness, which could consequently result in under- or over-estimation of regional growth curve and quantile estimates. Furthermore, the changes in sample properties and quantile estimates could differ between different cases of trend forms and fitted distributions.

The mean square error (MSE) of an estimator $\hat{\theta}$ with respect to the true parameter θ is defined as:

$$MSE(\hat{\theta}) = E((\hat{\theta} - \theta)^2) \quad (9.31)$$

The MSE is the second moment (about the origin) of the error, and thus incorporates both the variance of the estimator and its bias. It can be written as the sum of the variance and the squared bias of the estimator:

$$MSE(\hat{\theta}) = Var(\hat{\theta}) + (Bias(\hat{\theta}, \theta))^2 \quad (9.32)$$

For an unbiased estimator, the MSE is the variance. Like the variance, MSE has the same unit of measurement as the square of the quantity being estimated. In an analogy to standard deviation, taking the square root of the MSE yields the root mean squared error or RMSE, which has the same units as the quantity being

estimated; for an unbiased estimator, the RMSE is the square root of the variance, known as the standard error.

Two or more statistical models may be compared using their MSEs as a measure of how well they explain a given set of observations: the unbiased model with the smallest MSE is generally interpreted as best explaining the variability in the observations.

In the index flood method, the quantile function of the distribution at site i has the form of $Q_i = \mu_i x(F; \theta)$, where μ_i is the index flood at site i and $x(F; \theta)$ is the form of regional growth curve. θ represents the parameter or parameters of the regional growth curve. Let $\hat{\mu}_i$ and $\hat{\theta}$ be the estimator of μ_i and θ respectively, thus the estimator of the at-site quantile of nonexceedance probability F is $\hat{Q}_i(F) = \hat{\mu}_i x(F; \hat{\theta})$. This shows that the error in the estimated quantile comes from the variability and bias associated with the estimators of both at-site index flood and the frequency distribution of the growth curve. Hosking and Wallis (1997) derived an expression for the mean square error of the quantile estimate based on the L-moment algorithm and showed that the variability in the $\hat{Q}_i(F)$ estimate arises from the following sources:

- Variability of the sample mean, $\text{var}(\hat{\mu}_i)$; and
- Variability of the estimated regional growth curve, $\text{var}\left\{x(F; \hat{\theta})\right\}$, which arises from variability of the sample L-moment ratios;

while the bias arises from:

- Misspecification of the regional frequency distribution,
- Heterogeneity in the region,
- Variability of the sample L-moment ratios, which induces bias in the quantile estimate in consequence of the nonlinearity of the regional growth curve as a function of the L-moment ratios.

Detailed analytical expressions for the bias and variance of L-moments of the GEV distribution have been given by Lu and Stedinger (1992). These can be used to obtain good approximations to the variance of quantile estimates for at-site and regional frequency analyses when the true and fitted frequency distributions are both of the generalised extreme-value form (Stedinger and Lu, 1995).

Hosking and Wallis (1997) recommended the Monte Carlo simulation method as an effective tool for establishing the properties of complex statistical procedures such as the regional L-moment algorithm. The general procedure in such an investigation starts by defining a region, that is, by specifying the number of sites in the region, and the frequency distributions and record lengths at each site. Many sets of data are generated from the region. The data are then fitted by using a selected distribution and parameter estimation method. The estimated quantiles and growth curve are compared with the true values implied by the frequency distribution specified for each site, and accuracy measures are calculated for the estimators.

The procedure for simulating the regional L-moment algorithm is discussed in Section 9.3.1. The error associated with the growth curve and quantile estimates have been measured in terms of relative bias, $B_i(F)$ and relative root mean square error, RMSE, $R_i(F)$ rather than in terms of only bias and RMSE.

The relative bias and relative RMSE, expressed as percentages, of the site- i quantile estimator are estimated by

$$B_i(F) = \frac{1}{M} \sum_{m=1}^M \frac{\hat{Q}_i^{[m]}(F) - Q_i(F)}{Q_i(F)} \times 100\% \quad (9.33)$$

and

$$R_i(F) = \left[\frac{1}{M} \sum_{m=1}^M \left\{ \frac{\hat{Q}_i^{[m]}(F) - Q_i(F)}{Q_i(F)} \right\}^2 \right]^{1/2} \times 100\% \quad (9.34)$$

where M is the number of simulations.

To obtain a summary of the performance of an estimation procedure over all of the sites in the region, the regional average values have been computed as follows:

Regional average relative bias:

$$B^R(F) = \frac{1}{N} \sum_{i=1}^N B_i(F) \quad (9.35)$$

Regional average absolute relative bias:

$$A^R(F) = \frac{1}{N} \sum_{i=1}^N |B_i(F)| \quad (9.36)$$

and

Regional average relative RMSE

$$R^R(F) = \frac{1}{N} \sum_{i=1}^N R_i(F) \quad (9.37)$$

The regional average relative bias, $B^R(F)$, measures the tendency of quantile estimates to be uniformly too high or too low across the whole region. This tendency is apparent, for example, when a distribution with a heavy upper tail is fitted to a region in which the true frequency distributions have relatively light upper tails, or vice versa.

The regional average absolute relative bias, $A^R(F)$, measures the tendency of quantile estimates to be consistently high at some sites and low at others. This occurs in a heterogeneous region, in which the estimated regional growth curve tends to overestimate the true at-site growth curve at some sites and to underestimate it at others. In such cases, $A^R(F)$ indicates the magnitude of the bias at a typical site and is more useful than $B^R(F)$, in which the contributions of negative and positive biases may cancel out to give a misleadingly small value of the bias. In a homogeneous region, however, we would expect the bias to be the same at each site, and therefore $A^R(F)$ and $B^R(F)$ to be equal.

The regional average relative RMSE, $R^R(F)$, measures the overall deviation of estimated quantiles from true quantiles.

The accuracy of the quantile estimates has also been assessed in terms of standard error (se). The se of a quantile estimate, $\hat{Q}(F)$ is an indication of how reliable that estimate is. It is based on the assumption that the data upon which the estimate is based are randomly drawn from a single population. If an infinite number of similarly sized data sets were drawn from the same population and the value of quantile obtained from each set of data by the same procedure, then the se is defined as:

$se(\hat{Q}(F)) = \text{standard deviation of all possible set of } \hat{Q}(F) \text{ values.}$

This measure only represents the degree of scatter of the several estimates and does not refer to whether the mean of these equals the true value in the population.

If this latter equality holds, then the procedure by which $\hat{Q}(F)$ is calculated is said to be unbiased – otherwise it is said to be biased.

Theoretical expressions for standard errors of L-moments based estimates of at-site quantiles for both EV1 and GEV distribution have been given by Lu and Stedinger (1992). In the present study, the standard error of quantile estimate has been obtained from the above mentioned Monte Carlo simulation technique as proposed for the bias and RMSE.

The standard error of the site-*i* quantile estimator is obtained from the following expression:

$$SE_i(F) = \sqrt{(R_i(F))^2 - B_i(F)^2} \quad (9.38)$$

The regional average standard error of the estimated quantile is

$$SE^R(F) = \frac{1}{N} \sum_{i=1}^N SE_i(F) \quad (9.39)$$

In addition to the quantiles, the above accuracy measures have also been estimated for the growth curves. Comparison of the accuracy of the estimated growth curve and the estimated quantiles facilitates judgement of the relative importance of errors in estimating the index flood and errors in estimating the regional growth curve.

The above accuracy measures might be applicable for the no-trend scenario only. In any trend condition, these measures would rather estimate the effect of trends on the true quantiles. For example, the bias terms, $B_i(F)$ and $B^R(F)$ would measure the relative differences (increases/decreases) in quantile estimates to be caused by various trend slope magnitudes at the at-site and regional levels respectively. For a particular trend scenario, $\hat{Q}_i(F)$ in equation 9.33 will be the quantile estimate associated with this trend slope while $Q_i(F)$ will remain the true at-site quantile estimate.

9.4 RESULTS

9.4.1 Introduction

As mentioned earlier, initially the impacts of trends on population properties such as the first three moments, Mean, L-CV and L-Skewness, were investigated. Subsequently, the changes in the distribution parameters have been examined. Finally, any changes in the estimates of regional growth curves and at-site quantiles (over the stationary condition) were investigated for various trend scenarios.

Model simulations were carried out for 10,000 realisations of regions ($M = 10,000$). The results of the simulation experiments are presented in the following sections.

The changes in population properties and quantile values were calculated with respect to the true values on a regional scale basis as discussed in Section 9.3.6. The true values of the at-site L-moment ratios, distribution parameters and some at-site true quantile estimates for the region specified in Section 9.3.2 are given in the tables below, where **Table 9.2** corresponds to GEV distribution and **Table 9.3** is for EV1 distribution. The regional growth curve has been calculated from the harmonic mean of the at-site quantile estimates in each case.

Table 9.2: True at-site properties, distribution parameters and at-site quantile values for GEV distribution (reproduced from Hosking and Wallis, 1993; the mean of all populations is 1.0).

Site	L-CV	L-Skew.	n _i	GEV Parameters			True at-site Quantiles							
				u	alpha	k	0.010	0.100	0.500	0.800	0.900	0.950	0.990	0.999
1	0.200	0.200	30	0.828	0.276	-0.046	0.421	0.602	0.930	1.256	1.482	1.706	2.242	3.073
2	0.207	0.207	30	0.820	0.283	-0.057	0.407	0.590	0.925	1.263	1.499	1.735	2.307	3.213
3	0.214	0.214	30	0.812	0.289	-0.068	0.393	0.578	0.920	1.269	1.516	1.764	2.374	3.361
4	0.221	0.221	30	0.805	0.296	-0.079	0.379	0.566	0.915	1.275	1.532	1.793	2.442	3.514
5	0.229	0.229	30	0.797	0.302	-0.089	0.366	0.555	0.909	1.281	1.549	1.823	2.512	3.677
6	0.236	0.236	30	0.789	0.307	-0.100	0.354	0.543	0.904	1.286	1.565	1.852	2.584	3.846
7	0.243	0.243	30	0.781	0.313	-0.110	0.341	0.532	0.898	1.292	1.581	1.882	2.658	4.025
8	0.250	0.250	30	0.773	0.318	-0.121	0.329	0.521	0.893	1.297	1.597	1.911	2.732	4.210
9	0.257	0.257	30	0.765	0.324	-0.131	0.318	0.510	0.887	1.302	1.612	1.940	2.809	4.403
10	0.264	0.264	30	0.757	0.329	-0.142	0.306	0.499	0.881	1.306	1.628	1.970	2.888	4.608
11	0.271	0.271	30	0.749	0.333	-0.152	0.295	0.488	0.875	1.311	1.643	2.000	2.968	4.820
12	0.279	0.279	30	0.741	0.338	-0.162	0.284	0.478	0.869	1.315	1.658	2.030	3.051	5.045
13	0.286	0.286	30	0.733	0.342	-0.173	0.274	0.467	0.862	1.318	1.673	2.060	3.134	5.277
14	0.293	0.293	30	0.725	0.346	-0.183	0.264	0.457	0.856	1.322	1.688	2.090	3.220	5.522
15	0.300	0.300	30	0.717	0.350	-0.193	0.254	0.447	0.849	1.325	1.702	2.119	3.307	5.775
Regional growth curve (harmonic mean)							0.325	0.518	0.891	1.294	1.592	1.903	2.711	4.137

Table 9.3: True at-site properties, distribution parameters and at-site quantile values for EV1 distribution (Note: L-Skewness plays no role in determining the parameters and quantiles. The mean of all populations is 1.0)

Site	L-CV	L-Skew.	n _i	EV1 Parameters		True at-site Quantiles							
				u	Alpha	0.010	0.100	0.500	0.800	0.9	0.95	0.99	0.999
1	0.200	0.200	30	0.834	0.289	0.393	0.593	0.939	1.266	1.483	1.690	2.161	2.826
2	0.207	0.207	30	0.828	0.299	0.371	0.578	0.937	1.276	1.500	1.715	2.202	2.892
3	0.214	0.214	30	0.822	0.309	0.349	0.564	0.935	1.285	1.517	1.740	2.244	2.957
4	0.221	0.221	30	0.816	0.320	0.328	0.549	0.933	1.295	1.534	1.764	2.285	3.022
5	0.229	0.229	30	0.810	0.330	0.306	0.535	0.931	1.304	1.552	1.789	2.327	3.087
6	0.236	0.236	30	0.804	0.340	0.284	0.520	0.928	1.314	1.569	1.814	2.368	3.153
7	0.243	0.243	30	0.798	0.350	0.263	0.506	0.926	1.323	1.586	1.838	2.410	3.218
8	0.250	0.250	30	0.792	0.361	0.241	0.491	0.924	1.333	1.603	1.863	2.451	3.283
9	0.257	0.257	30	0.786	0.371	0.219	0.476	0.922	1.342	1.621	1.888	2.492	3.348
10	0.264	0.264	30	0.780	0.381	0.198	0.462	0.920	1.352	1.638	1.912	2.534	3.414
11	0.271	0.271	30	0.774	0.392	0.176	0.447	0.917	1.361	1.655	1.937	2.575	3.479
12	0.279	0.279	30	0.768	0.402	0.154	0.433	0.915	1.371	1.672	1.962	2.617	3.544
13	0.286	0.286	30	0.762	0.412	0.133	0.418	0.913	1.380	1.690	1.986	2.658	3.609
14	0.293	0.293	30	0.756	0.423	0.111	0.404	0.911	1.390	1.707	2.011	2.700	3.674
15	0.300	0.300	30	0.750	0.433	0.089	0.389	0.909	1.399	1.724	2.036	2.741	3.740
Regional growth curve (harmonic mean)						0.199	0.483	0.924	1.332	1.600	1.857	2.438	3.259

9.4.2 Population Properties

Changes in properties such as mean, L-CV and L-Skewness have been examined for different combinations of trend scenarios, forms and true distribution types.

Mean:

Figure 9.2 illustrates the changes in regional average sample mean for different trend scenarios, trend forms and true distribution types. The random samples associated with the upper two graphs in this figure have been drawn from GEV distribution, while the EV1 distribution is the corresponding distribution for the lower two graphs. The graphs on the left correspond to TF-1, while those on the right are for TF-2. Each graph illustrates the changes in regional average mean with the increase in trend slopes under three trend scenarios (SUT, SVT and Trend on single site).

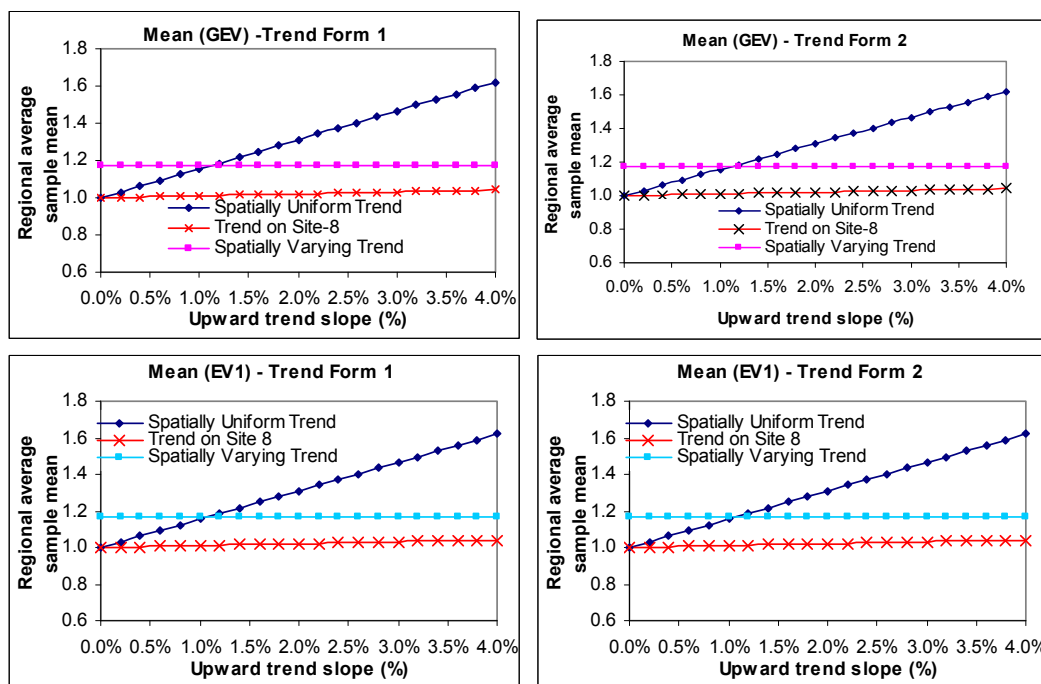


Figure 9.2: Changes in regional average mean with increase in upward trend slopes for all trend forms and true distribution types (left graphs are for TF-1 & right graphs are for TF-2). Samples were generated from GEV (upper graphs) and EV1 (lower graphs) distributions with sample properties presented in Tables 9.2 and 9.3 respectively.

It can be seen in the above graphs that the regional average mean increases with the increase in trend slopes in a similar fashion in both cases of trend forms and distribution types. It increases linearly with the increase in trend slope magnitudes for the SUT scenario. This increase in regional average mean can be expected as the linearly varying upward trend is applied in the true distribution mean (TF-1) and/or in the true data values (TF-2), thus giving increased values of at-site sample mean. For the upward trend slope of 1%, the true regional average sample mean

increases by 15.5% to 1.155 in both trend forms and distribution types. In the SVT case, it increases by 17% over the stationary condition in both cases of distribution and trend form scenarios. The effect of trend on a single site in the region is almost imperceptible on a regional scale.

L-CV:

Figure 9.3 illustrates the changes in regional average L-CV with the increases in trend slopes for different trend scenarios, trend forms and true distribution types. It can be seen in these graphs that the regional average L-CV changes in different fashions with the increase in trend slopes under the different trend forms and distribution types. In general, L-CV decreases in the case of SUT TF-1 and increases in the SUT TF-2 case. The patterns of changes are similar in the SUT trend scenario in both GEV and EV1 distributions, but are markedly different in the SVT trend scenario.

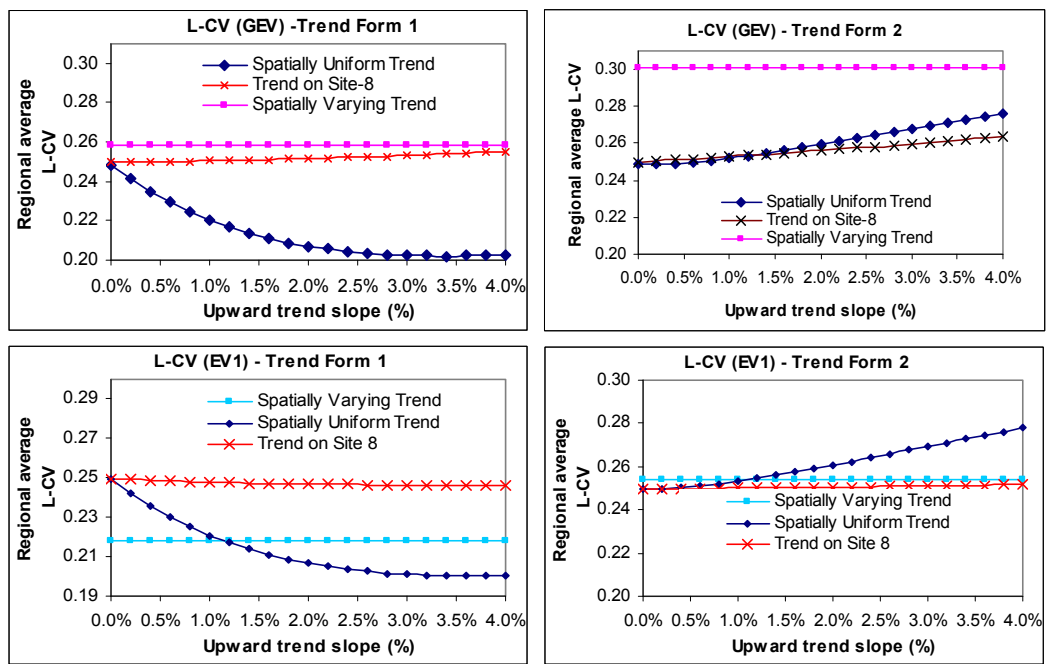


Figure 9.3: Changes in L-CV (regional average value) for various trend forms and types (left hand graphs – TF-1 & right hand graphs for TF-2). Samples were generated from GEV (upper graphs) and EV1 (lower graphs) distributions with population sample properties presented in Table 9.2 and 9.3 respectively.

GEV distribution:

In the GEV distribution case when trends were applied uniformly across all sites in the region in the trend form of TF-1, the regional average L-CV decreased in a curvilinear fashion up to an upward trend slope of 3%, thereafter it remained

unchanged for any further increases in trend slope, while in TF-2, L-CV increased almost linearly with the increase in trend slope. The change rate is markedly larger in the case of TF-1. In the SVT trend scenario, L-CV increases both in TF-1 and TF-2. L-CV is much higher in the TF-2 case than in the TF-1 case. Trend on a single site (site 8) in the region showed an imperceptible effect on the regional average L-CV in the case of TF-1, however, in the TF-2 case the change (increase) rate in L-CV is slightly more noticeable.

The above suggests that L-CV is very sensitive to TF-1 in the case of SUT trend scenario while sensitive to TF-2 in the SVT case. The former reduces the sample variability and the latter inflates it in GEV population. This can be explained by examining the changes in the at-site L-CV as presented in the L-moment ratio diagrams for all trend scenarios and forms for GEV distribution in **Figure 9.4**. It can be seen in these diagrams that in the SUT trend scenario, the sites with larger L-CVs are more sensitive to trend slopes, i.e. their L-CV values decrease more than that of the sites with lower L-CVs with the increase in trend slopes in the form of TF-1. In contrast, in the TF-2 case, the at-site L-CVs increase almost at an equal rate at all sites in the region. In the SVT case, the at-site L-CV increase for the sites with larger L-CV in both trend forms with significant increase in TF-2.

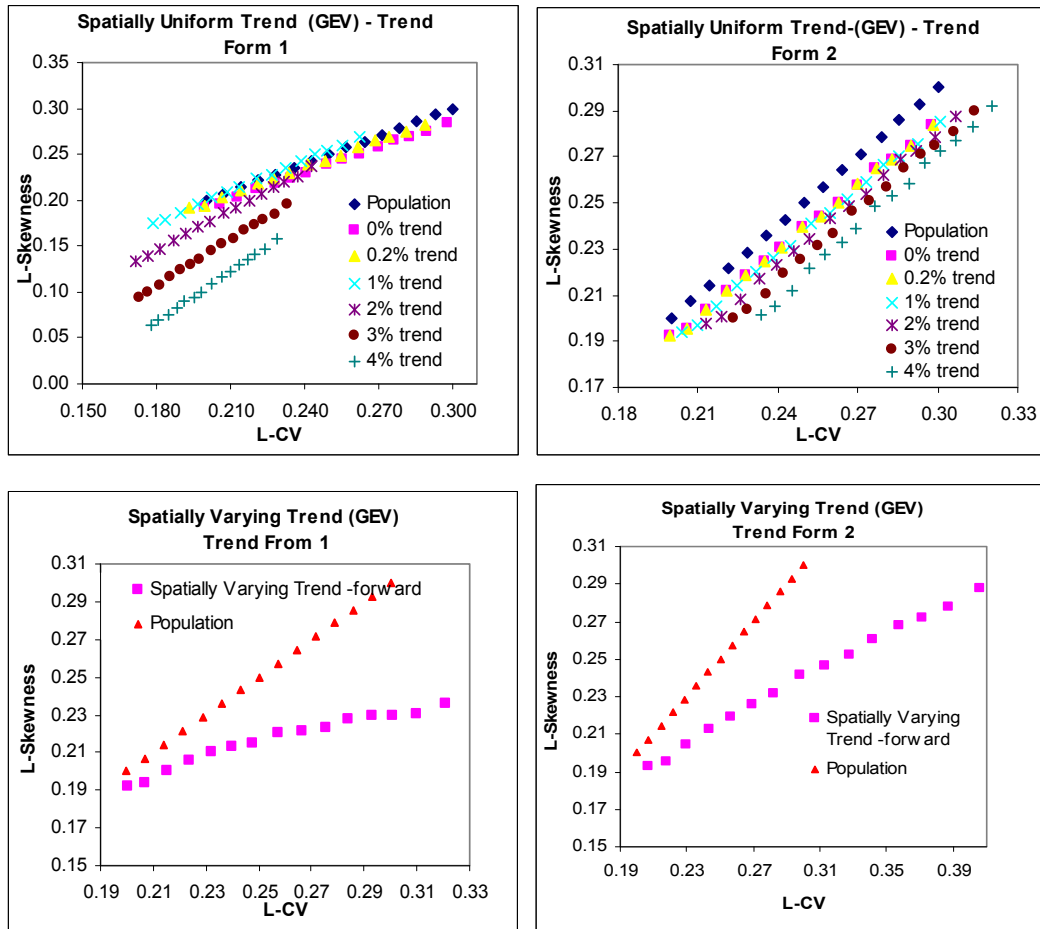


Figure 9.4: L-moment ratios for all sites in the region for different trend scenarios and forms (left hand graphs are for TF-1 and right hand graphs are for TF-2); Samples were generated from GEV distribution with population sample properties presented in Table 9.2.

EV1 distribution:

In the EV1 distribution case, the pattern of changes in L-CV is similar to that of GEV distribution for the SUT case in both trend forms. In the SVT case, changes in L-CV in both trend forms are markedly different than for the GEV distribution. The regional average L-CV decreases in TF-1, but increases very slightly in TF-2. Trend on a single site (site 8) in the region showed an imperceptible effect on regional average L-CV in both cases of trend forms.

The causes of the above mentioned changes in EV1 sample variability (L-CV) with the increase in trend slopes under different trend forms and scenarios can be explained by examining the changes in at-site L-CVs under these conditions. **Figure 9.5** presents the L-moment ratio diagrams for EV1 distribution for all trend scenarios and forms. It can be seen in these diagrams that in the SUT trend

scenario, the sites with larger L-CV are more sensitive to trend slopes, i.e. their L-CV values decrease more than that of the sites with lower L-CVs in the region in the case of TF-1. The opposite scenarios can be noticed in the case of TF-2. The changes are significantly larger in TF-1 than in TF-2. This explains why the regional average L-CV decreases in the case of TF-1, while it increases in the TF-2 case. In the SVT trend scenario, the variability shrinks markedly in TF-1, especially for the sites with larger L-CV while TF-2 introduces some slight increases in at-site sample variability. The regional average L-CV therefore decreases in TF-1 and increases slightly in TF-2.

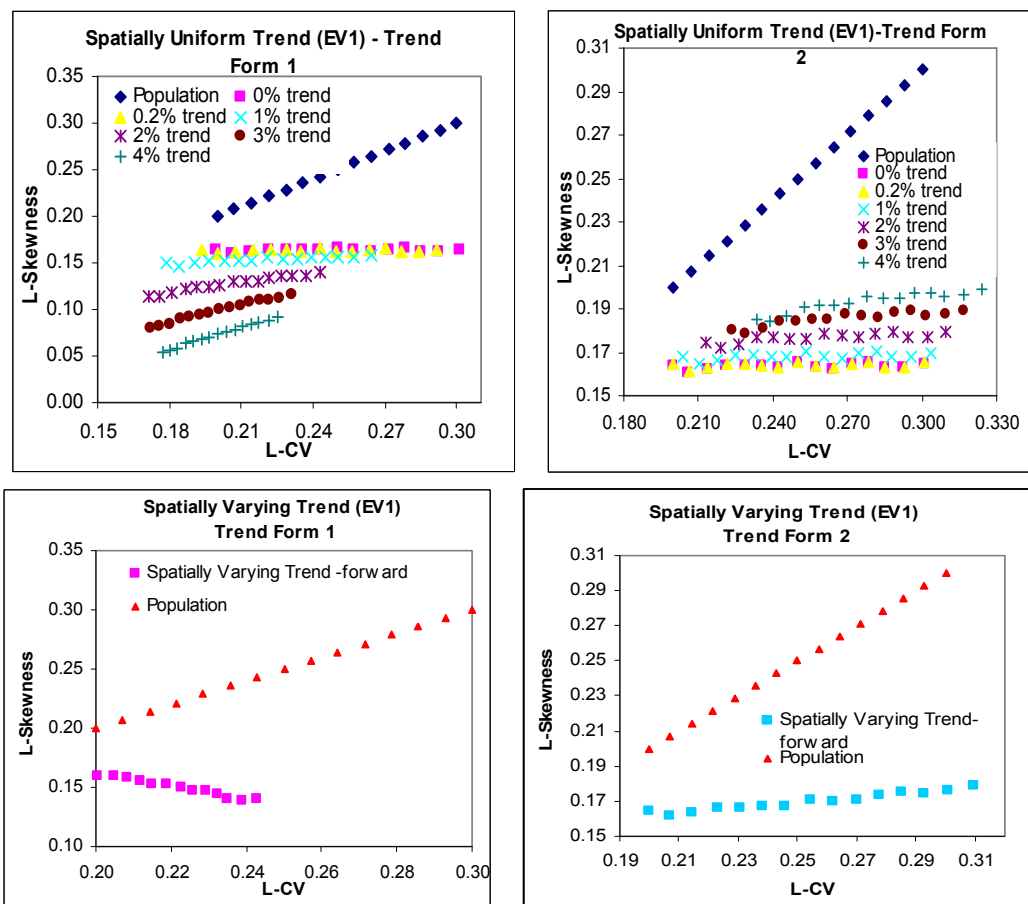


Figure 9.5: L-moment ratios for all sites in the region for different trend scenarios and forms (left graphs are for trend form-1 and right graphs are for TF-2); Samples were generated from EV1 distribution with population sample properties presented in Table 9.3.

L-Skewness:

Figure 9.6 illustrates the changes in regional average L-Skewness with the increase in trend slopes for various trend scenarios, forms and true distribution types. It can be seen in this figure that similar to L-CV, the regional average L-Skewness also changes in different fashions with the increase in trend slopes under the different trend forms and distribution types. In general, the regional average L-Skewness decreases in the case of TF-1 and increases in the TF-2 case with the increase in upward trend slopes, in both GEV and EV1 distributions.

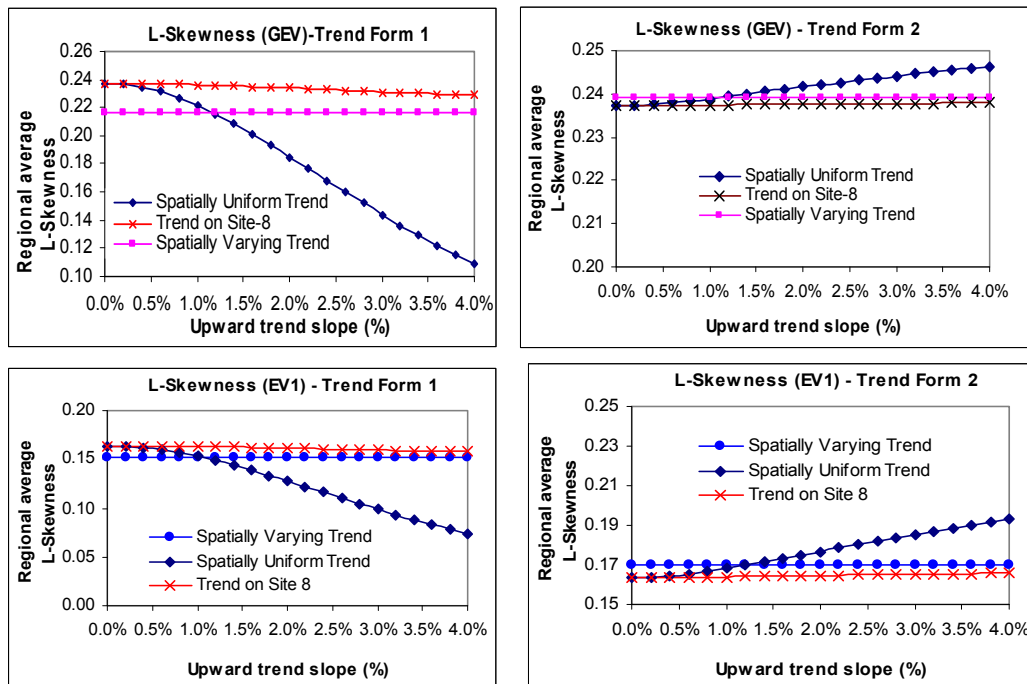


Figure 9.6: Changes in L-Skewness (regional average value) for various trend forms and types (left graphs are for TF-1 & right graphs are for TF-2). Samples were generated from GEV (upper graphs) and EV1 (lower graphs) distributions with population sample properties presented in Table 9.2 and 9.3 respectively.

GEV distribution:

In GEV distribution, L-Skewness is more sensitive to TF-1 than TF-2 in both SUT and SVT trend scenarios. In the SUT case, TF-1 reduces L-Skewness, while it increases in TF-2. The change rate in TF-1 is larger than in TF-2, in both cases changes occur linearly with the increase in trend slope. In the SVT case, L-Skewness reduces in both trend forms with a marked reduction in the TF-1. Trend on a single site in the region showed an imperceptible effect on the regional average L-Skewness in both trend forms.

The above changes can be explained by examining the changes in the at-site L-Skewness with the increase in trend slopes under both trend forms and trend types. **Figure 9.4** presents the L-moment ratio diagrams for GEV distribution for all sites with different trend slopes. It can be seen in these diagrams that in the SUT scenario, the rates of changes in the at-site L-Skewness with the increase in trend slope are almost equal at all sites in the region. TF-1 reduces at-site L-Skewness, while TF-2 inflates it. The change rate is higher in the TF-1 case than in TF-2. Due to these changes in at-site L-Skewness, regional average L-Skewness decreases in TF-1 and increases in TF-2. In the SVT case, the at-site L-Skewness decreases markedly for the sites with larger L-Skewness in TF-1, while in TF-2 at-site L-Skewness decreases slightly equally at all sites in the region.

EV1 distribution:

In the EV1 distribution case, the regional average L-Skewness decreases to 0.164 at the no-trend (0% trend slope) simulation scenario, which is approximately close to its fixed L-Skewness of 0.1699. In the SUT case, L-Skewness decreases further almost linearly with the increase in trend slopes under TF-1, while it increases in the case of TF-2. Similar to GEV distribution, the change rate is larger in TF-1. In the SVT case, changes in regional average L-Skewness are not significant in both cases of trend forms. In TF-1, L-Skewness decreases slightly over the no-trend condition, while in the TF-2 it remains almost unchanged. Trend on a single site in the region showed an imperceptible effect on regional average L-Skewness in both of trend forms.

The above changes in the regional average L-Skewness can be explained by examining the changes in the at-site L-Skewness as presented in the L-moment ratio diagrams for all trend scenarios and forms in **Figure 9.5**. Similar to GEV distribution, the rates of changes in the at-site L-Skewness are almost equal at all sites in the region in the case of SUT trend scenario. TF-1 reduces at-site L-Skewness while TF-2 inflates it. The change rate is higher in the TF-1 case than in the TF-2 case. In the SVT case, the at-site L-Skewness decreases and increases slightly at a higher rate for the sites with larger at-site L-Skewness in the TF-1 and TF-2 respectively.

From the above, it can be concluded that, in the SUT trend scenario, TF-1 deflates the regional average L-Skewness while TF-2 inflates in both GEV and EV1 distributions, and these deflation and inflation rates increase with the increase in trend slope magnitude. The change rates are slightly higher in the case of EV1 distribution in both trend forms. In the SVT case, L-Skewness reduces in both trend forms with a marked reduction in the TF-1 for GEV distribution.

Summary – Changes in population properties:

Table 9.4 compares the changes in regional average properties (mean, L-CV and L-Skewness) of GEV and EV1 distributions with the increase in trend slopes for both trend forms under the SUT scenario. **Figure 9.7** illustrates these changes. The left graphs are for GEV distribution, while the right ones are for EV1 distribution. As discussed earlier, the regional average ‘mean’ changes in a similar fashion in both cases of trend forms and distribution types. It increases linearly with the increase in trend slopes at the same rate in both distributions and trend forms. However, the patterns of changes in L-CV and L-Skewness are different in different trend forms. The regional average L-CV and L-Skewness decrease in the case of TF-1, while they increase in the TF-2 case with the increase in trend slopes. The changing rates are markedly larger in TF-1 than TF-2. These are true in both EV1 and GEV distributions.

From the above comparisons, it can be concluded that TF-1 reduces the variability and asymmetry while TF-2 inflates these properties. The subject properties are more sensitive to TF-1 than that to TF-2. These two scenarios are opposite; however both could occur in the real world due to the changing climate and/or due to any anthropogenic changes in the catchment characteristics.

Table 9.4: Comparison of the regional average mean, L-CV & L-Skewness for SUT trend scenario for both GEV and EV1 distributions for various trend slopes; (Samples were generated from GEV and EV1 distributions with population sample properties presented in Tables 9.2 and 9.3 respectively. The mean of all populations is 1.0).

Trend slope	GEV distribution						EV1 distribution					
	Mean		L-CV		L-Skewness		Mean		L-CV		L-Skewness	
	TF-1	TF-2	TF-1	TF-2	TF-1	TF-2	TF-1	TF-2	TF-1	TF-2	TF-1	TF-2
0.0%	1.000	1.000	0.248	0.248	0.237	0.237	1.000	1.000	0.250	0.250	0.164	0.164
0.2%	1.031	1.031	0.241	0.249	0.237	0.237	1.031	1.031	0.242	0.250	0.163	0.164
0.4%	1.062	1.062	0.235	0.249	0.235	0.238	1.062	1.062	0.236	0.250	0.162	0.165
0.6%	1.093	1.093	0.229	0.250	0.231	0.238	1.093	1.093	0.230	0.251	0.160	0.166
0.8%	1.124	1.124	0.224	0.251	0.227	0.238	1.124	1.124	0.225	0.252	0.157	0.167
1.0%	1.155	1.155	0.220	0.252	0.222	0.239	1.155	1.155	0.221	0.253	0.153	0.168
1.2%	1.186	1.186	0.217	0.253	0.215	0.239	1.186	1.186	0.217	0.255	0.149	0.170
1.4%	1.217	1.217	0.214	0.255	0.208	0.240	1.217	1.217	0.214	0.256	0.144	0.171
1.6%	1.248	1.248	0.211	0.256	0.201	0.240	1.248	1.248	0.211	0.258	0.139	0.173
1.8%	1.279	1.279	0.209	0.258	0.193	0.241	1.279	1.279	0.209	0.259	0.134	0.175
2.0%	1.310	1.310	0.207	0.259	0.185	0.242	1.310	1.310	0.207	0.261	0.128	0.177
2.2%	1.341	1.341	0.206	0.261	0.176	0.242	1.341	1.341	0.205	0.262	0.122	0.179
2.4%	1.372	1.372	0.204	0.263	0.168	0.243	1.372	1.372	0.204	0.264	0.116	0.180
2.6%	1.403	1.403	0.204	0.264	0.160	0.243	1.403	1.403	0.202	0.266	0.110	0.182
2.8%	1.434	1.434	0.203	0.266	0.152	0.244	1.434	1.434	0.202	0.268	0.104	0.184
3.0%	1.465	1.465	0.202	0.268	0.144	0.244	1.465	1.465	0.201	0.269	0.099	0.185
3.2%	1.496	1.496	0.202	0.270	0.136	0.245	1.496	1.496	0.201	0.271	0.093	0.187
3.4%	1.527	1.527	0.202	0.271	0.129	0.245	1.527	1.527	0.200	0.273	0.088	0.189
3.6%	1.558	1.558	0.202	0.273	0.122	0.245	1.558	1.558	0.200	0.274	0.083	0.190
3.8%	1.589	1.589	0.202	0.275	0.116	0.246	1.589	1.589	0.200	0.276	0.078	0.191
4.0%	1.620	1.620	0.203	0.276	0.109	0.246	1.620	1.620	0.201	0.278	0.073	0.193

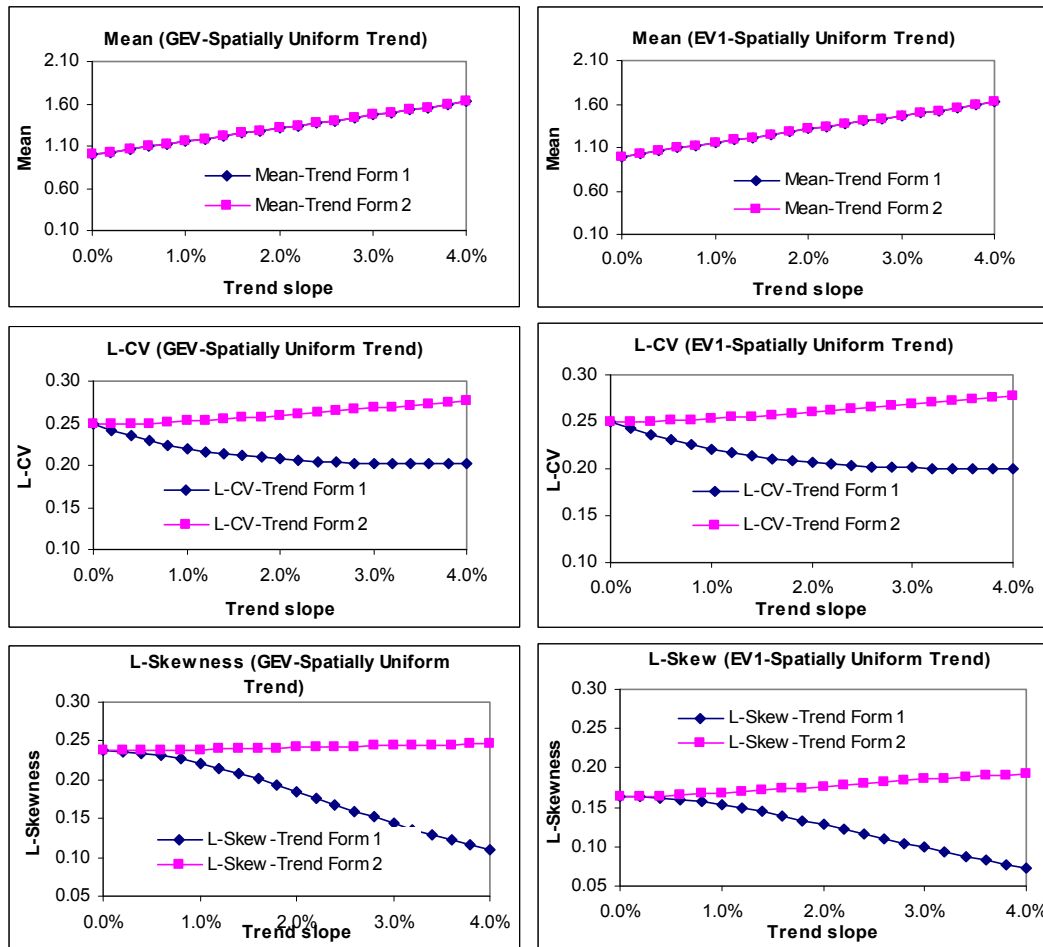


Figure 9.7: Comparison of the regional average mean, L-CV & L-Skewness for SUT scenario for various trend slopes; Samples were generated from GEV (left hand graphs) and EV1 (right hand graphs) distributions with population sample properties presented in Table 9.2 and 9.3 respectively.

9.4.3 Changes in Distribution Parameters

Changes in distribution parameters for both EV1 and GEV distributions with the increase in trend slopes have been investigated for various combinations of trend scenarios and forms.

GEV distribution:

Figure 9.8 illustrates the changes in the GEV location parameter for various trend scenarios and forms. The left hand graph illustrates the changes under TF-1 while the right hand graph is for TF- 2.

It can be seen from these graphs that in the SUT trend scenario, the regional average **GEV location parameter** increases with the increase in trend slopes in a similar fashion (linearly) in both trend forms. The rate of increase is slightly higher in TF-1 than in TF-2. In the SVT case, it increases slightly over the no-trend condition in both cases of trend forms. The presence of trend on a single site in the region shows insignificant effect on GEV location parameter in both cases of trend forms.

The increase in the GEV location parameter can be expected as it is proportional to the mean as can be seen in equation 9.40. Since the mean increases with the increases in trend slope magnitude as discussed earlier, the GEV location parameter also increases.

$$\hat{u} = l_1 - \frac{\hat{\alpha}}{\hat{k}} \left\{ 1 - \Gamma(1 + \hat{k}) \right\} \quad (9.40)$$

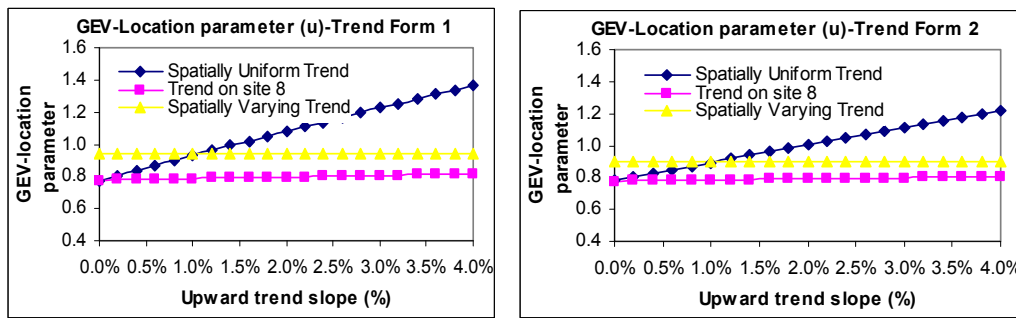


Figure 9.8: Changes in the GEV location parameter for various trend scenarios and forms (left hand graph is for TF-1 & right hand graph is for TF-2). Samples were generated from GEV distribution with population sample properties presented in Table 9.2.

The **scale parameter of GEV distribution** also increases with the increase in trend slopes in a similar fashion (linearly) in both cases of trend forms in the SUT trend scenario (**Figure 9.9**). In contrast to location parameter, the increase rate is slightly higher in TF-2 than in TF-1. This can be expected as TF-2 introduces more variability in the data series than TF-1. In the SVT case, the GEV scale parameter also increases in both trend forms in a similar fashion but with a slightly larger rate in TF-2. The presence of trend on a single site in the region shows insignificant effect on the regional average scale parameter in both cases of trend forms.

The causes of the above mentioned increases in GEV scale parameter can be explained from equation 9.41. It can be seen in this equation that the scale parameter is directly proportional to the data variability or L-scale. Since the L-scale

increases with the increases in trend slopes, the scale parameter therefore also increases.

$$\hat{\alpha} = \frac{\hat{l}_2 \hat{k}}{(1 - 2^{-\hat{k}}) \Gamma(1 + \hat{k})} \quad (9.41)$$

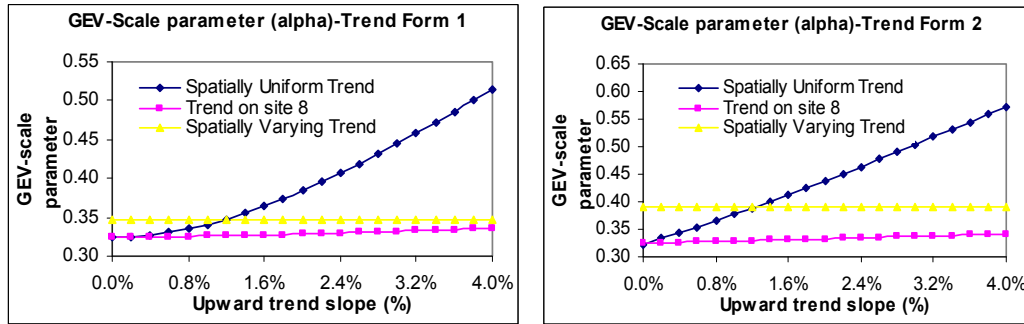


Figure 9.9: Changes in the GEV scale parameter (regional average value) for various trend scenarios and forms (left hand graph is for trend scheme 1 & right hand graph corresponds to trend scheme 2). Samples were generated from GEV distribution with population sample properties presented in Table 9.2.

The simulation results showed that in the SUT trend scenario, the regional average value of **GEV shape parameter** increases with the increase in trend slopes in the case of TF-1, while it decreases in TF-2 (**Figure 9.10**). The change rate is markedly larger in TF-1. This suggests that the shape parameter is very sensitive to TF-1. Similar to SUT, the GEV shape parameter also increases in TF-1 and decreases in TF-2 in the SVT trend scenario. The presence of trend on a single site in the region shows insignificant effect on the regional average GEV shape parameter in both cases of trend forms.

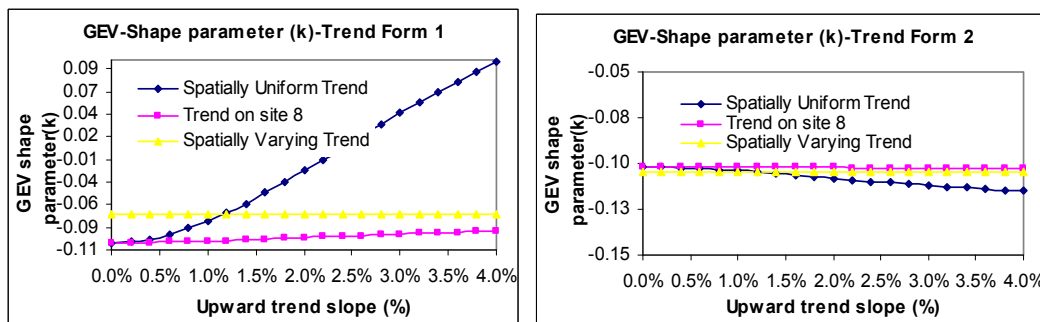


Figure 9.10: Changes in the GEV shape parameter (regional average value) for various trend scenarios and forms (left graph is for TF-1 & right graph corresponds to TF-2). Random samples were generated from GEV distribution with population sample properties presented in Table 9.2.

The above changes in the GEV shape parameter can be explained from the equation 9.42 (Hosking & Wallis, 1989). It can be seen in this equation that shape parameter, k , is inversely proportional to L-Skewness. **Figure 9.11** also illustrates this relationship in the case of TF-1 under SUT trend scenario. This suggests that any decrease in L-Skewness will increase the k -value and vice versa. Since the regional average L-Skewness decreases with the increases in trend slopes in the case of TF-1, the GEV shape parameter therefore increases; the opposite to this occurs in the TF-2 scenario.

$$\hat{k} \approx 7.8590c + 2.9554c^2 \quad (9.42)$$

$$\text{where } c = \frac{2}{3+t_3} - \frac{\ln 2}{\ln 3}$$

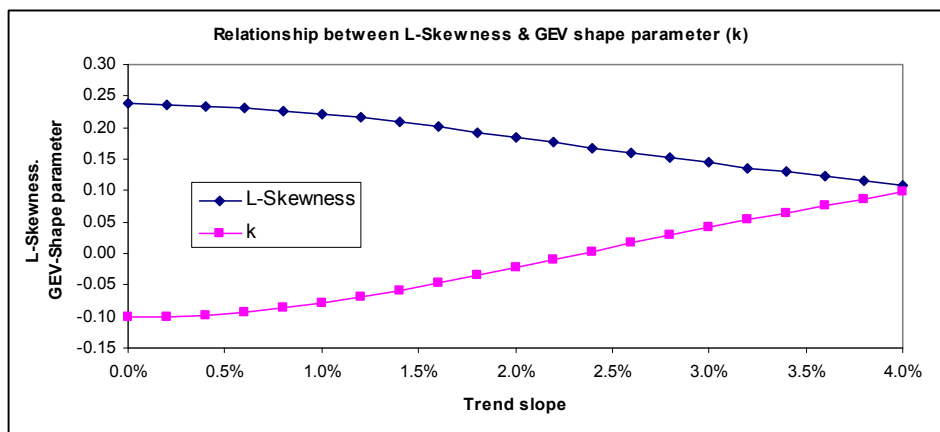


Figure 9.11: Relationship between L-Skewness & GEV shape parameter (k) for SUT trend scenario and TF-1

EV1 distribution:

In **EV1 distribution** the regional average **location parameter (u)** increases linearly with the increase in trend slopes (**Figure 9.12**) in both cases of trend forms under the SUT trend scenario. The increase rate is slightly higher in TF-1. In the SVT case, the EV1 location parameter also increases in both trend forms. The presence of trend on a single site in the region shows insignificant effect on the regional average EV1 location parameter in both cases of trend forms.

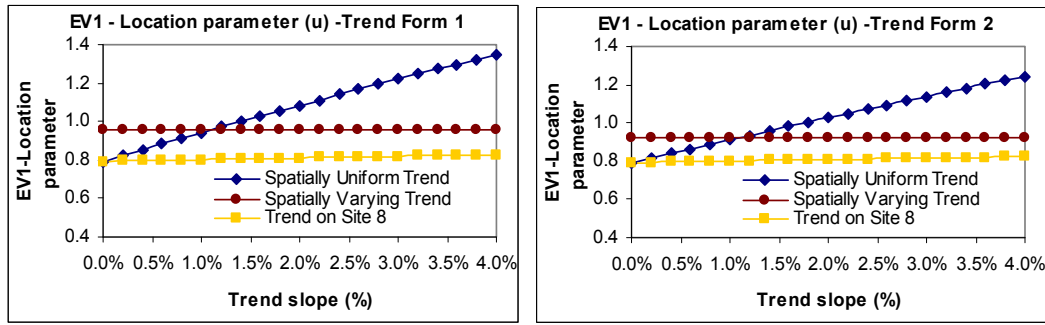


Figure 9.12: Changes in the EV1 location parameter (regional average value) for various trend scenarios and forms (the left graph is for TF-1 & the right graph correspond to TF-2). Samples were generated from EV1 distribution with population sample properties presented in Table 9.3.

The changes in EV1 location parameter can be easily explained from its relationship with mean. As can be seen in equation 9.43 that the EV1 location parameter is directly proportional to mean. Since the mean increases with the increase in trend slope, the EV1 location parameter also increases.

$$\hat{u} = l_1 - 0.5772 \hat{\alpha} \quad (9.43)$$

The simulation results also show that in the SUT trend scenario, the regional average value of the **EV1 scale parameter** increases with the increase in trend slopes (**Figure 9.13**) in both cases of trend forms. The change rate is markedly higher in TF-2. In the SVT trend scenario, TF-1 introduces almost imperceptible changes in regional average location parameter, while TF-2 introduces marked changes (increase).

Equation 9.44 shows that the scale parameter is directly proportional to L-scale. The regional average scale parameter of the EV1 distribution therefore increases with the increase in trend slopes, since the L-scale increases. The increase rate in scale parameter is slower in TF-1 than TF-2. This can be expected as the increase rate of L-scale and/or the variability is higher in the cases of TF-2.

$$\hat{\alpha} = \frac{l_2}{\ln 2} \quad (9.44)$$

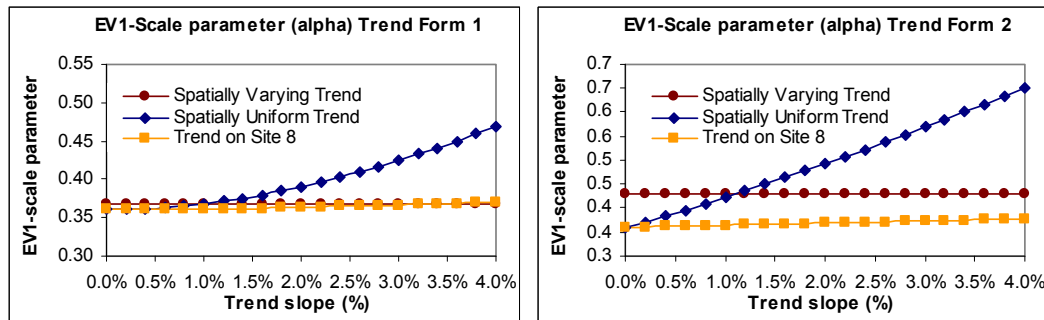


Figure 9.13: Changes in the EV1 scale parameter (regional average value) for various trend scenarios and forms (the left hand graph is for TF-1 & the right hand graph correspond to TF-2). Samples were generated from EV1 distribution with population sample properties presented in Table 9.3.

Summary – Changes in distribution parameters:

GEV distribution:

Table 9.5 compares the changes in the regional average values of the GEV distribution parameters (location, scale & shape) with the increase in trend slopes for both trend forms under the SUT trend scenario. **Figure 9.14** graphically illustrates these changes. It can be seen in this figure that the patterns of changes in the location and scale parameters are similar in both cases of the trend forms, i.e. they both increase with the increase in trend slopes in both trend forms. The increase rate in the location parameter is slightly higher in the case of TF-1; while the scale parameter increases in a slightly slower rate in this trend form scenario than TF-2. This is expected as TF-2 introduces more variability in the data series. The shape parameter increases with the increase in trend slopes in the case of TF-1, while it decreases in the TF-2 case. The changing rate is markedly higher in the case of TF-1. In general it can be concluded that TF-1 causes significant changes in the shape of upper tail of the distribution, while TF-2 causes significant spread in the over-all shape of the distribution. These are illustrated in **Figure 9.15**. In the case of TF-1 it can be expected, since it is shown earlier that in this trend form sample L-Skewness shrinks significantly than TF-2.

Table 9.5: Comparison of GEV distribution parameters (regional average values-location, scale and shape parameters) for uniform trend scenario; Samples were generated from GEV distribution with population sample properties presented in Table 9.2.

Trend slope	u		Alpha		k	
	Scheme 1	Scheme 2	Scheme 1	Scheme 2	Scheme 1	Scheme 2
0.0%	0.776	0.777	0.325	0.323	-0.102	-0.102
0.2%	0.807	0.801	0.325	0.333	-0.101	-0.102
0.4%	0.838	0.825	0.327	0.344	-0.098	-0.102
0.6%	0.868	0.848	0.331	0.354	-0.093	-0.103
0.8%	0.899	0.871	0.335	0.366	-0.087	-0.103
1.0%	0.929	0.894	0.341	0.377	-0.078	-0.104
1.2%	0.959	0.916	0.348	0.389	-0.069	-0.105
1.4%	0.989	0.939	0.356	0.401	-0.059	-0.106
1.6%	1.019	0.961	0.364	0.413	-0.047	-0.107
1.8%	1.049	0.983	0.374	0.426	-0.035	-0.107
2.0%	1.079	1.004	0.384	0.438	-0.022	-0.108
2.2%	1.108	1.026	0.395	0.451	-0.010	-0.109
2.4%	1.138	1.047	0.407	0.464	0.003	-0.110
2.6%	1.167	1.069	0.419	0.477	0.016	-0.111
2.8%	1.196	1.090	0.432	0.491	0.029	-0.111
3.0%	1.225	1.111	0.445	0.504	0.041	-0.112
3.2%	1.254	1.132	0.458	0.518	0.053	-0.113
3.4%	1.283	1.153	0.472	0.531	0.065	-0.113
3.6%	1.311	1.174	0.486	0.545	0.076	-0.114
3.8%	1.340	1.195	0.500	0.559	0.087	-0.114
4.0%	1.368	1.215	0.515	0.573	0.097	-0.115

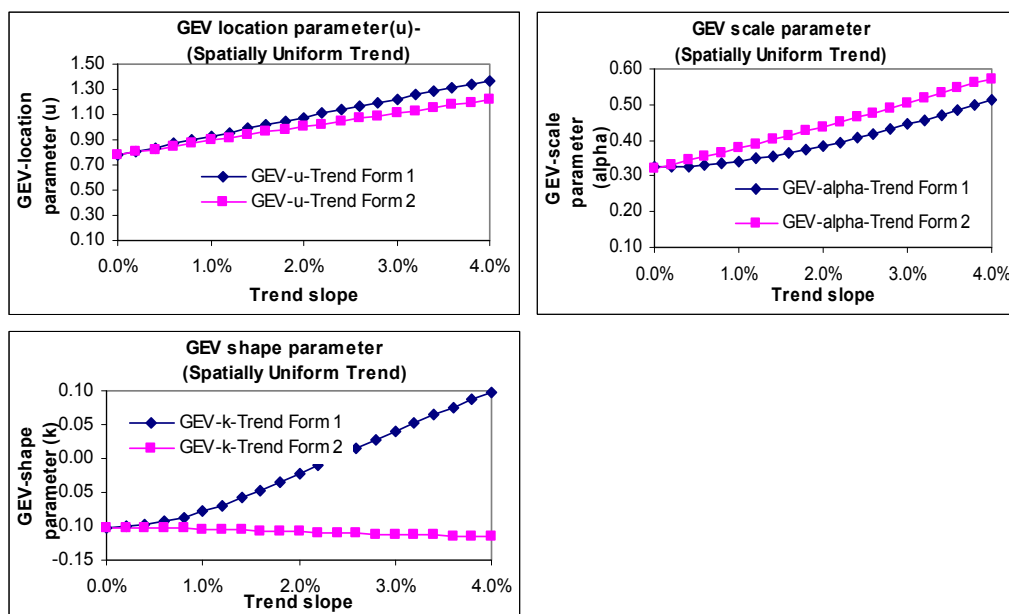


Figure 9.14: Comparison of GEV distribution parameters (regional average values-location, scale and shape parameters) for uniform trend scenario; Samples were generated from GEV distribution with population sample properties presented in Table 2.

The shape parameter k of GEV distribution governs the tail behaviour (tail shape and size) of the distribution and distinguishes between its constituent three types of distributions. For $k > 0$, the distribution corresponds to EV3 type distribution; for $k < 0$, the distribution has a thicker right-hand tail and corresponds to the EV2 distribution for maxima, while $k = 0$, the distribution takes the shape of EV1 distribution. It can be seen in **Figure 9.15** that under TF-1, the shape parameter approaches to almost zero at the trend slope of 2.4%, which suggests that GEV distribution takes the form of EV1 distribution at this SUT uniform trend slope. With further increases in trend slope, the shape parameter increase and thus takes the form of EV3 distribution (also see **Table 9.5**).

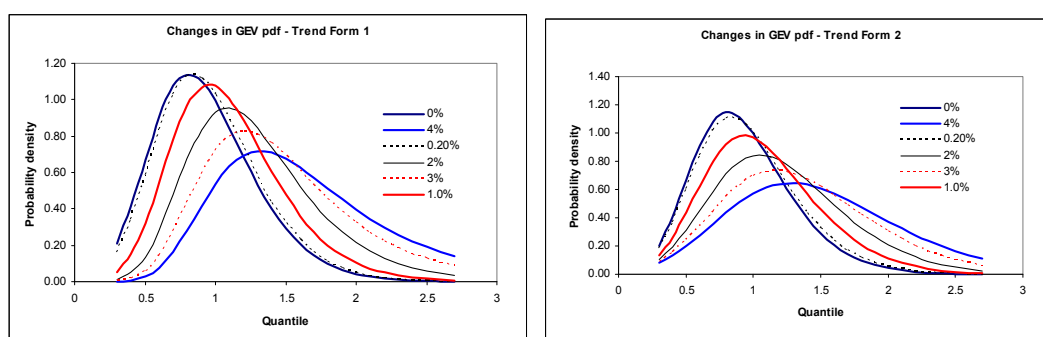


Figure 9.15: Changes in the shape of GEV pdf with the increase in uniform trend slope

EV1 Distribution:

Figure 9.16 illustrates the changes in the regional average values of the EV1 parameters (location and scale) with the increase in trend slope under the SUT trend scenario for both cases of trend forms (also see **Table 9.6**). It can be seen in this figure that the patterns of changes in the location and scale parameters are similar in both cases of trend forms, i.e. the both parameters increase with the increase in trend slopes in both cases. The increase rate in the location parameter is slightly higher in TF-1; while lesser in the scale parameter. The higher increase rate in the scale parameter is expected since TF-2 inflates sample variability.

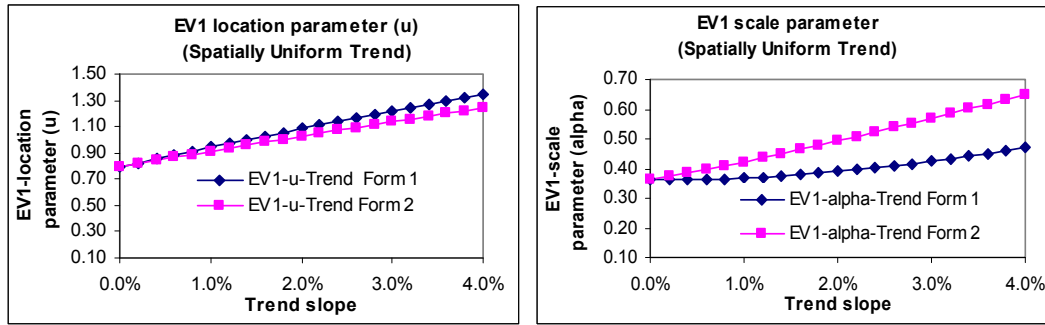


Figure 9.16: Comparison of EV1 distribution parameters (regional average values-location and scale parameters) for SUT scenario; Samples were generated from EV1 distribution with population sample properties presented in Table 9.3.

Table 9.6: Comparison of EV1 distribution parameters (regional average values-location and scale parameters) for uniform trend scenario; Samples were generated from EV1 distribution with population sample properties presented in Table 9.3.

Trend slope	u		Alpha	
	Scheme 1	Scheme 2	Scheme 1	Scheme 2
0.0%	0.792	0.792	0.360	0.360
0.2%	0.823	0.816	0.361	0.372
0.4%	0.853	0.840	0.362	0.384
0.6%	0.883	0.864	0.363	0.396
0.8%	0.913	0.888	0.365	0.409
1.0%	0.943	0.911	0.368	0.422
1.2%	0.972	0.934	0.371	0.436
1.4%	1.000	0.957	0.375	0.450
1.6%	1.029	0.980	0.380	0.464
1.8%	1.057	1.003	0.385	0.478
2.0%	1.085	1.026	0.390	0.493
2.2%	1.112	1.048	0.396	0.508
2.4%	1.139	1.070	0.403	0.523
2.6%	1.166	1.092	0.410	0.538
2.8%	1.193	1.114	0.417	0.554
3.0%	1.220	1.136	0.425	0.569
3.2%	1.246	1.158	0.433	0.585
3.4%	1.272	1.180	0.441	0.601
3.6%	1.298	1.202	0.450	0.617
3.8%	1.324	1.224	0.459	0.633
4.0%	1.349	1.245	0.469	0.649

9.4.4 Changes in Growth Curves

The changes in regional growth curves have been examined for the SUT trend scenario only, since it was found that the presence of varying nature of regional trend and also a random trend on a single site in the region have somewhat lesser effect on the population properties and also on the distribution parameters in the regional average scale.

Figure 9.17 presents the plots of growth curves for various combinations of true and fitted distributions under the specified two different trend forms. The left hand graphs are for TF-1, while the right hand graphs are for TF-2. Vertically these graphs are presented from, top to bottom, for the true and fitted distribution combinations of GEV-GEV, GEV-EV1, EV1-EV1 and EV1-GEV respectively. In each graphs, growth curves are plotted for a range of trend slopes, such as 0.2%, 0.4%, 0.8%, 1%, 1.2%, 1.4%, 1.6%, 1.8%, 2%, 3% and 4%. These are shown in different colours. In addition to these, two other growth curves corresponding to no-trend condition (0% slope, thin-dashed line) and the true regional growth curve (thick black line) which has been estimated as the harmonic mean of the true at-site growth curves are also included in each graph.

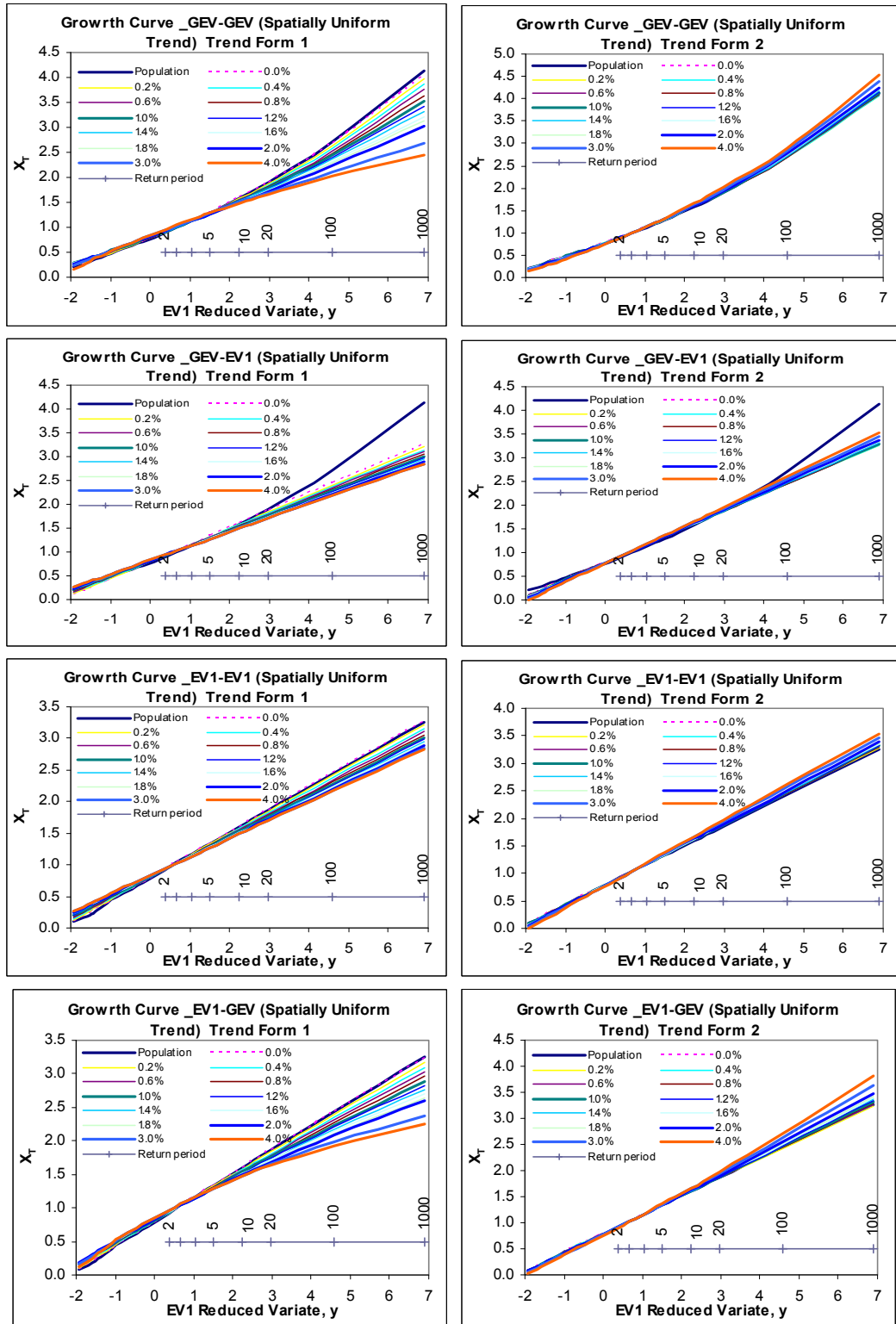


Figure 9.17: Comparison of growth curves for SUT scenario and for different combinations of true and fitted distributions (for example GEV-EV1 mean true distribution GEV and fitted distribution EV1)

It can be seen in these graphs that the growth curves in each combination of the true and fitted distributions in TF-1 get flatter and flatter as the trend slope magnitude increases. In contrast, in TF-2 growth curves in all distribution combinations get steeper with the increase in trend slopes except in the GEV-EV1 case. In the GEV-EV1 case growth curves get flatter with the increase in at-site trend slopes similar to TF-1. This suggests that, in TF-2 scenario, the growth factor associated with a particular return period, increases with the increase in at-site trend slope in the distribution combinations of GEV-GEV, EV1-EV1 and EV1-GEV, while it decreases in the GEV-EV1 case.

Tables 9.7 and **9.8** present the estimated relative differences in growth factors (percentage increase/decrease over the stationary condition, **Equation 9.35**) associated with the return periods of 10, 100 1000 years for various trend slopes and true and fitted distribution combinations for the trend forms of TF-1 and TF-2 respectively. These results are graphically presented in **Figure 9.18**.

Table 9.7: Relative differences in growth factors for various combinations for true and fitted distributions under TF-1 scenario.

Trend slope	F=0.90				F=0.99				F=0.999			
	GEV-GEV	GEV-EV1	EV1-EV1	EV1-GEV	GEV-GEV	GEV-EV1	EV1-EV1	EV1-GEV	GEV-GEV	GEV-EV1	EV1-EV1	EV1-GEV
0.0%	0.1%	0.5%	0.2%	0.1%	-1.1%	-9.9%	0.5%	-0.2%	-1.9%	-21.0%	0.7%	-0.6%
0.2%	-1.0%	-0.6%	-0.9%	-1.0%	-3.0%	-11.5%	-1.3%	-2.0%	-4.2%	-22.6%	-1.4%	-2.8%
0.4%	-1.9%	-1.6%	-1.9%	-1.9%	-4.8%	-12.8%	-2.8%	-3.7%	-6.7%	-24.0%	-3.2%	-4.9%
0.6%	-2.7%	-2.4%	-2.8%	-2.8%	-6.6%	-14.0%	-4.2%	-5.3%	-9.3%	-25.2%	-4.8%	-7.0%
0.8%	-3.4%	-3.2%	-3.5%	-3.6%	-8.3%	-15.1%	-5.4%	-6.8%	-11.9%	-26.3%	-6.2%	-9.1%
1.0%	-4.0%	-3.8%	-4.2%	-4.2%	-10.0%	-15.9%	-6.4%	-8.3%	-14.6%	-27.2%	-7.4%	-11.2%
1.2%	-4.5%	-4.3%	-4.8%	-4.8%	-11.5%	-16.7%	-7.3%	-9.6%	-17.2%	-28.0%	-8.5%	-13.2%
1.4%	-4.9%	-4.8%	-5.3%	-5.3%	-13.1%	-17.4%	-8.1%	-10.9%	-19.7%	-28.7%	-9.4%	-15.1%
1.6%	-5.3%	-5.2%	-5.7%	-5.8%	-14.5%	-17.9%	-8.8%	-12.1%	-22.1%	-29.2%	-10.2%	-17.0%
1.8%	-5.6%	-5.5%	-6.0%	-6.1%	-15.8%	-18.4%	-9.3%	-13.2%	-24.4%	-29.7%	-10.9%	-18.7%
2.0%	-5.8%	-5.8%	-6.3%	-6.4%	-17.1%	-18.8%	-9.8%	-14.3%	-26.6%	-30.1%	-11.4%	-20.4%
2.2%	-6.0%	-6.0%	-6.6%	-6.7%	-18.3%	-19.1%	-10.2%	-15.2%	-28.7%	-30.4%	-11.9%	-21.9%
2.4%	-6.2%	-6.2%	-6.8%	-7.0%	-19.4%	-19.3%	-10.5%	-16.1%	-30.5%	-30.7%	-12.3%	-23.3%
2.6%	-6.4%	-6.3%	-7.0%	-7.1%	-20.4%	-19.5%	-10.8%	-16.9%	-32.3%	-30.9%	-12.6%	-24.7%
2.8%	-6.5%	-6.4%	-7.1%	-7.3%	-21.3%	-19.7%	-11.0%	-17.7%	-33.8%	-31.0%	-12.8%	-25.9%
3.0%	-6.5%	-6.5%	-7.2%	-7.4%	-22.1%	-19.8%	-11.1%	-18.3%	-35.3%	-31.1%	-13.0%	-27.0%
3.2%	-6.6%	-6.5%	-7.2%	-7.5%	-22.9%	-19.8%	-11.2%	-18.9%	-36.6%	-31.2%	-13.1%	-28.0%
3.4%	-6.6%	-6.5%	-7.3%	-7.6%	-23.6%	-19.8%	-11.3%	-19.5%	-37.8%	-31.2%	-13.2%	-28.9%
3.6%	-6.7%	-6.5%	-7.3%	-7.7%	-24.2%	-19.8%	-11.3%	-20.0%	-38.8%	-31.2%	-13.2%	-29.7%
3.8%	-6.7%	-6.5%	-7.3%	-7.7%	-24.8%	-19.8%	-11.3%	-20.4%	-39.8%	-31.2%	-13.2%	-30.5%
4.0%	-6.7%	-6.5%	-7.2%	-7.7%	-25.3%	-19.7%	-11.2%	-20.8%	-40.7%	-31.1%	-13.1%	-31.1%

Table 9.8: Relative differences in growth factors for various combinations for true and fitted distributions under TF-2 scenario.

Trend slope	F=0.90				F=0.99				F=0.999			
	GEV-GEV	GEV-EV1	EV1-EV1	EV1-GEV	GEV-GEV	GEV-EV1	EV1-EV1	EV1-GEV	GEV-GEV	GEV-EV1	EV1-EV1	EV1-GEV
0.0%	0.1%	0.5%	0.2%	0.1%	-1.1%	-9.9%	0.5%	-0.2%	-1.9%	-21.0%	0.7%	-0.6%
0.2%	0.2%	0.5%	0.2%	0.2%	-1.0%	-9.9%	0.5%	-0.2%	-1.8%	-20.9%	0.7%	-0.5%
0.4%	0.2%	0.6%	0.3%	0.3%	-0.9%	-9.8%	0.6%	0.0%	-1.6%	-20.8%	0.9%	-0.2%
0.6%	0.3%	0.7%	0.4%	0.4%	-0.6%	-9.6%	0.8%	0.3%	-1.3%	-20.7%	1.1%	0.3%
0.8%	0.5%	0.8%	0.5%	0.5%	-0.3%	-9.4%	1.1%	0.7%	-0.8%	-20.5%	1.4%	0.9%
1.0%	0.6%	1.0%	0.7%	0.7%	0.0%	-9.2%	1.3%	1.2%	-0.3%	-20.2%	1.7%	1.7%
1.2%	0.8%	1.2%	0.9%	0.9%	0.4%	-8.9%	1.6%	1.7%	0.2%	-19.9%	2.0%	2.5%
1.4%	1.0%	1.4%	1.1%	1.1%	0.8%	-8.6%	2.0%	2.3%	0.8%	-19.6%	2.4%	3.4%
1.6%	1.3%	1.7%	1.3%	1.3%	1.3%	-8.3%	2.3%	2.9%	1.4%	-19.3%	2.9%	4.4%
1.8%	1.5%	1.9%	1.6%	1.5%	1.8%	-7.9%	2.7%	3.5%	2.1%	-18.9%	3.3%	5.4%
2.0%	1.7%	2.1%	1.8%	1.8%	2.2%	-7.6%	3.1%	4.2%	2.8%	-18.6%	3.7%	6.4%
2.2%	2.0%	2.4%	2.1%	2.0%	2.7%	-7.2%	3.5%	4.8%	3.5%	-18.2%	4.2%	7.5%
2.4%	2.2%	2.6%	2.3%	2.3%	3.2%	-6.9%	3.9%	5.5%	4.2%	-17.8%	4.7%	8.6%
2.6%	2.5%	2.9%	2.6%	2.5%	3.7%	-6.5%	4.3%	6.2%	4.9%	-17.5%	5.2%	9.6%
2.8%	2.7%	3.2%	2.9%	2.8%	4.3%	-6.1%	4.7%	6.9%	5.6%	-17.1%	5.7%	10.7%
3.0%	3.0%	3.4%	3.1%	3.1%	4.8%	-5.8%	5.1%	7.5%	6.2%	-16.7%	6.1%	11.8%
3.2%	3.2%	3.7%	3.4%	3.3%	5.3%	-5.4%	5.5%	8.2%	6.9%	-16.3%	6.6%	12.9%
3.4%	3.5%	3.9%	3.6%	3.6%	5.8%	-5.0%	5.9%	8.9%	7.6%	-15.9%	7.1%	14.0%
3.6%	3.7%	4.2%	3.9%	3.8%	6.3%	-4.7%	6.4%	9.5%	8.3%	-15.6%	7.6%	15.0%
3.8%	4.0%	4.5%	4.2%	4.1%	6.7%	-4.3%	6.8%	10.2%	8.9%	-15.2%	8.1%	16.1%
4.0%	4.2%	4.7%	4.4%	4.3%	7.2%	-3.9%	7.2%	10.8%	9.6%	-14.8%	8.5%	17.1%

The above results show that the differences between the zero trend growth factors and fitted growth factors are larger for the larger return periods in all cases of trend forms and distribution combinations. The effect of SUT trends on growth curve is larger in TF-1 than TF-2, i.e. the change rates of relative differences in growth curves with the increase in trend slopes are higher in TF-1 than TF-2. In the TF-1 case, growth factors decrease while in TF-2 they increase. This occurs because in TF-1, growth curves get flatter with the increase in trend slope while the opposite occurs in TF-2.

For example, in the TF-1 case, the relative differences for the 10, 100 and 1000 years return periods EV1-EV1 growth factors are -4.2%, -6.4%, -7.4% (decreases) respectively for a trend slope of 1%., while in TF-2 the corresponding differences are 0.7%, 1.3% and 1.7% (increases) and respectively (Tables 9.7 and 9.8).

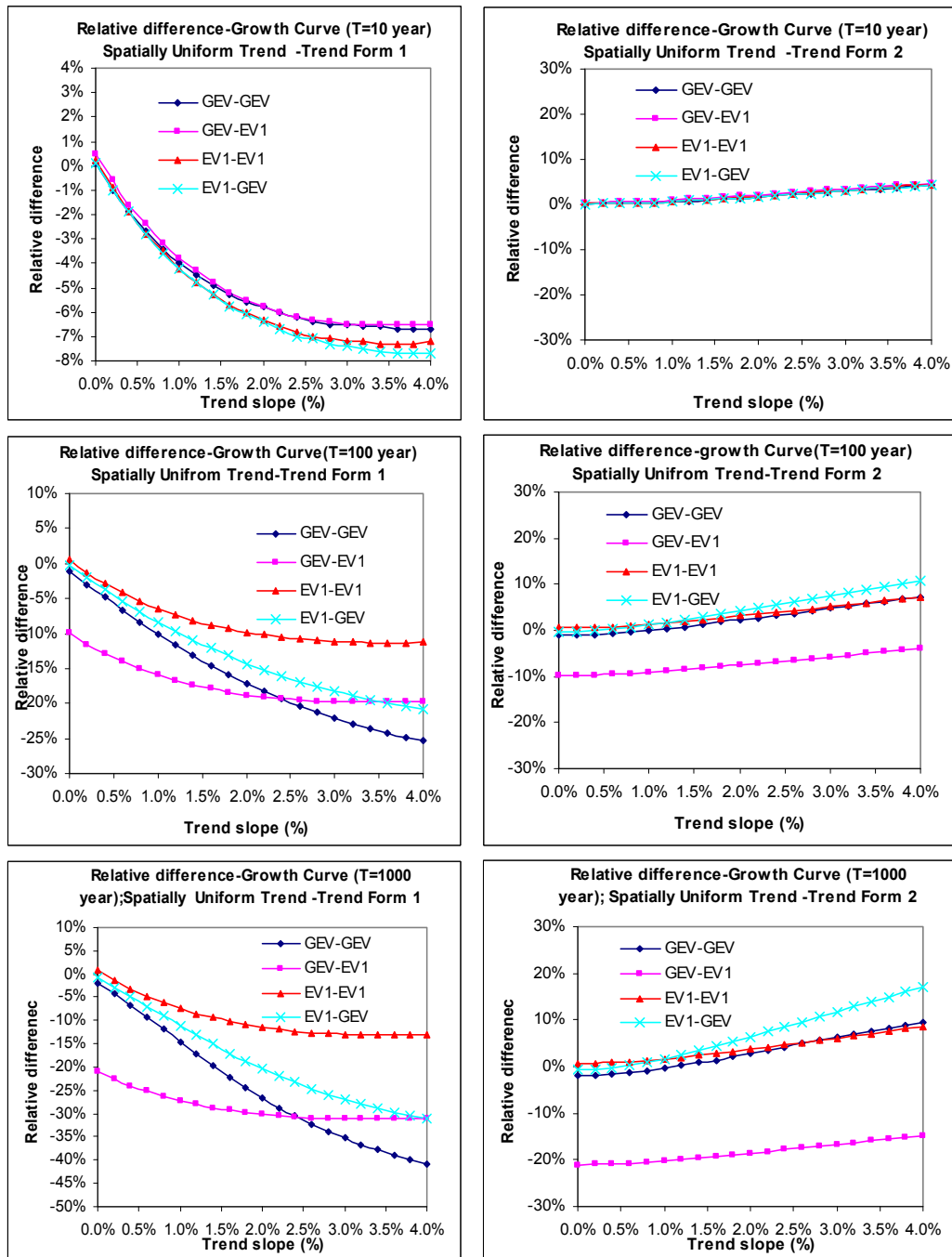


Figure 9.18: Comparison of relative differences in growth curves for different combinations of true and fitted distributions (left graphs correspond to TF-1 & right graphs are for TF-2).

The highest differences can be noticed in the GEV-GEV distribution combination followed by the EV1-GEV case in TF-1, while in TF-2, the highest differences can be noticed in the EV1-GEV distribution combination followed by GEV-EV1. This suggests that the upper tail of three-parameter distribution is more sensitive to trend

slope and thus introduces more bias or differences. It could be due to the fact that the true sample L-Skewness of GEV distribution decreases with the increase in trend slopes. This results a sample with low skewness, which might not fit the GEV distribution well and thus gives higher relative differences. It is also true in the case of no trend condition that bias/relative differences in the growth curve estimate increases when a thin tail distribution is fitted to a thick tailed distribution and vice versa In other words, bias in growth curve estimate increases when a two parameter fixed skew model is used to estimate growth curve when data are drawn from a population with high skewness model (Cunnane, 1989). This can be seen in **Figure 9.18** in the distribution combination of GEV-EV1. The performance of the two-parameter EV1 distribution in fitting a GEV sample with a high trend is better than its true distribution.

Figure 9.18 shows that at approximately 2.4% trend slope the growth factor estimates from both GEV-GEV and EV1-EV1 cases are equal meaning that the GEV distribution has $k=0$ at that this trend slope.

The above changes in growth curves can be explained with the help of corresponding growth curve equations and the changes in their parameters with the increases in trend slopes as discussed in the previous sections. The growth curve equations for the GEV and EV1 distributions are presented in Section 9.3.5.

The GEV growth curve and its parameters:

$$x(F) = 1 + \frac{\beta}{k} \{ \Gamma(1+k) - (-\ln(F))^k \}$$

where, $\beta = \frac{t_2 k}{(1 - 2^{-k}) \Gamma(1+k)}$ &

$$k \approx 7.8590c + 2.9554c^2, \quad \text{where } c = \frac{2}{3 + \tau_3} - \frac{\ln 2}{\ln 3}$$

It can be seen in the above growth curve equation that, the growth factor, $x(F)$ corresponding to any non-exceedance probability of F is directly proportional to parameter β , and inversely proportional to the shape parameter k . Again, the β parameter is directly proportional to L-CV, and the shape parameter is inversely proportional to L-Skewness. As discussed in Section 9.4.2, the regional average L-CV and L-Skewness decrease with the increase in trend slope in the case of TF-1.

This suggests that the β parameter will be decreased and the k parameter will be increased with the increase in trend slopes. Consequently, the slope factor β/k will be decreased which will result in a flatter growth curve and reduced growth factor. In the case of TF-2, the L-CV and L-Skewness values increase with the increase in trend slope, thus the β parameter increases and k value decreases, which consequently give a higher value of growth factor for a particular non-exceedance probability.

Similar logic applies to the EV1 distribution case as can be seen from its growth curve equation:

$$x(F) = 1 + \beta \{-\ln(-\ln F) - \gamma\}$$

where parameter, $\beta = \frac{t_2}{\ln 2}$.

The above EV1 growth curve equation suggests that the slope of the growth curve will get flatter in the case of TF-1, because the regional average L-CV value decreases with the increase in trend slopes, which consequently reduces the scale parameter and thus decreases the slope of growth curve. In TF-2, the opposite scenario occurs, i.e β increases and hence the growth curve gets steeper with the increase in trend slopes.

The above results suggest that the SUT type trends in a pooling group will have some effects on the regional growth curves. The magnitude of this effect depends on the forms of the trend in the at-site data series in the region. This effect would result from the changes in the true sample and distribution parameters. Irrespective of the trend forms, the estimated effects of the SUT type trends in a pooling group on the true GEV 100 year growth factor could range for a trend slope of 1% from 0% to -15.9% (**Tables 9.7 and 9.8**).

9.4.5 Changes in At-site Quantiles

Similar to growth curve, the changes in the at-site quantile estimates have also been investigated for the SUT trend scenario only. The at-site quantiles for the sites 1, 8 and 15 have been examined.

Figures 9.19, 9.20 and 9.21 illustrate the quantile functions for the sites 1, 8 and 15 respectively. Quantile functions for various combinations of true and fitted distributions (GEV-GEV, GEV-EV1, EV1-EV1 and EV1-GEV) and trend forms (TF-1 and TF-2) are included in these figures. The left graphs in these figures are for TF-1, while the right graphs correspond to TF-2. In each graph, quantile functions for a range of trend slopes, such as 0.2%, 0.4%, 0.8%, 1%, 1.2%, 1.4%, 1.6%, 1.8%, 2%, 3% and 4% are plotted. These are shown in different colours. In addition to these, quantile functions associated with the true and no-trend condition (i.e. trend slope of 0%) have also been included in each of the graphs, which are shown in a thick black solid line and in a thin-dashed line respectively.

It can be seen in these graphs that the at-site quantiles in each combination of the true and fitted distributions increase with the increase in at-site trend slope magnitudes in both trend forms with some exception in the GEV-GEV distribution combination in TF-1. In this case, for any trend slope greater than **1.2%**, (see **Figure 9.22**) the estimated quantiles get smaller than the no-trend condition estimates, especially for $T \geq 500$ years. The increase rate is larger for the larger return periods in both trend forms. Given the moderately heterogeneous nature of the region, the regional quantile estimate for Site 1 (lowest L-CV & L-Skewness) is higher than its true estimate, while for Site 15 (highest L-CV and L-Skewness) it is smaller than the true estimates.

Tables 9.9 and 9.10 present the estimated relative differences in quantile estimates for (percentage increase/decrease over the stationary condition, Equation 9.35) associated with the return periods of 10, 100 1000 years for various trend slopes and true and fitted distribution combinations for the trend forms of TF-1 and TF-2 respectively. These results are graphically presented in **Figure 9.23**.

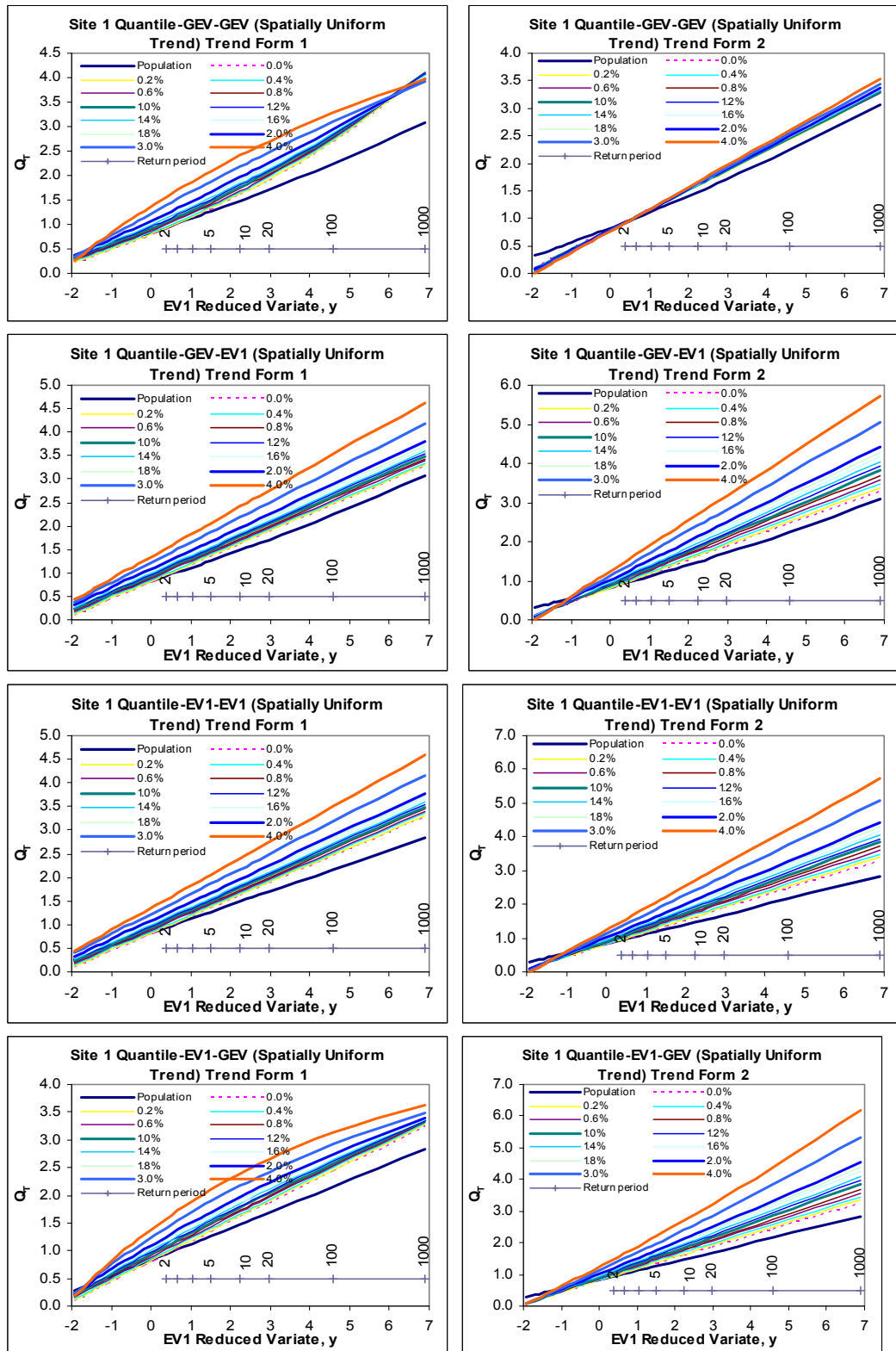


Figure 9.19: Comparison of Site 1 quantiles for different combinations of trend forms and true and fitted distributions (left graphs are for TF-1 & the right graphs correspond to TF-2).

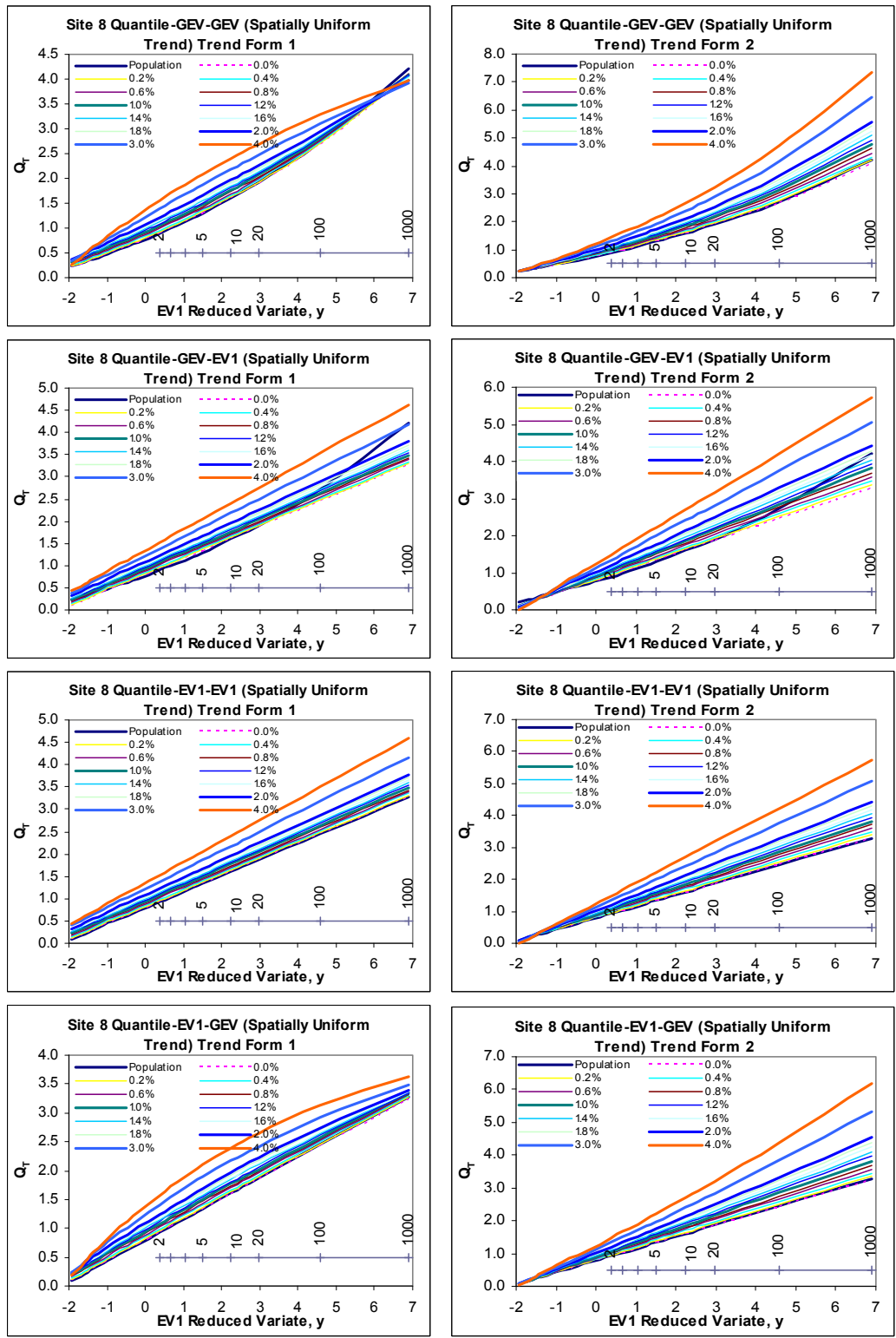


Figure 9.20: Comparison of Site 8 quantiles for different combinations of trend forms and true and fitted distributions (left graphs are for TF-1 & the right graphs correspond to TF-2).

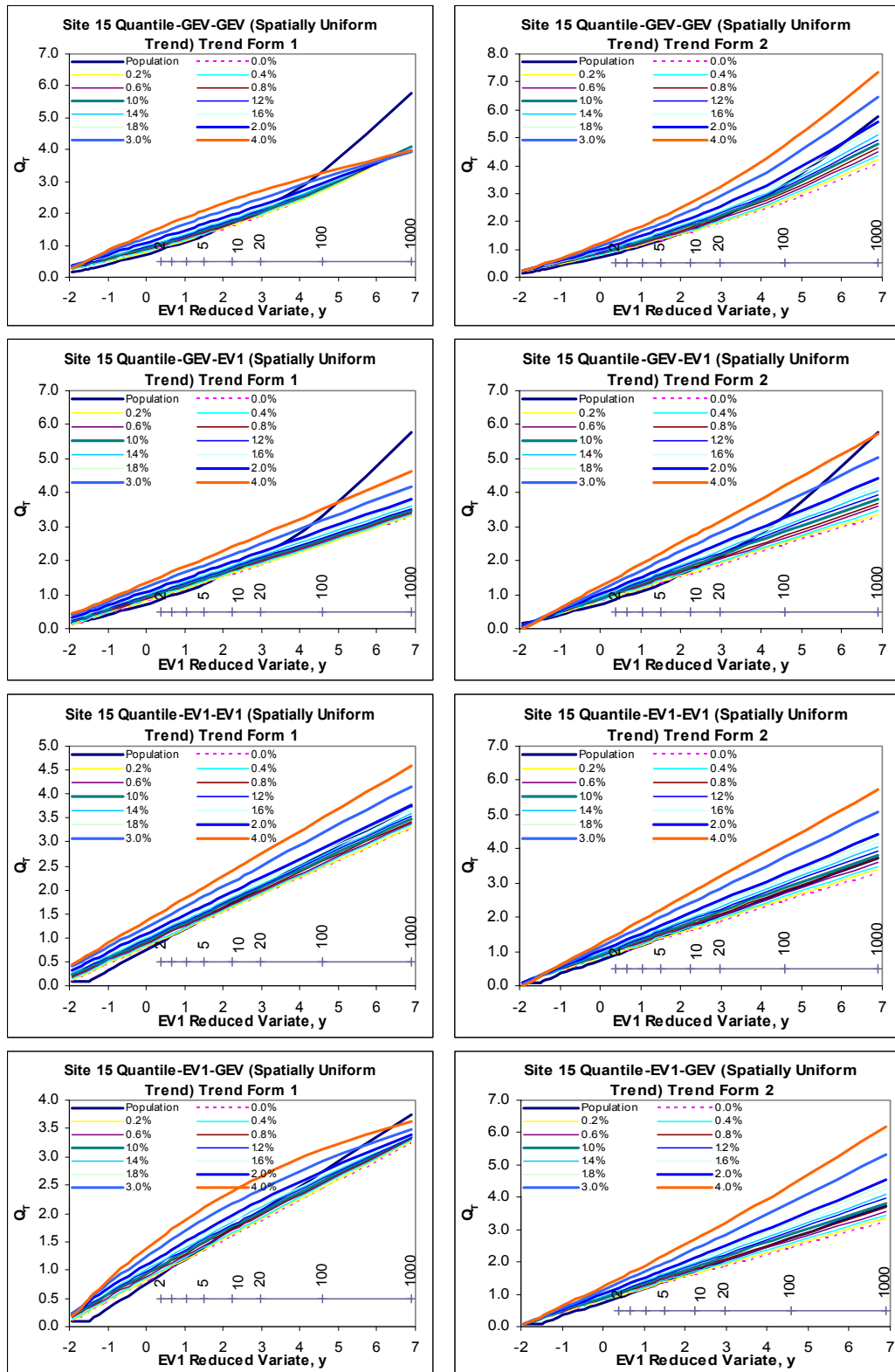


Figure 9.21: Comparison of Site 15 quantiles for different combinations of trend forms and true and fitted distributions (left graphs are for TF-1 & the right graphs correspond to TF-2).

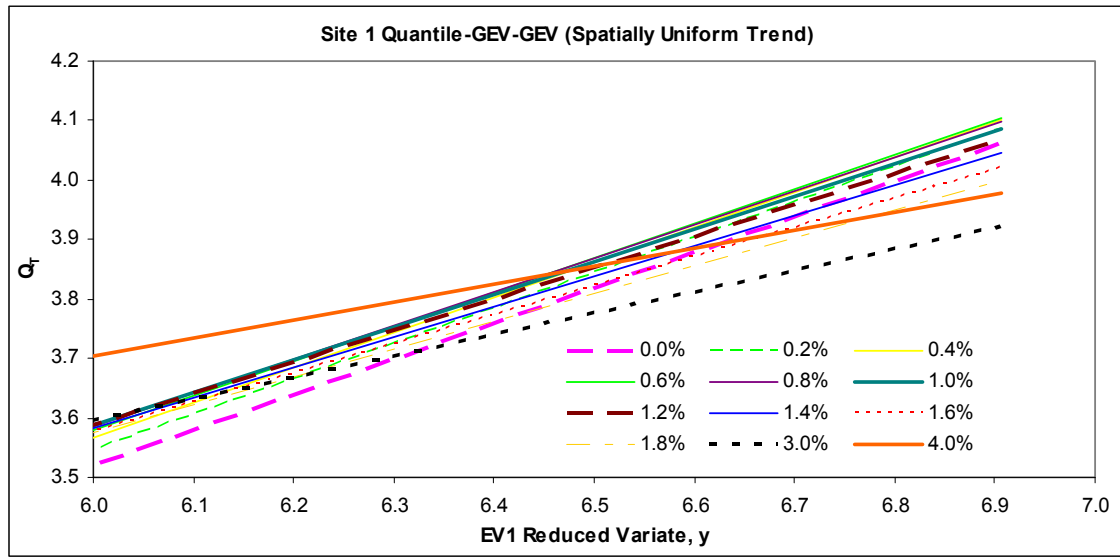


Figure 9.22: At-site quantiles for Site 1 (GEV-GEV) for TF-1

Table 9.9: Relative differences in regional average at-site quantile estimates for various combinations for true and fitted distributions under trend form TF-1.

Trend slope	F=0.90				F=0.99				F=0.999			
	GEV-GEV	GEV-EV1	EV1-EV1	EV1-GEV	GEV-GEV	GEV-EV1	EV1-EV1	EV1-GEV	GEV-GEV	GEV-EV1	EV1-EV1	EV1-GEV
0.0%	0.1%	0.5%	0.2%	0.1%	-1.0%	-9.9%	0.5%	-0.2%	-1.8%	-21.0%	0.7%	-0.6%
0.2%	2.1%	2.5%	2.1%	2.1%	0.1%	-8.7%	1.8%	1.0%	-1.2%	-20.2%	1.7%	0.2%
0.4%	4.2%	4.5%	4.2%	4.1%	1.1%	-7.4%	3.2%	2.3%	-0.9%	-19.3%	2.8%	1.0%
0.6%	6.4%	6.7%	6.3%	6.2%	2.1%	-6.0%	4.7%	3.5%	-0.8%	-18.2%	4.1%	1.6%
0.8%	8.6%	8.9%	8.4%	8.4%	3.1%	-4.5%	6.4%	4.7%	-0.9%	-17.1%	5.4%	2.1%
1.0%	10.9%	11.1%	10.7%	10.6%	4.0%	-2.9%	8.1%	5.9%	-1.2%	-15.9%	6.9%	2.6%
1.2%	13.3%	13.5%	13.0%	12.9%	4.9%	-1.2%	9.9%	7.2%	-1.7%	-14.6%	8.5%	3.0%
1.4%	15.7%	15.9%	15.3%	15.2%	5.8%	0.6%	11.9%	8.4%	-2.2%	-13.2%	10.2%	3.3%
1.6%	18.2%	18.3%	17.7%	17.6%	6.8%	2.4%	13.9%	9.7%	-2.8%	-11.7%	12.1%	3.6%
1.8%	20.8%	20.9%	20.2%	20.1%	7.7%	4.4%	16.0%	11.0%	-3.3%	-10.1%	14.0%	4.0%
2.0%	23.4%	23.4%	22.7%	22.5%	8.6%	6.4%	18.2%	12.3%	-3.8%	-8.4%	16.0%	4.3%
2.2%	26.0%	26.1%	25.3%	25.1%	9.6%	8.5%	20.4%	13.7%	-4.3%	-6.7%	18.1%	4.7%
2.4%	28.7%	28.7%	27.9%	27.7%	10.7%	10.7%	22.8%	15.1%	-4.6%	-4.9%	20.4%	5.2%
2.6%	31.4%	31.4%	30.5%	30.3%	11.8%	12.9%	25.2%	16.6%	-4.9%	-3.0%	22.7%	5.7%
2.8%	34.1%	34.2%	33.2%	32.9%	12.9%	15.2%	27.7%	18.1%	-5.1%	-1.1%	25.0%	6.3%
3.0%	36.9%	37.0%	36.0%	35.6%	14.1%	17.6%	30.2%	19.7%	-5.1%	0.9%	27.5%	7.0%
3.2%	39.7%	39.9%	38.8%	38.3%	15.4%	20.0%	32.8%	21.3%	-5.1%	3.0%	30.0%	7.8%
3.4%	42.6%	42.7%	41.6%	41.1%	16.7%	22.4%	35.5%	23.0%	-4.9%	5.1%	32.6%	8.6%
3.6%	45.4%	45.6%	44.5%	43.9%	18.1%	24.9%	38.2%	24.7%	-4.7%	7.2%	35.3%	9.5%
3.8%	48.3%	48.6%	47.3%	46.7%	19.6%	27.5%	41.0%	26.5%	-4.3%	9.4%	38.0%	10.5%
4.0%	51.2%	51.5%	50.3%	49.5%	21.1%	30.1%	43.8%	28.3%	-3.9%	11.6%	40.8%	11.6%

Table 9.10: Relative differences in regional average at-site quantile estimates for various combinations for true and fitted distributions under trend form TF-2.

Trend slope	F=0.90				F=0.99				F=0.999			
	GEV-GEV	GEV-EV1	EV1-EV1	EV1-GEV	GEV-GEV	GEV-EV1	EV1-EV1	EV1-GEV	GEV-GEV	GEV-EV1	EV1-EV1	EV1-GEV
0.0%	0.1%	0.5%	0.2%	0.1%	-1.0%	-9.9%	0.5%	-0.2%	-1.8%	-21.0%	0.7%	-0.6%
0.2%	3.3%	3.6%	3.3%	3.3%	2.1%	-7.1%	3.6%	2.9%	1.3%	-18.5%	3.9%	2.6%
0.4%	6.4%	6.8%	6.5%	6.5%	5.3%	-4.2%	6.9%	6.2%	4.6%	-15.9%	7.1%	6.0%
0.6%	9.7%	10.1%	9.7%	9.7%	8.7%	-1.2%	10.2%	9.7%	8.0%	-13.3%	10.5%	9.6%
0.8%	12.9%	13.4%	13.0%	13.0%	12.1%	1.9%	13.6%	13.2%	11.6%	-10.6%	13.9%	13.4%
1.0%	16.3%	16.7%	16.3%	16.3%	15.6%	4.9%	17.0%	16.9%	15.2%	-7.8%	17.4%	17.4%
1.2%	19.6%	20.1%	19.7%	19.6%	19.1%	8.1%	20.5%	20.7%	18.9%	-5.0%	21.0%	21.6%
1.4%	23.0%	23.5%	23.1%	23.0%	22.8%	11.3%	24.1%	24.5%	22.8%	-2.1%	24.7%	25.9%
1.6%	26.4%	26.9%	26.5%	26.4%	26.5%	14.5%	27.7%	28.4%	26.7%	0.8%	28.4%	30.3%
1.8%	29.8%	30.3%	29.9%	29.9%	30.2%	17.8%	31.4%	32.4%	30.7%	3.7%	32.1%	34.8%
2.0%	33.3%	33.8%	33.4%	33.3%	34.0%	21.1%	35.0%	36.5%	34.8%	6.7%	35.9%	39.4%
2.2%	36.7%	37.3%	36.9%	36.8%	37.8%	24.4%	38.8%	40.6%	38.9%	9.7%	39.8%	44.2%
2.4%	40.2%	40.8%	40.4%	40.3%	41.7%	27.8%	42.5%	44.8%	43.0%	12.7%	43.6%	49.0%
2.6%	43.8%	44.4%	43.9%	43.9%	45.6%	31.2%	46.3%	49.0%	47.2%	15.8%	47.6%	53.9%
2.8%	47.3%	48.0%	47.5%	47.4%	49.6%	34.6%	50.2%	53.3%	51.5%	18.9%	51.5%	58.8%
3.0%	50.9%	51.5%	51.1%	51.0%	53.6%	38.1%	54.0%	57.6%	55.8%	22.1%	55.5%	63.9%
3.2%	54.4%	55.1%	54.7%	54.6%	57.6%	41.6%	57.9%	61.9%	60.1%	25.2%	59.5%	69.0%
3.4%	58.0%	58.8%	58.3%	58.2%	61.6%	45.1%	61.8%	66.3%	64.5%	28.4%	63.6%	74.1%
3.6%	61.6%	62.4%	61.9%	61.8%	65.6%	48.6%	65.7%	70.7%	68.8%	31.6%	67.6%	79.3%
3.8%	65.2%	66.0%	65.5%	65.4%	69.7%	52.1%	69.7%	75.1%	73.3%	34.8%	71.7%	84.5%
4.0%	68.9%	69.7%	69.2%	69.0%	73.8%	55.7%	73.6%	79.6%	77.7%	38.0%	75.9%	89.8%

The above results show that the quantiles estimates increase with increase in trend slopes in all cases of trend forms and distribution combinations. In contrast to growth curve, the effect of SUT trends on the regional estimate of at-site quantile is larger in TF-2 than TF-1, i.e. the change rates of relative differences in quantile estimates with the increase in trend slopes are higher in TF-2 than TF-1. This occurs because in TF-1, growth curves get flatter (or growth factors decrease) with the increase in trend slope while the opposite occurs in TF-2.

For example, in the TF-1 case, the relative differences for the 10, 100 and 1000 years return periods EV1-EV1 quantile estimates are 10.7%, 8.1% and 6.9% respectively for a trend slope of 1%., while in TF-2 the corresponding differences are 16.3%, 17.0% and 17.4% and respectively (**Tables 9.9 and 9.10**).

The differences between the various distribution combinations are imperceptible for the smaller return period in both cases of trend forms. However, these become significant with the increase in return periods. The highest differences can be

noticed in the EV1-EV1 distribution combination followed by the GEV-EV1 case in TF-1, while in TF-2, the highest differences can be noticed in the EV1-GEV distribution combination followed by the GEV-EV1 and GEV-GEV combinations. For 1000 year return period, the GEV-GEV distribution combination shows decreasing trend in quantile estimates with the increase in at-site trend slope.

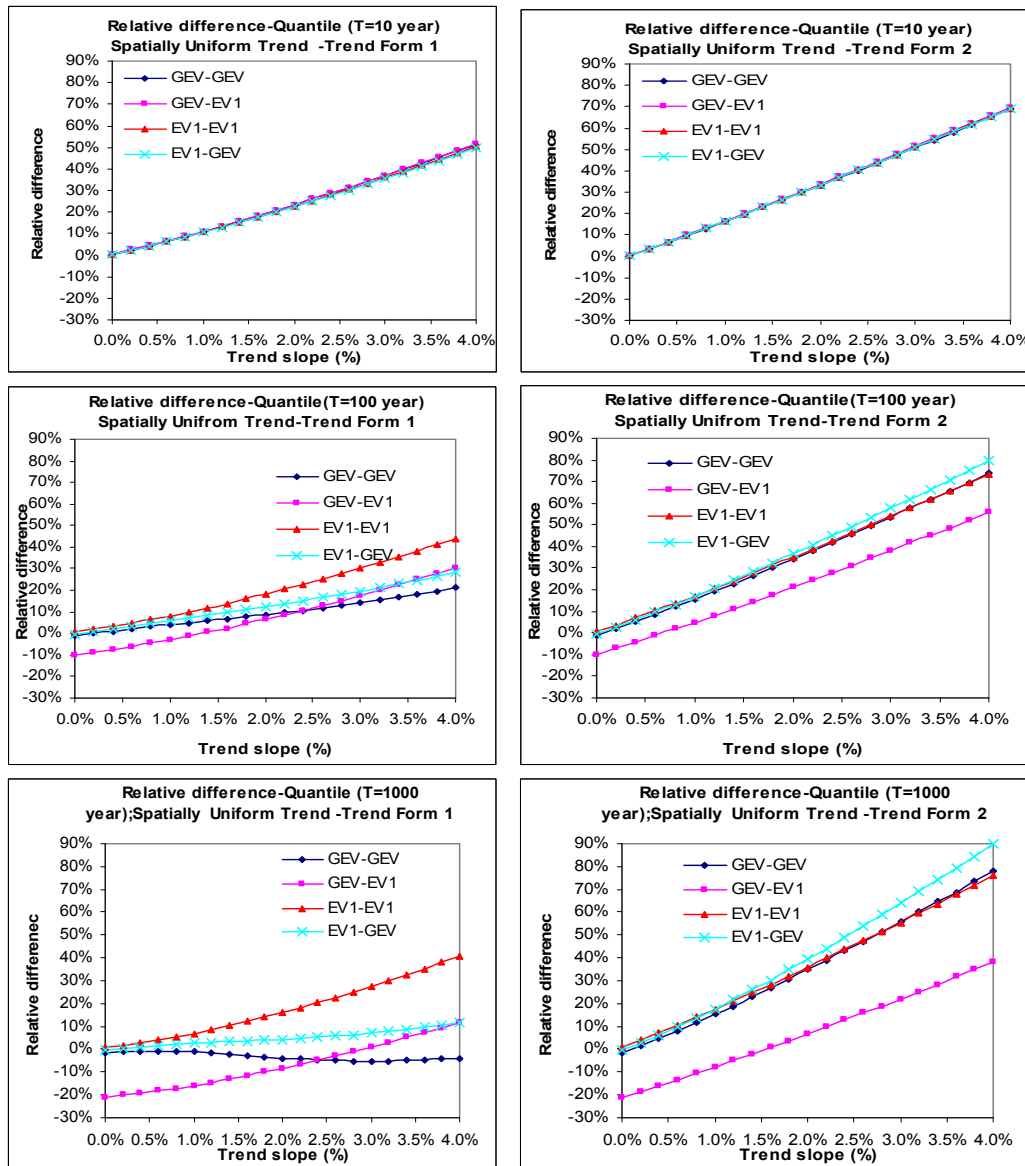


Figure 9.23: Comparison of relative differences in quantile estimates for different combinations of true and fitted distributions (left graphs correspond to TF-1 & right graphs are for TF-2).

It can also be seen in the **Figure 9.23** that the differences in quantile estimates for the distribution combinations of GEV-GEV and GEV-EV1 are almost same at the trend slope of 2.4%. The means that the at this trend slope the GEV distribution

takes the form of EV1 distribution i.e. the shape parameter becomes near to zero, as can be seen in **Table 9.5**. Any further increase in trend slopes, the shape parameter increases, thus the quantile functions become concave upward and therefore the quantile estimates at the larger return periods become smaller than the true estimates. This can be clearly seen in the bottom left graph in **Figure 9.23**.

It should be mentioned here that, at the no-trend condition there are some associated percentage differences between the true and fitted functions. These differences are the biases in the estimates which mainly results from misspecification of distribution type. For example, the bias of quantile estimate associated with the 100 year return period in the EV1-EV1 distribution combination is 0.5% under the TF-1 scenario.

The above changes in the quantile functions can be explained with the help of corresponding changes in growth curves and at-site sample mean with the increases in trend slopes as discussed in the sections 9.4.2 and 9.4.4. This explanation is appropriate, since the index flood method uses these two variables in estimating the at-site quantile estimates, i.e. $Q_T = Q_{mean} \times X_T$.

As was shown earlier that the at-site sample mean increases with the increase in trend slope in a linear fashion in both cases of trend forms. The growth curves also increase with the increase in trend slopes in the cases of TF-2. Thus it is obvious that the quantile estimates will be increased with the increase in trend slopes under this trend form scenario. On the other hand, the growth factors decrease with the increase in trend slopes in the TF-1 scenario. However, this decrease rate is slower than the increase rate of the at-site sample mean. Thus, the quantile estimates in the case of TF-1 increase with the increase in trend slopes. The differences between various true and fitted distribution combinations in the case of quantile estimation are similar to the corresponding differences in the growth curve estimates as discussed in Section 9.4.4.

The above results suggest that the SUT type trends in a pooling group will have some effects on the regional estimates of at-site quantiles. The magnitude of this effect depends on the forms of the trend in the at-site data series in the region. This effect would results from the changes in the true sample and distribution parameters. Irrespective of the trend forms, the estimated effects of the SUT type

trends in a pooling group on the true GEV 100 year quantile estimate (GEV-GEV case) for could range from 4% to 15.6% (Tables 9.9 and 9.10) for a trend slope of 1%. The corresponding effect on the EV1 true quantile could vary from 8.1% to 17% (EV1-EV1 case).

9.4.6 Suitability of various Distributions in Trend Impact Study

9.4.6.1 Robustness Assessment of various True and Fitted Distribution Combinations

A procedure is said to be robust if it yields estimates of Q_T that are good (low bias and low standard error-high efficiency) even if the procedure is based on an assumption that is not true. Since we do not know the distribution of AM floods in nature it is necessary to tends us to seek out and find a distribution and an estimating procedure which together are robust when dealing with distributions which give random samples which have a flood-like behaviour.

A suitable method of testing the robustness of any distribution and parameter estimation procedure involves simulating random samples from a parent distribution in which the Q-T relationship is known exactly (Hosking et al., 1985a). A number of such studies for various combinations of distribution and parameter estimation procedures were carried out for the at-site/regional level in the past, such as Kuczera (1982), Hosking et al. (1985a), Lettenmaier et al. (1985), Wallis and Wood (1985), Lettenmaier & Potter (1985), Arnell & Gabrielle (1985, 1988) and Landwehr et al. (1987). The results of these studies are summarised by Cunnane (1989) in the World Meteorological Organisation's Operational Hydrology Report No. 33. The results of these studies which are relevant to our study are summarised below:

- The results from Kuczera (1982a) show that 2 parameter estimators, LN2 and EV1, have smaller RMSE values than 3 and 4 parameter estimators especially in small samples. A considerable proportion of RMSE is due to bias in the 2 parameter estimators while that proportion is almost negligible in the 3 and 4 parameter estimators. In other words the more flexible 3 and 4 parameter estimators have negligible bias but very large sampling error while the less flexible 2 parameter estimators have considerable bias but much smaller standard error. Similar conclusions were drawn by Lettenmaier et al.

(1985) in relation to EV1 and GEV quantile estimators, the latter having negligible bias and very large standard errors while the former exhibit tight confidence intervals but with considerable bias when the population is GEV ($k < 0$). Thus the 2-parameter models have high efficiency but are biased while in contrast 3-parameter models can be unbiased but quite inefficient. The 2-parameter model bias can be damaging while the 3-parameter inefficiency make 3-parameter models unattractive for at-site use alone (Cunnane, 1989).

- Lettenmaier et al. (1985) study shows that when a two parameter fixed skew model is used to estimate quantiles when data are drawn from a population with higher skewness than that implied by the model results in negative bias, whether used in at-site or at-site/regional mode. When used in at-site mode it has much smaller standard error than a typical 3-parameter model, while the latter has much less bias. Corresponding but opposite remarks apply when the model skewness exceeds that of the parent.
- The use of two-parameter distributions such as the Gumbel is not recommended in regional frequency analysis (Hosking and Wallis, 1996). Use of a two-parameter distribution is beneficial only if the investigator has complete confidence that the distribution's L-Skewness and L-kurtosis are close to those of the frequency distributions at the sites in the region; otherwise large biases in quantile estimates will result.
- Misspecification of the frequency distribution introduces bias into quantile estimates, however it is important only for quantiles far into the tails of the distribution ($F > 0.99$).
- Heterogeneity introduces bias into estimates at sites not typical of the region as a whole. This bias can easily be the major source of error in the estimated quantiles and growth curve.
- At extreme quantiles ($F \geq 0.999$) the advantage of regional over at-site estimation is greater. For these quantiles, heterogeneity is less important as a source of error, whereas misspecification of the frequency distribution is more important.

This study supports the above findings as can be seen in **Table 9.11**, where various accuracy measures for growth curve and quantile estimates corresponding to return periods of 10 and 1000 years obtained from various combinations of true and fitted distributions are presented.

The accuracy measures (as discussed in Section 9.3.6) for the trend slopes of 0.2% and 1% in both cases of trend forms have also been included in **Table 9.11**. It was stated earlier that in any trend conditions, these accuracy measures do not provide the same meaning as that of the no-trend condition, since the quantile estimates are obtained from the non-stationary samples which are different from the true sample; these measures rather estimates the effects of trend on the true estimates. However, comparisons of these measures for various trend form scenarios can give an idea about the various effects of trends on the true estimates. For example, it can be seen **Table 9.11** that the RMSE values associated with the TF-2 are higher than for the TF-1 in any trend condition, particularly for larger return periods. This suggests that the TF-2 introduces more variability in the at-site samples and thus the region becomes more heterogeneous. Furthermore, it can be seen that the patterns of the accuracy measures for various distribution combinations under various trend scenarios are similar to that of the no-trend condition.

Table 9.11: Regional Average Relative bias, Abs. bias, RMSE and Standard Error of growth curves and quantiles for various trend slopes estimated from various combinations of trend forms and true and fitted distributions.

Trend Form	Trend Slope	Statistics	Growth curve				Quantile			
			GEV-GEV	GEV-EV1	EV1-EV1	EV1-GEV	GEV-GEV	GEV-EV1	EV1-EV1	EV1-GEV
F=0.90										
No-trend	0%	Abs. BIAS	3.7%	3.7%	4.0%	4.0%	3.7%	3.7%	4.0%	4.0%
		BIAS	0.1%	0.5%	0.2%	0.1%	0.1%	0.5%	0.2%	0.1%
		RMSE	4.1%	4.1%	4.4%	4.4%	10.2%	10.3%	9.7%	9.7%
		SE	4.1%	4.1%	4.4%	4.4%	10.2%	10.3%	9.7%	9.7%
TF-1	0.20%	Abs. BIAS	3.8%	3.7%	4.1%	4.1%	4.0%	4.1%	4.3%	4.3%
		BIAS	-1.0%	-0.6%	-0.9%	-1.0%	2.1%	2.5%	2.1%	2.1%
		RMSE	4.1%	4.1%	4.4%	4.4%	10.4%	10.6%	9.9%	9.9%
		SE	4.0%	4.1%	4.3%	4.3%	10.2%	10.3%	9.7%	9.7%
	1.00%	Abs. BIAS	4.8%	4.7%	5.1%	5.1%	10.9%	11.1%	10.7%	10.6%
		BIAS	-4.0%	-3.8%	-4.2%	-4.2%	10.9%	11.1%	10.7%	10.6%
		RMSE	5.1%	5.0%	5.3%	5.4%	14.6%	14.8%	14.0%	13.9%
		SE	3.1%	3.3%	3.3%	3.3%	9.7%	9.8%	9.0%	9.0%
TF-2	0.20%	Abs. BIAS	3.7%	3.7%	4.0%	4.0%	4.4%	4.6%	4.8%	4.7%
		BIAS	0.2%	0.5%	0.2%	0.2%	3.3%	3.6%	3.3%	3.3%
		RMSE	4.1%	4.1%	4.4%	4.4%	11.0%	11.2%	10.5%	10.5%
		SE	4.1%	4.1%	4.4%	4.4%	10.5%	10.6%	10.0%	10.0%
	1.00%	Abs. BIAS	3.7%	3.8%	4.1%	4.1%	16.3%	16.7%	16.3%	16.3%
		BIAS	0.6%	1.0%	0.7%	0.7%	16.3%	16.7%	16.3%	16.3%
		RMSE	4.1%	4.2%	4.4%	4.4%	19.9%	20.3%	19.4%	19.4%
		SE	4.0%	4.1%	4.3%	4.3%	11.5%	11.5%	10.6%	10.6%
F=0.999										
No-trend	0%	Abs. BIAS	16.7%	22.0%	7.5%	7.5%	16.6%	22.0%	7.5%	7.5%
		BIAS	-1.9%	-	0.7%	-0.6%	-1.8%	-	0.7%	-0.6%
		RMSE	20.7%	22.4%	8.1%	11.5%	23.1%	24.2%	12.1%	14.5%
		SE	20.6%	7.7%	8.1%	11.5%	23.0%	12.0%	12.1%	14.5%
TF-1	0.20%	Abs. BIAS	16.6%	23.1%	7.5%	7.7%	16.7%	21.5%	7.6%	7.5%
		BIAS	-4.2%	-	-1.4%	-2.8%	-1.2%	-	1.7%	0.2%
		RMSE	20.5%	23.5%	8.1%	11.5%	23.0%	23.6%	12.1%	14.4%
		SE	20.1%	6.4%	8.0%	11.2%	23.0%	12.3%	12.0%	14.4%
	1.00%	Abs. BIAS	18.6%	27.2%	9.2%	11.5%	16.7%	19.2%	9.2%	7.7%
		BIAS	-14.6%	-	-7.4%	-	-1.2%	-	6.9%	2.6%
		RMSE	21.9%	27.4%	9.7%	14.2%	22.4%	21.2%	13.2%	14.1%
		SE	16.4%	3.2%	6.2%	8.8%	22.4%	14.1%	11.3%	13.8%
TF-2	0.20%	Abs. BIAS	16.7%	22.0%	7.5%	7.5%	16.9%	20.5%	8.1%	7.7%
		BIAS	-1.8%	-	0.7%	-0.5%	1.3%	-	3.9%	2.6%
		RMSE	20.7%	22.3%	8.1%	11.5%	23.6%	22.8%	12.9%	15.0%
		SE	20.6%	7.8%	8.1%	11.5%	23.6%	13.4%	12.3%	14.8%
	1.00%	Abs. BIAS	16.8%	21.5%	7.6%	7.6%	21.6%	16.9%	17.4%	17.4%
		BIAS	-0.3%	-	1.7%	1.7%	15.2%	-7.8%	17.4%	17.4%
		RMSE	20.9%	21.9%	8.2%	11.8%	28.9%	19.9%	21.1%	23.4%
		SE	20.9%	8.3%	8.1%	11.7%	24.6%	18.3%	11.9%	15.6%

9.4.6.2 Unrealistic Results for GEV Distribution

As discussed earlier in Section 9.4.5, in the GEV-GEV distribution case, the at-site quantile estimates for any return period larger than $F=0.998$ (500 year return period) decrease with the increase in trend slopes, particularly when trend slope goes over 1.2% in the case of TF-1 (see **Table 9.9**). **Figure 9.24** illustrates this fact for the at-site quantile estimates of the sites 1, 8 and 15. In reality, it seems unrealistic, since the mean increases linearly with the increase in trend slopes. In other distribution combinations, the at-site quantile estimates generally increases with the increase in trend slopes.

The causes of the above unrealistic results in the case of GEV-GEV distribution can be attributed to the following:

- (i) **Inherent properties of GEV distribution's shape parameter:** The GEV distribution combines three types of extreme value distributions called the extreme value types I, II and III (EV1, EV2 and EV3). The GEV distribution is a three-parameter distribution with location (u), scale (α) and shape (k) parameter. The shape parameter (k) governs the tail behaviour (tail shape and size) of the distribution and distinguishes between the above three types of distributions. For $k>0$, the distribution has a finite upper bound at $u + \alpha / k$ and corresponds to EV3 type distribution; for $k<0$, the distribution has a thicker right-hand tail and corresponds to the EV2 distribution for maxima and when $k=0$, the distribution takes the shape of EV1 distribution which has a relatively thinner right-hand tail.

Thus the GEV distribution's upper tail is strongly related to its shape parameter. If $k>0$, the distribution's frequency curve is concave downwards, while for $k<0$ it is concave upwards. In the EV1 type the frequency curve is a straight line.

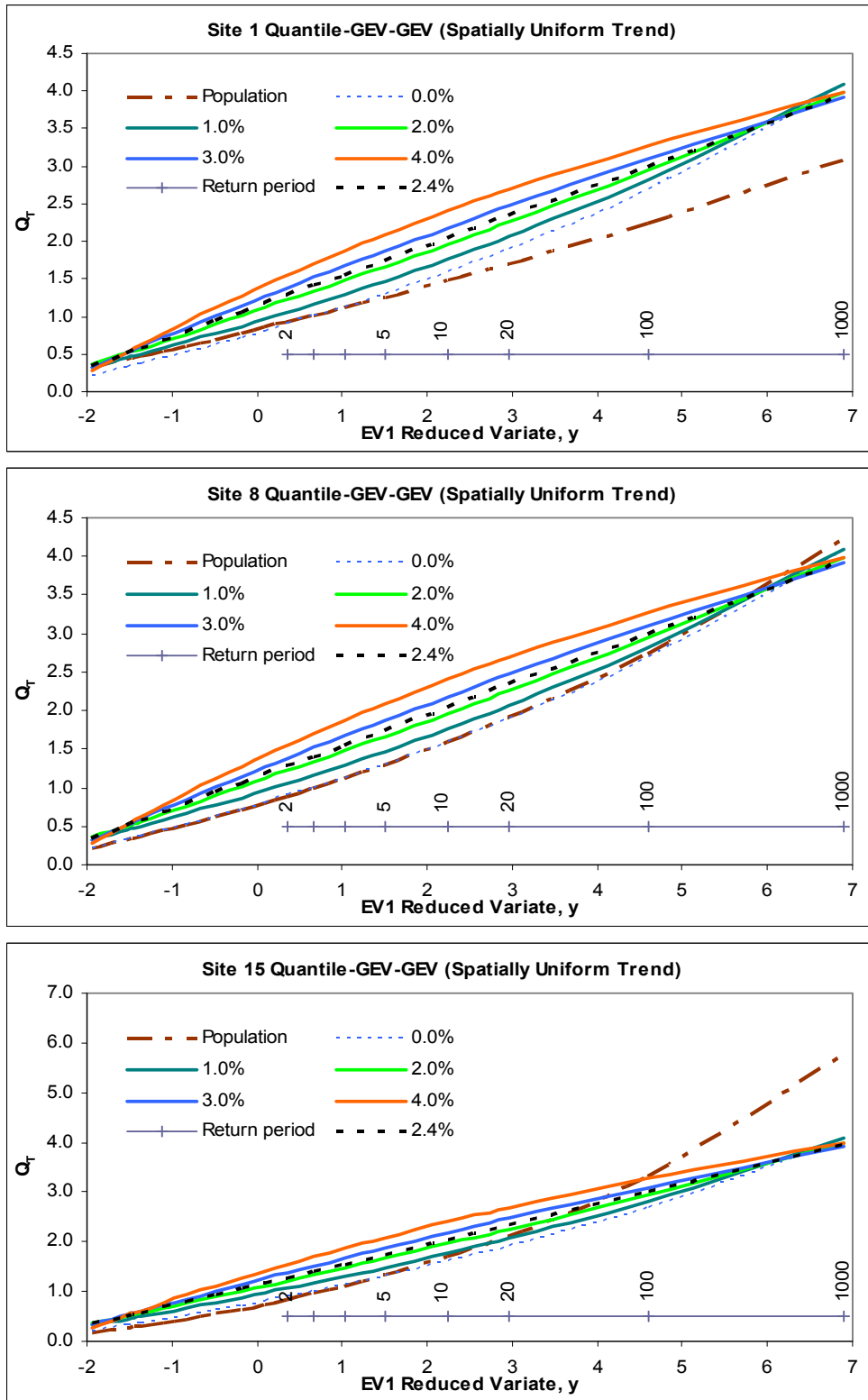


Figure 9.24: Unrealistic quantile estimates in the case of GEV-GEV distribution combination under TF-1 scenario (SUT)

It was shown earlier that the L-Skewness of the true distribution decreases with the increase in upward trend slope magnitude, which consequently results in an increase in the shape (k) parameter. This increase in shape parameter causes increasingly downward curvature at the upper tail of the flood frequency curve, which consequently causes decrease in quantile estimates for the larger return periods. However, it is realistically expected that with the increase in trend slopes, quantile estimates for any return periods will be increased, contrary to the above finding.

The above thus suggests that the GEV distribution gives unrealistic quantile estimates for upward trend slope greater than 1.2%, particularly when the return period is very large ($T > 500$ years) and this occurs due to its very strong relationship with the shape parameter.

- (ii) **Shorter record length for estimation of very large return period quantile:** The size of the pooling group plays an important role in estimating any quantile for a specified return period with sufficient accuracy. The analysis carried out in the UK FEH (1999) suggests that no one pooling-group size is optimal. The FEH recommendation is that the number of station-years in the pooling group should be set at five times the return period: the 5T rule.

Thus in order to estimate any quantile with a return period of 1000 year, the recommended pooling group size should be 5000 station-years. In our study, the size of the pooling group used is 450 station-years, which seems very small for the 1000 year return period quantile estimate.

A sensitivity study for the GEV-GEV distribution combination has been carried out for different at-site record lengths of 30, 40, 50, 60, 70, 80, 90, 100, 200, 300 years to determine a pooling group size, which will provide a realistic quantile estimate for 1000-year return period at different trend slope conditions. The L-moment algorithm as discussed in Section 9.3.1 has been used to estimate this quantile. The relative differences of the regional average growth curve and quantile estimates for different trend slopes have been estimated for all of the above mentioned record lengths which are

presented in **Tables 9.12** and **9.13** respectively for $F=0.999$. It can be seen in these tables that in order to get a realistic estimate for a 1000 year return period quantile for a uniform trend slope of 1%, at least 200 years of record length will be required at each of the sites in the region which is equivalent to a pooling group size of 3000 station-years (i.e. pooling group size should be at least three times of return period-3T). **Figure 9.25** illustrates the changes in the shape of the quantile functions for Site 1 at the upper tails for the at-site record lengths of 100, 200 and 300 years. This means that if the record length is large enough the downward curvature is not so severe and the large quatile estimates are more realistic.

Table 9.12: Relative differences in 1000 year return period growth factor for various record lengths in the case GEV-GEV distribution and TF-1.

Trend slope	30 year	40 year	50 year	60 year	70 year	80 year	90 year	100 year	200 year	300 year
0.0%	-1.9%	-1.0%	-0.4%	-0.1%	0.2%	0.4%	0.6%	0.7%	1.3%	1.6%
1.0%	-14.6%	-18.2%	-21.8%	-25.3%	-28.5%	-31.4%	-33.9%	-36.0%	-45.7%	-47.2%
2.0%	-26.6%	-32.3%	-36.6%	-39.9%	-42.2%	-43.8%	-45.0%	-45.8%	-47.0%	-45.6%
3.0%	-35.3%	-40.3%	-43.4%	-45.2%	-46.3%	-46.9%	-47.1%	-47.3%	-45.7%	-44.0%
4.0%	-40.7%	-44.3%	-46.1%	-47.0%	-47.3%	-47.3%	-47.2%	-47.0%	-44.5%	-42.8%

Table 9.13: Relative differences in 1000 year return period quantile for various record lengths in the case GEV-GEV distribution and TF-1.

Trend slope	30 year	40 year	50 year	60 year	70 year	80 year	90 year	100 year	200 year	300 year
0.0%	-1.8%	-1.0%	-0.4%	0.0%	0.3%	0.5%	0.6%	0.8%	1.3%	1.6%
1.0%	-1.2%	-1.3%	-1.8%	-2.5%	-3.1%	-3.5%	-3.8%	-3.7%	8.9%	32.4%
2.0%	-3.8%	-4.5%	-4.3%	-3.2%	-1.1%	1.7%	5.1%	8.9%	59.7%	117.9%
3.0%	-5.1%	-3.6%	0.0%	4.9%	11.0%	17.7%	25.0%	32.6%	118.2%	209.0%
4.0%	-3.9%	1.4%	8.9%	17.7%	27.6%	38.0%	48.9%	60.0%	178.8%	301.4%

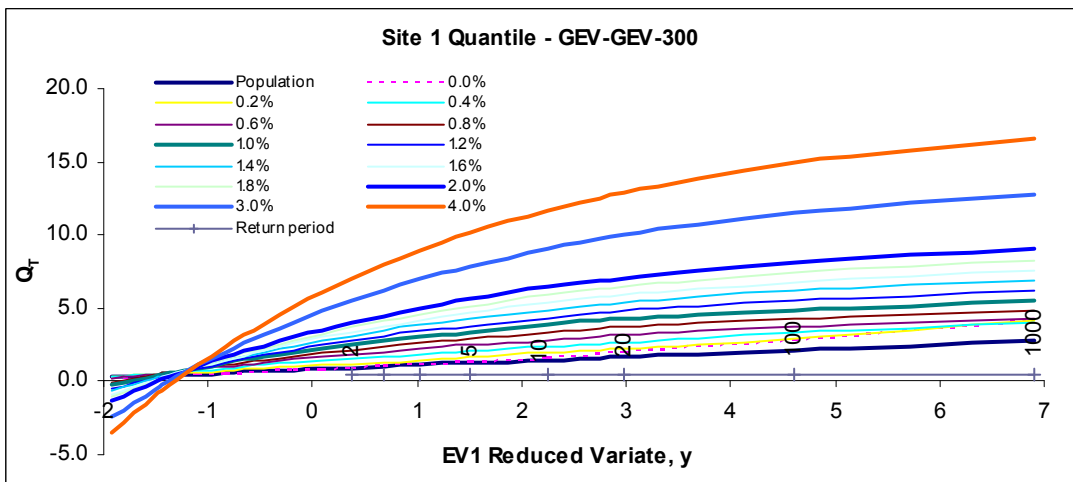
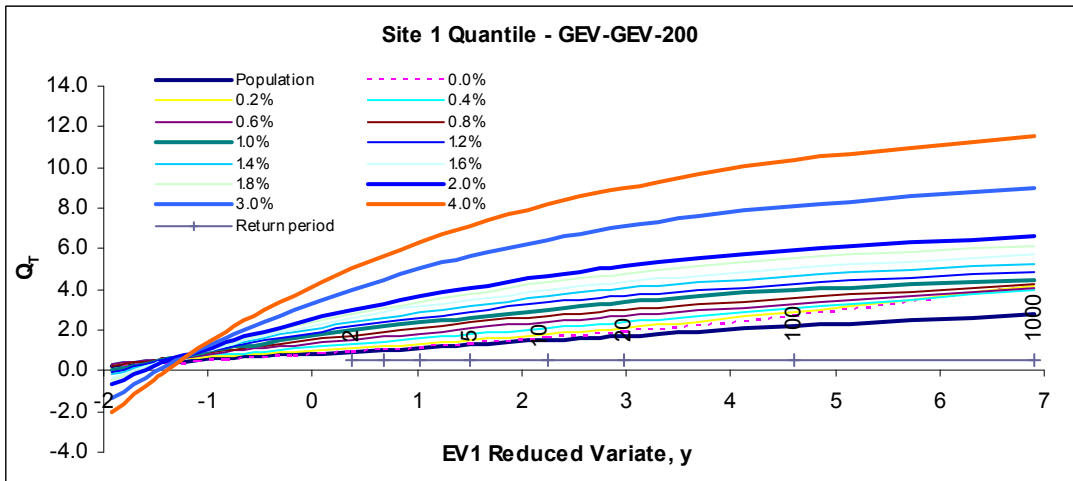
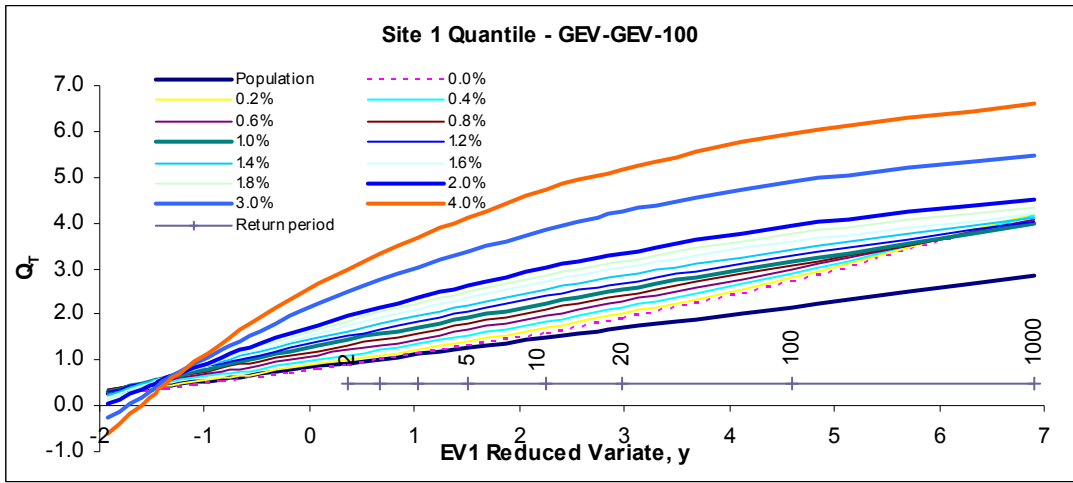


Figure 9.25: Changes in quantile functions for Site 1 estimated by GEV-GEV for different larger at-site record lengths (from top to bottom, 100, 200 and 300 years respectively)

9.4.7 Result Summary and Discussions

The following conclusions can be drawn from this study:

- It is found, as expected, that any trends in a time series would cause changes in its true sample properties. The significance of these changes depends on the form and magnitude of trend slope and also on the distributions types to which the sample belongs. It is found that, the population mean increases linearly with the increase in trend slope in all cases of trend scenarios (SUT, SVT & RD), forms (TF-1 & TF-2) and true distribution types (GEV & EV1). However the effects of trends on variability (L-CV) and skewness (L-Skewness) are different in different cases of trend scenario, form and distribution types. In the SUT trend scenario, the variability and skewness decreases with the increase in trend slope in both GEV and EV1 distributions in TF-1. The opposite occurs in TF-2. This suggests that TF-1 reduces variability and skewness, while TF-2 inflates these properties in both distributions. In the SVT trend scenario, effects are markedly different in the two distributions. It reduces variability markedly in the EV1 distribution in TF-1 and slightly increases in TF-2. The changes in L-Skewness are not significant in both cases of trend forms. In TF-1, L-Skewness decreases slightly while in the TF-2 case it remains almost unchanged. In the GEV distribution, L-CV increases both in TF-1 and TF-2 while L-Skewness reduces in both trend forms with a marked reduction in the TF-1. Trend on a single site (Site 8) in the region showed an imperceptible effect on the regional average mean, L-CV and L-Skewness in both trend forms and distribution.
- The changes in the population properties cause changes in the population distribution parameters. In the case of GEV distribution, the patterns of changes in the location and scale parameters are similar in both cases of the trend forms. These increase with the increase in trend slope in both cases of trend forms. TF-2 introduces more spread in the distribution shape than TF-1. In the trend form TF-1, the shape parameter of GEV distribution increases, while it decreases in the case of TF-2 with the increase in trend slope. The changes in EV1 distribution parameters are similar to that of the GEV location and scale parameters. Similar results are obtained in the case of SVT trend scenario in both distributions. Trend on a single site (Site 8) in

the region showed an imperceptible effect on the distribution parameters in both distributions.

- The Spatially Uniform Trend in a pooling group will have some effects on the regional growth curve. The magnitudes of these effects depend on the forms of the trend in the at-site data series in the region. Growth curves in each combination of the true and fitted distributions get flatter and flatter as the trend slope magnitude increases in TF-1. In contrast, in TF-2 growth curves in all distribution combinations get steeper with the increase in trend slopes except in the GEV-EV1 case. In the GEV-EV1 case growth curves get flatter with the increase in at-site trend slopes similar to TF-1.

Irrespective of the trend forms, the estimated effects of the SUT type trends on the true GEV 100 year growth factor could range from 0% to -15.9% (decrease) for a trend slope of 1% (GEV-GEV case). In the TF-1 case, the relative differences for the 10, 100 and 1000 years return periods EV1 growth factors (EV1-EV1 case) are -4.2%, -6.4%, -7.4% (decreases) respectively for a trend slope of 1%, while in TF-2 the corresponding differences are 0.7%, 1.3% and 1.7% (increases) respectively. This suggests that the effects are larger for the larger return periods in both cases of trend forms, which is not unexpected.

The results also show that fitting an EV1 distribution to a non-stationary sample of true GEV population could result in a reduction of true growth factor by 9% to 15.9% for T=100 for a trend slope of 1%, while fitting the non-stationary sample by the parent GEV distribution would reduce the 100 year growth factor by 0 to 10% depending on the forms of trends present in the data series.

- The differences in the effects of trends on the regional growth curves between the different true and fitted distribution combinations are very small for the smaller return periods in both cases of trend forms. However these become noticeably larger with the increase in return periods. The highest relative differences (difference between the true and fitted growth factors) were found in the GEV-GEV distribution combination followed by the

EV1-GEV in TF-1, while in TF-2 the highest relative differences were found in the EV1-GEV distribution combination followed by GEV-EV1. This suggests that the upper tail of a three-parameter distribution is more sensitive to trend slope and thus introduces more bias or differences. It could be due to the fact that the true sample L-Skewness of GEV distribution decreases with the increase in trend slopes. This results in a sample with low skewness, which might not fit the GEV distribution well and thus, gives higher relative differences. It is also true, particularly in the no-trend condition that bias/relative differences in the growth curve estimate increases when a thin tail distribution is fitted to a thick tailed distribution and vice versa. In other words, bias in growth curve estimate increases when a two parameter fixed skew model is used to estimate growth curve when data are drawn from a population with high skewness model (Cunnane, 1989). The performance of the two-parameter EV1 distribution in fitting a GEV sample with a high trend is better than its true distribution.

- The simulation results also shows that at the trend slope of 2.4% the growth factor estimates in both GEV-GEV and EV1-EV1 cases are equal, meaning that the GEV distribution has $k=0$ at that this point.
- The regional estimates of the at-site quantiles increase with the increase in trend slopes in all cases of trend forms and distribution combinations with some exceptions in the GEV-GEV distribution combination in TF-1. In this case, for any trend slope greater than 1.2%, the estimated quantiles get smaller than the no-trend condition estimates, especially for $T \geq 500$. In contrast to growth curves, the effects of the SUT type trends on the at-site quantiles are larger in TF-2 than in TF-1. This occurs because in TF-1, growth curves get flatter (or growth factors decrease) with the increase in trend slope while the opposite occurs in TF-2. This occurs due to the changes in the population properties, particularly in the 'mean' and in the growth curve distribution parameters.

Irrespective of the trend forms, the estimated effects of the SUT type trends in a pooling group on the true GEV 100 year quantile estimate could range from 4 to 15.6% (increases) for a trend slope of 1% (GEV-GEV case). The

corresponding effect on the EV1 true quantile could vary from 8.1% to 17% (EV1-EV1 case). In the TF-1 case, the relative differences for the 10, 100 and 1000 years return periods EV1-EV1 quantile estimates are 10.7%, 8.1% and 6.9% respectively for a trend slope of 1%, while in TF-2 the corresponding differences are 16.3%, 17.0% and 17.4% and respectively. This suggests that the increased rates of relative differences (effects) are slightly higher for smaller return periods in the trend form TF-1.

- The differences in the effects of trends on the at-site quantiles between the various distribution combinations are imperceptible for the smaller return periods in both cases of trend forms. However, these become noticeable with the increase in return periods. The highest relative differences were found in the EV1-EV1 distribution combination followed by GEV-EV1 in TF-1, while in TF-2, the highest relative differences were found in the EV1-GEV distribution combination followed by the GEV-EV1 and GEV-GEV combinations. These variations in the different distribution combinations can be attributed to the changes that occur in the true distribution parameters in the presence of trends and the suitability of fitting the true and other distributions to the non-stationary data.
- The simulation results also show that the relative differences in the quantile estimates for the distribution combinations of GEV-GEV and GEV-EV1 are almost the same at the trend slope of 2.4%. This means that at this trend slope the GEV distribution takes the form of EV1 distribution i.e. the shape parameter becomes near to zero. Any further increase in trend slopes, the shape parameter increases, thus the quantile functions become concave downwards and therefore the quantile estimates at the larger return periods become smaller than the true estimates.
- As mentioned earlier, in the trend form TF-1, for any trend slope greater than 1.2%, the estimated quantiles from GEV-GEV distribution are smaller than the no-trend condition estimates, especially for $T \geq 500$. Thus the GEV distribution gives unrealistic results for the larger return periods. This occurs due to its very strong relationship with the shape parameter and also due to estimating these extremely larger return period quantiles from a

comparatively shorter pooling group size (450 station-years). A sensitivity analysis for various pooling group sizes showed that in order to get a realistic estimate for a 1000 year return period quantile for any trend slope of 1%, at least 200 years of record length will be required at each of the sites in the region which is equivalent to a pooling group size of 3000 station-years (i.e. pooling group size should be at least three times of return period-3T).

- In flood frequency analysis, a major assumption is that all observations in a data set are independent and identically distributed. If trend is present in the data, the stationarity assumption would not be valid and therefore the current procedures of estimation of design flood based on statistical theory would give misleading results. The application of the existing statistical procedure on this non-stationary data would result in under- and/or over-estimation of a design flood quantile.

The simulation results suggest that due to the presence of trend in data series, the regional growth curves get flatter in TF-1 and steeper in TF-2. However in both cases, the quantile estimates increase. This may be due to increase in sample mean. The increase rate in the at-site quantiles may not be significant for very smaller trend slopes. Therefore the application of the conventional frequency analysis techniques on the non-stationary sample may not have significant effect on the design flood estimation and consequently on the costs and safety of the project. However, for a larger trend slope the effect could be significant. In this context careful attention should be given to estimate the design flood quantile when non-stationary properties are present in the data series. In this case the conventional frequency analysis method would need to be revised.

Since until now no such acceptable procedure has been developed and/or adopted to deal with the non-stationary properties of data series, the findings of the current study could help hydrologists/engineers to make an allowance in the estimated design flood using the current statistical procedure. This can be done by estimating the extent of trend (trend slope) present in the subject data series and applying an allowance based on the estimated relative differences reported above associated with the design flood estimate. The

slope of trend in the data series can be estimated from the Theil (1950) and Sen (1968) proposed method or from the regression slope method.

10 CONCLUSIONS AND RECOMMENDATIONS

10.1 CONCLUSIONS

The present study focused on the estimation of low and high flows for Irish River catchments, particularly for ungauged catchments and in the context of changing climatic condition which is believed to be causing non-stationarity in the stream flow time series. The study was carried out in two parts, therefore, the findings of the studies and associated conclusions are presented separately for each part.

Part-A: Low-Flow Estimation for Ungauged River Catchments in Ireland

The following conclusions can be drawn from the studies carried out on low-flows for Irish River catchments:

- (i) It was found that a regression based 2-parameter logarithmic type model provides a good approximation to the lower three-quarter part of the Period-of-Record (POR) daily Flow-duration Curves (FDC) at most of the 125 gauging sites in Ireland. Given the complex shape of the observed FDC and the higher variability in the high-flow sections of the FDCs, this study focused on modelling of only the lower three-quarter section of FDC (25%ile to 99.99%ile). The model parameters are found to be strongly correlated (the parameter '*b*' is approximately 4.6558 times the parameter '*a*'). Based on this, the two-parameter FDC model has been approximated by a single parameter model. This approximation of parameter '*b*' was found to be more reliable than estimating it from a catchment physiographic and climatic characteristics based regression procedure. The parameter of the proposed model has been estimated from the easily measurable/obtainable catchment physiographic and climatological characteristics, such as catchment area (AREA), mean annual rainfall (SAAR), mean annual potential evapotranspiration (PE). Two alternative regression based models were proposed for estimating the parameter '*a*' namely (i) AREA-SAAR Model and (ii) MF-Model. The AREA-SAAR Model under-estimates the Q_{95} flows by 7.6% while the MF-Model under-estimates Q_{95} flows by 12.12%. They both perform reasonably well for 25%, 50% and 75%ile flow estimations but less well for the 95%ile flow estimation.

- (ii) A sensitivity analysis on the mean daily flow records for 10 Irish River catchments showed that at least 15 to 20 years of observed streamflow records are required to obtain a reliable long-term POR equivalent estimate of the FDCs and associated low-flow indices. The requirement of this longer record length in the Irish context can be attributed to the significant irregular pattern in decadal climate variability and its impacts on streamflows in contrast to the usual interannual and seasonal variability. The study also showed that the Q_{95} flow estimate from 10 years of records at a site in the study region could deviate (under- or over-estimation) by 20% from the long-term equivalent estimate.

Part-B: Non-Stationarity in Flood Flows and Its Effect on Flood Frequency Growth Curves for Irish River Catchments

The following general conclusions can be drawn from the studies carried out on the non-stationarity in AMF records and its effect on flood frequency growth curves for Irish river catchments. The details of the conclusions have already been presented in Chapters 7.6, 8.4 and 9.4.7.

- (i) Non-stationarity in Irish AMF records:

The results demonstrate that the Irish river catchments are dominated by positive (increasing) trends and these results are comparable with other studies carried out in European rivers. Some temporal variations in the trend test results are also apparent in Irish AMF records. The Annual Maximum Rainfall (AMR) records of Ireland (1955-2008) also showed significant increasing trends, with longer rainfall durations showing greater tendency of trend. Some evidence of spatial patterns in trends in AMF and AMR series was detected by a mapping exercise indicating that climate change may be responsible for the AMF trend.
- (ii) Power of the trend identification test:

The findings of the simulation experiments carried out to identify the power of different trend identification tests (MK, SPR and SLR tests) showed that, in general, the power of a trend test is an increasing function of the trend slope and sample size, i.e. power increases with the increase in trend slope and

sample size in all tests. The simulation results also showed that the sample variance plays a very important role in detecting whether trend exists or not in the records.

(iii) Effects of trend on growth curves and at-site quantiles:

Two different forms of trends were applied, TF-1 and TF-2, in three different spatial patterns. The simulation results show that any trend causes changes in the population parameters, depending on the form and magnitude of trend and type of population distribution. TF-1 generally causes a flattening of growth curves, while TF-2 has the opposite effect. These changes can be as large as 16% at T=100 and trend slope of 1%. Trend effect on quantiles is generally positive, largely caused by an increase in the index flood, with increases up to 17% at T=100 and 1% trend slope. Some unrealistic results emerged in the GEV-GEV simulation case, where large return period floods showed a decrease caused by the estimated GEV k value being (unexpectedly) positive when estimated from the data containing trends.

The simulation results suggest that the increase rate in the at-site quantiles may not be noticeable for a very small trend slope. However, for larger trend slopes the effects could be more noticeable and might have an impact on project safety and costs. In this context careful attention should be given to estimating the design flood quantile where non-stationary properties exist in the data.

10.2 RECOMMENDATIONS

The following recommendations are made for further research:

- (i) Further improvement of the developed low-flow model performance for Ireland can be obtained by incorporating more gauging sites and additional catchment characteristics in estimating the model parameter. It is recommended that 2km x 2km grid based maps of 'Potential Evapotranspiration (PE)' and Net Annual Rainfall (NAR) be prepared for Ireland to assist in estimating the model parameter.

- (ii) It is recommended that an appropriate improved procedure for estimating low-flows from short records should be developed for Ireland. However, the estimated absolute error of 20% might be applied as an adjustment factor for estimating the long-term equivalent Q_{95} flow from 10 years of short records. In the case of low-flow estimates, it is generally advisable to reduce the short-sample estimate by this factor, to avoid any risk of uncertainty in design failure (such as water supply scheme or water quality management measures). A more reliable regional adjustment factor can be obtained by incorporating more sites and forming a larger homogeneous region.

- (iii) The spatial correlations between the significant increasing trends in AMF and AMR records should be investigated through a statistical test to establish the effect of climate change on AMF series in Ireland. A further site-specific study along with the examination of other changes in the catchment characteristics (such as urbanization, forestation, drainage improvement works, flow regulations or abstractions, etc.) should be carried out before coming to a conclusion on the climate change impact on Irish AMF records.

- (iv) Since until now no such acceptable procedure has been developed and/or adopted to deal with the non-stationary properties of data series, the findings of the current study could help hydrologists/engineers to make an allowance in the estimated design flood using the current statistical procedure. This can be done by estimating the extent of trend (trend slope) present in the subject data series and applying an allowance based on the estimated relative differences reported above associated with the design flood estimate. The slope of trend in the data series can be estimated from the Theil (1950) and Sen (1968) proposed method or from the regression slope method.

References

REFERENCES

Part A: Low Estimation for Ungauged Catchments

- Ando, Y., Takahasi, Y., Ito, K., 1986. Regionalisation of parameters by basin geology for use in a groundwater runoff recession equation. IAHS Publication No. 156, pp. 151–159.
- Armbruster, J.T., 1976. An infiltration index useful in estimating low-flow characteristics of drainage basins. *J. Res. USGS* 4 (5), 533–538.
- Armentrout, G.W., Wilson, J.F., 1987. Assessment of low flows in streams in northeastern Wyoming. USGS Water Resources Investigations Report, 85-4246, 30 pp.
- Balco, M., 1976. Relation of the catchment area and its mean runoff to low-flows. *Vodohospodarsky Casopis* 24 (3), 248–257.
- Balco, M., 1977. Multi-parameter regression analysis of low flows. *Vodohospodarsky Casopis* 26 (4), 378–385.
- Barnes, C.R., 1986. Methods for estimating low-flow statistics for ungauged streams in the lower Hudson River basin, NY. USGS Water Resources Investigations Report 85-4070, 22 pp.
- Beard, L.R., 1943. Statistical analysis in hydrology. *Trans ASCE* 1943; vol.108: 1110-60.
- Bingham, R.H., 1986. Regionalization of winter low-flow characteristics of Tennessee streams. USGS Water-Resources Investigations Report 86-4007, 88 pp.
- Bosch, J.M., Hewlett, J.D., 1982. A review of catchment experiments to determine the effect of vegetation changes on water yield and evapotranspiration. *J. Hydrol.* 55, 3–23.
- Bowles, D.S., Riley, J.P., 1976. Low flow modeling in small steep watersheds. *J. Hydraul. Div., ASCE* 102 (HY9), 1225–1239.
- Box GEP, Cox DR. An analysis of transformations. *J R Stat Soc Ser B* 1964; 26: 211-52.
- Bree, T., MacCarthaigh, M., Quinn, R., Fitzpatrick, J., Walsh, R., 2010. Estimation of flow for ungauged catchments for Ireland. Presented at a Continuing Professional Development Event of the Institution of Engineers of Ireland on 29th April, 2010.
- Brilly, M., Kobold, M., Vidmar, A., 1997. Water information management system and low flow analysis in Slovenia. In: *FRIEND'97 — Regional Hydrology: Concepts and Models for Sustainable Water Resource Management*, IAHS Publication No. 246, pp. 117–124.
- Brogan, L., and Cunnane, C, 2006. Low flows and low flow distributions for Ireland. Irish National Hydrology Seminar, 2006, Tullamore, Ireland. pp. 85-92. www.opw.ie/hydrology.
- Browne, T.J., 1981. Derivation of a geologic index for low-flow studies. *Catena* 8, 265–280.
- Brutsaert, W., Neiber, J.L., 1977. Regionalised drought flow hydrographs from a mature glaciated plateau. *Water. Resour. Res.* 13 (3), 637–643.
- Burn, D.H., 1990a. An appraisal of the “region of influence” approach to flood frequency analysis. *Hydrological Science Journal.*, 35, 149-165.
- Burn, D.H., 1990b. Evaluation of regional flood frequency analysis with a region of influence approach. *Water Resources Research*, 26, 2257-2265.

Carty, G. and Cunnane, C., 1990. An evaluation of some methods for determining storage yield relationships for impounding reservoirs. *Journal of the Institution of Water and Environmental Management*, Vo. 4, No. 1 February, 1990.

Castellarin A, Vogel RM, Barth A. A stochastic index flow model of flow duration curves. *Water Resources Research* 2004; 40:W03104. doi:1029/2003WR002524.

Castellarin et al., 2004. Regional flow-duration curves: reliability for ungauged basins. *Advances in Water Resources* 27 (2004) 953-965.

Cervione, M.A., Richardson, A.R., Weiss, L.A., 1993. Low-flow characteristics of selected streams in Rhode Island. *USGS Water-Resources Investigations Report* 93-4046, 16 pp.

Chang, M., Boyer, D.G., 1977. Estimates of low flows using watershed and climatic parameters. *Water Resour. Res.* 13 (6), 997–1001.

Chiew, F.H.S. and T.A. McMahon, 2002: Global ENSO-streamflow teleconnection, streamflow forecasting and interannual variability. *Hydrological Sciences Journal*, 47: 505-522.

Claps P, Fiorentino M. probabilistic flow duration curves for use in environmental planning and management. In: Harmancioglu NB et al., Editors. *Integrated approach to environmental data management systems*. NATO-ASI series. Vol. 2(31). Dordrecht, The Netherlands: Kluwer; 1997, p. 255-66.

Clausen, B., Pearson, C.P., 1995. Regional frequency analysis of annual maximum streamflow drought. *J. Hydrol.* 173, 111–130.

Croker, K.M., A.R. Young, M.D. Zaidman and H.G. Rees, 2003: Flow duration curve estimation in ephemeral catchments in Portugal. *Hydrological Sciences Journal*, 48(3): 427-439.

Cumming Cockburn Ltd, 1990. *Low flow characteristics in Ontario*. Ontario Ministry of the Environment, Canada. 23 pp.

Demuth, S., 1989. Application of the west German IHP Recommendations for the analysis of data from small research basins. *FRIENDS in Hydrology*, IAHS Publication No. 187, pp. 47–60.

Demuth, S., 1993: *Untersuchungen zum Niedrigwasser in West Europa*. Freiburger Schriften zur Hydrologie, Institut für Hydrologie Band 1.

Demuth, S., 1994. Regionalisation of low flows using a multiple regression approach—a review. *Proceedings of the XVIIth Conference of Danube countries*, Budapesht, vol. 1, pp. 115–122.

Demuth, S., 2004: Self Guided Tour - Estimation of low flow indices at the ungauged site. In: *Hydrological Drought Processes and Estimation Methods for Streamflow and Groundwater* (L.M. Tallaksen and H.A.J. van Lanen, eds). *Developments in Water Science*, Elsevier, Amsterdam.

Dingman, S.L., 1978. Synthesis of flow-duration curves for unregulated streams in New Hampshire. *Water Resour. Bull.* 14 (6), 1481–1502.

Dingman, S.L., 2002: *Physical Hydrology*. Second edition, Prentice Hall, New Jersey, United States.

- Dingman, S.L., Lawlor, S.C., 1995. Estimating low flow quantiles from drainage-basin characteristics in New Hampshire and Vermont. *Water Resour. Bull.* 31 (2), 243–256.
- Dooge, J.C.I., 1985. Droughts in Irish History. In de Buitlear, E., (Ed.) *Irish Rivers*, Country House Press, Dublin, pp. 26-28.
- Downer, R.N., 1981. Low-flow studies for Vermont—a prognosis for success. *Hydro Power and Its Transmission in the Lake Champlain Basin. Proceedings of the Eighth Annual Lake Champlain Basin Environmental Conference*, pp. 43–51.
- Fennessey, N., Vogel, R.M., 1990. Regional flow-duration curves for ungauged sites in Massachusetts. *J. Water Resour. Plan. Manag.* 116 (4), 530–549.
- Ferguson, B.K., Suckling, P.W., 1990. Changing rainfall–runoff relationships in the urbanizing peachtree creek watershed, Atlanta, Georgia. *Water Resour. Bull.* 26 (2), 313–322.
- Fleig, A., L.M. Tallaksen, H. Hisdal and S. Demuth, 2006: A global evaluation of streamflow drought characteristics. *Hydrology and Earth System Sciences*, 10: 535-552.
- Franchini M, Suppo M. Regional analysis of flow duration curves for a limestone region. *Water Resour Manage* 1996;10:199-218.
- FREND: Flow Regimes From Experimental And Network Data, 1989. I: Hydrological Studies; II: Hydrological Data, Wallingford, UK.
- FRIEND: Flow Regimes From International Experimental And Network Data, 1994. IAHS Publication No. 221, 525 pp.
- Furness, L.W., 1959. Kansas streamflow characteristics-part 1 – Flow duration. Kansas Water Resources Board technical report no. 1, 1959. 213 p.
- Ganora et al., 2009. A approach to estimate nonparametric flow duration curves in ungauged basins. *Water Resources Research*, vol. 45, W10418, doi: 10. 1029/2008WR007472, 2009.
- Green, C.S., 1986. Preliminary notes on the processing and analysis of hydrological data for groundwater assessment. Department of Mineral Resources Internal Document, Government of Fiji.
- Green, I.R.A., Stephenson, D., 1986. Criteria for comparison of single event models. *Hydrol Sci. J.* 31, 395–411.
- Gustard et al., 2009. Manual on Low-flow Estimation and Prediction. Operational Hydrology Report No. 50. World Meteorological Organisation, WMO-No. 1029.
- Gustard, A., A. Bullock and J.M. Dixon, 1992: Low Flow estimation in the United Kingdom. Institute of Hydrology Report No. 108, Wallingford, United Kingdom.
- Gustard, A., Bullock, A., Dixon, J.M., 1992. Low Flow estimation in the United Kingdom. Institute of Hydrology, Report No. 108, 88 pp., append.
- Gustard, A., Rees, H.G., Croker, K.M., Dixon, J.M., 1997. Using regional hydrology for assessing European water resources.
- Haan, C.T., 1977. *Statistical Methods in Hydrology*. Iowa State University Press, Ames, IA.
- Haines, A.T., Finlayson, B.L., McMahon, T.A., 1988. A global classification of river regimes. *Appl. Geogr.* 8, 255–272.

- Hamilton, D., 1985. Preliminary data compilation for selected drainage basins in Nova Scotia for a low flow regional analysis study. Environment Canada, Inland Waters Directorate, Atlantic Region, Water Planning and Management Branch, Dartmouth, NS. 85-92, 18 pp.
- Hayes, D.C., 1992. Low-flow characteristics of streams in Virginia. USGS Open-File Report 89-586, 85 pp.
- Hisdal, H., B. Clausen, A. Gustard, E. Peters and L.M. Tallaksen, 2004: Event definitions and indices. In: Hydrological Drought - Processes and Estimation Methods for Streamflow and Groundwater (L.M. Tallaksen and H.A.J. van Lanen, eds). Developments in Water Science, 48, Elsevier Science B.V., Amsterdam: 139-198.
- Holmes, M.G.R. and A.R. Young, 2002: Estimating seasonal low flow statistics in ungauged catchments. Proceedings of the British Hydrological Society Eighth National Symposium (Birmingham, 2002).
- Holmes, M.G.R., A.R. Young, A. Gustard and R. Grew, 2002a, 2002b: A region of influence approach to predicting flow duration curves within ungauged catchments. Hydrology and Earth System Sciences, 6 (4): 721-731.
- Holmes, M.G.R., A.R. Young, A. Gustard and R. Grew, 2002a: A new approach to estimating mean flow in the United Kingdom. Hydrology and Earth System Sciences, 6(4): 709-720.
- Holmes, M.G.R., A.R. Young, A.G. Gustard and R. Grew, 2002: A region of influence approach to predicting flow duration curves within ungauged catchments. Hydrology and Earth System Sciences, 6(4): 721-731.
- Hopkinson, C., Young, G.J., 1998. The effect of glacier wastage on the flow of the Bow River at Banff, Alberta, 1951–1993. Hydrol. Processes 12 (10–11), 1745–1762.
- Hughes, D.A., Smakhtin, V.Y., 1996. Daily flow time series patching or extension: a spatial interpolation approach based on flow duration curves. Hydrol. Sci. J. 41 (6), 851–871.
- Hutchinson, P.D., 1990. Regression estimation of low flow in New Zealand. Hydrology Centre Christchurch, NZ Publication 22, 51 pp.
- Hutchinson, P.D., 1993. Calculation of a base flow index for New Zealand catchments. Ministry of Works and Development, Christchurch, NZ Report WS818, 18 pp.
- Institute of Hydrology, 1980. Low Flow Studies (1–4), Wallingford, UK.
- Institute of Hydrology, 1987. Low Flow estimation in Scotland, Wallingford, UK.
- Kachroo, R.K., 1992. Storage required to augment low flows: a regional study. Hydrol. Sci. J. 37, 247–261.
- King, M.C., 1985. A low flow frequency analysis for Irish rivers,. M.Eng.Sc. Thesis, University College, Galway, Ireland, p. 213.
- Kobold, M., Brilly, M., 1994. Low-flow discharge analysis in Slovenia. FRIEND — Flow Regimes from International Experimental and Network Data. IAHS Publication No. 221, pp. 119–131.
- Kundzewicz, Z.W., Robson, A.J., 2000. Detecting trend and other changes in hydrological data. World Climate Change Programme – Data and monitoring, WCDMP-45, WMO/TD-No.1013. CEH Wallingford, UK.
- Laaha, G., Blöschl, G., 2004b. A comparison of low flow regionalization methods – catchment grouping. Journal of Hydrology 2004.

- Laaha, G., Blöschl, G., 2005. Low flow estimates from short stream flow records – a comparison of methods. *Journal of Hydrology* 2005 30692005) 264-286.
- Lacey, G.C., Grayson, R.B., 1998. Relating baseflow to catchment properties in south-eastern Australia. *J. Hydrol.* 204, 231–250.
- LeBoutillier, D.W., Waylen, P.R., 1993. Stochastic model of flow duration curves. *Water Resour. Res.* 29 (10), 3535–3541.
- Leith, R.M., 1978. Streamflow Regionalisation in British Columbia, No. 4: Regression of Low Flows on Physiographic parameters. Report series No. 75, 26 pp.
- Ludwig, A.H., Tasker, G.D., 1993. Regionalization of Low-Flow Characteristics of Arkansas Streams. USGS Water-Resources Investigations Report 93-4013, 19 pp.
- Lundquist, D., Krokli, B., 1985. Low Flow analysis. Norwegian Water Resources and Energy Administration, Oslo, Norway.
- Mac Cárthaigh, M., 1987. "A Statistical Analysis of River Flows - The Southern Water Resource Region". An Foras Forbartha. December 1987.
- Mac Cárthaigh, M., 1984. "A Statistical Analysis of River Flows – The South-eastern Water Resources Region." An Foras Forbartha, Ireland.
- Mac Carthaigh, M., 2002. Parameters of low flow and data on low flows in selected Irish Rivers. National Hydrology Seminar 2002; pp. 64-70.
- MacCarthaigh, M., 1992. Assessment and forecasting of drought flow conditions in Irish rivers. Paper presented to Water and Env. Eng. Section, Inst. Eng. Ire. , Nov. 1992, 33p.
- MacCarthaigh, M., 1999. Surface water resources in Ireland, paper presented to Inst. Eng. Ireland. Water Course, EPA, Dublin, 18p.
- Martin, J.V. and Cunnane, C., 1977. Analysis and prediction of low-flow and drought volumes for selected Irish rivers. The Institution of Engineers of Ireland. 101, 1976-77, 21-28.
- McCummiskey, M., 1981. A review of Ireland's Water Resources. *Irish J. Env. Science.*, 1(2).
- Meigh, J.R., 1987. Low flow analysis of selected catchments in Malawi and Zimbabwe. Preliminary report on the Basement Aquifer Project, Institute of Hydrology, Wallingford, UK.
- Midgley, D.C., Pitman, W.V., Middleton, B.J., 1994. Surface water resources of South Africa 1990. Water Research Commission Report No 298/5.1/94, Pretoria, South Africa.
- Mimikou, M., 1984. Regional relationships between basin size and runoff characteristics. *Hydrol. Sci. J.* 29 (1), 63–73.
- Mimikou, M., Kaemaki, S., 1985. Regionalization of flow duration characteristics. *J. Hydrol.* 82, 77–91.
- Musiake, K., Takahasi, Y., Ando, Y., 1984. Statistical analysis on effects of basin geology on river flow regime in mountainous areas of Japan. Proc. Fourth Cong. Asian & Pacific Reg. Div. Int. Assoc. Hydraul. Res., Bangkok, APD-IAHR/Asian Institute Technology, vol. 2, pp. 1141–1150.
- Nathan, R.J. and T.A. McMahon, 1990: Practical aspect of low-flow frequency analysis. *Water Resources Research*, 26(9): 2135-2141.
- Pater, J.A., 2007. Evaluation of low-flow estimation techniques for ungauged catchments. *Water and Environmental Journal*, 21 ISSN 1747-6585; 2007.

- Pelletier, P.M., Bilozor, W., Glennie, R.A., 1986. Low flow characteristics of selected streams in southern Manitoba. Proceedings of the 16th Canadian Hydrology Symposium: Drought - the Impending Crisis? Regina, Saskatchewan, pp. 159–174.
- Pereira, L.S., Keller, H.M., 1982. Recession characteristics of small mountain basins, derivation of master recession curves and optimization of recession parameters. IAHS Publication No. 138. pp. 243–255.
- Pilon, P.J., Condie, R., 1986. Median drought flows at ungauged sites in southern Ontario. Proceedings of the 16th Canadian Hydrology Symposium: Drought — the Impending Crisis? Regina, Saskatchewan, pp. 189–196.
- Pirt, J., Simpson, M., 1983. The Estimation of river flows. Severn Trent Water Authority, UK, 41 pp., append.
- Pol, R.A., 1985. Flow duration and low flow frequency analyses for selected watersheds in the Atlantic Provinces. Environment Canada, Inland Waters Directorate, Atlantic Region, Water Resources Branch, vols. 85–80, 20 pp.
- Quimpo, R.G., Alejandrino, A.A., McNally, T.A., 1983. Regionalised flow duration curves for Philippines. J. Water Res Plan. Manag., ASCE 109 (4), 320–330.
- Ries III, K.G., 1994. Development and application of generalized least- squares regression models to estimate low-flow. USGS Water-Resources Investigations Report 94-4155, 33 pp.
- Risle, J.C., 1994. Estimating the magnitude and frequency of low flows of streams in Massachusetts. USGS Water-Resources Investigations Report 94-4100, 34 pp.
- Robson, A., and Reed, D.W., 1999. Statistical Procedures for Flow Frequency Estimation. Flood Estimation Handbook. Vol. 3. Institute of Hydrology, Wallingford, UK.
- Sakovich, V.M., 1995. Regional estimation method of minimum river flows from river basin characteristics. Proceedings of the International Symposium on Runoff Calculations for Water Projects. St. Petersburg, Russia.
- Searcy, J.C., 1959. Flow duration curves. United States Geological Survey, Washington, DC, Water Supply Paper 1542A.
- Singh RD, Mishra SK, Chowdhury H. Regional flow-duration models for large number of ungauged Himalayan catchments for planning microhydro projects. J. Hydrol Eng 2001;6(4):310-6
- Singh, K.P., 1971. Model flow duration and streamflow variability. Water Resour. Res. 7 (4), 1031–1036.
- Smakhtin V.Y., Watkins, D.A., 1997. Low-flow estimation in South Africa. Water Research Commission Report No. 494/1/97, Pretoria, South Africa.
- Smakhtin, V.U. and B. Masse, 2000: Continuous daily hydrograph simulation using duration curves of precipitation index. Hydrological Processes, 14: 1083-1100.
- Smakhtin, V.U., 2001: Low Flow Hydrology: A Review. Journal of Hydrology, 240 (3-4): 147-186.
- Smakhtin, V.U., E. Creuse-Naudine and D.A. Hughes, 1997: Regionalisation of daily flow characteristics in part of the Eastern Cape, South Africa. Hydrological Sciences Journal, 42(6): 919-936.

- Smith, R.W., 1981. Rock type and minimum 7-day/10-year flow in Virginia streams. Virginia Water Resource Research Center, Virginia Polytechnique Institute and State University, Blacksburg, Bulletin, vol. 116, 43 pp.
- Smyth, A.J., 1984. An Analysis of low flow data. M. Eng. Sc. Thesis. University College Galway, Ireland. p. 171.
- Srikanthan, R., McMahon, T.A., 1986. Recurrence interval of long hydrologic events. J. Hydraul. Eng. 112, 518–538.
- Stahl, K., Demuth, S., 1999. Linking streamflow drought to the occurrence of atmospheric circulation pattern. Hydrol. Sci. J. 44 (3), 467–482.
- Studley SE. Estimated flow-duration curves for selected ungauged sites in Kansas. US Geological Survey. Water-resources investigations report 01-4142, 2001.
- Tallaksen, L.M. and H.A.J. van Lanen (eds), 2004: Hydrological Drought: Processes and Estimation Methods for Streamflow and Groundwater. Developments in Water Science, 48, Elsevier Science B.V., Amsterdam.
- Tallaksen, L.M., 2000: Streamflow drought frequency analysis. In: Drought and Drought Mitigation in Europe (J.V. Vogt and F. Somma, eds). Advances in Natural and Technological Hazards Research, 14, Kluwer Academic Publishers, Dordrecht, the Netherlands, pp. 103-117.
- Tallaksen, L.M., H. Madsen and B. Clausen, 1997: On the definition and modelling of streamflow drought duration and deficit volume. Hydrological Sciences Journal, 42(1): 15-33.
- Tallaksen, L.M., H. Madsen and H. Hisdal, 2004: Frequency analysis. In: Hydrological Drought - Processes and Estimation Methods for Streamflow and Groundwater (L.M. Tallaksen and H.A.J. van Lanen). Developments in Water Sciences 48, Elsevier B.V., the Netherlands, pp. 199-271.
- Tallaksen, L.M., Hisdal, H., 1997. Regional analysis of extreme streamflow drought duration and deficit volume. FRIEND'97 – Regional Hydrology: Concepts and Models for Sustainable Water Resource Management, IAHS Publication No. 246, pp. 141–150.
- Tallaksen, L.M., Madsen, H., Clausen, B., 1997. On the definition and modeling of streamflow drought duration and deficit volume. Hydrol. Sci. J. 42 (1), 15–33.
- Tasker, G.D., 1989. Regionalization of low flow characteristics using logistic and GLS regression. New directions for surface water modeling. Proceedings of the Baltimore Symposium. IAHS Publication No. 181, pp. 323–331.
- Tjomsland, T., Ruud, E., Nordseth, K., 1978. The physiographic influence on recession runoff in small Norwegian rivers. Nordic Hydrol. 9, 17–30.
- Vogel, R.M., Fennessey, N.M., 1990. Regional flow duration curves for ungauged sites in Massachusetts. Journal of Water Resources Planning and Management, ASCE 1990:116(4):530-549.
- Vogel, R.M., Fennessey, N.M., 1994. Flow duration curves. I. A new interpretation and confidence intervals. J. Water Resour. Plan. Manag. 120 (4), 485–504.
- Vogel, R.M., Fennessey, N.M., 1995. Flow duration curves. II. a review of applications in water resource planning. Water Resour. Bull. 31 (6), 1029–1039.
- Vogel, R.M., Kroll, C.N., 1989. Low-flow frequency analysis using probability-plot correlation coefficients. J. Water Res. Plan. Manag. (ASCE) 115 (3), 338–357.

- Vogel, R.M., Kroll, C.N., 1991. The value of streamflow record augmentation procedures in low-flow and flood-flow frequency analysis. *J. Hydrol.* 125, 259–276.
- Vogel, R.M., Kroll, C.N., 1992. Regional geohydrologic - geomorphic relationships for the estimation of low-flow statistics. *Water Resour. Res.* 28 (9), 2451–2458.
- Vogel, R.M., Kroll, C.N., 1996. Estimation of baseflow recession constants. *Water Resour. Manag.* 10, 303–320.
- Vogel, R.M., Stedinger, J.R., 1985. Minimum variance streamflow record augmentation procedures. *Water Resour. Res.* 21 (5), 715–723.
- Vogel, R.M., Wilson, I., 1996. Probability distribution of annual maximum, mean, and minimum streamflows in the United States. *J. Hydrol. Eng.* 1 (2), 69–76.
- White, E.L., 1977. Sustained flow in small Appalachian watersheds. *J. Hydrol.* 32, 71–86.
- Wilcock, D.N., Hanna, J.E., 1987. Derivation of flow duration curves in Northern Ireland. *Proc. Inst. Civil Engrs.* 83 (2), 381–396.
- World Meteorological Organisation, (WMO), 1974. *International Glossary of Hydrology*, WMO, Geneva.
- Yevjevich, V., 1972. *Probability and Statistics in Hydrology*. Water Resources Publications, Fort Collins, CO, USA, 302 pp.
- Yevstigneev, V.M., 1990. *Rechnoj stok and gidrologicheskie raschety (River runoff and hydrological calculations)*. Moscow University, Moscow, 304 pp.
- Young, A.R., 2006: Stream flow simulation within UK ungauged catchments using a daily rainfall-runoff model. *Journal of Hydrology*, 320(1-2): 155-172.
- Young, A.R., A. Gustard, A. Bullock, A.E. Sekulin and K.M. Croker, 2000: A river network based hydrological model for predicting natural and influenced flow statistics at ungauged sites. *Science of the Total Environment*, 251-252: 293-304.
- Young, A.R., R. Grew and M.G.R. Holmes, 2003: LowFlows 2000: A national water resources assessment and decision support tool. *Water Science and Technology*, 48(10): 119-126.
- Yu PS, Yang TC, Wang YC. Uncertainty analysis of regional flow duration curves. *J Water Resour Plann Manage*, ASCE 2002;128(6): 424-30.

Part B: Non-stationarity in Flood Flows and Its Effect on Flood Frequency Growth Curves for Irish River Catchments

Adamowski, K., Bocci, C., 2001. Geostatistical regional trend detection in river flow data. *Hydrological Processes* 15, 3331–3341.

Arnell, N. 2006. The implication of climate change from hydrological regimes and water resources; An overview. Irish National Hydrology Seminar, 2006. pp. 1-7.

Anrnell, N.W. and Gabrielle, S., S., 1985. Regional flood frequency analysis with the two-component extreme value distribution: An assessment using computer simulation experiments. Workshop on combined efficiency of direct and indirect estimations for point and regional flood prediction, Perugia, Italy, December.

Anrnell, N.W. and Gabrielle, S., S., 1988. The performance of the two component extreme value distribution in regional flood frequency analysis. *Water Resources Research*, 24(6), 879-887.

Adlouni, S. El., Ouarda, T.B.M.J., Zhang, X., Roy, R. and Bobée, B., 2007. Generalised maximum likelihood estimators for the non-stationary generalized extreme value model. *Water Resources Research*, Vol. 43, W03410, doi: 1029/2005WR00545, 2007.

Barlow, M., S. Nigam and E.H. Berbery. 2001. ENSO, Pacific decadal variability, and U.S. summertime precipitation, drought, and stream flow. *J. Climate* 14: 2105-2127.

Barnard, G.A., 1959. Control charts and stochastic processes. *Journal of the Royal Statistical Society, Series B*, 21:239-244.

Bloomfield, P. & Steiger, W. L., 1983. *Least Absolute Deviations: Theory, Applications, and Algorithms*. Birkhauser, Boston, Massachusetts, USA.

Buishand, T. A., 1982. Some methods for testing the homogeneity of rainfall records. *J. Hydrol.* 58, 11–27.

Buishand, T. A., 1984. Tests for detecting a shift in the mean of hydrological time series. *J. Hydrol.* 73, 51–69.

Burn, D.H. 1994a. Hydrologic effects of climate change in west-central Canada. *Journal of Hydrology* 160, 53-70.

Burn, D.H. 1994b. Identification of a data collection network for detecting climate change, *Canadian Water Resources Journal* 19, 27-38.

Burn, D.H. and M.A. Hag Elnur. 2002. Detection of hydrologic trend and variability. *J. Hydrol.* 255: 107-122.

Burn, D.H., 1990: Evaluation of regional flood frequency-analysis with a region of influence. *Water Resources Research*, 26, 2257-2265.

Castellarin, A., Burn, D.H., and Brath, A. 2001. Assessing the effectiveness of hydrological similarity measures for flood frequency analysis, *J. Hydrology*, 241, 270-285.

Chiew, F. H. S. & McMahon, T. A., 1993. Detection of trend or change in annual flow of Australian rivers. *Int. J. Climatol.* 13, 643–653.

- Cleary, J.A., Levenbach, H., 1982. *The Professional Forecaster*. Lifetime Learning Publications, Belmont, California.
- Cleveland, W. S., 1994. *The Elements of Graphing Data*. Hobart Press, New Jersey, USA.
- Coles, S., 2001. *An Introduction to Statistical Modeling of Extreme Values*. Springer, London (208 pp).
- Cox, D.R., Isham, V.S. and Northrop, P.J., 2002. Floods: some probabilistic and statistical approaches. *Philosophical Transactions of Royal Society London, Series A* vol. 360, 1389-1408.
- Cunderlik, J.M. and D.H. Burn. 2002. Local and regional trends in monthly maximum flows in southern British Columbia. *Can. Water Resour. J.* 27: 191-212.
- Cunderlik, J.M. and D.H. Burn. 2003. Non-stationary pooled flood frequency analysis. *Journal of Hydrology* 276 (2003) 210-223.
- Cunnane, C., 1988. Methods and merits of regional flood frequency analysis. *Journal of Hydrology*, 100, 269-90.
- Cunnane, C., 1989. Statistical Distributions for flood frequency analysis. WMO., Operational Hydrology Report No. 33. WMO. No. 718.
- Das, S., Cunnane, C., 2011. Examination of homogeneity of selected Irish pooling groups. *Hydrol. Earth Syst. Science*, 15, 819-830.
- Davidson, A. C. & Hinkley, D. V., 1997. *Bootstrap Methods and Their Application*. Cambridge University Press, Cambridge, UK.
- Dixon, H., Lawler, D.M., Shamseldin, A.Y., 2006. Streamflow trends in western Britain. *Geophys. Res. Lett.* 32. doi:10.1029/2006GL027325.
- Douglas, E.M., Vogel, R.M., Knoll, C.N., 2000. Trends in flood and low flows in the United States: impact of spatial correlation. *J. Hydrol.* 240, 90–105.
- Ecology and Hydrology. *Flood Estimation Handbook Vol 1-5*, 1999
- Efron, B. & Tibshirani, R. J., 1998. *An Introduction to the Bootstrap*. Chapman & Hall, London, UK (436pp.)
- Efron, B., 1982. The jackknife, the bootstrap, and other resampling plans, Society for Industrial and Applied Mathematics, Philadelphia.
- El-Adlouni, S., Ouarda, T.B.M.J., Zhang, X., Roy, R., Bobee, B., .2005. Generalised maximum likelihood estimators for the nonstationary GEV model. *Water Resources Research*, vol. 43, W03410, doi:1029/2005WR004545, 2007.
- Elmore, K.L., Baldwin, M.E., Schultz, D.M., 2006. Field significance revisited: spatial bias errors in forecasts as applied to the eta model. *Monthly Weather Rev.* 134, 519–531.
- F. Chiew, L.Siriwardena, Sylvan Arene and J. Rahman, 2005. TREND software for tren/change detection in hydrological data. University of Melbourne, Catchment Research Centre for Catchment Hydrology, (www.toolkit.net.au/trend), 2005.
- Fitzgerald, D.L. 2007. Estimation of Point Rainfall Frequencies, Met Eireann Technical Note No. 61.

Good, P., 1993. *Permutation Tests: A Practical Guide to Resampling Methods for Testing Hypotheses*. Springer-Verlag, Berlin, Germany.

Greenwood, J.A., Landwehr, J.M., Matalas, N.C., and Wallis, J.R. 1979. Probability weighted moments – definition and relation to parameters of several distributions expressible in inverse form, *Water Resources Research*, 15, 1049-1054.

GREHYS, 1996. Presentation and review of some methods for regional flood frequency analysis. *Journal of Hydrology* 18691-4, 63-84.

Grubb, H. & Robson, A., 2000. Exploratory/visual analysis. In: *Detecting Trend and Other Changes in Hydrological Data* (ed. by Z. W. Kundzewicz & A. Robson), 19–47. World Climate Programme—Water, World Climate Data and Monitoring Programme, WCDMP-45, WMO/TD no. 1013. World Meteorological Organization, Geneva, Switzerland.

Haan, C.T., 1977. *Statistical Methods in Hydrology*. The Iowa State University Press, Ames, Iowa (378 pp).

Hannaford, J., Marsh, T., 2006. An assessment of trends in UK runoff and low flows using a network of undisturbed catchments. *Int. J. Climatol.* 26, 1237– 1253.

Harvey, K.D., P.J. Pilon and T.R. Yuzyk. 1999. Canada's reference hydrometric basin network (RHBN). In *Proceedings of the CWRA 51st Annual Conference*, Nova Scotia.

Helsel, D. R. & Hirsch, R. M., 1992. *Statistical Methods in Water Resources*. Studies in Environmental Science 49. Elsevier, Amsterdam, The Netherlands.

Hipel, K.W. and McLeod, A.I., 1989. Intervention analysis in environmental engineering. *Environmental Monitoring Assessment*. 12: 185-201.

Hipel, K.W., 1985. *Time Series Analysis in Water Resources*. American Water Resources Association, Bethesda, Maryland.

Hipel, K.W., McLeod, A.I. and Weiler, R.R., 1988. Data analysis of water quality time series in Lake Eire. *Water Resources Bulletin* 24(3) 533-544.

Hipel, K.W., McLeod, A.I., 1994. *Time Series Modeling of Water Resources and Environmental Systems*. Elsevier, Amsterdam (p. 853-938).

Hirsch, R. M. & Slack, J. R., 1984. A nonparametric test for seasonal data with seasonal dependence. *Water Resour. Res.* 20, 727–732.

Hirsch, R. M., Slack, J. R. & Smith R. A., 1982. Techniques of trend analysis for monthly water quality data. *Water Resour. Res.* 18, 107–121.

Hirsch, R.M., Alexander, R.B., Smith, R.A., 1991. Selection of methods for the detection and estimation of trends in water quality. *Water Resources Research*, 27, 803-813.

Hisdal, H., Stahl, K., Tallaksen, L.M., Demuth, S., 2001. Have streamflow droughts in Europe become more severe or frequent? *Int. J. Climatol.* 21, 317–333.

Holder, R.L., 1985. *Multiple Regression in Hydrology*. Institute of Hydrology, Wallingford, UK.

Hollander, M. and Wolfe, D.A., 1973. *Nonparametric Statistical methods*. Wiley, New York.

Hosking J.R.M, Wallis, J.R., and Wood, E.F., 1985a. An appraisal of the regional flood frequency procedure in the UK Flood Studies report, *Hydrol. Sc. J.*, 30(1), 85-109.

- Hosking, J.R.M and Wallis, J.R., 1993: Some statistics useful in regional frequency analysis. *Water Resources research*, 29, 271-281, 1993.
- Hosking, J.R.M. and J.R. Wallis , 1997: *Regional frequency analysis: An approach based on L-moments*. Cambridge University Press.
- Hosking, J.R.M., 1990: L-moments: Analysis and estimation of distributions using linear combinations of order statistics. *Journal of the Royal Statistical Society*, B 52(1): 105-124.
- Hosking, J.R.M., Wallis, J.R. and Wood, E.F. (1985b). Estimation of the generalised extreme value distribution by the method of probability – weighted moments. *Technometrics*, 27, 251-261.
- IPCC, 2007. *Climate Change 2007. The Physical Science Basis. Contribution of Working Group I to the Fourth Assessment Report of the Intergovernmental Panel on Climate Change (IPCC)*.
- IPCC. *Climate Change 2007. The Physical Science Basis - Summary for Policymakers. Contribution of Working Group I to the Fourth Assessment Report of the Intergovernmental Panel on Climate Change*. February 2007.
- IPPC, 1996. *Climate change 1995. The second IPC Scientific assessment*. In: Houghton, J.T., Meria Filho, L.A., Callender, B.A. (Eds). *Intergovernmental Panel on Climate Change*. Cambridge University Press, Cambridge, UK.
- IPPC, 2001. *Climate Change 2001. Impacts, Adoption and Vulnerability. Contribution of Working Group II to the Third Assessment of the IPCC on Climate change*. Cambridge University Press, Cambridge, UK.
- IPPC, 2001. *Climate Change 2001. The Scientific Basis. Contribution of Working Group I to the Third Assessment Report of IPCC on Climate change*. Cambridge University Press, Cambridge, UK.
- Jain, S., Lall, U., 2001. Floods in changing climate: does the past represent the future? *Water Resources Research* 37 (12) 3193-3205.
- Jenkins, G.M. and Watts, D.G., 1968. *Spectral analysis and its applications*. Holden-day, San Francisco.
- Katz, R.W., Parlange, M.B., Naveau, P., 2002. Statistics of extremes in hydrology. *Adv. Water Resour.* 25, 1287–1304.
- Kendall, M.G., Stuart, A., Ord, J.K. 1983. *The Advanced Theory of Statistics, Volume 3*. Griffin, London.
- Kendall, M.G., 1975. *Rank Correlation Methods*. Charless Griffin, London.
- Khaliq, M.N., Ouarda, T.B.M.J., Gachon, P., 2009. Identification of temporal trends in annual and seasonal low flows occurring in Canadian rivers: The effect of short- and long-term persistence. *Journal of Hydrology*, 369(2009) 183-197.
- Khaliq, M.N., Ouarda, T.B.M.J., Gachon, P., Sushama, L. and St-Hilarie, A., 2009. Identification of hydrological trend in the presence of serial and cross correlations: A review of selected methods and their application to annual flow regimes of Canadian rivers. *Journal of Hydrology*, 368(2009) 117-130.

Khaliq, M.N., Ouarda, T.B.M.J., Gachon, P., Sushama, L., 2008. Temporal evolution of low flow regimes in Canadian rivers. *Water Resour. Res.* 44, W08436. doi:10.1029/2007WR006132.

Khaliq, M.N., Ouarda, T.B.M.J., Ondo, J.-C., Gachon, P., Bobée, B., 2006. Frequency analysis of a sequence of dependent and/or non-stationary hydrometeorological observations: a review. *J. Hydrol.* 329, 534–552.

Kiely, G., Albertson, J.D., Parlange, M.B., 1998. Recent trends in diurnal variation of precipitation at Valentia on the west coast of Ireland. *Journal of Hydrology*, 207, 270-279.

Kiely, G., 1999. Climate change in Ireland from precipitation and streamflow observations. *Advances in Water Resources* 23(1999) 141-151.

Kim, P. J. and Jennrich, R. I. (1973). Tables of the exact sampling distribution of the two-sample Kolmogorov-Smirnov criterion, D_{mn} , $m \leq n$. In *Selected Tables in Mathematical Statistics* (Edited by H. L. Harter and D. B. Owen), Vol. I. American Mathematical Society.

Kjeldsen, T.R. and Jones, D. A., 2009. A formal statistical model for pooled analysis of extreme floods. *Hydrol. Research*, 40, 465-480.

Kuczera, G., 1982. Robust flood frequency models. *Water Resources Research*, 18(2), 315-324.

Kuczera, G., 1982a. Combining site-specific and regional information. An empirical bayes approach. *Water Resources Research*, 18(20), 306 – 314.

Kulkarni, A., von Storch, H., 1995. Monte Carlo experiments on the effect of serial correlation on the Mann–Kendall test of trend. *Meteorol. Z.* 4 (2), 82–85.

Kundzewicz, Z. W. & Robson, A. (eds) (2000) *Detecting Trend and Other Changes in Hydrological Data*. World Climate Programme—Water, World Climate Programme Data and Monitoring, WCDMP-45, WMO/TD no. 1013. World Meteorological Organization, Geneva, Switzerland.

Kundzewicz, Z.W. 2004. Detection of change in world-wide hydrological time series of maximum annual flow. GRDC Report Series, Report No. 32.

Kundzewicz, Z.W. 2004. Searching for change in hydrological data. *Hydrological Science Journal*. 49(1) (2004) 3-6.

Kundzewicz, Z.W., 2005. Change detection in high river flows in Europe. 49(1) (2004) 7-19. Regional Hydrological Impacts of Climate Change – Hydroclimatic Variability. Proceedings of symposium S6 held during the 7th IAHS Scientific Assembly at Foz do Iguacu, Brazil, April 2005, IAHS Publ. 296, 71-80.

Kundzewicz, Z.W., Graczyk, D., Maurer, T., Pinskiwar, I., Radziejewsky, M., Svensson, C., Szwed, M., 2005. Trend detection in river flow series: 1. Annual maximum flow. *Hydrol. Sci. J.* 50 (5), 797–810.

Kundzewicz, Z.W., Robson, A.J., 2004. Change detection in hydrological records – a review of the methodology. *Hydrological Science Journal*. 49(1) (2004) 7-19.

Landwehr, J.M., Tasker, G.D. and Jarret, R.D., 1987. Discussion of “Relative Accuracy of log-Pearson III procedures” by Wallis and Wood (1985). *ASCE, Journal of Hydraulic Engineering*, 113(9), 1206-1210.

- Lang, M., Ouarda, T.B.M.J., Bobee, B., 1999. Towards operational guidelines for over-threshold modeling. *Journal of Hydrology* 225, 103-117.
- Leahy, P., Kiely, G. 2009. Ireland's changing precipitation patterns. HMRC Flood Defences & Coastal Seminar, University College, Cork, January 2009.
- Leclerc, M. and Ouarda, T.B.M.J., 2007. Non-stationary regional flood frequency analysis at ungauged sites. *Journal of Hydrology*, 343, 254-265.
- Lehmann, E.L., 1975. *Nonparametric: Statistical Methods Based on Ranks*. Holden-Day, Oakland, California.
- Lettenmaier, D.P., 1976. Detection of trend in water quality data from records with dependent observations. *Water Resour. Res.* 12 (5), 1037-1046.
- Lettenmaier, D.P., Burges, S.J., 1978. Climate change: detection and its impact on hydrologic design. *Water Resour. Res.* 14 (4), 679-687.
- Lettenmaier, D.P. and Potter, K.W., 1985. Testing flood frequency estimation methods using regional flood generation model. *Water Resources research*, 21, 1903-14.
- Lettenmaier, D.P., Wallis, J.R. and Wood, E.F., 1987. Effect of regional heterogeneity on flood frequency estimation. *Water Resources Research*, 23, 313-323, 1987.
- Lettenmaier, D.P., Wood, E.F., Wallis, J.R., 1994. Hydro-climatological trends in the continental United States, 1948-88. *J. Climate* 7 (4), 586-607.
- Lettenmaier, D.P., Wallis J.R., and Wood, E.F., 1985. Note on the comparative robustness of estimates of extreme flood quantiles. Presented at American Geophysical Union, Spring Meeting Baltimore.
- Lindstrom, G. and Bergstrom, S., 2004. Runoff trends in Sweden 1807-2002. *Hydrological Science Journal*, 49(1), 69-83.
- Lins, H.F., Slack, J.R., 1999. Streamflow trends in the United States. *Geophys. Res. Lett.* 26 (2), 227-230.
- Lu, L.H. and Stedinger, J.R., 1992b. Variance of two- and three- parameter GEV/PWM quantile estimators: Formulae, confidence intervals, and a comparison. *Journal of Hydrology*, 138, 247-67.
- Lu, L.H. and Stedinger, J.R. 1992. Sampling variance of normalised GEV PWM quantile estimators and a regional homogeneity test. *J. Hydrology*, 138, 223-245.
- M. Radziejewski and Z.W. Kundzewicz. HYDROSPECT – software for detecting changes in hydrological data, June 2004.
- Madsen, H., Pearson, C.P., Rosbjerg, D., 1997b. Comparison of annual maximum series and partial duration series methods for modeling extreme hydrologic events. 2. Regional modelling. *Water Resources Research* 33(4), 759-769.
- Madsen, H., Rasmussen, P.F., Rosbjerg, D., 1997a. Comparison of annual maximum series and partial duration series methods for modeling extreme hydrologic events. 1. At-site modelling. *Water Resources Research* 33(4), 747-757.
- Mann, H.B., 1945. Non-parametric tests against trend. *Econometrica* 13, 245-259.

- McGilchrist, C. A. & Woodyer, K. D. (1975) Note on a distribution-free CUSUM technique. *Technometrics* 17(3), 321–325.
- McLeod, A.I., Hipel, K.W. and Bodo, B.A., 1991. Trend analysis methodology for water quality time series. *Environmetrics* 292): 169-200.
- Milly, P.C.D., Wetherald, R.T., Dunne, K.A. and Delworth, T.L., 2002. Increasing risk of great floods in a changing climate, *Nature* 415, 514-517.
- Mortsch, L., Hengeveld, H., Lister, M., Lofgren, B., Quinn, F., Slivitzky, M., Wenger, L., 2000. Climate change impacts on the hydrology of the Great Lakes-St. Lawrence system. *Canadian Water Resources Journal* 25(2), 153-179.
- Mudelsee, M., Börngen, M., Tetzlaff, G., Grünewald, U., 2003. No upward trends in the occurrence of extreme floods in central Europe. *Nature* 421, 166-169.
- Mudelsee, M., Börngen, M., Tetzlaff, G., Grünewald, U., 2004. Extreme floods in central Europe over the past 500 years: role of cyclone pathway “Zugstrasse Vb”. *Journal of Geophysical Research* 109, 1–21. doi:[10.1029/2004JD005034](https://doi.org/10.1029/2004JD005034).
- Mudelsee, M., Deutsch, M., Börngen, M., Tetzlaff, G., 2006. Trends in flood risk of the river Werra (Germany) over the past 500 years. *Hydrological Sciences Journal* 51 (5), 818–833 (Special Issue Historical Hydrology).
- NERC (Natural Environment Research Council). Flood Studies Report. 1975.
- Nobillis, F. and Lorenz, P., 1997. Flood trends in Austria. IAHS Publ. 239 IAHS Press, Wallingford, UK.
- OPW Flood Studies Update Programme, Work-Package 2.2 “ Flood Frequency Analysis” - Analysis of Trend in Irish Annual Maximum Flood Series, July 2009, National University of Ireland, Galway, Department of Engineering Hydrology.
- Ouarda, T.B.M.J., M. Lang, B. Bobée, J. Bernier, P. Bois, 1999. Synthèse de modèles régionaux d’estimation de crue utilisés en France et au Québec. *Rev.Sci. Eau*, 12, 155-182.
- Petrow, T. and Merz, Bruno, 2009. Trends in flood magnitude, frequency and seasonality in Germany in the period 1951-2002. *Journal of Hydrology* 371 (2009) 129-141.
- Pettitt, A. N., 1979. A non-parametric approach to the change point problem. *Appl. Statist.* 28, 126–135.
- Pilon, P. (2000) Criteria for the selection of stations in climate change detection network. In: *Detecting Trend and Other Changes in Hydrological Data* (ed. by Z. W. Kundzewicz & A. Robson), 121–131. World Climate Programme— Water, World Climate Data and Monitoring Programme, WCDMP-45, WMO/TD no. 1013, World Meteorological Organization, Geneva, Switzerland.
- Pilon, P.J. and S. Yue. 2002. Detecting climate-related trends in streamflow data. *Water Sci. Technol.* 8(45): 89-104.
- Porporato, A., Roidolfi, L., 1998. Influence of week trends in exceedance probability. *Stochastic Hydrology and Hydraulics* 12, 1-14.
- Potter, K.W. and Lettenmaier, D.P., 1990. A comparison of regional flood frequency estimation methods using a resampling method. *Water Resources research*, 26, 415-24.

- Radziejewski, M., Bardossy, A. & Kundzewicz, Z. W. (2000) Detection of change in river flow using phase randomization. *Hydrol. Sci. J.* **45**(4), 547–558.
- Ramesh, N.I., Davison, A.C., 2002. Local models for exploratory analysis of hydrological extremes. *Journal of Hydrology* 256, 106-119.
- Robson A.J. and Reed D.W., 1996. Non-stationarity in UK flood records. Flood Estimation Handbook Note No. 24, Report to MAFF, Project FD 0409, Institute of Hydrology, Wallingford, Oxfordshire, U.K., 1996.
- Robson, A. J., Jones, T. A. & Reed, D. W., 1998. A study of national trend and variation in UK floods. *Int. J. Climatol.* **18**, 165–182.
- Robson, A.J., 2002. Evidence for trends in UK flooding. *Philosophical Transactions of the Royal Society of London A* 360, 1327–1343.
- Rood, S.B., Samuelson, G.M., Weber, J.K., Wywrot, K.A., 2005. Twentieth-century decline in streamflows from the hydrological apex of North America. *J. Hydrol.* 306, 215–233.
- Salas, J.D. and D.C. Boes, 1980: Shifting level modelling of hydrologic series. *Advances in Water Resources*, 3: 59-63.
- Salas, J.D., 2000: Stochastic analysis and modelling for simulation and forecasting, Consulting report for Hydro-Quebec, Colorado State University.
- Salas, J.D., Delleur, J.W., Yevjevich, V.M., Lane, W.L., 1980. Applied Modeling of Hydrologic Time Series. Water Resources Publications, Littleton, Colorado (484 pp).
- Sen, P.K., 1968. Estimates of the regression coefficient based on Kendall's tau. *Journal of the American Statistical Association* 63, 1379–1389.
- Siegel, S. & Castellan, N. J., 1988. *Non-parametric Statistics for the Behavioural Sciences*. McGraw-Hill, New York, USA.
- Siegel, S., 1956. *Nonparametric Statistics for Behavioural Sciences*. McGraw-Hill, New York.
- Sneyers, R., 1975. *Sur l'analyse statistique des series d'observations*. WMO Technical Note no. 143. World Meteorological Organization, Geneva, Switzerland.
- Sneyers, R., 1990. On the Statistical Analysis of series of Observations. World Meteorological Organisation. Technical Note no. 143, WMO no. 415.
- Srikanthan, R. and McMahon, T.A. and J.L. Irish, 1983. Time series analysis of annual flows of Australian rivers. *Journal of Hydrology* 66; 213-276, 1983.
- Stedinger, J.R. and Lu, L.H., 1995. Appraisal of regional and index flood quantile estimators, *Stoch. Hydrology and Hydraulics*, 9, 49-75.
- Stedinger, J.R., Vogel, R.M., and Foufoula Georgiou, E., 1992. Frequency analysis of extreme events. In *Handbook of Hydrology*, edited by D.R. Maidment, Chapter 18, McGraw-Hill, New York.
- Strupczewski, W.G., Kaczmarek, Z., 2001. Non-stationary approach to at-site frequency modelling II. Weighted least squares estimation. *Journal of Hydrology* 248, 143-151.
- Strupczewski, W.G., Singh, V.P., Feluch, W., 2001a. Non-stationary approach to at-site flood frequency modeling I. Maximum likelihood estimation. *J. Hydrol.* 248, 123–142.

- Strupczewski, W.G., Singh, V.P., Mitosek, H.T., 2001b. Non-stationary approach to at-site flood frequency modeling III. Flood analysis of Polish rivers. *J. Hydrol.* 248, 152–167.
- Svensson, C. and Kundzewicz, Z.W. and Maurer, T. 2004a. Trends in flood and low flow series. Report to the World Climate Programme – Water and Global Runoff Data Centre. ECASP-64, WMO Geneva, Switzerland.
- Svensson, C., Hannaford, J., Kundzewicz, Z., Marsh, T., 2006. Trends in river flows: why is there no clear signal in observations? In: *Frontiers in Flood Research*, IAHS Publ. 305, pp. 1–18.
- Svensson, C., Kundzewicz, Z.W., Maurer, Th., 2005. Trend detection in river flow series: 2 flood and low-flow index series. *Hydrological Sciences Journal* 50 (5), 811–824.
- Tong, H., Thanoon, B., Gudmundsson, G., 1985. Threshold time series modelling of two Icelandic riverflow systems. *Water Resources Bulletin*, 21(4):651-661.
- Tufte, E. R. (1983) *The Visual Display of Quantitative Information*. Graphics Press, Cheshire, Connecticut, USA.
- Tukey, J.W., (1977). *Exploratory Data Analysis*. Addison-Wesley, Reading, Massachusetts.
- Von Storch, H., 1995. Misuses of statistical analysis in climate research. In: von Storch, H., Navarra, A. (Eds.), *Analysis of Climate Variability: Applications of Statistical Techniques*. Springer-Verlag, Berlin, pp. 11–26.
- Von Storch, H., Cannon, A.J. (Eds.), 1995. *Analysis of Climate Variability – Applications of Statistical Techniques*. Springer Verlag, New York. 334 pp.
- Walpole R.E. and Myers R.H., 1978. *Probability and statistics for Engineers and Scientists*. MacMillan Publishing Company, New York, pp. 615-646.
- Wallis, J.R. and Wood, E.F., 1985. Relative accuracy of log-Pearson III procedures. *ASCE Journal of Hydraulic Engineering*, 111(7), 1043 – 1056.
- Wallis, J.R. and Wood, E.F., 1987. Reply to discussion by Beard (1987) and by Landwehr et al. (1987) of “Relative accuracy of log-Pearson III procedures” by Wallis and Wood (1985). *ASCE, Journal of Hydraulic Engineering*, 113(9), 1210-1214.
- Wang, X.L., Swail, V.R., 2001. Changes of extreme wave heights in northern hemisphere oceans and related atmospheric circulation regimes. *J. Climate* 14, 2204–2221.
- Westmacott, J.R., Burn, D.H., 1997. Climate change effects on the hydrologic regime within the Churchill-Nelson River basin. *J. Hydrol.* 202, 263–279.
- Whitfield, P.H. and A.J. Cannon. 2000. Recent variation in climate and hydrology in Canada. *Can. Water Resour. J.* 25: 19-65.
- Whitfield, P.H., Cannon, A.J., 2000. Recent variations in climate and hydrology in Canada. *Can. Water Resour. J.* 25 (1), 19–65.
- WMO (World Meteorological Organisation) (1988). *Analysis Long term series of hydrological data with respect to Climate variability and change. WCAP-3. WMO/TD no. 224*. WMO, Geneva, Switzerland.

- WMO (World Meteorological Organisation) (1988) *Analysing Long Time Series of Hydrological Data with Respect to Climate Variability and Change*. WCAP-3, WMO/TD no. 224, WMO, Geneva, Switzerland.
- Xiong, L., Shenglian, G., 2004. Trend test and change-point detection for the annual discharge series of the Yangtze River at the Yichang hydrological station. *Hydrol. Sci. J.* 49 (1), 99–112.
- Xu, Z.X., Takeuchi, K., Ishidaira, H., 2003. Monotonic trend and step changes in Japanese precipitation. *Journal of Hydrology* 27992003) 144-150.
- Yu, S., Wang, C.Y., 2002. Applicability of prewhitening to eliminate the influence of serial correlation on the Mann-Kendall test. *Water Resources Research* 38(6), 41-47.
- Yue, S., P.J. Pilon and B. Phinney. 2003. Canadian streamflow trend detection: impacts of serial and cross correlation. *J. Hydrol. Sci.* 48(1): 51-64.
- Yue, S., P.J. Pilon, B. Phinney and G. Cavadias. 2002b. The influence of autocorrelation on the ability to detect trend in hydrological series. *Hydrolog. Process.* 16(9): 1807-1829.
- Yue, S., P.J. Pilon, G. Cavadias and B. Phinney. 2002a. Power of the Mann-Kendall and Spearman's rho tests for detecting monotonic trends in hydrological series. *J. Hydrol.* 259: 254-271.
- Yue, S., Pilon, P., 2004. A comparison of the power of the t test, Mann–Kendall and bootstrap tests for trend detection. *Hydrol. Sci. J.* 49 (1), 21–37.
- Yue, S., Pilon, P., Cavadias, G., 2002a. Power of the Mann–Kendall and Spearman's rho tests for detecting monotonic trends in hydrological series. *J. Hydrol.* 259, 254–271.
- Yue, S., Pilon, P., Phinney, B., Cavadias, G., 2002. The influence of autocorrelation on the ability to detect trend in hydrological time series. *Hydrological Processes* 16, 1807–1829.
- Yue, S., Pilon, P., Phinney, B., Cavadias, G., 2002b. The influence of autocorrelation on the ability to detect trend in hydrological series. *Hydrol. Process.* 16, 1807– 1829.
- Yue, S., Wang, C.Y., 2004. The Mann–Kendall test modified by effective sample size to detect trend in serially correlated hydrological series. *Water Res. Manage.* 18, 201–218.
- Yulianti, J.S., Burn, D.H., 1998. Investigating links between climatic warming and low streamflow in Prairies region of Canada. *Can. Water Resour. J.* 23 (1), 45–60.
- Zhang, X., Harvey, K.D., Hogg, W.D., Yuzyk, T.R., 2001. Trends in Canadian streamflow. *Water Resour. Res.* 37 (4), 987–998.

APPENDIX A

Data and Catchment Characteristics

Part A: Low Estimation for Ungauged Catchments (Study catchments)

Station	Waterbody	Location	Record Length (yrs)	25%ile flow (m ³ /s)	50%ile flow (m ³ /s)	75%ile flow (m ³ /s)	95% ile flow (m ³ /s)	99% ile flow (m ³ /s)	Mean flow (m3/s)	Area km ²	Rain Ave 61-90 (mm)
01042	Finn	Dreenan	29	9.67	5.03	2.22	0.75	0.18	6.45	347.7	1,937
01054	Bunadaowen	Croaghmagowna Frst.	7	0.44	0.15	0.04	0.02	0.01	0.35	4.9	1,916
03051	Blackwater	Faulkland	28	3.44	1.52	0.69	0.15	0.05	2.68	142.6	1,079
03055	Mountain Water	Glaslough	17	1.51	0.51	0.22	0.06	0.03	1.34	71.0	1,062
06013	Dee	Charleville	29	5.75	2.73	1.09	0.43	0.24	4.25	307.8	873
06014	Glyde	Tallanstown	27	6.20	2.93	1.14	0.44	0.27	4.46	269.2	928
06030	Big	Ballygoly	31	0.32	0.16	0.08	0.03	0.02	0.28	10.4	1,156
07001	Tremblestown	Tremblestown	27	3.12	1.72	0.76	0.32	0.18	2.37	150.7	913
07002	Deel	Killyon	26	6.60	3.80	1.78	0.85	0.69	4.76	283.8	920
07003	Blackwater (Enfield)	Castlerickard	30	2.94	1.66	0.84	0.40	0.25	2.39	180.8	809
07006	Moynalty	Fyanstown	18	3.92	1.83	0.72	0.29	0.12	2.87	176.7	936
07009	Boyne	Navan Weir	28	36.60	18.50	7.59	3.68	2.71	24.70	1,651.4	868
07033	Blackwater (Kells)	Virginia Hatchery	26	4.15	1.24	0.49	0.13	0.04	2.49	124.4	1,032
08011	Nanny	Duleek D/S	25	3.04	1.18	0.44	0.10	0.04	2.28	181.0	820
08012	Stream	Ballyboghill	16	0.31	0.12	0.03	0.01	0.00	0.25	25.8	799
09001	Ryewater	Leixlip	47	2.96	1.34	0.43	0.11	0.06	2.35	208.8	783
09002	Griffeen	Lucan	47	0.55	0.31	0.17	0.04	0.02	0.43	34.8	754
09009	Owendoher	Willbrook Road	23	0.56	0.35	0.23	0.13	0.11	0.48	20.5	916
09011	Slang	Frankfort	22	0.11	0.06	0.04	0.02	0.02	0.10	5.4	770
09037	Tolka	Botanic Gardens	7	2.00	0.96	0.50	0.29	0.24	2.21	137.3	792
09049	Lyreen	Maynooth	6	1.09	0.51	0.16	0.05	0.04	1.03	87.1	768
09102	Santry	Cadbury's	5	0.17	0.09	0.05	0.03	0.03	0.15	10.4	725
10002	Avonmore	Rathdrum	43	10.30	5.47	2.84	1.07	0.54	8.26	229.9	1,529
10021	Shanganagh	Common's Road	26	0.53	0.30	0.14	0.06	0.04	0.44	32.4	800
10022	Cabinteely	Carrickmines	22	0.21	0.11	0.05	0.02	0.01	0.17	12.9	822
10028	Aughrim	Knocknamohill	20	7.38	4.41	2.30	1.09	0.79	5.66	202.1	1,396
10038	Stream	Druids Glen	6	0.41	0.23	0.12	0.06	0.05	0.32	15.9	915
11001	Owenavorrigh	Boleany	35	2.77	1.16	0.54	0.29	0.21	2.42	154.5	930
12016	Boro	Dunanore	23	5.19	3.02	1.67	0.80	0.64	3.99	173.6	1,121
14007	Stradbally	Derrybrock	22	2.10	1.08	0.52	0.20	0.11	1.57	118.1	814
14014	Triogue	Portlaoise	6	0.67	0.35	0.17	0.10	0.09	0.49	42.5	874
14019	Barrow	Levitstown	37	25.80	15.00	8.15	4.12	3.02	20.20	1,690.5	862
14033	Owenass	Mountmellick	25	2.14	1.00	0.42	0.12	0.06	1.78	78.6	1,145
14057	Bothogue	Timolin	10	0.37	0.25	0.13	0.08	0.06	0.30	32.1	941

Station	Waterbody	Location	Record Length (yrs)	25%ile flow (m ³ /s)	50%ile flow (m ³ /s)	75%ile flow (m ³ /s)	95% ile flow (m ³ /s)	99% ile flow (m ³ /s)	Mean flow (m ³ /s)	Area km ²	Rain Ave 61-90 (mm)
14101	Boghlonge	Kyleclonhobert	7	0.27	0.10	0.03	0.01	0.00	0.18	9.8	935
14104	Greese	Greesemount	6	1.40	0.94	0.55	0.34	0.31	1.12	51.4	890
15001	Kings	Annamult	34	9.15	4.03	1.51	0.57	0.37	6.99	442.6	935
15003	Dinin	Dinin Br.	33	7.32	3.27	1.16	0.42	0.27	6.16	298.0	933
15005	Erkina	Durrow Ft. Br.	30	7.82	4.35	1.99	0.72	0.42	5.75	377.9	885
15006	Nore	Brownsbarn	34	51.80	27.80	12.30	5.90	4.25	39.90	2,408.9	942
15010	Goul	Ballyboodin	24	1.95	1.15	0.64	0.29	0.17	1.35	158.4	889
16001	Drish	Athlummon	35	2.55	1.39	0.69	0.19	0.11	2.02	134.5	916
16003	Clodiagh	Rathkennan	47	7.63	3.86	1.48	0.52	0.29	5.62	242.3	1,192
16009	Suir	Caher Park	51	41.50	22.40	11.40	5.72	3.81	31.50	1,576.7	1,079
16010	Anner	Anner	30	8.62	4.47	2.26	1.22	0.65	6.47	435.5	985
16012	Tar	Tar Br.	38	8.72	5.26	3.30	1.86	1.31	7.09	228.8	1,320
16013	Nire	Fourmilewater	34	4.54	2.36	1.21	0.57	0.32	3.73	93.2	1,472
18001	Bride	Mogeely	29	12.30	5.46	2.60	0.95	0.48	8.47	332.8	1,158
18002	Blackwater	Ballyduff	51	80.20	45.30	22.80	12.70	8.65	61.10	2,324.8	1,201
18004	Awbeg	Ballynamona	32	7.22	4.44	2.43	1.19	0.85	5.75	309.1	986
18005	Funshion	Downing Br.	31	11.80	6.69	3.90	1.96	1.50	8.96	377.1	1,187
19001	Owenboy	Ballea	31	2.89	1.45	0.70	0.24	0.12	2.30	102.9	1,176
19009	Butlerstown	Brookhill	9	1.53	0.79	0.27	0.10	0.07	1.10	42.8	1,191
19016	Ovens	Bride(Lee)	23	4.13	1.92	0.83	0.23	0.06	3.24	117.4	1,278
19032	Glashaboy	Meadowbrook	5	2.60	1.36	0.65	0.28	0.22	2.16	75.8	1,183
19044	Martin	Kilmona	8	1.93	0.95	0.42	0.14	0.07	1.38	38.8	1,212
20002	Bandon	Curranure	30	19.80	9.50	3.87	1.35	0.86	14.90	422.2	1,667
21001	Cummeragh	Cummeragh Weir	27	4.74	2.51	1.25	0.52	0.30	3.12	47.0	2,271
21002	Coomhola	Coomhola	27	5.16	1.78	0.67	0.20	0.09	4.79	64.5	2,580
21004	Mealagh	Inchilough	32	2.58	1.07	0.43	0.11	0.04	2.28	44.8	1,880
22003	Maine	Riverville	28	12.60	5.91	2.71	0.99	0.57	9.70	270.2	1,345
22006	Flesk(Laune)	Flesk	43	16.40	7.50	3.93	1.91	1.08	13.40	327.5	1,822
22007	Caragh	Caragh	9	15.10	6.83	2.82	0.99	0.52	11.30	162.3	2,561
22009	Deenagh (Laune)	White Bridge	24	1.43	0.79	0.42	0.21	0.14	1.11	35.3	1,175
22039	Clydagh	Clydagh Br.	7	4.13	1.60	0.84	0.48	0.34	3.51	56.8	1,884
22042	Cappagh	Cappagh	7	1.01	0.33	0.13	0.05	0.03	0.87	10.1	2,585
22043	Stream	Toormore Br. Weir	7	0.18	0.07	0.04	0.01	0.01	0.14	3.3	1,179
22044	Stream	Rahanane Weir	7	0.53	0.23	0.11	0.04	0.02	0.40	10.0	1,157
22045	Stream	Knockauncore Weir	7	0.11	0.05	0.02	0.01	0.00	0.09	2.8	1,170

Station	Waterbody	Location	Record Length (yrs)	25%ile flow (m ³ /s)	50%ile flow (m ³ /s)	75%ile flow (m ³ /s)	95% ile flow (m ³ /s)	99% ile flow (m ³ /s)	Mean flow (m ³ /s)	Area km ²	Rain Ave 61-90 (mm)
23001	Galey	Inch Br.	45	5.44	2.05	0.80	0.23	0.12	4.70	191.0	1,087
23002	Feale	Listowel	57	26.30	9.98	3.98	1.46	0.83	20.90	644.3	1,346
23005	Allaghaun	Goulburn	24	2.38	1.00	0.43	0.14	0.06	1.93	61.9	1,253
23017	Smearlagh	Trienearagh	25	5.46	1.70	0.66	0.19	0.10	4.20	118.6	1,332
23022	Big	Tralee Clonalour	21	0.42	0.16	0.06	0.02	0.01	0.33	10.9	1,127
24008	Maigue	Castleroberts	27	16.60	7.74	3.38	1.38	0.92	12.50	803.0	939
24022	Mahore	Hospital	22	0.85	0.41	0.15	0.04	0.02	0.68	41.1	942
24030	Deel	Danganbeg	26	6.27	2.71	1.10	0.42	0.31	4.84	257.9	1,051
24033	White	Ballyhahill	26	1.59	0.57	0.21	0.03	0.02	1.64	51.7	1,099
25001	Mulkear	Annacotty	24	19.50	10.30	5.33	2.64	1.57	15.70	645.1	1,165
25002	Newport	Barrington's Br.	43	7.42	3.60	1.76	0.61	0.21	5.65	220.8	1,298
25004	Bilboa	New Bridge	21	5.52	2.67	1.36	0.71	0.51	3.84	121.8	1,333
25005	Dead	Sunville	22	4.97	1.95	0.82	0.36	0.25	3.60	191.9	1,025
25014	Silver	Millbrook	28	2.93	1.77	0.95	0.51	0.35	2.32	163.8	1,013
25022	Camcor	Syngefield	48	3.73	2.22	1.27	0.67	0.47	2.96	160.7	984
25027	Ollatrim	Gourdeen	30	2.87	1.54	0.67	0.30	0.21	2.19	118.4	1,020
25030	Graney	Scarriff	34	11.20	5.63	2.56	0.76	0.37	8.16	278.9	1,185
25038	Nenagh	Tyone	9	4.63	2.22	1.12	0.55	0.48	3.45	135.6	1,250
25040	Bunow	Roscrea	22	0.53	0.30	0.13	0.04	0.01	0.41	27.9	989
25044	Kilmastulla	Coole	37	2.54	1.24	0.61	0.30	0.19	2.00	92.2	1,187
25107	Little	Crancreagh	7	0.26	0.13	0.08	0.05	0.03	0.24	15.7	850
25222	Boor	Gorteen Br.	5	0.26	0.12	0.05	0.02	0.02	0.20	26.9	876
26004	Island	Bookala	6	3.67	2.03	1.00	0.19	0.03	2.83	131.7	1,089
26007	Suck	Bellagill	29	37.80	18.00	7.61	2.68	1.73	25.20	1,202.3	1,045
26012	Boyle	Tinacarra	44	16.80	9.01	3.78	1.09	0.64	11.60	517.8	1,143
26014	Lung	Banada Bridge	10	7.91	3.75	1.85	0.71	0.43	5.58	214.3	1,198
26018	Owenure	Bellavahan	30	3.90	1.78	0.43	0.13	0.09	2.49	119.0	1,044
26021	Inny	Ballymahon	30	28.00	16.00	6.75	2.76	1.96	21.80	1,094.3	945
26029	Shannon	Dowra	32	6.31	2.34	0.88	0.30	0.16	4.91	116.5	1,759
26056	Mountnugent	Mountnugent Br.	24	1.79	0.66	0.29	0.10	0.07	1.79	88.0	991
26058	Inny Upper	Ballinrink Br.	25	1.56	0.86	0.44	0.18	0.11	1.13	59.7	973
27001	Claureen	Inch Br.	9	1.94	0.70	0.25	0.07	0.02	1.55	46.5	1,478
27002	Fergus	Ballycorey	49	14.70	7.64	2.99	0.70	0.27	10.00	562.0	1,337
28001	Inagh	Ennistimon	31	7.66	2.54	0.91	0.22	0.09	5.92	168.7	1,422
30012	Clare	Claregalway	10	28.60	13.30	5.03	1.59	1.02	21.00	1,068.5	1,099
30021	Robe	Christina's Br.	26	3.63	1.73	0.75	0.22	0.13	2.76	103.2	1,168

Station	Waterbody	Location	Record Length (yrs)	25%ile flow (m ³ /s)	50%ile flow (m ³ /s)	75%ile flow (m ³ /s)	95% ile flow (m ³ /s)	99% ile flow (m ³ /s)	Mean flow (m ³ /s)	Area km ²	Rain Ave 61-90 (mm)
30033	Glensaul	Toormakeady	10	1.56	0.44	0.16	0.07	0.05	1.17	24.2	2,388
31002	Cashla	Cashla	28	3.84	1.81	0.86	0.33	0.17	2.67	71.1	1,530
32004	Owenglin	Clifden	16	2.25	0.94	0.41	0.16	0.09	1.85	32.2	1,849
32011	Bunowen	Louisburg Weir	26	3.83	1.46	0.61	0.23	0.14	3.10	69.8	1,613
32012	Newport	Newport Weir	25	8.85	4.49	1.97	0.78	0.42	6.05	145.5	1,784
32024	Glaishwy	Glaishwy Bridge	5	0.12	0.05	0.03	0.01	0.00	0.10	4.5	1,700
33006	Owenduff	Srahnamanragh	23	7.87	3.15	1.17	0.57	0.45	6.19	118.2	1,585
34024	Pollagh	Kiltimagh	30	4.17	1.90	0.79	0.35	0.24	3.10	126.7	1,177
34031	Charlestown	Charlestown	10	0.79	0.43	0.21	0.11	0.09	0.65	23.0	1,276
36010	Annalee	Butlers Br.	26	20.90	9.22	2.74	0.39	0.11	13.70	768.5	968
36018	Dromore	Ashfield	27	6.33	2.90	0.78	0.14	0.03	4.01	233.4	950
36019	Erne	Belturbet	41	41.70	20.90	7.08	1.33	0.44	26.90	1,485.5	971
36020	Blackwater	Killywillin	20	4.09	1.97	0.77	0.20	0.09	2.98	93.1	1,573
36021	Yellow	Kiltybardan	22	1.39	0.53	0.23	0.09	0.05	1.07	23.3	1,570
36027	Woodford	Bellaheady	18	13.60	7.47	2.81	0.80	0.48	8.80	332.4	1,373
36029	Rag	Tomkinroad Bridge	17	1.06	0.45	0.19	0.07	0.03	0.89	34.6	1,120
38001	Owenea	Clonconwal Ford	26	7.22	2.80	1.12	0.36	0.16	5.32	110.8	1,752
38005	Owengarve	Nr. Glenties	7	0.76	0.33	0.13	0.02	0.01	0.49	8.4	1,876
39021	Owennasop	Meanahernish	5	0.74	0.29	0.12	0.05	0.03	0.61	14.2	1,643

Part B: Non-stationarity in AMF Records (Study catchment)

Hydr. Station	Waterbody	Location	Record length (yrs)	Area (km2)	Rainfall (61-90) (mm)	Main stream length (km)	Stream lengths (km)	Stream frequency (STMFRQ)	Drainage density (DRAIND)	S1085 (slope)	FARL (catchment attenuation index)	BFI
06011	Fane	Moyles Mill	51	229	1028.98	33.15	130.88	114	0.571	2.695	0.874	0.000
06013	Dee	Charleville	34	309	873.08	53.97	345.39	275	1.117	2.553	0.971	0.617
06014	Glyde	Tallanstown	34	270	927.45	34.39	234.08	235	0.866	3.071	0.927	0.634
06025	Dee	Burley	34	176	908.31	38.63	175.53	124	0.997	3.635	0.956	0.000
06026	Lagan (Glyde)	Aclint	50	148	940.87	25.43	151.96	154	1.023	4.724	0.915	0.658
07009	Boyne	Navan Weir	33	1658	868.55	69.07	683.13	552	0.976	1.714	0.911	0.713
07033	Blackwater (Kells)	Virginia	25	125	1032.22	25.76	141.45	237	1.311	3.961	N/A	0.439
08002	Naul	Delvin	21	33	791.12	19.15	91.78	112	1.098	4.259	N/A	0.597
08008	Broadmeadow	Broadmeadow	29	108	810.61	24.28	202.39	148	1.113	3.046	0.999	0.000
09001	Ryewater	Leixlip	52	210	783.26	27.01	175.52	191	1.132	1.583	1	0.507
09002	Lucan	Griffeen	25	35	754.75	21.61	138.59	228	1.47	20.931	0.958	0.674
10021	Common's Road	Shanganagh	24	33	799.07	5.95	21.62	23	1.671	10.155	N/A	0.654
11001	Owenavorrhagh	Boleany	36	155	931.07	89.28	1101.02	1302	1.068	2.053	0.999	0.500
14005	Barrow	Portarlington	52	405	1014.90	52.71	730.51	668	0.687	3.106	1	0.501
14006	Barrow	Pass Br	55	1064	899.07	20.53	64.67	35	0.545	3.847	N/A	0.571
14009	Cushina	Cushina	29	68	831.24	20.72	64.04	37	0.395	0.936	N/A	0.667
14013	Burren	Ballinacarrig	50	154	887.98	114.49	1746.46	1430	0.722	0.45	0.999	0.000
14018	Barrow	Royal Oak	55	2419	857.46	83.71	995.37	794	0.586	0.697	1	0.665
14019	Barrow	Levitstown	55	1697	861.46	137.92	2086.49	1763	0.751	0.528	0.999	0.624
15003	Dinin	Dinin Br.	55	299	933.86	56.84	525.97	447	1.07	0.867	0.998	0.000
15004	Nore	Mcmahons Br.	55	491	1067.46	39.33	273.39	230	0.721	1.903	0.999	0.000
16002	Suir	Beakstown	55	486	932.15	29.86	274.92	288	1.13	5.264	0.999	0.634
16003	Clodiagh	Rathkennan	55	243	1192.01	32.67	209.30	156	0.915	1.803	1	0.550
16004	Suir	Thurles	51	229	941.36	29.03	118.44	183	1.41	6.563	N/A	0.579
16005	Multeen	Aughnagross	34	84	1153.57	27.77	119.51	205	1.577	5.887	0.994	0.560

Hydr. Station	Waterbody	Location	Record length (yrs)	Area (km2)	Rainfall (61-90) (mm)	Main stream length (km)	Stream lengths (km)	Stream frequency (STMFRQ)	Drainage density (DRAIND)	S1085 (slope)	FARL (catchment attenuation index)	BFI
16008	Suir	New Bridge	55	1090	1029.63	85.44	1585.17	1810	1.002	1	0.998	0.635
16009	Suir	Caher Park	56	1583	1078.57	116.48	2240.00	2743	1.045	0.936	0.998	0.631
18005	Funshion	Downing Br.	54	378	1190.37	24.04	107.91	98	1.045	3.738	N/A	0.707
19001	Owenboy	Ballea	52	103	1175.68	15.49	67.17	59	1.063	10.672	N/A	0.640
19020	Ballyedmond	Owennacurra	28	74	1179.07	21.08	84.30	79	1.087	6.437	N/A	0.664
20001			48	N/A	N/A	N/A	N/A	N/A	N/A	N/A	N/A	0.000
20002	Bandon	Curranure	35	424	1668.87	35.91	310.87	322	1.146	5.075	1	0.526
23001	Galey	Inch Br.	46	192	1084.01	50.54	718.61	861	1.111	4.281	N/A	0.322
24008	Maigue	Castleroberts	34	806	939.47	32.67	307.30	251	1.093	2.234	1	0.535
24082	Maigue	Islandmore	32	763	941.70	53.24	888.27	1030	1.372	4.067	0.999	0.518
25002	Newport	Barrington's Br.	55	222	1299.96	42.34	545.38	623	1.367	4.741	0.998	0.000
25003	Mulkear	Abington	55	399	1106.40	24.99	229.92	238	1.194	3.214	0.999	0.497
25005	Dead	Sunville	47	193	1023.31	67.32	846.17	629	0.728	0.876	0.955	0.474
25006	Brosna	Ferbane	56	1163	931.99	75.90	852.50	633	0.722	0.828	0.956	0.708
25014	Silver	Millbrook	58	164	1007.65	31.69	178.37	133	0.648	5.939	0.999	0.671
25017	Shannon	Banagher	59	7980	1024.05	27.95	190.53	160	0.967	1.89	0.999	0.000
25021	Little Brosna	Croghan	48	479	927.77	22.31	129.46	83	0.802	9.831	N/A	0.000
25023	Little Brosna	Milltown	56	114	922.49	29.68	103.89	69	0.644	2.599	0.995	0.654
25025	Ballyfinboy	Ballyhooney	35	161	904.54	27.79	111.40	90	0.937	3.925	0	0.730
25027	Ollatrim	Gourdeen	47	119	1021.15	38.12	259.72	216	0.887	4.826	0.997	0.651
25029	Nenagh	Clarianna	37	293	1108.68	37.32	341.46	351	1.219	3.687	0.85	0.578
25030	Graney	Scarriff	52	280	1183.81	72.33	512.26	458	0.799	0.5	0.979	0.542
26002	Suck	Rookwood	57	641	1067.03	96.71	820.88	691	0.756	0.41	0.981	0.605
26005	Suck	Derrycahill	55	1085	1054.40	28.82	174.12	171	0.942	0.959	0.97	0.560
26006	Suck	Willsbrook	57	185	1120.64	107.36	908.56	761	0.753	0.386	0.983	0.540
26007	Suck	Bellagill	57	1207	1045.62	34.79	316.71	296	1.13	1.024	0.855	0.653
26008	Rinn	Johnston's Br.	54	280	1035.47	17.47	94.34	68	0.96	2.886	0.936	0.611

Hydr. Station	Waterbody	Location	Record length (yrs)	Area (km2)	Rainfall (61-90) (mm)	Main stream length (km)	Stream lengths (km)	Stream frequency (STMFRQ)	Drainage density (DRAIND)	S1085 (slope)	FARL (catchment attenuation index)	BFI
26009	Black	Bellantra Br.	39	98	1018.79	20.54	128.02	132	1.354	2.168	0.937	0.000
26017			53	N/A	N/A	N/A	N/A	N/A	N/A	N/A	N/A	0.000
26018	Owenure	Bellavahan	53	119	1043.90	35.81	229.22	155	0.906	0.631	0.986	0.721
26019	Camlin	Mullagh	55	253	979.62	5.19	5.42	3	0.044	8.124	N/A	0.537
26020	Camlin	Argar	33	122	1003.36	90.24	816.98	607	0.744	0.273	0.807	0.000
26021	Inny	Ballymahon	34	1099	945.25	13.92	23.99	7	0.388	3.549	N/A	0.828
26022	Fallan	Kilmore	37	62	915.82	70.03	461.73	326	0.876	0.237	0.825	0.579
26059	Finnea Br.	Inny	23	257	976.44	17.13	47.79	59	0.333	4.511	0.912	0.910
27001	Claureen	Inch Br.	36	47	1476.89	40.39	303.14	391	0.537	1.257	0.835	0.284
27002	Fergus	Ballycorey	55	564	1336.35	21.04	81.89	113	0.492	3.885	0.922	0.697
27003	Fergus	Corrofin	52	166	1567.43	30.91	238.25	298	1.406	2.533	0.938	0.000
27070	Baunkyle	L. Inchiqui	29	144	1592.48	27.32	154.96	146	1.251	5.126	0.804	0.631
29001	Raford	Rathgorgin	44	115	1089.74	28.84	69.37	47	0.571	2.697	0.993	0.000
29004	Clarinbridge	Clarinbridge	35	121	1107.47	39.48	253.60	254	0.934	2.074	0.969	0.616
29011	Dunkellin	Kilcolgan	26	354	1079.37	30.97	171.33	260	1.416	5.459	0.935	0.633
29071	Cutra	L. Cutra	29	124	1212.48	84.54	711.83	547	0.663	0.769	0.994	0.551
30007	Clare	Ballygaddy	35	470	1115.06	79.61	1055.82	1618	1.185	0.613	0.629	0.646
31002	Cashla	Cashla	26	71	1530.25	21.90	295.35	781	2.641	3.213	0.636	0.529
32012	Newport Weir	Newport	24	146	1784.36	17.65	119.05	152	1.564	10.64	0.998	0.595
33070	Carrowmore	Carrowmore L.	28	88	1422.25	69.18	2478.47	3270	1.375	0.982	0.817	0.000
34001	Moy	Rahans	39	1975	1322.66	44.55	379.95	455	1.229	1.658	0.901	0.776
34003	Foxford	Moy	29	1802	1339.66	31.92	173.18	185	1.361	1.477	0.922	0.797
34009	Owengarve	Curraghbonaun	37	117	1256.71	42.47	688.24	807	1.421	3.976	0.988	0.399
34011	Manulla	Gneeve Bridge	34	143	1247.57	23.74	152.79	258	1.602	3.06	0.732	0.000
34018	Castlebar	Turlough	33	95	1554.59	24.73	356.47	433	1.19	0.298	0.923	0.658
34024	Kiltimagh	Pollagh	29	127	1177.46	41.72	381.21	514	1.681	2.935	0.98	0.521
35001	Owenmore	Ballynacarrow	35	299	1172.84	25.66	151.05	289	1.701	13.512	0.986	0.598

Hydr. Station	Waterbody	Location	Record length (yrs)	Area (km2)	Rainfall (61-90) (mm)	Main stream length (km)	Stream lengths (km)	Stream frequency (STMFRQ)	Drainage density (DRAIND)	S1085 (slope)	FARL (catchment attenuation index)	BFI
35002	Owenbeg	Billa Br.	34	89	1380.56	26.51	138.13	113	1.181	2.334	0.994	0.422
35005	Ballysadare	Ballysadare	61	640	1198.32	34.21	425.43	584	1.451	4.081	0.978	0.609
35071	Lareen	L. Melvin	31	247	1364.46	15.42	83.32	67	1.225	13.75	0.823	0.000
35073			30	N/A	N/A	N/A	N/A	N/A	N/A	N/A	N/A	0.000
36010	Annalee	Butlers Br.	54	772	967.55	49.70	322.13	297	1.005	1.189	0.792	0.000
36011	Erne	Bellahillan	53	321	979.63	36.10	241.20	224	0.92	1.191	0.756	0.785
36012	Erne	Sallaghan	50	262	985.45	24.45	146.97	204	0.96	3.158	0.955	0.000
36015	Finn	Anlore	37	153	1090.72	44.96	488.06	516	0.963	2.44	0.816	0.000
36018	Dromore	Ashfield	54	234	950.12	78.58	1506.34	1508	1.01	1.297	0.761	0.692
36019	Erne	Belturbet	51	1492	971.21	20.52	130.86	112	1.4	11.216	0.839	0.787
36021	Yellow	Kiltybardan	31	23	1569.64	49.96	381.03	384	1.141	1.108	0.72	0.270
36031	Lisdarn	Cavan	30	64	910.43	122.78	2947.25	4182	0.94	0.519	0.663	0.481
39008			37	N/A	N/A	N/A	N/A	N/A	N/A	N/A	N/A	0.000
39009	Fern O/L	Aghawoney	33	207	1570.26	5.88	15.05	31	1.552	13.344	0.737	0.000

APPENDIX B

**CRITICAL VALUES FOR THE STANDARDISED LINEAR REGRESSION BASED
TEST STATISTIC (b_s)**

CRITICAL VALUES FOR THE STANDARDISED LINEAR REGRESSION BASED TEST STATISTIC (b_s)

N	BSMIN	BSBEAN	BSMAX	b_s critical										STDEVBS	SKEWBS
				$\alpha=0.005$	$\alpha=0.01$	$\alpha=0.025$	$\alpha=0.05$	$\alpha=0.10$	$\alpha=0.90$	$\alpha=0.95$	$\alpha=0.975$	$\alpha=0.99$	$\alpha=0.995$		
15	-0.0695	-0.0003	0.0634	-0.0445	-0.0406	-0.0336	-0.0282	-0.0223	0.0219	0.0274	0.0333	0.0405	0.0439	0.0172	0.0048
16	-0.0603	0.0001	0.0547	-0.0404	-0.0365	-0.0308	-0.0255	-0.0197	0.0201	0.0256	0.0304	0.0355	0.0388	0.0154	-0.0354
17	-0.0628	-0.0001	0.0551	-0.0378	-0.0344	-0.0281	-0.0237	-0.0183	0.0181	0.0230	0.0274	0.0328	0.0362	0.0142	-0.0435
18	-0.0575	0.0001	0.0549	-0.0328	-0.0308	-0.0257	-0.0216	-0.0166	0.0168	0.0219	0.0262	0.0311	0.0348	0.0132	0.0412
19	-0.0457	0.0000	0.0468	-0.0310	-0.0280	-0.0236	-0.0197	-0.0156	0.0155	0.0200	0.0237	0.0279	0.0311	0.0120	0.0209
20	-0.0420	0.0002	0.0418	-0.0302	-0.0269	-0.0219	-0.0182	-0.0141	0.0146	0.0186	0.0217	0.0257	0.0287	0.0112	-0.0403
21	-0.0432	0.0000	0.0412	-0.0270	-0.0244	-0.0203	-0.0174	-0.0134	0.0135	0.0173	0.0204	0.0239	0.0267	0.0104	-0.0144
22	-0.0361	0.0000	0.0432	-0.0255	-0.0235	-0.0189	-0.0158	-0.0120	0.0123	0.0162	0.0196	0.0232	0.0256	0.0097	0.0424
23	-0.0315	0.0000	0.0345	-0.0235	-0.0213	-0.0180	-0.0151	-0.0118	0.0117	0.0149	0.0176	0.0209	0.0232	0.0091	-0.0143
24	-0.0316	-0.0001	0.0322	-0.0226	-0.0203	-0.0170	-0.0144	-0.0115	0.0110	0.0140	0.0167	0.0199	0.0220	0.0087	-0.0217
25	-0.0342	0.0000	0.0291	-0.0214	-0.0193	-0.0158	-0.0132	-0.0103	0.0104	0.0133	0.0160	0.0190	0.0215	0.0081	0.0027
26	-0.0286	0.0001	0.0284	-0.0192	-0.0171	-0.0144	-0.0122	-0.0095	0.0097	0.0123	0.0149	0.0179	0.0201	0.0075	0.0171
27	-0.0296	0.0000	0.0309	-0.0184	-0.0167	-0.0142	-0.0119	-0.0093	0.0091	0.0117	0.0138	0.0165	0.0186	0.0072	-0.0227
28	-0.0283	0.0000	0.0328	-0.0177	-0.0157	-0.0134	-0.0112	-0.0088	0.0088	0.0111	0.0135	0.0162	0.0175	0.0068	0.0307
29	-0.0230	0.0000	0.0238	-0.0163	-0.0146	-0.0127	-0.0105	-0.0083	0.0082	0.0106	0.0126	0.0149	0.0166	0.0064	0.0120
30	-0.0247	-0.0001	0.0206	-0.0161	-0.0146	-0.0121	-0.0101	-0.0078	0.0076	0.0096	0.0116	0.0136	0.0154	0.0060	-0.0387
31	-0.0251	-0.0001	0.0190	-0.0147	-0.0134	-0.0113	-0.0094	-0.0074	0.0073	0.0094	0.0112	0.0133	0.0150	0.0057	0.0101
32	-0.0191	0.0000	0.0213	-0.0147	-0.0135	-0.0110	-0.0092	-0.0072	0.0071	0.0091	0.0108	0.0132	0.0146	0.0056	-0.0047
33	-0.0207	0.0000	0.0193	-0.0137	-0.0123	-0.0105	-0.0089	-0.0069	0.0067	0.0085	0.0103	0.0124	0.0138	0.0053	-0.0264
34	-0.0202	0.0000	0.0178	-0.0133	-0.0122	-0.0100	-0.0084	-0.0065	0.0065	0.0083	0.0100	0.0118	0.0130	0.0051	-0.0371
35	-0.0180	0.0000	0.0170	-0.0124	-0.0113	-0.0095	-0.0081	-0.0064	0.0063	0.0082	0.0098	0.0114	0.0124	0.0049	0.0375
36	-0.0178	0.0000	0.0200	-0.0124	-0.0108	-0.0091	-0.0077	-0.0060	0.0060	0.0078	0.0092	0.0110	0.0125	0.0047	0.0271
37	-0.0159	0.0000	0.0163	-0.0124	-0.0103	-0.0086	-0.0073	-0.0056	0.0057	0.0073	0.0087	0.0104	0.0114	0.0044	0.0075
38	-0.0177	0.0000	0.0160	-0.0124	-0.0101	-0.0086	-0.0071	-0.0055	0.0054	0.0069	0.0083	0.0098	0.0110	0.0043	-0.0472
39	-0.0145	-0.0001	0.0156	-0.0124	-0.0095	-0.0081	-0.0070	-0.0054	0.0053	0.0068	0.0080	0.0097	0.0110	0.0041	0.0478
40	-0.0153	0.0000	0.0154	-0.0124	-0.0090	-0.0078	-0.0065	-0.0051	0.0050	0.0065	0.0077	0.0092	0.0102	0.0040	-0.0028

N	BSMIN	BSBEAN	BSMAX	b_s critical										STDEVBS	SKEWBS
				$\alpha=0.005$	$\alpha=0.01$	$\alpha=0.025$	$\alpha=0.05$	$\alpha=0.10$	$\alpha=0.90$	$\alpha=0.95$	$\alpha=0.975$	$\alpha=0.99$	$\alpha=0.995$		
41	-0.0143	0.0000	0.0163	-0.0124	-0.0090	-0.0075	-0.0063	-0.0048	0.0049	0.0064	0.0076	0.0089	0.0099	0.0038	0.0058
42	-0.0158	0.0000	0.0145	-0.0124	-0.0086	-0.0072	-0.0060	-0.0047	0.0048	0.0061	0.0073	0.0088	0.0097	0.0037	0.0098
43	-0.0150	0.0000	0.0126	-0.0124	-0.0085	-0.0072	-0.0059	-0.0046	0.0045	0.0059	0.0070	0.0083	0.0092	0.0036	-0.0121
44	-0.0136	0.0001	0.0130	-0.0124	-0.0078	-0.0067	-0.0056	-0.0044	0.0044	0.0056	0.0067	0.0080	0.0092	0.0034	0.0006
45	-0.0127	0.0000	0.0122	-0.0124	-0.0078	-0.0067	-0.0055	-0.0043	0.0043	0.0055	0.0066	0.0080	0.0089	0.0034	0.0112
46	-0.0137	0.0000	0.0112	-0.0124	-0.0075	-0.0063	-0.0054	-0.0042	0.0042	0.0053	0.0063	0.0074	0.0081	0.0032	-0.0045
47	-0.0109	0.0000	0.0120	-0.0124	-0.0072	-0.0062	-0.0053	-0.0040	0.0040	0.0051	0.0061	0.0073	0.0081	0.0031	0.0155
48	-0.0133	0.0000	0.0117	-0.0124	-0.0070	-0.0059	-0.0049	-0.0039	0.0039	0.0050	0.0060	0.0071	0.0077	0.0030	-0.0024
49	-0.0108	0.0000	0.0128	-0.0124	-0.0069	-0.0057	-0.0048	-0.0037	0.0038	0.0049	0.0058	0.0071	0.0077	0.0029	0.0328
50	-0.0123	0.0000	0.0111	-0.0124	-0.0065	-0.0055	-0.0046	-0.0035	0.0037	0.0047	0.0056	0.0068	0.0075	0.0028	0.0461
51	-0.0101	0.0000	0.0099	-0.0124	-0.0063	-0.0054	-0.0045	-0.0035	0.0036	0.0046	0.0054	0.0064	0.0071	0.0028	0.0440
52	-0.0107	0.0000	0.0093	-0.0124	-0.0061	-0.0052	-0.0044	-0.0034	0.0034	0.0044	0.0053	0.0062	0.0070	0.0027	0.0452
53	-0.0097	0.0000	0.0096	-0.0124	-0.0060	-0.0051	-0.0043	-0.0033	0.0033	0.0041	0.0049	0.0059	0.0065	0.0026	-0.0482
54	-0.0088	0.0000	0.0095	-0.0124	-0.0059	-0.0050	-0.0042	-0.0033	0.0032	0.0041	0.0049	0.0058	0.0064	0.0025	0.0171
55	-0.0096	0.0000	0.0084	-0.0124	-0.0059	-0.0049	-0.0041	-0.0032	0.0032	0.0040	0.0049	0.0058	0.0063	0.0025	-0.0466
56	-0.0090	0.0000	0.0103	-0.0124	-0.0057	-0.0048	-0.0041	-0.0031	0.0031	0.0039	0.0047	0.0056	0.0062	0.0024	-0.0030
57	-0.0082	0.0000	0.0099	-0.0124	-0.0054	-0.0046	-0.0038	-0.0030	0.0030	0.0038	0.0046	0.0054	0.0061	0.0023	0.0338
58	-0.0090	0.0000	0.0088	-0.0124	-0.0053	-0.0045	-0.0037	-0.0029	0.0030	0.0038	0.0045	0.0054	0.0059	0.0023	0.0182
59	-0.0086	0.0001	0.0090	-0.0124	-0.0051	-0.0043	-0.0036	-0.0028	0.0029	0.0037	0.0044	0.0053	0.0058	0.0022	0.0020
60	-0.0077	0.0000	0.0091	-0.0124	-0.0051	-0.0042	-0.0035	-0.0028	0.0028	0.0036	0.0043	0.0050	0.0055	0.0022	0.0349

APPENDIX C

HETEROGENEITY TEST MEASURES

APPENDIX C: HETEROGENEITY TEST MEASURES

The heterogeneity test measures proposed by Hosking and Wallis (1997) are based on (1) L-CV alone (the H_1 statistic) and (2) L-CV, L-Skewness jointly (the H_2 statistic). These tests measure the sample variability of the L-moment ratios among the samples in the pooling group and compare it to the variation that would be expected in a homogeneous pooling group. The sample variability of the L-moment ratios is measured as the standard deviation of the at-site sample L-moment ratios weighted proportionally to the sites' respective record lengths.

1. The measure of the sample variability based on L-CV alone:

$$V_1 = \frac{\sum_{i=1}^M n_i (t_2^i - t_2^R)^2}{\sum_{i=1}^M n_i} \quad (C1)$$

2. The measure of sample variability based on both the L-CV and the L-Skewness:

$$V_2 = \frac{\sum_{i=1}^M n_i \left[(t_2^i - t_2^R)^2 + (t_3^i - t_3^R)^2 \right]^{1/2}}{\sum_{i=1}^M n_i} \quad (C2)$$

where t_2^R and t_3^R are the group mean of L-CV and L-Skewness respectively; t_2^i , t_3^i , and n_i are the values of L-CV, L-Skewness and sample size for site i ; and M is the number of sites in the pooling group.

The expected mean value and standard deviation of these dispersion measures for a homogeneous group, μ_{V_k} and σ_{V_k} , respectively, are assessed through repeated simulations, by generating homogeneous groups of basins having the same record lengths as those of the observed data following the methodology proposed by Hosking and Wallis (1997). The heterogeneity measures are then evaluated using the following expression:

$$H_k = \frac{V_k - \mu_{V_k}}{\sigma_{V_k}}; \text{ for } k = 1, 2 \quad (\text{C3})$$

Hosking and Wallis (1997) suggested that a group of sites may be regarded as “acceptably homogeneous” if $H_k < 1$, “possibly heterogeneous” if $1 \leq H_k < 2$, and “definitely heterogeneous” if $H_k \geq 2$. The authors also pointed out that H_2 statistic lacks power to discriminate between homogeneous and heterogeneous regions, whereas H_1 , has much better discriminatory power. However, the H_2 statistic as the heterogeneity measure was adopted by FEH (1999) for testing the homogeneity of pooling groups as both the L-CV and L-skewness are required for fitting pooled growth curves with a Generalised Logistic (GLO) or a Generalised Extreme Value distribution (GEV). FEH (1999) revised the heterogeneity criteria based on the H_2 statistic, suggesting that if $2 < H_2 < 4$, a region could be considered as heterogeneous whereas if $H_2 > 4$ it could be considered as strongly heterogeneous.